



저작자표시-비영리-변경금지 2.0 대한민국

이용자는 아래의 조건을 따르는 경우에 한하여 자유롭게

- 이 저작물을 복제, 배포, 전송, 전시, 공연 및 방송할 수 있습니다.

다음과 같은 조건을 따라야 합니다:



저작자표시. 귀하는 원저작자를 표시하여야 합니다.



비영리. 귀하는 이 저작물을 영리 목적으로 이용할 수 없습니다.



변경금지. 귀하는 이 저작물을 개작, 변형 또는 가공할 수 없습니다.

- 귀하는, 이 저작물의 재이용이나 배포의 경우, 이 저작물에 적용된 이용허락조건을 명확하게 나타내어야 합니다.
- 저작권자로부터 별도의 허가를 받으면 이러한 조건들은 적용되지 않습니다.

저작권법에 따른 이용자의 권리는 위의 내용에 의하여 영향을 받지 않습니다.

이것은 [이용허락규약\(Legal Code\)](#)을 이해하기 쉽게 요약한 것입니다.

[Disclaimer](#)

A DOCTORAL DISSERTATION

**Characteristics of Underwater Capillary Discharge and its
Application for Antibacterial Activity**

DEPARTMENT OF NUCLEAR AND ENERGY ENGINEERING

GRADUATE SCHOOL

JEJU NATIONAL UNIVERSITY

Muhammad Waqar Ahmed

December, 2016

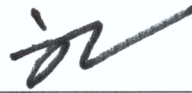
Characteristics of Underwater Capillary Discharge and Its Application for Antibacterial Activity

Muhammad Waqar Ahmed
(Supervised by Professor Heon-Ju Lee)

A thesis submitted in partial fulfillment of the requirement for the degree of Doctor
of Nuclear and Energy Engineering.

2016. 12.

This thesis has been examined and approved.



Thesis director, Heon-Ju Lee, Prof. of Nuclear and Energy Engineering

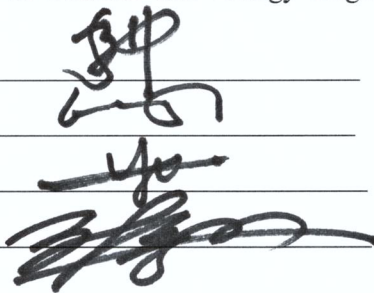
Suk Jae Yoo

Sooseok Choi

Young Hun Yu

Dong Kee Jeong

(Name and signature)



2016. 12.

Date

Department of Nuclear & Energy Engineering
GRADUATE SCHOOL
JEJU NATIONAL UNIVERSITY

TO MY SON.....

HUZAFI WAQAR

ACKNOWLEDGEMENTS

First and foremost I want to thank my Professor Heon-Ju Lee. It has been an honor to be his Ph.D. student. I appreciate all his contributions of time, ideas, and funding to make my Ph.D. experience productive and stimulating. The joy and enthusiasm he has for his research was contagious and motivational for me, even during tough times in the Ph.D. pursuit. I am also thankful for the excellent example he has provided as a successful physicist and professor. His though provoking seminars and discussion and pursuing me for attending and participating various conferences and seminars will be admired and cherished by me forever. The members of the plasma group have contributed immensely to my personal and professional tenure at plasma applications laboratory.

I can never forget the most important person Dr. Nauman Malik who introduced me in plasma applications laboratory of Jeju national university. His encouragement and nice attitude increased my confidence to come here for doctor course.

I am Thankful to Prof. Young-Sun Mok who delivered very useful and informative lectures during course work that are deeply related to my research work. Special thanks to Professor Soosok Choi for useful discussion and presentations during course work. I would like to acknowledge honorary laboratory member Dr. Konstantin Lyakhov who was here as a research professor a couple years ago. We discussed together on several theoretical aspects of underwater plasma discharge. Special thanks to Dr. Ulugbek Shaislamov for co-working in Nano-technology research field and helping to overcome Korean language barrier for purchasing components and technical equipment. I am grateful to my research fellow Rai Suresh for assisting the development and installation of underwater plasma discharge systems. I am thankful to Dr. Muhammad Abrar (Assistant professor, CIIT Islamabad) for having useful advices, critics and discussion on experimental results especially spectral analysis of underwater plasma discharge. Special thanks to Dr. Anil Kumar Khambampati (research professor, JEJUNU) for his guidance during research and for useful informative presentations in course work. I am highly grateful to Prof. Dong Kee Jeong from faculty of Biotechnology, for permitting collaboration work and providing bacterial test facility in his laboratory. I appreciate the impressive

skills of Dr. Raj Kumar Mongre on *E. coli* growth and testing mechanisms for non-treated and plasma treated water. The growth of bacteria, agar plate's preparation, optical density measurement and *E. coli* preservations would never had been possible without his cooperation.

I am highly grateful to Mr. Shahid Aziz from advance mechatronics laboratory for his guidance to learn very useful design skills using pro-engineer software. I am thankful to the other members of mechatronics laboratory including Dr. Zubair, Ghayas Siddiqui and Memoon Sajid for useful technical discussion on computing and chemistry. I am grateful to Mr. Waseem Abbas for providing matlab codes to evaluate electrical parameters of underwater plasma discharge. He developed smart codes that made my work easy to analyze the large amount of data points quickly and effectively. For social gathering I would like to highlight members of international student's organization for providing such fascinating events during hard time of doctoral course. I am thankful to my roommate Ghayas siddiqui for having such nice time and encouragement during stay at university dormitory. I am thankful to my lab mate Mr. Shahin-ur-Rahman who joined our laboratory as master's student, for useful discussion on electrical systems and for assistance in electrical wiring while working with 3-phase system. I am highly grateful to my Korean friends for their valuable cooperation. Special thanks to Mr. Jong Keun Yang for his efforts and participation in all aspects during my research especially documents preparations and other technical aspects. I would like to mention all Pakistani students for such a fascinating time at Jeju national university.

Lastly, I would like to mention to those who are actually behind the motivation an inspiration for me for this long doctoral program that is my family, their love and encouragement. For my parents who raised me with a love and supported me in all my pursuits. For my son Huzaifa Waqar who always watched me on Skype and waited for my degree completion since he was four months old when I left him, up-to four and half years of his age. This time will never come back in his life as I missed his childhood and he missed my love. I really appreciate tolerance of my wife and I have no words to explain her participation during this long and tough time. Her loving, supportive, encouraging, and patient attitude supported me during the final stages of this Ph.D. I am thankful to my younger brother

Bilal for his cooperation to start this Ph.D. course. Without his efforts and time that he gave me it was impossible to get attested documents from HEC, ministry of foreign affairs and Embassy of Republic of Korea.

Thank You

M. Waqar Ahmed

CONTENTS

List of Figures	v
List of Tables	xii
Abstract	xiii
Thesis outline	xvi
1. Underwater Plasma Discharge	1
1.1 What is plasma?	1
1.2 Introduction to underwater plasma discharges	4
1.2.1 <i>Literature review on plasma water treatment</i>	7
1.2.2 <i>Conventional methods of electrical breakdown in water</i>	8
1.3 Fundamentals of underwater plasma discharge	11
1.3.1 Electrical breakdown in gas phase	11
(a) <i>Townsend Breakdown mechanism</i>	11
(b) <i>Spark Breakdown Mechanism</i>	13
1.3.2 Electrical breakdown in liquid phase	14
(a) <i>Dense gas approximation</i>	14
(b) <i>Semiconductor Approximation</i>	15
1.4 Reactive species generated by underwater discharge	16
1.4.1 <i>OH· Radicals</i>	17
1.4.2 <i>Reactive oxygen</i>	18
1.4.3 <i>Reactive hydrogen</i>	18
1.4.4 <i>Ozone</i>	18
1.4.5 <i>Hydrogen peroxide</i>	20
1.4.6 <i>UV radiations</i>	20
1.4.7 <i>Shock waves</i>	21
1.5 Applications of underwater plasmas	21
2. Diagnostics Techniques	22
2.1 Electrical diagnostics	22
(a) <i>Volt-Ampere characteristics curves</i>	23
(b) <i>Matlab codes</i>	25
2.2 Spectral diagnostics	27
(a) <i>Emission spectroscopy</i>	27
(b) <i>Absorption spectroscopy</i>	29

2.3 Imaging diagnostics	29
(a) <i>High speed camera photography</i>	29
(b) <i>Thermal camera photography</i>	30
2.4 Statistical diagnostics	31
(a) <i>Gaussian distribution functions</i>	31
(b) <i>Stark broadening</i>	31
(c) <i>Intensity ration method</i>	32
2.5 Diagnostics of oxidant species	33
(a) <i>OH radicals</i>	33
(b) <i>Hydrogen Peroxide</i>	33
(c) <i>Ozone</i>	33
(d) <i>Reactive hydrogen and oxygen</i>	34
2.6 Diagnostics of bacterial ineffectiveness	34
(a) <i>Heterotrophic plate counting (HPC)</i>	34
(b) <i>Optical density measurement (OD)</i>	35
3. Investigation of DC Underwater Capillary Discharge	37
3.1 Introduction	37
3.2 Experimental setup	38
3.3 Methodology	38
3.4 Results and Discussions	41
3.4.1 Electrical diagnostics	41
3.4.2 Spectral diagnostics	48
(a) <i>Emission Spectrum</i>	48
(b) <i>Gaussian function and OH· radicals</i>	50
3.4.3 Imaging diagnostics	51
(a) <i>High speed camera imaging</i>	51
(b) <i>Thermal camera imaging</i>	52
3.5 Conclusion	54
4. Appraisal of Plasma Electron Temperature and Number Density and Their Effect on Chemical Reactive Species in Negative DC Capillary Discharge	55
4.1. Introduction	55
4.2. Materials and Methods	57
4.3. Results and Discussion	59
4.3.1 <i>Electrical results</i>	59

4.3.2	<i>Hydrogen Emission Profiles</i>	62
4.3.3	<i>Calculation of Electron Temperature (T_e)</i>	65
4.3.4	<i>Calculation of Electron Number Density (N_e)</i>	67
4.3.5	<i>Effect of Electron Temperature on Chemical Reactive Species</i>	70
i.	<i>\cdotOH Radicals</i>	70
ii.	<i>Hydrogen Peroxide</i>	73
iii.	<i>Ozone</i>	76
4.4	Conclusions	79
5.	High Frequency Underwater Capillary Discharge	80
	5.1 Diagnostics of Argon Injected Hydrogen Peroxide Added High Frequency Underwater Capillary Discharge	80
1.	Introduction	80
2.	Experiment set-up	82
3.	Results and Discussion	85
3.1	<i>Electrical Results</i>	85
3.2	<i>Spectral Results</i>	89
4.	Conclusions	92
	5.2 Effect of Water Conductivity on the Generation of OH\cdot Radicals in High Frequency Underwater Capillary Discharge	93
1.	Introduction	93
2.	Experiment-setup	95
3.	Methodology	97
4.	Results and Discussion	97
4.1	<i>Electrical Results</i>	97
4.2	<i>Spectral Results</i>	101
5.	Conclusions	104
6.	Large Volume Underwater Discharge	105
1.	Introduction	105
2.	Experiment set-up	106
3.	Results and Discussion	108
3.1	<i>Electrical Results</i>	108
3.2	<i>Spectral Results</i>	108
4.	Conclusions	110
7.	High Frequency Underwater Plasma Discharge Application in Antibacterial Activity	111
7.1	Introduction	111

7.2 Materials and methods	114
7.2.1 <i>E. coli</i> strains and growth conditions	114
(a) <i>Micro-well dilution coliform assay</i>	114
(b) <i>Agar-well diffusion coliform assay</i>	115
7.3 Experiment Set-up and methodology	115
7.4 Results and discussion	117
7.4.1 <i>Volt-Ampere characteristics</i>	118
7.4.2 <i>Spectral</i>	121
7.4.3 <i>Ozone Concentration</i>	123
7.4.4 <i>Plasma discharge inhibits rapid propagation and inactivation of E. coli.</i>	122
7.5 Conclusions	130
8. Summary	132
Acknowledgements	135
References	136
Publications	148

List of Figures

Fig.1.1 Transformation stages of plasma formation under influence of heating	2
Fig.1.2 Some typical natural plasma exist in (a) sun (b) moon (c) galaxies (d) Aurora (e) atmospheric electricity	2
Fig.1.3 Range of upper atmosphere plasmas	3
Fig.1.4 Schematic of plasma application in various fields	4
Fig.1.5 Electric polarization of water molecules	7
Fig.1.6 Multichannel discharge generated between two stainless steel electrodes	9
Fig.1.7 Schematics of some typical electrodes configurations	9
Fig.1.8 Schematics of different electrode configurations for bubble discharge	10
Fig.1.9 Flow chart of Theoretical models in underwater plasma discharge mechanism	12
Fig.1.10 Electron Avalanche process	13
Fig.1.11 Mechanism of streamer propagation	14
Fig.1.12 Schematic of charge transformation in (a) Semiconductors (b) In dielectric liquids under influence of high electric field	16
Fig.1.13 Ozone decomposition scheme in water and formation of resultant reactive species	19
Fig.1.14 Applications of underwater plasma discharge	21
Fig.2.1 (a) Typical IV curves of pulsating underwater discharge with DC power source	23
Fig.2.1 (b) Typical IV curves underwater discharge with high frequency power source	24
Fig.2.2 Processing scheme of spectral diagnostics	27
Fig.2.3 Typical emission spectrum of underwater plasma discharge	28
Fig.2.4 Schematic of plasma absorption spectroscopy	29
Fig.2.5 (a, b) Images of bubbles and discharge taken by fast speed camera	30
Fig.2.6 Typical discharge image taken by thermal camera	31
Fig. 2.7 A typical Agar plate for bacteria count also known as HPC method	35

Fig. 2.8 Schematic of optical density measurement	36
Fig.3.1 (Color online) Schematic view of the experiment set-up	40
Fig.3.2 (Color online) Visual view of capillary discharge	40
Fig.3.3 (Color online) IV characteristics of air-injected discharges with (a) 1-mm and (b) 2-mm gap distances	42
Fig.3.4 (Color online) IV characteristics of oxygen-injected discharges with (a) 1-mm and (b) 2-mm gap distances	42
Fig.3.5 (Color online) Average time interval as a function of the gas flow rate for two different gap distances: (a) air and (b) oxygen	44
Fig.3.6 (Color online) Breakdown voltage as a function of the gas flow rate at two different gap distances: (a) air and (b) oxygen	45
Fig.3.7 (Color online) Average energy per pulse as function of gas flow rate for 1-mm and 2-mm gap distances (a) air and (b) oxygen	46
Fig.3.8 (Color online) Average pulse duration as a function of the gas flow rate for 1-m and 2-mm gap distances: (a) air and (b) oxygen	47
Fig.3.9 (Color online) Average power of the pulses occurring per second as a function of the gas flow rate for 1-mm and 2-mm gap distances: (a) air and (b) oxygen	47
Fig.3.10 (Color online) Emission spectrum of OH radicals for (a)1-mm and (b) 2-mm inter electrode gaps and various air injection rates	49
Fig.3.11 (Color online) Emission spectrum of the OH radicals for (a) 1-mm and (b) 2-mm inter electrode gaps and various oxygen injection rates	49
Fig. 3.12 (Color online) Concentration of OH radicals by using a Gaussian function for various gas injection rates and two different inter electrode gap distances: (a) air injection and (b) oxygen injection	50
Fig.3.13 (Color online) Oxygen injected discharges	51
Fig.3.14 (Color online) Air injected discharges	52

Fig. 3.15 The discharge structure obtained by thermal camera at 2mm inter-electrode gap distance for various air injection rates	53
Fig. 3.16 The discharge structure obtained by thermal camera at 2mm inter-electrode gap distance for various oxygen injection rates	54
Fig. 4.1 Experimental Setup for underwater capillary Discharge	58
Fig. 4.2 Visual view of the discharge	58
Fig. 4.3 (Color online) Typical Volt-Ampere characteristics of the gas injected discharge	60
Fig.4.4 (Color online) Break down voltage (a) 1-mm and (b) 2-mm gap distance	61
Fig.4.5 (Color online) variations in power of discharge pulses under different gas injection rates (a) 1- mm and (b) 2mm gap distance	61
Fig.4.6 (Color online) Emission spectrum of hydrogen lines at various argon injection rates. (a) 1- mm and (b) 2-mm inter-electrode gaps	62
Fig.4.7 (Color online) Emission spectrum of hydrogen lines at various air injection rates. (a) 1-mm and (b) 2-mm inter-electrode gaps	63
Fig.4.8 (Color online) Emission spectrum of hydrogen lines at various oxygen injection rates. (a) 1-mm and (b) 2-mm inter-electrode gaps	64
Fig.4.9 (Color online) Electron Temperature for various gas injection rates and power of discharge pulses at 1-mm and 2-mm gap distances	66
Fig.4.10 (Color online) Electron number density under different experimental conditions and inter-electrode gap distances	69
Fig.4.11 (Color online) Emission spectrum of OH radicals for various argon injection rates at (a) 1-mm and (b) 2-mm inter electrode gap distances	71
Fig.4.12 (Color online) Emission spectrum of OH radicals for (a) 1-mm and (b) 2-mm inter electrode gaps and various air injection rates	72
Fig.4.13 (Color online) Emission spectrum of OH radicals for various oxygen injection rates at (a) 1-mm and (b) 2-mm inter electrode gap distances	73

Fig.4.14 (Color online).Concentration of OH radicals by using Gaussian function (a-c) Electron temperature dependent (d-f) Electron number density dependent for 1 mm and 2 mm gap distances.	74
Fig.4.15 (Color online) (a) Absorption spectrum of pertitanic acid yellow complex solution (b-d) electron temperature dependent hydrogen peroxide concentration.	75
Fig.4.16 (Color online) (a-c) Electron Number density dependent Hydrogen peroxide concentration.	76
Fig.4.17 (Color online) (a) Absorption spectrum of ozone containing water sample (b-d) electron temperature dependent ozone concentration.	78
Fig.4.18 (Color online) Electron Number density dependent ozone concentrations.	79
Fig.5.1.1(Color online) Schematic view of experiment set-up.	84
Fig. 5.1.2(Color online) Visual view of the capillary discharge.	84
Fig. 5.1.3(Color online)Typical Volt-Ampere characteristics of non-gas injected discharge for different amounts of hydrogen peroxide addition (a) 0ml/l H ₂ O ₂ (b) 0.05 ml/L H ₂ O ₂ (c) 0.20 ml/L H ₂ O ₂ (d) 0.35 ml/L H ₂ O ₂ .	86
Fig. 5.1.4 (Color online)Typical Volt-Ampere characteristics of 500 sccm Ar gas injected discharge for different amounts of hydrogen peroxide addition (a) 0ml/l H ₂ O ₂ (b) 0.05 ml/L H ₂ O ₂ (c) 0.20ml/L H ₂ O ₂ (d) 0.35 ml/L H ₂ O ₂ .	86
Fig. 5.1.5 (Color online). Variation in breakdown voltage for different Ar injection rates and various hydrogen peroxide addition.	88
Fig. 5.1.6 (Color online). Variation in electrical power of discharge pulses for different Ar injection rates and various hydrogen peroxide additions.	88
Fig. 5.1.7 (Color online). Variation in frequency of discharge pulses for different Ar injection rates and various hydrogen peroxide additions.	89
Fig. 5.1.8 (Color online). Average time difference between the occurrence of discharge pulses for different Ar injection rates and various hydrogen peroxide additions.	89

Fig. 5.1.9 (Color online). Emission Spectrum of •OH radicals and other reactive species for different Ar injection rates and various hydrogen peroxide addition (a) 0ml/l H ₂ O ₂ (b) 0.05 ml/L H ₂ O ₂ (c) 0.20 ml/L H ₂ O ₂ (d) 0.35 ml/L H ₂ O ₂ .	91
Fig. 5.1.10 (Color online). Variation in concentration of •OH radicals for different Ar injection rates and various hydrogen peroxide addition.	92
Fig. 5.2.1(Color online) Schematic view of experiment set-up.	96
Fig. 5.2.2 (Color online) Visual view of the capillary discharge.	96
Fig. 5.2.3 (Color online) Typical Volt-Ampere characteristics for non-gas and Argon injected values at different gap distances	98
Fig. 5.2.4 (Color online) Variation of breakdown voltage at various conductivities and different inter-electrode gaps (a) No gas injection (b) 200sccm Argon injection.	99
Fig. 5.2.5 (Color online) Variation in average electrical power of discharge pulses at various conductivities and inter-electrode gaps (a) Non-gas injected (b) 200sccm Argon.	100
Fig. 5.2.6 (Color online) Emission spectrum of OH• radicals at various conductivities for (a) 1-mm (b)-10mm Inter-electrode gaps without argon gas injection.	102
Fig. 5.2.7(Color online) Emission spectrum of OH• radicals at various conductivities for (a) 1-mm (b) 10-mm inter-electrode gaps at 200 sccm argon gas injections.	102
Fig. 5.2.8 (Color online) Concentration of OH• radicals for various conductivities and different inter-electrode gaps (a) non gas injection (b) 200sccm Argon injection.	103
Fig. 6.1 Schematic diagram of parallel capillaries experimental set-up.	107
Fig. 6.2 (Color online) (a) Typical volt-ampere characteristics curve (b) Variation in Breakdown Voltage; for parallel capillaries assembly.	108
Fig. 6.3 (color online) Emission Spectrum of Oxygen Injected capillary discharge.	109
Fig. 7.1 (Color online) Schematic view of experiment set-up.	116
Fig. 7.2 (Color online) Visual view of capillary discharge.	116
Fig. 7.3 (color online) Dependence of typical Volt-Ampere characteristics of High Frequency	

Underwater Plasma Discharges occurred in bubbles containing water without and with H₂O₂ addition on oxygen injected rate (rate of O₂-injection).

(a): rate of O₂-injection – 0 sccm, and H₂O₂ addition - 0 ml/L;

(b): rate of O₂-injection – 100 sccm, and H₂O₂ addition - 0.35 ml/L;

(c): rate of O₂-injection – 600 sccm, and H₂O₂ addition - 0.35 ml/L;

(d): rate of O₂-injection – 800 sccm, and H₂O₂ addition - 0.35 ml/L.

119

Fig. 7.4 Dependences of electrical parameters due to oxygen injected bubbles and increasing in power and in energy of discharge pulses on oxygen injection rate.

(a): variation in breakdown voltage in presence and absence of hydrogen peroxide addition;

(b): increasing in power of discharge pulses;

(c): increase in energy of discharge pulses.

120

Fig. 7.5 (color online) The typical optical emission spectra of reactive chemical

species useful for *E. coli* inactivation which have enhanced yield rate due to mixing H₂O₂ and O₂ and have been observed in High Frequency Underwater Plasma Discharges for various values of O₂ injection rates and H₂O₂ additions in water, accordingly, (a), (b), (c), (d), (e) and (f).

122

Fig. 7.6 Concentration of ozone (O₃) generated after discharge occurrence under different experimental conditions.

123

Fig. 7.7 Visual comparison of *E. coli* colonies concentration existence.

(a): High concentration of *E. coli* colonies in agar plate with pure *E. coli* Strain concentration too numerous to count (TNTC).

(b): Reduced to countable colonies after mixing 100 µl of strain to 1 liter water, before plasma treatment.

(c): the countable colonies after Plasma Treatment without oxygen injection and 0 ml/L H₂O₂; (d): the countable colonies after Plasma Treatment without oxygen injection and with 0.35ml/L H₂O₂.

125

Fig. 7.8 Typical results of ineffective action on *E. coli* by plasma treatment without any addition of hydrogen peroxide.

(a): after plasma treatment of pure *E. coli* strain concentration in water;

(b): after plasma treatment with 100 sccm O₂ injection;

(c): after plasma treatment with 400 sccm O₂ injection;

(d) after plasma treatment with 800 sccm O₂ injection.

126

Fig. 7.9 Typical examples of the effective inactivation of *E. coli* by plasma treatment in

discharges with the H₂O₂ -adding in water and injection of O₂.

- (a): after plasma treatment of pure *E. coli* strain concentration in water;
- (b): after plasma treatment with 100 sccm O₂ injection and adding of 0.35 ml/L H₂O₂;
- (c): after plasma treatment with 400 sccm O₂ injection and adding of 0.35 ml/L H₂O₂;
- (d) after plasma treatment with 800 sccm O₂ injection and adding of 0.35 ml/L H₂O₂. 127

Fig. 7.10 (color online) Dependences of the *E. coli* inactivation efficiency, η and the Kill rate, $\ln \frac{N}{N_0}$ (the reduction in *E. coli* colonies) versus the rate of O₂-injection in underwater plasma discharges with the add of H₂O₂ in water.

- (a): *E. coli* inactivation efficiency, η ;
- (b): the Kill rate of *E. coli* colonies. 129

Fig. 7.11 Typical images of untreated and treated water samples.

- (a): sample with Pure *E. coli* strain;
- (b): sample with untreated water containing *E. coli*;
- (c): sample with H₂O₂ mixed water containing *E. coli* which treated by plasma discharge without oxygen injection;
- (d): sample with H₂O₂ mixed water containing *E. coli* which treated by plasma discharge with oxygen injection. The oxygen injected and H₂O₂ mixed plasma discharge effectively sterilized water from *E. coli*. 129

Fig. 7.12 (Color online) The % of viable bacteria in water containing *E. coli* after its underwater discharge treatment versus the rate of oxygen injection for two conditions related to adding of hydrogen peroxide in the water. 130

List of Tables

Table 1.1 Redox potential of different chemical reactive species.	5
Table 5.1.1 The possible chemical reactions list that takes place when discharge occurs in liquid.	81
Table 5.1.2 Properties of selected species involved in advance oxidation process (AOP) are through electrical discharge in water discharge.	83
Table 5.2.1 Reactions considered in non-gas and Argon gas injected discharge.	94

Abstract

Formation of underwater plasma discharge has been an attractive avenue for the researchers since last few decades due to some rare and critical applications. Underwater plasma discharges have wide range of applications in environmental, biological, industrial and semi-conductor industry. The basic understanding of the physical and chemical characteristics of these underwater discharges is of extensive importance for their future applications and research. Due to the high dielectric constant of water the control on power consumption is first challenge for researchers working for liquid plasma. Various methods were adopted in past to reduce power consumption and to generate plasma in large volume of water effectively. Among them use of different electrode assemblies with pulse power source, high frequency power sources, and wave-heated sources were adopted to generate plasma at low power consumption. Using some electrical, spectral and imaging diagnostic techniques some work has been done on the characterization of liquid plasmas.

The aim of this research work was to generate flowing water discharge at low power consumption by injecting stream of gas. Moreover the determination of best experimental conditions to yield high concentration of reactive species and their advance antibacterial application was another objective of this research work.

To achieve these objectives a flowing water capillary discharge method has been adopted in this research for the diagnostics and applications of underwater plasma discharge. The discharge was created in a quartz tube with two different power sources, negative DC and high frequency AC. The tungsten electrodes were installed in pin-pin electrode assembly and discharge was created in flowing water. In order to reduce the power consumption gas bubbles were introduced in capillary tube. Three different gasses argon, oxygen and air were used in all experiments to compare the electrical, spectral and chemical effects of each of them. Two types of water was used, a tap water and high conductivity water to compare the physical and chemical characteristics of two types of water. Hydrogen peroxide was also mixed in water for different amounts to observe its effect on the yield rate of oxidant species. The observed oxidant species were $OH\cdot$ radicals, ozone (O_3), hydrogen peroxide, reactive hydrogen

and reactive oxygen. Various spectral and chemical mechanisms were adopted for the determination of these oxidant species generated by underwater plasma discharge.

In negative DC discharge air and oxygen injected discharge was compared. The effect of each gas on electrical parameters like breakdown voltage, frequency, time between the occurrence of discharge pulses, energy per discharge pulse and power of discharge pulses were determined and compared. The effect of each gas on the yield rate of $OH\cdot$ radicals has been explored. Oxygen was proved to be more efficient compared to air from above mentioned prospects.

Electron temperature and number density was determined in argon air and oxygen injected negative DC discharge and their effect on the concentration of oxidant species including $OH\cdot$ radicals, ozone and hydrogen peroxide has been explored. A direct relation of electron temperature and oxidant species was determined.

In high frequency capillary discharge the effect of hydrogen peroxide addition along with argon injection for tap water and water with various conductivities was performed. In tap water the effect of hydrogen peroxide addition and argon injection on the electrical and spectra characteristics was determined. While in case of higher conductivities than tap water the effect of water conductivity on the electrical and spectral characteristics were explored. Hydrogen peroxide was observed ineffective for electrical parameters of discharge like break down voltage, power and frequency of discharge pulses while it effected highly the concentration of $OH\cdot$ radicals. High conductivity of water reduced required breakdown voltage and enhances the concentration of $OH\cdot$ radicals.

On the basis of DC and high frequency AC underwater capillary discharge conclusions large volume flowing water sterilization was obtained by plasma discharge at low input power. Twenty capillaries were connected in parallel and high flow rate (0.2L/min) of water was treated by high frequency power source. Total 4 L/min water sterilization was obtained by this mechanism.

Based on spectral and electrical diagnostics of underwater capillary discharge, its application on the antibacterial activity (Gram-negative *E. Coli*) was observed. The oxygen injected and hydrogen peroxide added capillary discharge was adopted for the disinfection of bacterial effect in drinking

water. The addition of oxygen and hydrogen peroxide mixing resulted in high yield rate of ozone, $OH\cdot$ radicals, hydrogen peroxide, reactive hydrogen and reactive oxygen, which played a vital role in bacterial disinfection.

Thesis Outline

The outline of the different chapters of this thesis is as follow:

Chapter 1 represents a brief introduction of underwater plasma discharge. The mechanisms of discharge occurrence, the resultant of underwater discharge in form of oxidant species have been explained. The application area of underwater plasma discharge has been mentioned.

Chapter 2 discusses the diagnostic techniques of underwater plasma discharge adopted in this research. Spectral, electrical, imaging, statistical and computing methods are explained in this chapter.

Chapter 3 demonstrates the diagnostics of negative dc flowing water capillary discharge with air and oxygen injection. A comparison of air and oxygen injection in underwater discharge with respect to electrical parameters and concentration of $OH\cdot$ radicals has been explored.

Chapter 4 illustrates a relation between physical and chemical characteristics of negative dc; gas injected (argon, air, oxygen) flowing water capillary discharge. The electron number density and electron temperature were calculated and their effect on the oxidant species ($OH\cdot$, H_2O_2 and O_3) was presented.

Chapter 5 explains the characteristics of high frequency alternating current voltage flowing water capillary discharge. This chapter is composed of three parts. In first part the effect of argon injection and hydrogen peroxide addition on the generation of $OH\cdot$ radicals was presented, while in second part of this chapter, effect of water conductivity on electrical spectral and on effect on the yield rate of $OH\cdot$ radicals were explained.

Chapter 6 represents the sterilization of large volume of water. Multiple capillaries were joined in parallel, to sterilize large volume of water quickly. Since one capillary could sterilize water at flow rate of maximum 0.2 L/min, so twenty capillaries were connected in parallel to sterilize 4 L/min flowing water. The electrical and spectral results are presented in this section of large volume sterilization.

Chapter 7 presents the application of underwater capillary discharge in antibacterial activity. The effect of oxygen injection and hydrogen peroxide addition on the inactivation of gram negative *Escherichia coli* (*E. coli*) was explored.

Chapter 8 gives the conclusions of this thesis for various diagnostics and application background.

1. Underwater Plasma Discharge

1.1 What is plasma?

Else than solid liquid and gas there exists another state of matter known as “Plasma” named by Irvin Langmuir in 1920’s [1]. “A quasi-neutral gas, consisting of charged and neutral particles, exhibiting collective behavior is called plasma” [2]. Before concept of plasma three states of matter were considered known as solid liquid and gas. Solids are state of matter where atoms are arranged in specific positions, and they cannot move inside the bulk of material, but they can oscillate about their mean positions. When temperature is applied to the solids (above their melting point) these solids transformed to the liquid state. In liquid state of matter, the atoms and molecules venders inside the bulk of material, as they have enough kinetic energies, which can overcome the potential energies due to mutual interactions. Due to the existence of surface potential experienced by liquid molecule they cannot leave the surface of the liquid. Now if further heating is applied to the liquid (above or equal to their vaporization temperature) these liquids convert into their gaseous form. In this gaseous state the molecules have enough kinetic energy that they can move freely and some sort of container or vessel is required to enclose that gas [3]. Further if some sort of energy or heating ($>10^3$ Kelvin) either from electrical field, electromagnetic (EM) waves, laser or from any RF source is applied, then gas will be ionized and this ionized gas is called “*PLASMA*” [4]. This ionized (partially or in ideal case fully ionized) gas contains charged and neutral particles. Fig. 1.1 shows the schematic of transformation process.

Two main sources of plasma exists 1). Natural plasma. 2). Laboratory plasma. In nature plasma exists in sun, moon, galaxies and stars [5]. Fig. 1.2 represents some typical forms of upper atmosphere plasmas [6]. The range of upper atmospheric plasmas depends upon electron density. Fig. 1.3 represents the range of typical upper atmosphere plasmas [7].

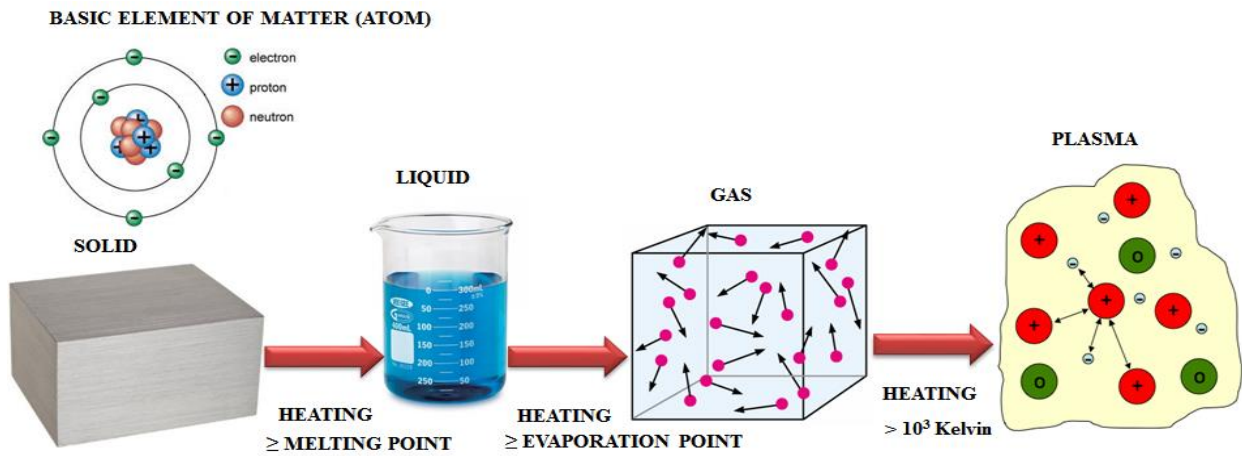


Fig. 1.1 Transformation stages of plasma formation under influence of heating.

In laboratory some plasma can also be generated by ionizing gas at atmospheric pressure or at low pressure by applying electric field across the electrodes. By heating gas through electric fields, EM waves, RF waves or laser can cause generation of plasmas.

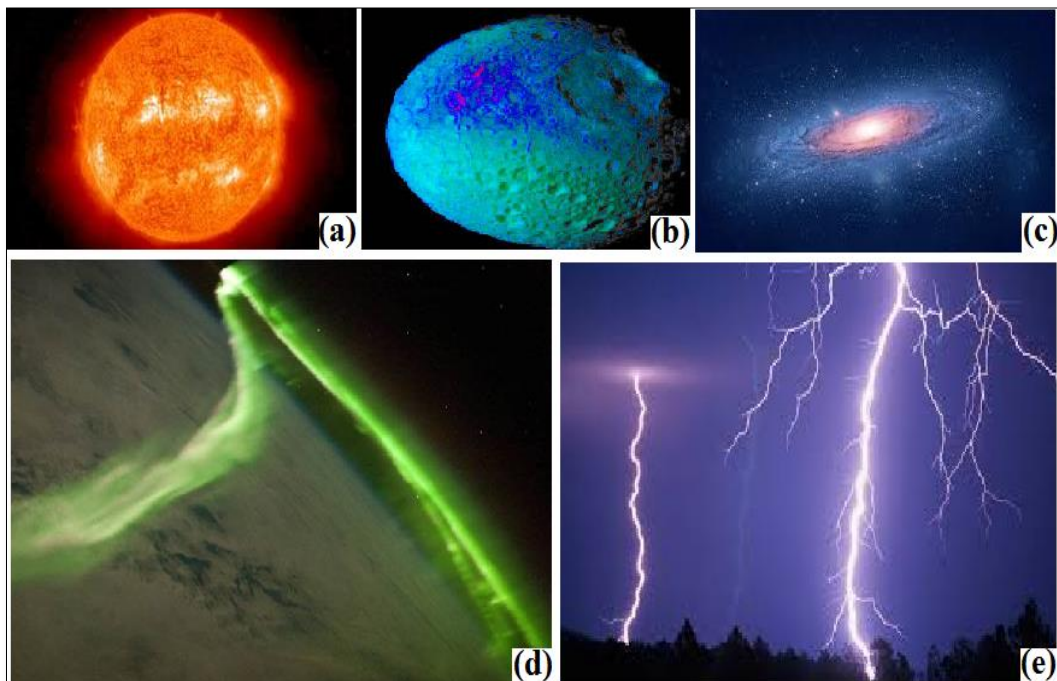


Fig. 1.2 Some typical natural plasma exist in (a) sun (b) moon (c) galaxies (d) Aurora (e) atmospheric electricity.

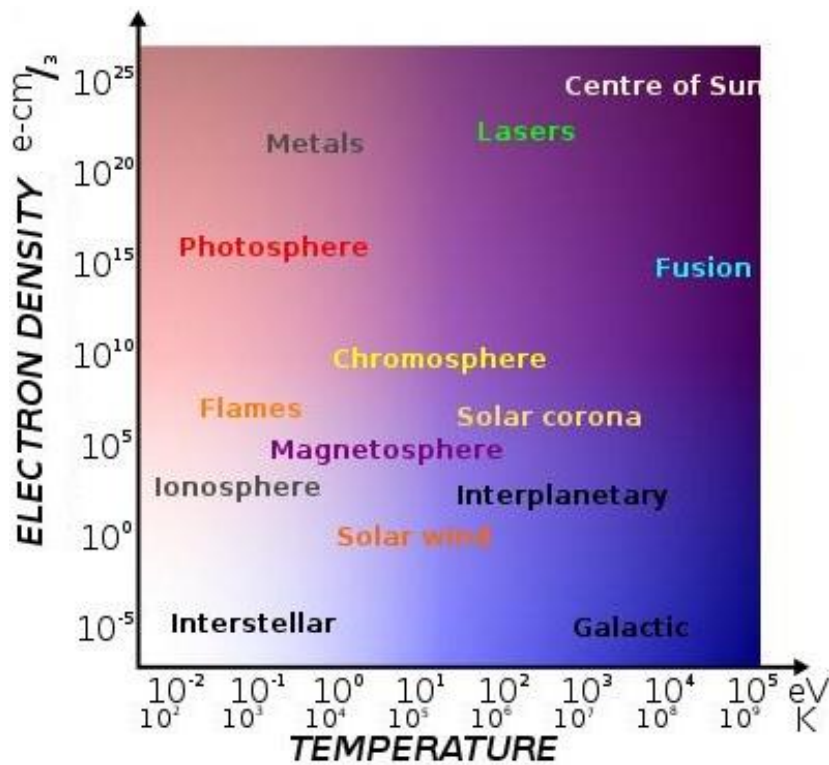


Fig. 1.3 Range of upper atmosphere plasmas.

The laboratory plasma can be induced in gas, vacuum or within liquid also. The technological or laboratory plasmas can be divided into two types [8]:

- 1). Thermal plasmas
- 2). Non-thermal plasmas.

Thermal plasmas have $T_e = T_{i, n}$ (where T_e represents the electron temperature and $T_{i, n}$ are heavy particle temperature like ions and neutral atoms). In the core of the plasma these temperatures can reach values up to 10^3 K and the gas is highly ionized. The characteristic of different excited states gave a specific property to the active species like atoms. Atmospheric pressure non-thermal plasmas have a very high electron temperature T_e , while that of heavy particles the $T_{i, n}$ remains at the local areas. A small density and low degree of ionization exists as well. The electrons and ions never achieve local thermodynamic equilibrium, which is the reason why gas remains at room temperature or very slightly above it.

Plasmas (either high temperature or low temperature) have wide range of various applications. Plasma can be generated in different media like gas, vacuum, solid and liquid. Fig. 1.4 shows schematic diagram of plasma applications in various fields [9].

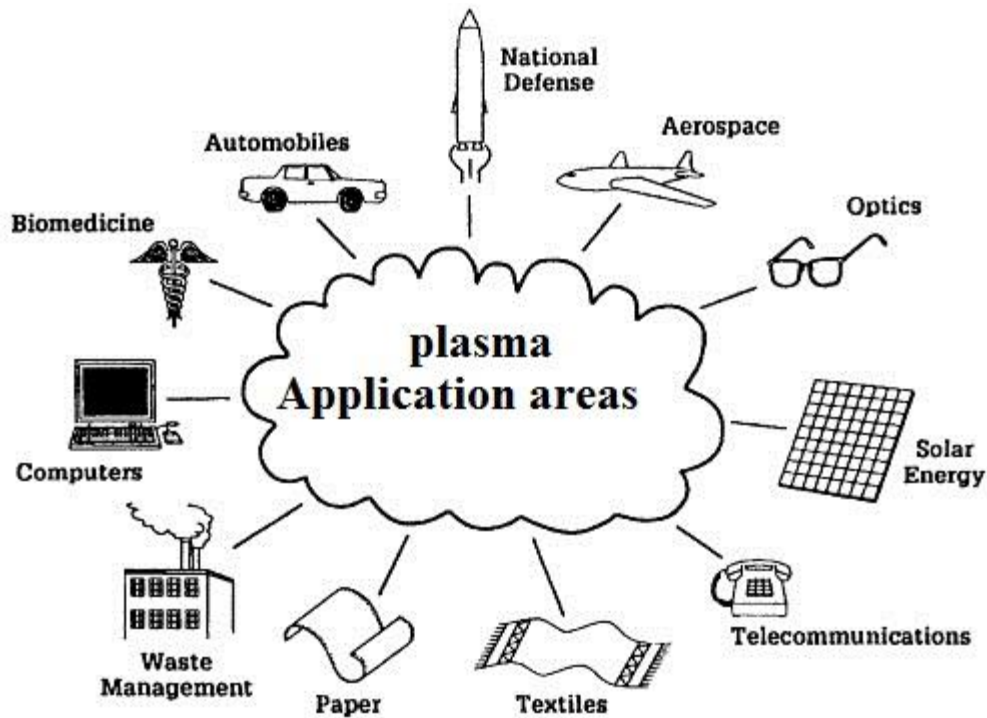


Fig. 1.4 Schematic of plasma application in various fields.

In this research we will focus on the diagnostics and applications of underwater plasma discharge.

1.2 Introduction to underwater plasma discharges

The disinfection of water and wastewater through plasma processing has become an attractive avenue for plasma researchers due to its maximum disinfection rate ($\sim 99.6\%$) and minimum treatment time (~ 8 seconds) [10].

The increases in the population and industrial activities have caused an increase in chemical pollutants and harmful species (dyes, phenol, benzenes, organic pollutants, and microorganisms) in aqueous systems.

Initially, chemical methods like chlorination were adopted for water disinfection and to rid water from its undesirable odor. This method, however, requires a large treatment time and results in a lower disinfection rate. Moreover, such disinfection methods generate some harmful ingredients, such as N-

nitrosodimethylamine (NDMA), trihalomethane (THMS), and halo acetic acids (HAAs), which cause rectal cancer and increase the risk of miscarriage as well as birth defects and fetal growth in women [11]. These chemicals also severely affect the human eyes and brain [12]. All these factors reduce the effectiveness of the chlorination process. The advanced oxidation processes (AOPs) were thus developed to replace the chlorination method. In AOPs, chemical, electrical, or radiation energy was used for generating highly reactive oxidants that cause water disinfection, and among these oxidants, the $OH\cdot$ radicals have been proven to be the most effective for water sterilization because of their large redox potential (2.80 V) [13]. Table 1.1 shows the redox potentials of different chemical species. The major AOPs for water treatment and for generating a large amount of $OH\cdot$ radicals are ultraviolet (UV) radiation, ozone treatment, hydrogen-peroxide (H_2O_2) treatment, and treatments with various combinations of H_2O_2 , UV, and ozone [14].

Oxidant Species	Redox Potential (Volts)
Hydroxyl Radicals	2.80
Ozone	2.07
Hydrogen Peroxide	1.78
Permanganate	1.69
Chlorine dioxide	1.69
Chlorine	1.36
Oxygen	1.23

Table 1.1. Redox potential of different chemical reactive species.

The AOP's also having some disadvantages. UV radiation can sterilize industrial water, but its efficiency for a large amount of water is too low, especially in flowing water [15]. Ozone (O_3) has also been proven to be a powerful disinfectant that destroys microorganisms through direct oxidation, but it is less popular than the other disinfectants because ozone equipment is expensive and ozone can cause damage if its dose is uncontrolled. The combination of H_2O_2 and O_3 also acts as a water disinfectant source as together they produce $OH\cdot$ radicals that are strong disinfectants [16]. Their combination, however, requires a special storage arrangement and deteriorates with time, which has made it also less popular than the other existing disinfectants. The combinations of ozone treatment and UV radiation and of UV radiation and hydrogen peroxide treatment also generate $OH\cdot$ radicals, but the water

turbidity affects the $OH\cdot$ radicals' production rate [17, 18]. By means of ultrasound in water, the cavitation effects can create micro bubbles. As a result of the implosion of these micro bubbles, hot plasma can be generated in their interior, which causes the generation of $OH\cdot$ radicals [19]. This process, however, has also been proven to be less efficient because of it has low energy efficiency and also it requires the use of supplemental oxidants like UV, ozone, or hydrogen [20]. Water can also be disinfected by striking it directly with a high-energy beam of electrons with energies of several MeV [21], but the electron range limits the thickness of the water layer that can be treated. Membranes also used in water disinfection [22], but the requirement for continuous cleaning and replacement reduces their use. Underwater plasma discharge share the potential to overcome all these limitations of the advanced oxidation processes; although compared to gas discharges, the physics of underwater discharge is very complicated, and many aspects of it are still largely not understood [23]. Due to their potential in solving several technological problems, however, such as in the field of water cleaning, underwater plasmas consisting of streamers (both positive and negative); are attracting much interest [24]. A plasma discharge in water is based on the following two theories [25]:

(1) The electron theory, according to which the water molecules are ionized and dissociated by a strong applied electric field and the plasma that is generated; and (2) The thermal (bubble) theory, according to which liquid is strongly heated by the passing current; thus, micro bubbles are generated, a potential gradient occurs inside the bubbles, and a discharge is ignited. The contribution of both the bubbles and electrons causes the breakdown of the liquid, the dissociation of the water molecules, and the generation of $OH\cdot$ radicals and other reactive species. The bubbles can also be induced by injecting a stream of gas from external source. When electrical energy is used for generating plasma, the applied electric field dissociates the water molecules through a four-step electrical polarization process, as shown in Fig. 1.5.

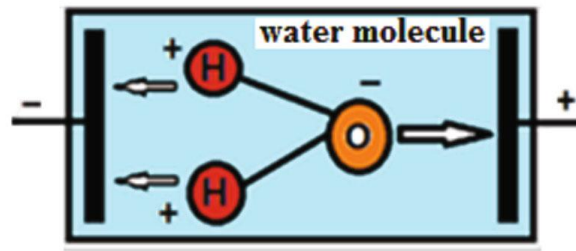


Fig 1.5. Electric polarization of water molecules.

In the first step, opposite polarities are applied across two electrodes. In the second step, the water molecules become electrically charged. In the third step, due to electric polarization, the water's stability is weakened by the hydrogen and the oxygen atoms. Finally, in the fourth step, due to the existing voltage, the attraction to the water molecules splits up the water molecules into atoms and produce various reactive radicals ($OH\cdot$, H, O, and HO_2), as well as molecular species like H_2O_2 , H_2 , and O_3 [26]. Depending upon the applied voltage, the type of applied voltage (pulse or continuous, DC or AC), and the existence of an opposite polarity attraction, the electric polarization continues. The intense electric field kills only the microorganisms, but the taste and the nutrient content of the water remain invariable [27]. The expansion of the plasma in the surrounding water causes the generation of shockwaves with a pressure amplitude on the order of hundreds of mega Pascal. These shockwaves also participate in the generation of reactive species through electrohydraulic cavitation [28]. All these processes participate in water disinfection and other environmental applications.

1.2.1 Literature review on plasma water treatment

The research is under process since last few decades. Many research groups participated so far in liquid discharges; an overview is given here. Historically the electrical engineers first time studied the plasma discharge in liquids [29, 30]. Ham and Balaster in 1973 [31], Ohgiyama, and Clements in 1996 [32], Sato and Clements in 1999 [33] studied about partial electrical discharge and arc or spark discharge. The process of increase in time lag to water break down with increasing pressure through bubble mechanism in sub-microsecond discharge was studied by Jones and Kunhardt in 1994,1995 [34]. The cavitation mechanism of discharge in bubbles was determined by Beroual, Zahn and Badent in 1993 and 1998 [35]. The electronic process inside bubbles generated by any mechanism with in

water was also studied by Akiyama in 2000 [36]. The process of bulk heating via ionic current, evaporation process and streamers propagation was studied by Lisitsyn et al. in 1999 [37]. The generation of ultra violet (UV) radiations, shock waves generation and formation of thermal plasma channel was studied by Sunka et al. in 1999 [38] and Lee et al. in 2003. The electric breakdown fields of megavolts per centimeter have been reported by Sato et al. in 2006 [39]. The generation of ultra violet (UV) radiations, reactive species and shock waves simultaneously were reported by B. R. Locke et al. in 2006 [40]. About the physics of discharge, chemical reactions taking place in discharge and different kinds of discharge were reported by Bridgeman and Leys in 2009 [41].

Since then and currently several groups around the world are actively involved in underwater plasma discharge and discharge in direct liquid chemicals for advance applications in various fields.

1.2.2 Conventional methods of electrical breakdown in water

Several methods have been reported so far for creating discharge in water through different electrodes configurations and various power sources. Fig. 1.6 represents discharge generated between two stainless steel disc electrodes having a dielectric layer [42]. Fig. 1.7 represents various electrode assemblies used for generating plasma discharge in water [42].

The generation of discharge in micro bubbles either generated by ohmic heating or by external gas injection is of large interest due to less dielectric constant of gas inside bubbles.

Fig. 1.8 represents some typical examples of electrode configurations and discharge generating mechanism inside bubbles and liquid medium simultaneously [42].

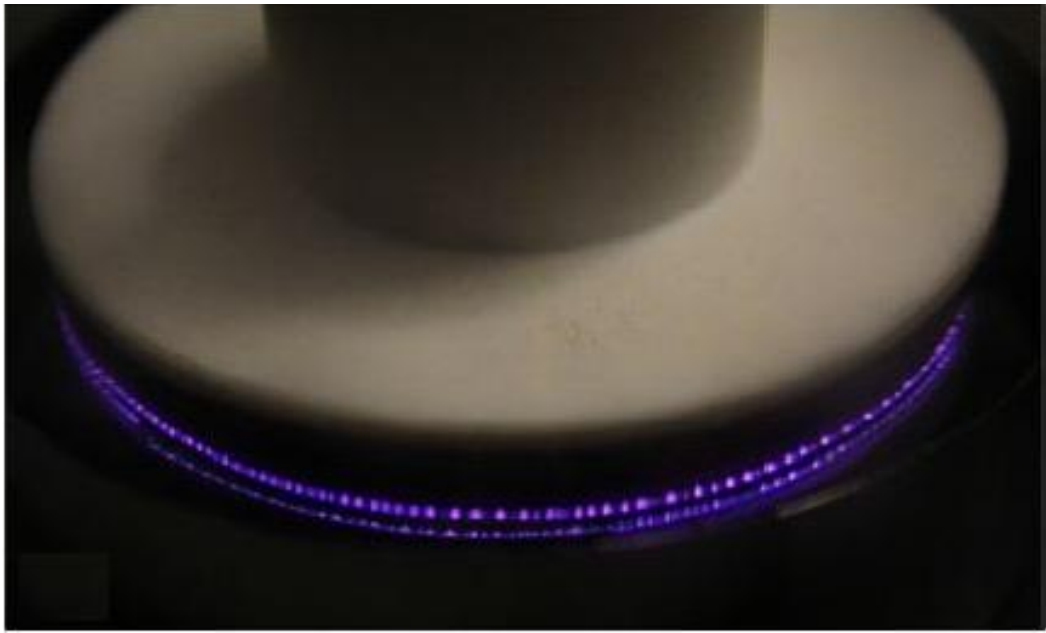


Fig. 1.6 Multichannel discharge generated between two stainless steel electrodes (Yang, Kim et al. 2011a).

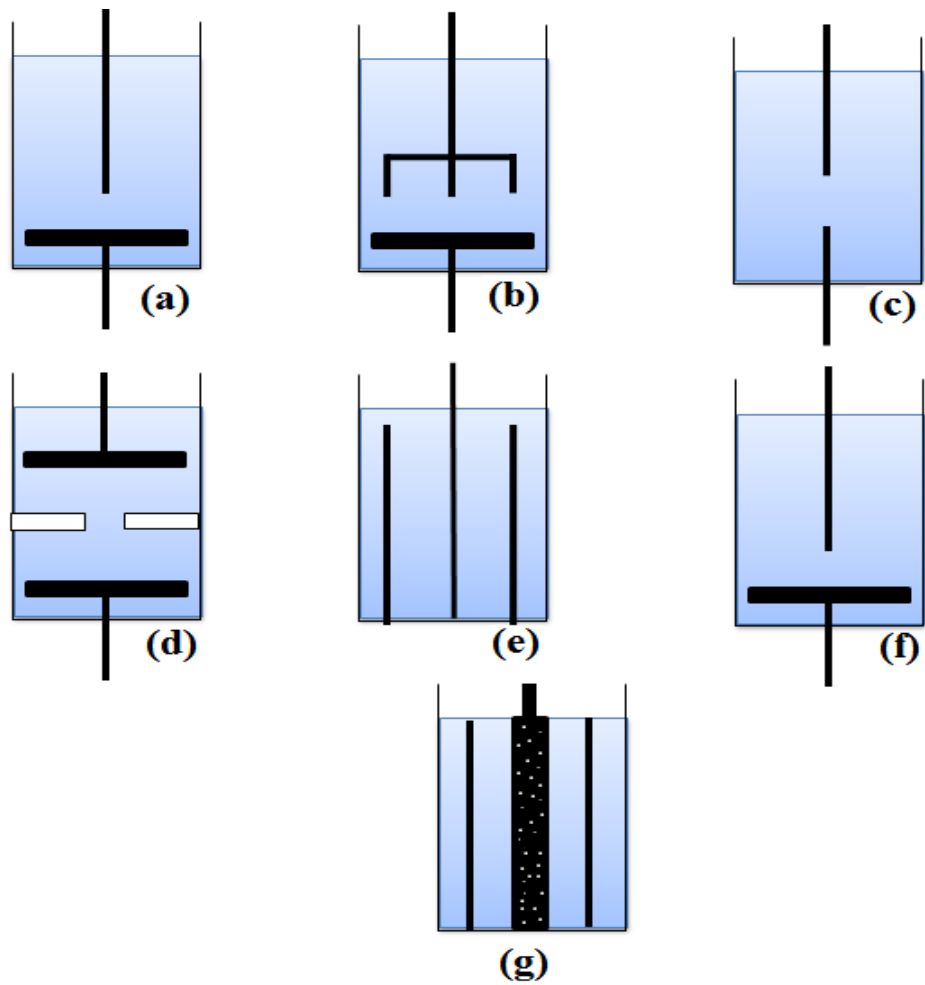


Fig. 1.7 Schematics of some typical electrodes configurations

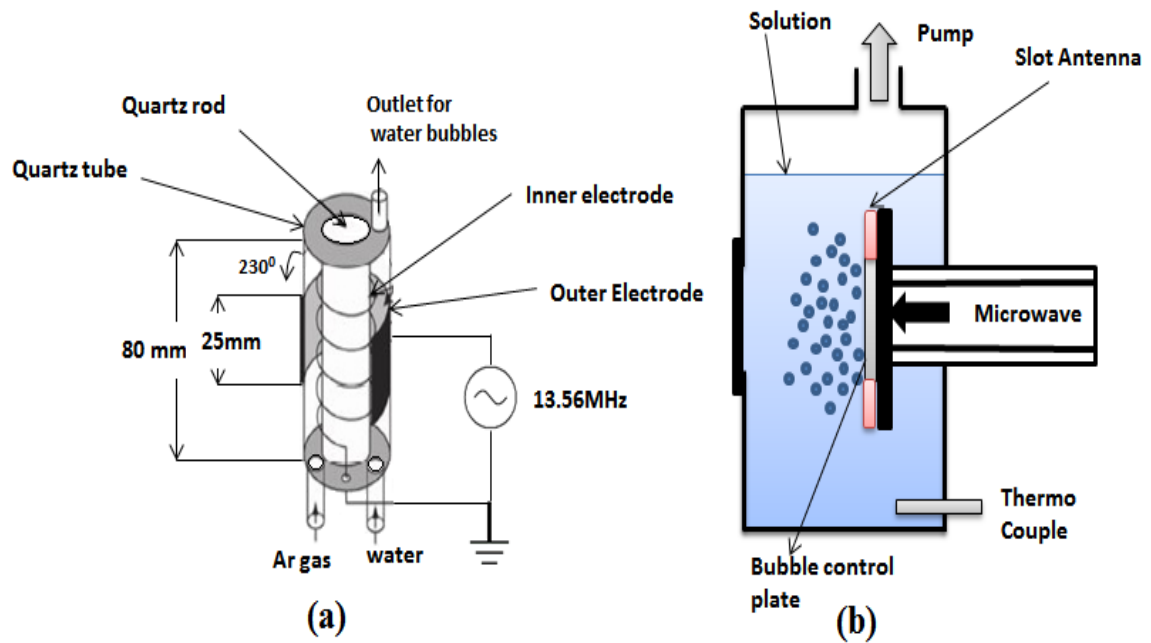


Fig. 1.8 Schematics of different electrode configurations for bubble discharge [42].

Due to high dielectric strength of water, high voltage and high power is needed for generating discharge in water. The high power consumption makes underwater plasma discharge an expensive technique for various applications and disadvantageous edge. To overcome this problem bubbles are usually introduced in water and at comparatively low voltage plasma can be induced inside these bubbles, whose implosion participates in occurrence of discharge with in water. The bubbles can be induced by various mechanisms, including heating of water by high power and generation of micro bubbles due to joule's heating effect, that will make the temperature of liquid too high, which is often undesirable specially for applications where low temperature is needed. For such conditions, non-thermal plasma can be generated by the injection of gas externally to generate bubbles in liquid and to induce plasma within bubbles at liquid gas interface. The injection of external gas not only proved useful for generating low power plasma but also depending upon the characteristics of the injected gas, the chemical characteristics can be controlled. Also generation of bubbles by wave heating and sound cavitation process are more familiar methods for inducing bubbles and discharge creation within that bubbles. The process of bubbles generation and discharge creation within these bubbles

drastically reduced the power consumption problem. Moreover use of high frequency voltages, radio frequency (RF) heated plasmas also proved effective for large volume discharge creation. Multi-phase input (3-phase to 12-phase) alternating current (AC) voltages also effectively reduced the power consumption problem [43].

In this research, due to flexibility of use of many capillaries in parallel, we adopted capillary discharge method having pin-pin electrodes assembly for research purpose, with external gas injection. The power consumption was drastically reduced by this method, which will be discussed in next chapters of thesis.

1.3 Fundamentals of underwater plasma discharge

The discharge mechanism in water can be divided into two categories; of pure water medium and bubble containing water [44, 45]: Since underwater discharge takes place in two mediums existing in water; one is pure water medium and other are bubbles, either created by joule's heating or by external gas injection. Therefore underwater plasma discharge process can be explained by two theories that are further divided into four different categories. Fig. 1.9 represents the flow chart of theories that explain the underwater plasma discharge mechanism.

In underwater discharge the medium where discharge occurs composed of gas containing bubbles or water at the interface of bubbles. Therefore breakdown mechanisms can be explained by two theories; one related to gas breakdown process and other related to liquid breakdown process.

1.3.1 Electrical breakdown in gas phase

Depending upon pressure and inter-electrode gap where plasma can be induced, the electrical breakdown in gas phase (bubbles and gas channels) can be explained by two mechanisms:

(a) Townsend breakdown mechanism

This mechanism resembles to breakdown process in gas discharges. At high frequency and short breakdown period the gas inside bubble become conductive and discharge occurs. The electron avalanche process initiates the discharge mechanism inside bubbles.

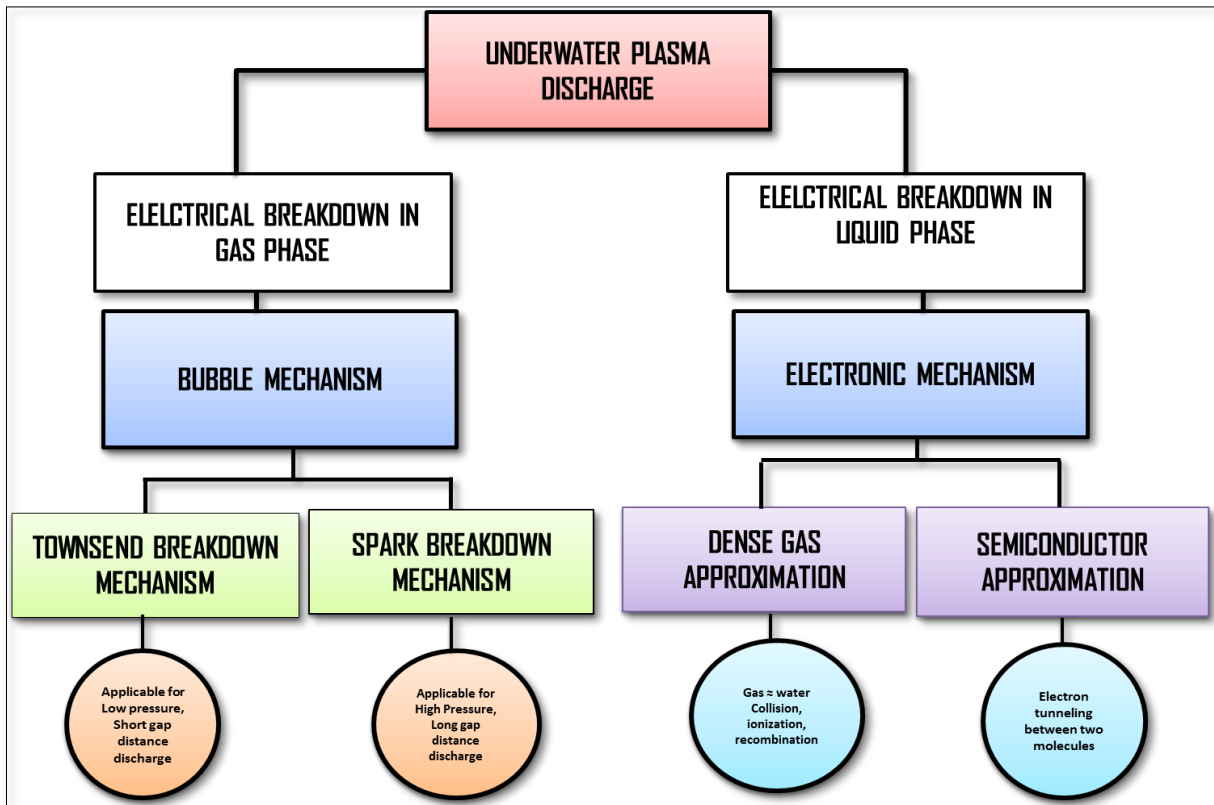


Fig. 1.9 Flow chart of Theoretical models in underwater plasma discharge mechanism.

The basis of Townsend is the generation of successive secondary avalanches to induce breakdown. Due to background radiations (cosmic radiations), radioactivity and thermal affects some primary electrons already present with in gaseous medium of bubbles before application of any electrical field or in the presence of weak electric field. When the field strength becomes sufficiently high, then due to collisions with neutral particles of gas, more ions and free electrons can be generated. These electrons known as secondary electrons will be able to further ionize neutral particles by collision leading to excess of electrons and ions. The process is cumulative, and the number of charge particles will go on increasing under the influence of the electric field. The multiplication of electrons number density will continue, and per unit length along electric field is given as [46]:

$$N_e = N_{e0} \cdot \text{Exp}^{\alpha x} \dots \dots \dots (1)$$

- N_{e0} = initial electron density
- N_e = electron number density after electric field influence
- α = Townsend ionization co-efficient

The Townsend discharge co-efficient is the number of ionizing collisions per unit length that a single electron undergoes. It depends upon, applied electric field, pressure and inter-electrode gap where plasma needed to be generated. The swarm of electrons and positive ions produced in this way is called an electron avalanche as schematically shown in Fig. 1.10.

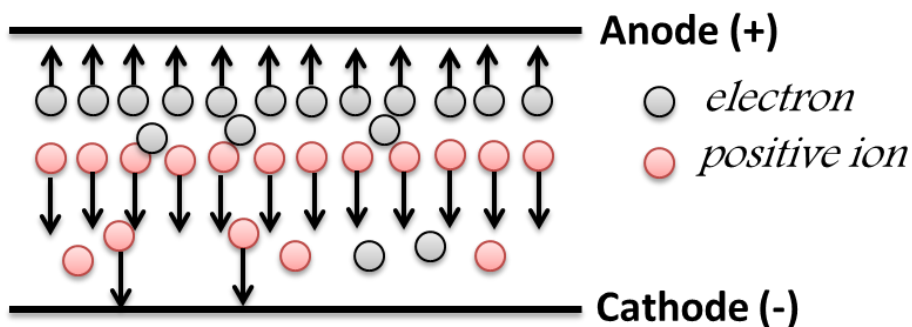


Fig. 1.10. Electron Avalanche process

When the gas medium within bubbles become full of electrons and ions, then under influence of applied electric field across two electrodes breakdown occurs, the implosion of bubbles participate overall discharge occurrence. The Townsend discharge mechanism is only applicable for low pressure and for discharge in short gap distances [47].

(b) Spark breakdown mechanism

For larger inter-electrode gap distances and high pressure discharges the phenomena can be explained by spark breakdown process. The spark breakdown process is based on the concept of streamers propagation between two electrodes within water, which arises due to the addition of space charge field of single avalanche with in gas medium. Fig. 1.11 represents the concept of streamer and its propagation direction [48]. Electrons being less massive and highly mobile will drift quickly towards anode leaving behind massive positive charge ions, giving a water drop shape of streamer. The field will increase in front of the head of streamer, while behind head, the field between the electrons and positive ions becomes in the opposite direction to the applied field, reducing the resultant field strength. At the head of the streamer near anode, electric field rapidly increases, resulting increase in

space charge and further strengthen the electric field near anode. The process is quick and results in formation of streamers [49].

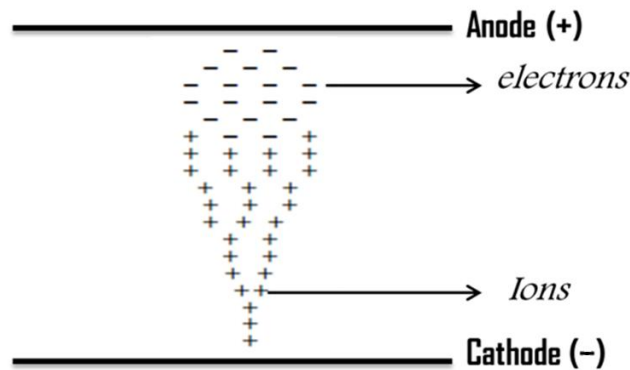


Fig. 1.11 Mechanism of streamer propagation

1.3.2 Electrical breakdown in liquid phase

Compared to gas discharge, in underwater plasma discharge due to multi-dynamics system and interaction of many particles, many aspects about the liquid discharge model are unresolved. The density difference of liquid and gas is the major cause. Being highly dense in water, the impact cross section of electron-neutral molecules and electron to charge particles is entirely different. Due to high density many body collision takes place quickly. Also due to dense plasma the Boltzmann distribution of electrons does not exist, due to multi-particle collisions, therefore collisional integral cannot be calculated from binary collision approximation [50]. Moreover the conductivity of liquids, chemical composition of liquids, and variation in energies of electrons generated by different simultaneous processes, like electric fields dissociation, by ionization, UV ionization and shockwaves interactions are also different [51]. Therefore the discharge occurrence in water cannot be approximated as equivalent to Townsend discharge mechanism. But there are some approximate models that lead to the discharge occurrence process more closely by considering some assumptions [52]:

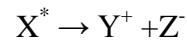
(a) Dense gas approximation

In dense gas approximation, like gas discharge, it is assumed that two body collisions are applicable. Although high density of liquid could cause rise in multi particle collision, but the strong bonds between the neutral molecules of the liquid is also another factor. Neglecting the many particles

collisions and assuming two body collisions and equalizing liquid to dense gas, some parameters in liquid discharge can be obtained [52].

(b) Semiconductor approximation

The second approximation for liquid discharge model is semiconductors approximation. In dielectric liquids the charge particle exists due to dissociation of neutral molecules under influence of energy supplied sufficient to create ionization by electrical or by heating process.



The ionization rate depends upon the dielectric strength of liquid and/or the binding forces between molecules of that liquid. In polar liquids like water the dissociation/ ionization is more than non-polar liquid due to the permittivity difference. Water has high permittivity that weakens the coulombs attraction between cations and anions, thus high rate of ionization exists [52].

In semiconductors, under the influence of applied electric field the electron move from cathode to anode, leaving a vacancy of electron called hole (+ve charge). To fill up this vacancy a similar electron from neighboring position transfer to that position and shift vacancy (hole) to the next position. This rapid process cause electron movement towards anode while vacancies transformation towards cathode. This cause transformation of current in semiconductors (electronic current due to electrons and conventional current due to holes/vacancies). While in liquids, like water, H_2O combines with a portion H^+ and forms a complex molecule H_3O^+ . This complex can transfer an excessive proton H^+ to the neighboring water molecule and forms complex H_3O^+ . Since this transformation takes place due to the displacement of electrons like in semiconductors under influence of strong electric field while protons remains stationary like vacancies or holes in semiconductors [52]. On the basis of this similarity in charge transfer the liquid discharge model can be assumed as semiconductors approximation. Under the influence of high electric fields, the electron and holes tunnel from one molecule to other. The applied electric field ' \vec{E} ' for this process should be higher than the barrier potential ' V ' between two molecules. The distance between two molecules also influences the

tunneling process. Fig. 1.12 indicates the schematic of charge transformation process in two approximations [52].

Compared to dense gas approximation where two body collisions are assumed, semiconductor approximation is better for explaining the breakdown process in liquid.

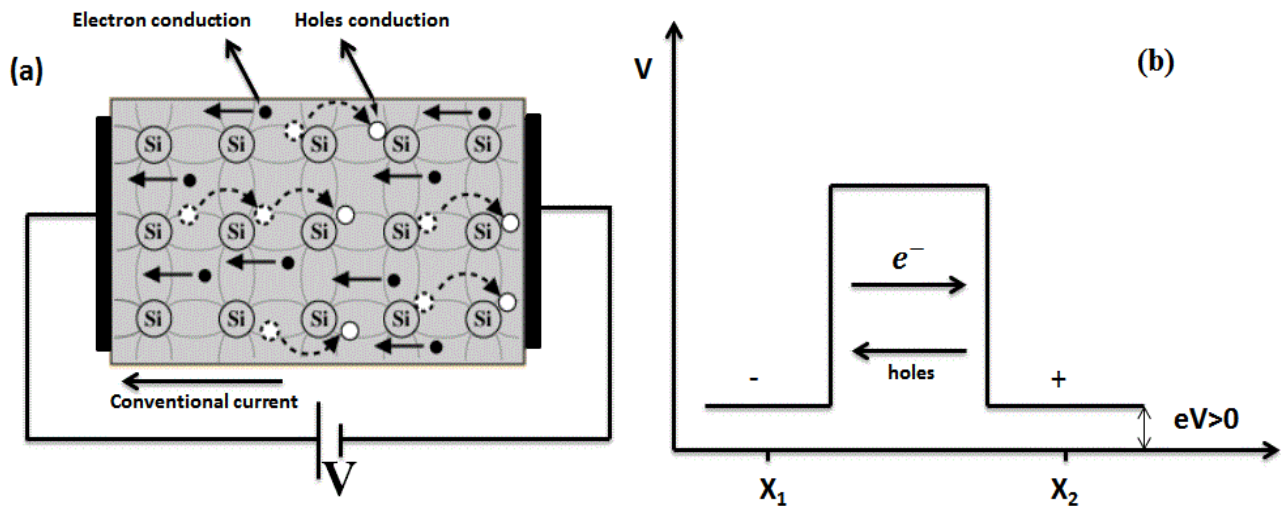


Fig. 1.12. Schematic of charge transformation in (a) Semiconductors (b) In dielectric liquids under influence of high electric field.

All above explained theoretical aspects of underwater plasma discharge were referenced and summarized from Alexander Friedman et. al book [52].

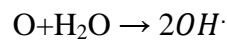
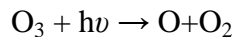
1.4 Reactive species generated by underwater discharge

Under effect of strong applied electric field from different power sources like DC, pulsed DC, high frequency AC or from RF source cause splitting of water molecule and generation of reactive oxidant species through physical and chemical processes. The other processes like UV radiations and shock waves of several orders of magnitudes (few Pascal to Mega Pascal) also cause the generation of reactive species [53, 54].

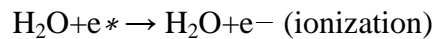
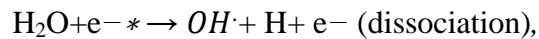
Many species can be generated through discharge process that has ability to sterilize water, remove harmful elements from water and can cause useful chemical reactions.

1.4.1 $OH\cdot$ radicals

The hydroxyl radical ($OH\cdot$) is the neutral form of the hydroxide ion (OH^-). The hydroxyl radicals are highly reactive and are consequently short-lived (~ 1 ms) [55]. In nature, ($OH\cdot$) radicals exist in the atmosphere, having been formed by photolysis in the upper atmosphere with ozone [56]. The high-energy and lower-wavelength UV photons dissociate the ozone molecules into atomic and molecular forms, and the atomic form can react with the water vapor present in the upper atmosphere to form $OH\cdot$ radicals [57]:



In laboratories, the $OH\cdot$ radicals can be induced by combining various chemicals, and by using electrical discharges [58]. In this experiment, electrical energy was used to generate $OH\cdot$ radicals through a plasma discharge without any chemical addition. The applied electrical energy generated non-thermal plasmas in the water, and as a result, dissociation and ionization took place in the water, which generated $OH\cdot$ radicals [59]:

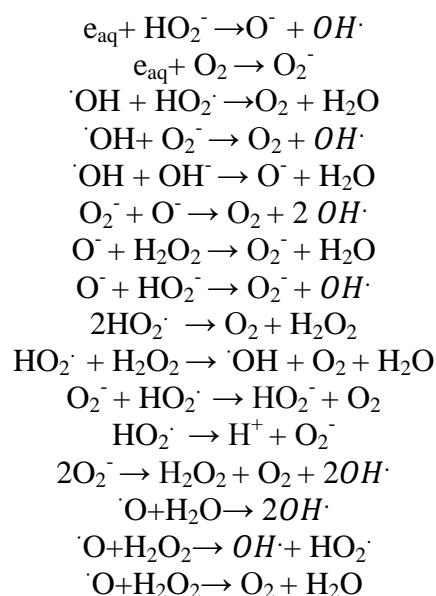


(*indicates the high-energy stage of the electron)

The generated $OH\cdot$ radicals have an important application in water sterilization when they react chemically to destroy dangerous bacteria (*E. coli*, salmonella, shigella, *etc.*) [60].

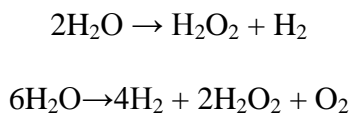
1.4.2 Reactive oxygen

The occurrence of plasma discharge in water cause splitting of water molecule that generates reactive oxygen which can be measured and identified through emission spectrum at 777nm and 844 nm. The possible chemical reactions for the generation of oxygen and its chemical reaction with other reactive species were reported by [61, 62], as follows:



1.4.3 Reactive hydrogen

The occurrence of discharge can cause reactive hydrogen production that can be measured by emission spectrum at H_β (444 nm) and H_α (656 nm). Some possible chemical reactions reported by [63]:



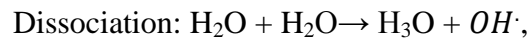
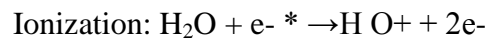
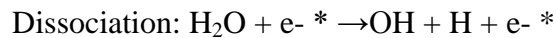
1.4.4 Ozone

Since long time ozone (O_3) has been used as disinfectant for industrial, chemical and waste water, due to its characteristic of powerful oxidant and effective thermodynamic oxidation potential [64]. In water treatment ozone proved to be useful for enhancing pleasant taste of water, removing unpleasant odor from water, for benefiting congelation and filtration process and acts as first obstacle for micro-

Also, if the temperature of the system is too high, the ozone molecules are basically decomposed therefore, electrical discharge method has been found as a very helpful method for successful ozone generation, decomposition of ozone and fusion of ozone with other reactive species [69].

1.4.5 Hydrogen peroxide

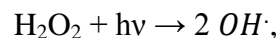
The generation of electrical discharge in water cause the generation of hydrogen peroxide due to the combination of hydroxyl radicals with possible chemical reactions is [70]:



The hydrogen peroxide can be measured by various mechanisms in which the most dominant is calorimetric method and using absorption spectroscopy.

1.4.6 UV radiations

The occurrence of discharge in water causes generation of high intensive UV radiations. The intensity of UV radiations can be measured by photodiodes, actinometrical methods and UV detectors [71-72]. The disinfection rate in water by UV radiations depends upon the intensity of radiations and the dose injected to the water. Thus, emission intensity of the UV radiations can be directly related to the discharge pulse power [73]. The water molecules dissociate into reactive species under influence UV radiations by following reactions:



The bactericidal disinfection by UV radiation, UV light (190–280 nm) of the corona discharge and (200–300 nm) with doses of several (0.1–10) mWcm⁻² was reported effective to cells [74].

1.4.7 Shock waves

The generation of shock waves due to plasma discharge in water was reported by many researchers [75]. Due to high intensity of these shock waves these are capable of destroying the DNA structure of dangerous bacteria like E.coli, Salmonella etc. [76]. The shock waves can be measured by

hydrophones or high resolution and high speed cameras [77]. The expansion of shock waves and their intensity cause disinfection of bacteria in drinking water. These waves do not influence the taste and nutrition of water and only sterilize it [78]. This mechanism is free from chemicals and proved very effective for water sterilization.

1.5 Applications of underwater plasmas

Generation of underwater plasmas has been an interesting subject due to some rare and important applications [79]. Underwater plasma discharges have wide range of applications in environmental [80], biological [81], industrial [82] and semi-conductor industry [83]. The basic understanding of the physical and chemical characteristics of these underwater discharges is of extensive importance for their future applications and research. Fig. 1.14 shows schematic of underwater plasma discharge applications.

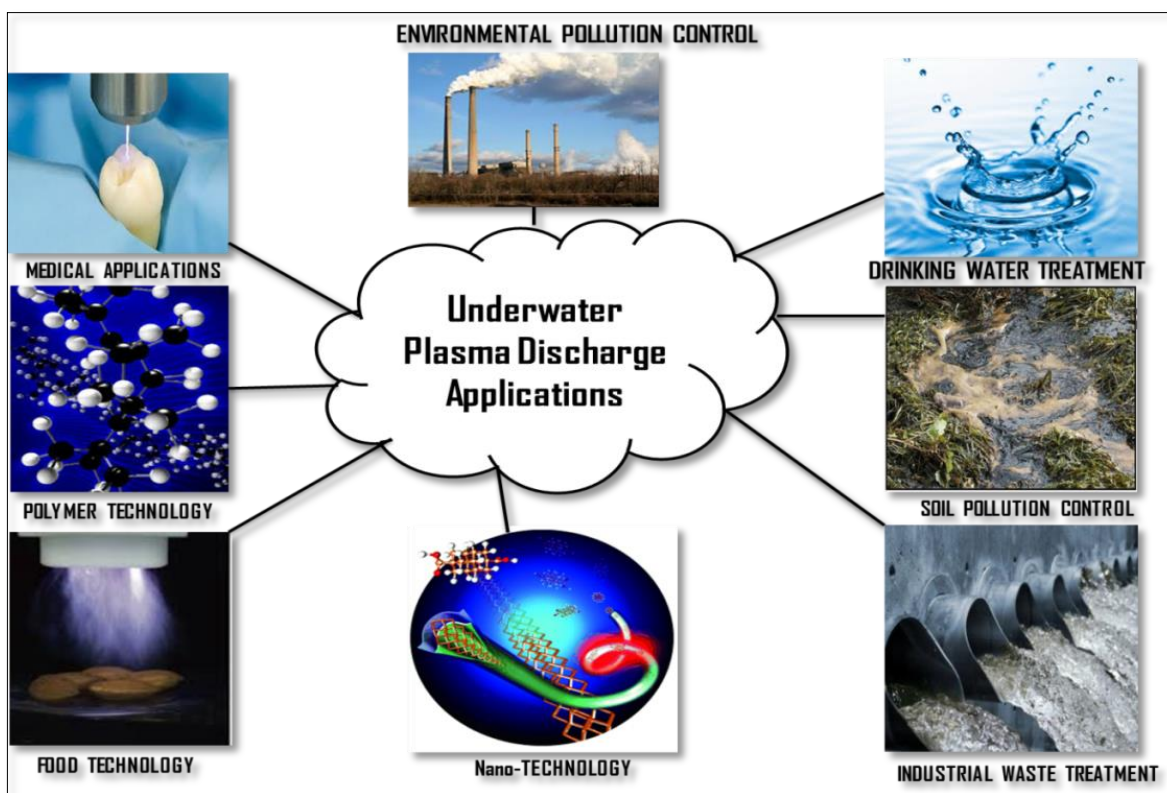


Fig. 1.14 Applications of underwater plasma discharge.

2. Diagnostic Techniques of Underwater Plasma Discharge

The physical and chemical processes occurring in underwater plasma discharge comprised of complicated and many simultaneous procedures, therefore many aspects are still largely unknown [84]. The major problem is the dielectric strength of water that is higher than gas, which requires high electrical power consumption for initiation of discharge and to sustain it [85]. The investigation of physical and chemical characteristics is therefore very important to solve such problem. Moreover, underwater plasma discharge could be generated many chemical oxidant reactive species that are very important for various applications, therefore the qualitative and quantitative investigation of such species is too necessary. Various diagnostics schemes are available for investigating discharge in water [86]. Depending upon the source of underwater plasma discharge and field of applications, different diagnostic methods were adopted in this research and presented in coming sections of this chapter.

2.1 Electrical diagnostics

The volt-ampere characteristics curves indicate the required breakdown voltage, discharge current, frequency of plasma discharge, pulse width, power consumption and nature of discharge (stable or pulsating). The high voltage and current probes are required for the measurement of electrical characteristics. Digital oscilloscopes connected with these probes and having data storage facility is convenient for taking large data values quickly. A Tektronix digital oscilloscope (DPO-2024) was used in this research for the measurement of electrical characteristics of underwater plasma discharge. The obtained data was evaluated by Matlab codes and various and various basic electrical engineering formulas. The discharge either occurs in pure water medium or bubbles containing water medium, therefore depending upon the nature of medium the electrical characteristics of discharge can be obtained.

(a) Volt-Ampere Characteristics curves

The Volt-ampere (IV) characteristic curve shape depends upon the nature of medium and input power source (A.C, D.C or RF). A typical volt-ampere characteristic curve of plasma discharge generated by DC power source is shown in Fig. 2.1 (a), while a typical high frequency power source IV curve is shown in Fig. 2.1 (b).

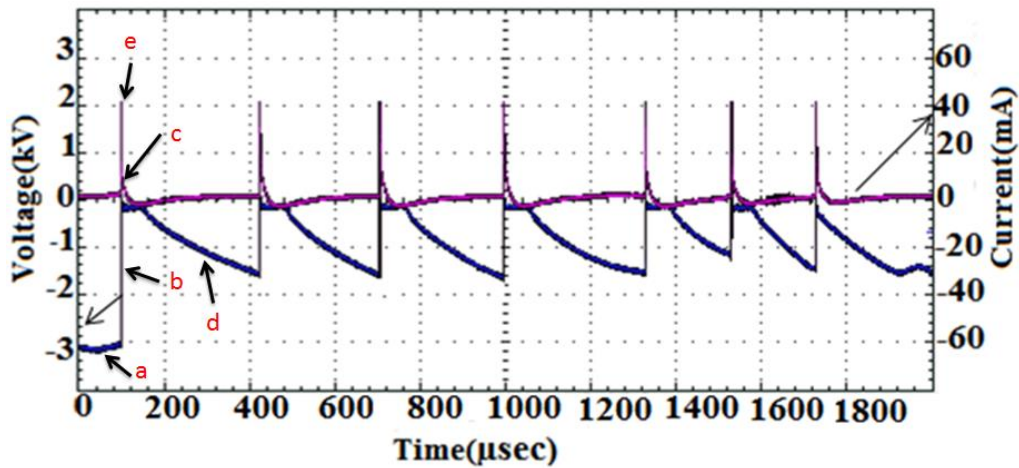


Fig. 2.1 (a) Typical IV curves of pulsating underwater discharge with DC power source.

The existence of bubbles and gas channels, occurrence of discharge within these gas channels and bubbles results in pulsating nature of discharge normally, which depends upon the characteristics of input power source, its frequency, rate of ionization and excitation in water and gaseous medium. In case of negative DC power source the shape of discharge pulses is of complex, sharpe and rapid pulsed wave form. As shown in Fig. 2(a), point 'a' is the applied voltage representation across two electrodes inserted in underwater discharge chamber, when discharge current starts increasing the voltage start decreasing as indicated by point 'b' at maximum required voltage also known as breakdown voltage the discharge occurs the discharge current is at the peak position and voltage is at lowest value as discharge current is at highest point as indicated by point 'c', again for next phase voltage began to increase and current reduces as indicated by point 'd'. Point 'e' represents the maximum value of discharge current, where complete discharge occurs.

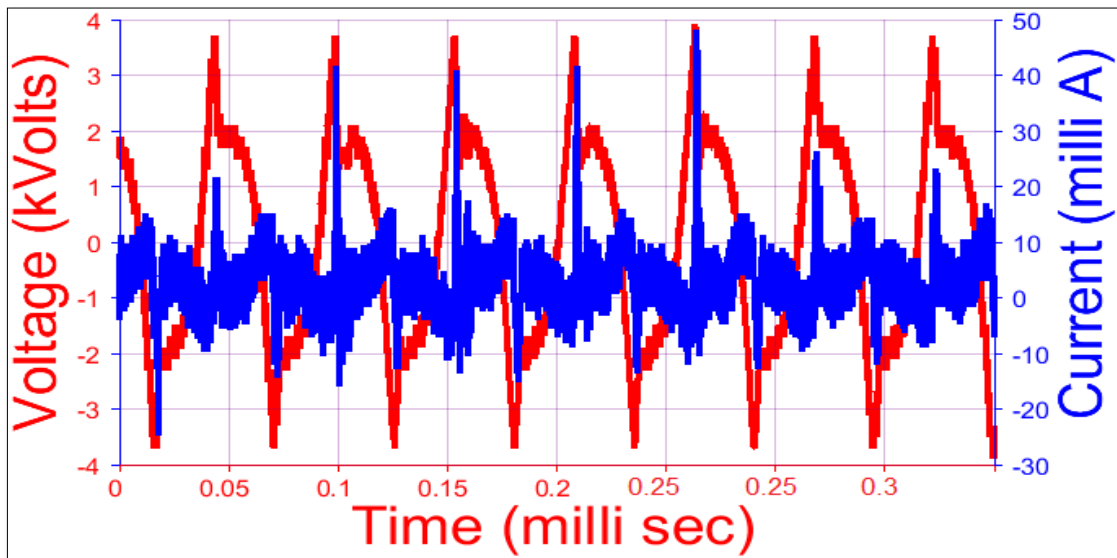


Fig. 2.1 (b) Typical IV curves underwater discharge with high frequency power source.

The discharge occurs at the intervals of micro and Nano seconds. The existence of gas channels and gas bubbles between two electrodes is a statistical process; moreover the discharge simultaneously occurs in liquid as well as gas phase therefore the waveforms are of pulsating nature.

The power of discharge pulses is an important parameter regarding to the physical characteristics of underwater plasma discharge. In case of DC source the power can be evaluated by simple relation $P=VI$, whereas for complex waves obtained it can be evaluated by equation $P=V_{rms}I_{rms}$. As the reciprocal of time period is frequency i. e $f = \frac{1}{T}$, therefore the time scale can provide the frequency of discharge pulses [87]. The time difference between occurrences of two consecutive discharge pulses can provide gap between the occurrences of discharge pulses.

(b) Matlab codes

The electrical data comprised of large data points that can easily evaluated by Matlab codes. Following are some codes for DC and A.C input power sources to evaluate breakdown voltage, discharge current, frequency and power.

(i) DC power source

```
*****
*****

%%
clear;clc
[file folder]=uigetfile('*.csv','Click on the data file');
[n,t,r]=xlsread([folder file],'A17:E125016');
%%
Time=n(:,1);
Voltage=n(:,3);
Current=n(:,5);
Fig.('units','normalized','outerposition',[0 0 1 1])
[hAx,hLine1,hLine2] =plotyy(Time,Voltage,Time,Current);
set(gca,'linewidth',2)
set(hAx(1),'fontsize',20)
set(hAx(2),'fontsize',20)
set(hAx(1),'Xgrid','on')
set(hAx(1),'Ygrid','on')
set(hAx(2),'Xgrid','on')
set(hAx(2),'Ygrid','on')
xlabel('Time (seconds)')
ylabel(hAx(1),'Voltage (Volts)') % left y-axis
ylabel(hAx(2),'Current (Amps)')
xlim([min(Time) max(Time)])
grid on

*****
*****
```

(ii) *AC power source*

```
*****
*****

%% data reading
clear;clc
[file folder]=uigetfile('*.*txt','Click on the data file')
[data] = textread([folder file],",','delimiter',';');
%% plotting code
Fig.('units','normalized','outerposition',[0 0 1 1])
[hAx,hLine1,hLine2] =plotyy(data(:,1),data(:,2),data(:,1),data(:,3));
set(gca,'linewidth',2)
set(hAx(1),'fontsize',20)
set(hAx(2),'fontsize',20)
xlabel('Time (seconds)')
ylabel(hAx(1),'Voltage (Volts)') % left y-axis
ylabel(hAx(2),'Current (mAmps)')
%% to be put in paper
V=data(:,2)*1000; % voltage (converted from kVolts to Volts)
I=data(:,3)/1000; % current (converted from milliAmps to Amps)
Vrms=sqrt(mean(V.^2)); % rms voltage
Irms=sqrt(mean(I.^2)); % rms current
Prms=Vrms*Irms % rms power
Pinst=V.*I;
Prms1=sqrt(mean(Pinst.^2)) % rms power (calculated from instantaneous
power)

*****
*****
```

2.2 Spectral diagnostics

An atom or ion immersed in plasma will emit radiations between various energy states that occur in optical range of plasma. Several energy states are produced after discharge occurrence, more effectively these energy states are produced by recombination of charge particles as well. The atoms and molecules depending upon applied energy excite to these energy states and on de-excitation emit radiations of several intensities and characteristics. The emitted radiations are allowed to pass through optical assembly and the spectrum with several intensities can be obtained. A typical plasma spectrum is composed of several atomic emission and absorption lines, corresponding to transitions of neutral atoms or ions of those atomic species contribute to the plasma. The obtained spectrum is the processed by several mechanisms and optical data can be evaluated that reveals several physical and chemical processes [88]. Fig. 2.2 indicates the scheme of spectrum evaluation.

Since underwater plasma discharge comprised of complex phenomena and many generated oxidant species are short lived like $OH\cdot$ Radicals, therefore its analysis is perfect by spectroscopy. Two types of spectrums exist mainly for underwater plasma discharge characterization, explained below.

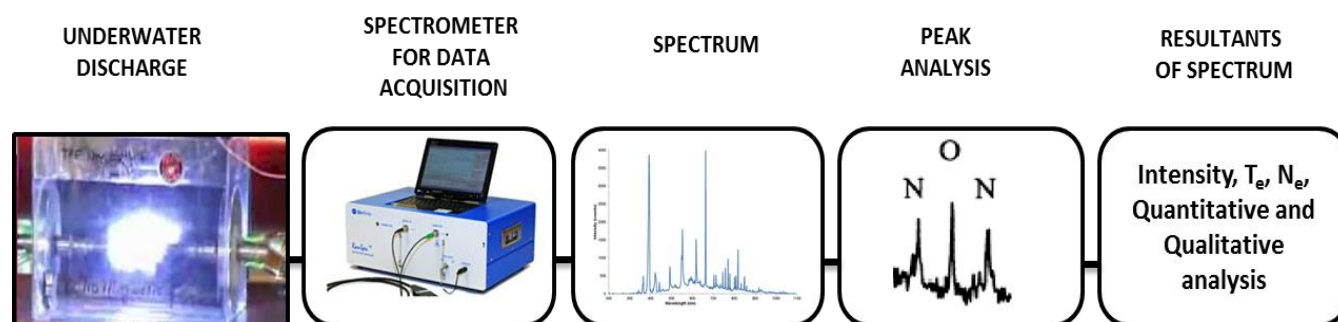


Fig. 2.2 Processing scheme of spectral diagnostics

(a) Emission spectroscopy

After discharge occurrence the atoms excite from lower to several higher energy levels in optical range, on de-excitation these atoms emit radiations known as electromagnetic radiations that can be

studied by emission spectrum. Emitted radiations can be analyzed by spectrometers with respect to their frequency and wavelength [89].

The emission intensity of spectrum is represented by arbitrary units (a. u) while wavelength that is the distance between two adjacent peaks can be measured in nanometers (nm) or centimeters (cm^{-1}). Range of spectrum can be adjusted by spectrometer [90].

Fig. 2.3 represents a typical emission spectrum obtained after discharge occurrence in water. Emission spectrum is widely used for the characterization of underwater plasma discharge specially for determining oxidant species.

The determination of some physical characteristics like electron temperature (T_e), electron number density (N_e) and plasma composition can be simply estimated by intensity and width of emission spectrum [91, 92].

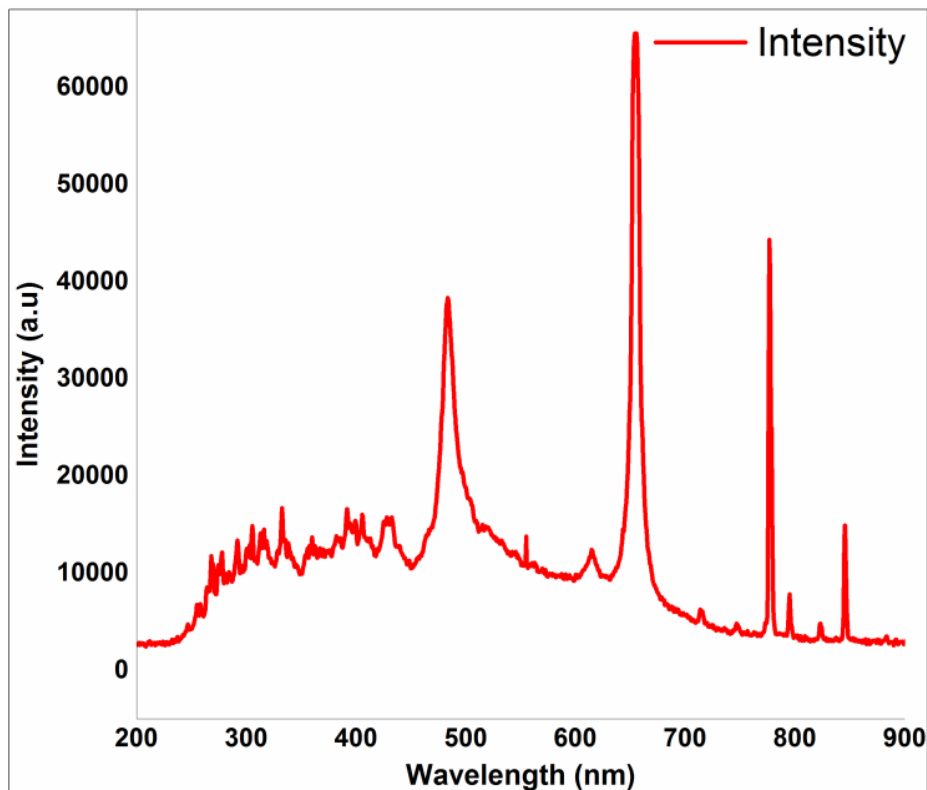


Fig. 2.3 Typical emission spectrum of underwater plasma discharge.

(b) Absorption spectroscopy

The quantitative analysis of reactive species existing in plasma can be made by absorption spectrum. The absorption of various wavelengths by visible lights in plasma can give absorption spectrum [93]. A simple assembly of absorption spectrum is shown in Fig. 2.4.

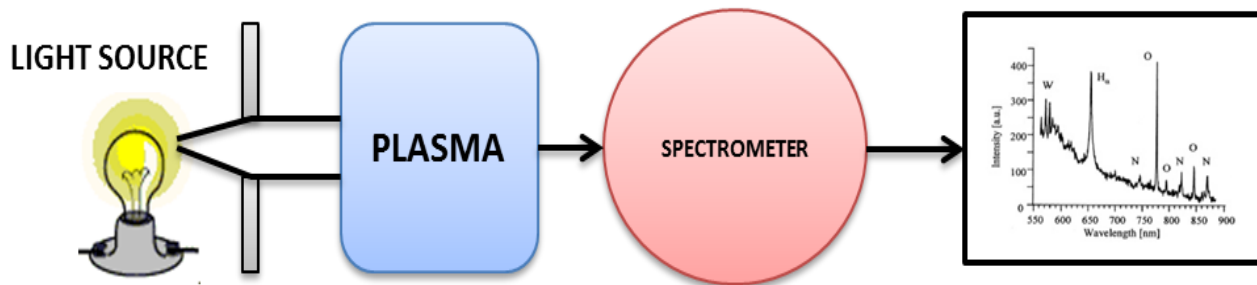


Fig. 2.4 Schematic of plasma absorption spectroscopy.

This method is used for the determination of reactive species concentration generated in plasma.

2.3 Imaging diagnostics

The discharge structure, propagation criterion and the expansion in water and bubble medium can be visually studied by imaging diagnostic methods. Such diagnostics provides the physical dimension and thermal effects in different regions of plasma at various distances from the main electrode [94]. In this research two imaging diagnostic techniques were adopted and presented.

(a) High speed camera photography

A high speed camera can give the structure of discharge variation with respect to time evolution in very short intervals of time. Fig. 2.5 (a, b) represents typical images taken by high speed camera (500fps) for bubbles propagation and discharge propagation.

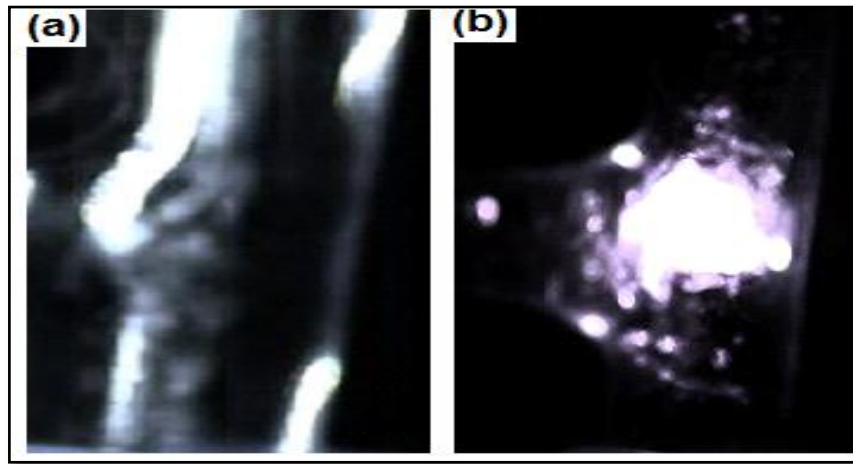


Fig. 2.5(a, b) Images of bubbles and discharge taken by fast speed camera.

The propagation of bubbles and discharge streamers propagation within these bubbles, as well as discharge expansion in the surroundings of electrodes and water can be identified conveniently by fast speed camera.

(b) Thermal camera photography

The occurrence of discharge cause high temperature in plasma zone, that varies with respect to the distance variation from center of discharge. Thermal imaging diagnostics represents the temperature variation along with discharge expansion [95]. Fig. 2.6 represents typical image of underwater capillary discharge expansion. A thermal camera TV-BM002 was used for thermal imaging of capillary discharge. The strength of discharge also depends upon the temperature of liquid that causes the generation of micro bubbles in the liquid which in turn causes the breakdown in liquid and within the bubbles. Therefore thermal diagnostics provide useful information concerning to the discharge strength at various points that effects yield rate of chemical reactive species.

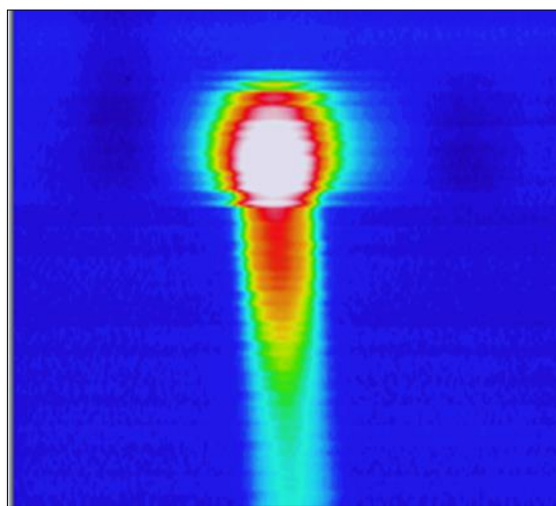


Fig. 2.6 Typical discharge image taken by thermal camera.

2.4 Statistical diagnostics

The application of various mathematical and numerical formulas on experimentally obtained results could give reasonable estimated results, where experimental or simulation approach is complicated [96]. In this research quantitative analysis of experimental data was performed to determine various physical and chemical quantities, as explained below:

(a) *Gaussian distribution functions*

Generally area under the curve can provide concentration of concerning quantity. Since OH radicals are highly oxidant reactive species among other chemical reactive species, therefore the quantitative determination of such radical's is of highly interest under different experimental conditions. Using Gaussian distribution function and full width at half of maximum on $OH\cdot$ radical's peak (309nm) the quantitative determination of OH radical's is possible [97]. The results used relation of this method has been explained in coming chapters of thesis.

(b) *Stark broadening*

The emission spectrum of Ballmer hydrogen lines (H_α , H_β , H_γ , H_δ and above) have probability of broadening due to various factors. The most dominant effects are local broadening mechanisms that

include mainly natural broadening, Doppler broadening, Stark /pressure/collisional broadening, instrumental broadening and Vander-waals broadening [98].

The emission spectrum line can be broadened by different broadening mechanisms. These mechanisms can cause shift in the energy levels of emitter atoms and the participation of each broadening mechanism depends upon the experimental conditions. At high electron densities Stark broadening is so dominant that Doppler and Van der Waal broadening with half width of about 0.3 and 0.03 \AA respectively is negligible. An instrumental broadening ($\leq 0.3 \text{\AA}$) is also negligible. The other factors like self-absorption and boundary layer effects depend upon experimental conditions [99]. The profiles coming from these mechanisms are either Gaussians or Lorentzian profiles. The mechanisms like Doppler broadening provide Gaussian profiles, while Van der Waals broadening, natural broadening and Stark broadening provides Lorentzian profiles. The total FWHM of Gaussian profiles can be calculated as $\Delta\lambda_{\text{Gauss}}^2 = \Delta\lambda_1^2 + \Delta\lambda_2^2$, while FWHM of Lorentzian profile can be found by relation $\Delta\lambda_{\text{Lorentz}} = \Delta\lambda_1 + \Delta\lambda_2$ and the convolution of these two phenomena gives Voigt profile, while deconvolution of Lorentzian from Voigt can provide Stark full width at half of maximum (FWHM), using the values of Lorentzian FWHM electron number density can be calculated [100].

(c) Intensity ratio method

Comparing intensities of emission peaks, the electron temperature can be determined. The emission lines intensity provides physical characteristics of plasma. If the condition of LTE for population densities of upper energy levels of two lines is fulfilled then intensity ratio method is straight forward for the determination of T_e [101]. In this research hydrogen emission lines were taken to determine electron temperature, for two transition states and the parameter values were determined from NIST database [102, 103]. The detail and results by this method are explained in coming sections of thesis.

2.5 Diagnostics of oxidant species

Various chemical, physical, optical and electrical methods are available for determination of oxidant species generated by underwater plasma discharge [104]. The adopted methods in this research are given below:

(a) OH radicals

Since the life time of $\cdot\text{OH}$ radicals is very short $\sim 10^{-8}$ sec, therefore convenient method for its detection is emission spectroscopy [105]. The intensity and width of emission spectrum indicates the concentration of OH radicals that is represented by area under the curve using mathematical approach as Gaussian distribution function used in this research.

(b) Hydrogen Peroxide

The most dominant method for hydrogen peroxide determination is colorimetric method proposed by Eisenberg [106]. In this research same photometric analysis for the determination of H_2O_2 generated in water was adopted after occurrence of plasma discharge. In this method sample of plasma treated water was mixed with equal amount of titanium sulfate reagent. The chemical reaction occurs and a yellow color solution can be obtained. The absorption spectrum of this yellow color complex solution was measured at 407 nm. The absorbance at this wave length corresponds to the concentration of H_2O_2 generated in water as result of plasma discharge [107]. The detail of process applied in this research is given in coming chapters of thesis.

(c) Ozone

A common method presented by Hoigne [108] called indigo method was used in this research for ozone measurement. In this process aqueous ozone concentration can be determined by allowing its chemical reaction with a color dye, under presence of various other chemicals like sulphuric acid (H_3PO_4), and sodium di-hydrogen phosphate (NaH_2PO_4). The comparison of absorption spectrums of blank and ozone mixed water samples provided ozone concentration in water phase. The complete

detail is given in coming section of thesis where it is applied on ozone determination in capillary discharge.

(d) Reactive hydrogen and oxygen

Using emission spectrum the concentration of reactive hydrogen ($H_{\beta}=484\text{nm}$, $H_{\alpha}=656\text{nm}$) and reactive oxygen (777nm, 844nm) can be determined conveniently [109].

2.6 Diagnostics of bacterial ineffectiveness

To test the efficacy of the plasma treatment against efficient colony forming *E. coli* bacteria, we have organized the following strategies as [110]:-

(a) Heterotrophic plate counting (HPC) method

(b) Optical density measurement (OD) method

(a) Heterotrophic plate counting (HPC) method

A common method of finding heterotrophic bacteria in drinking water and counts of colony formation on culture media is called Heterotrophic plate count (HPC) [111]. Generally, it can be used to investigate the microbiological quality of drinking water. The HPC method does not indicate the bacteria sources but it indicates the presence of culture-able organisms, with a precision of as low as 1% of the total bacteria present in the water. Moreover, the important parameters that affect this mechanism or type of medium used to grow the bacteria, temperature used for incubation, incubation duration, chemistry of water samples and concentration of bacteria existing in the water. This method indicates the number of colonies existing in water, which in turn represents the standard of water. Depending upon the type of bacteria and media, it is being used for preparing plates the number of colonies and their concentration can be changed due to dilution factor. Fig. 2.7 represents a typical Luria Broth (LB) agar plate having *E. coli* bacteria on the surface that can be calculated by the following formulae [112]:-

$$CFU = \frac{(\text{Number of colonies}) \times (\text{Dilution factors})}{V_o} \dots\dots\dots (1)$$



Fig. 2.7 A typical Agar plate for bacteria count also known as HPC method.

(b) Optical density measurement (OD) method

Basically the wavelength of measurement (WM) of OD depends on growth of the bacterial culture. The rapidly growth by bacteria strain which is "huge" growth then it form a linear part of relation between cell number and OD. On the other hand, optical density (OD) measurement is based on the process of light scattering by water having bacterial culture rather than amount of light absorbed. The basic phenomenon behind the optical density of bacterial culture depends on the number of growing *E.coli* in the bacterial culture; it is actually turbidity which is given term absorbance, because only few strong cells such as phototrophic bacteria can absorb significant light along with scattering. When scattered and less intense light (after absorption) falls on photometer OD measuring device then following considerations for OD measurement:

- a. Since light scattering and OD of culture depends upon wavelengths, therefore shortwave lengths scattering is more than long wavelengths, therefore choosing any wavelength will give OD of that culture particularly at that wavelength, as in this research for *E. coli* it was 595nm.

- b. Since OD measurement depends upon geometry of light therefore device dedication for single experiment is necessary.
- c. In order to measure the absorption of light caused by cells, the obtained absorption must be subtracted from blank spectrum. For all different values calculation keep the blank spectrum constant on one value.
- d. For small OD values ≤ 0.4 , the values are acceptable as cell density, but above these or higher values are not considered to be true results.

$$\% \text{ of Survival E. coli} = \frac{OD \text{ of test group} - OD \text{ of blank}}{OD \text{ of control} - OD \text{ of blank}} \times 100 \dots\dots\dots (2)$$

All above explanation was summarized from [113]. Fig. 2.8 represents the scheme of optical density measurement.

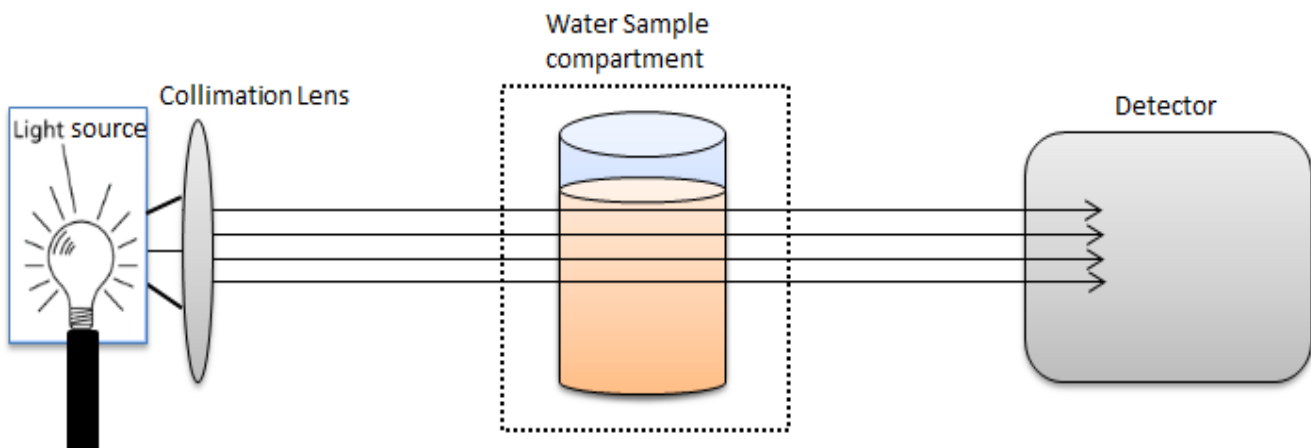


Fig. 2.8 Schematic presentation of optical density (OD) measurement method.

3. Investigation of DC Underwater Capillary Discharge

3.1 Introduction

Negative DC discharges are of large interest at laboratory scale underwater plasma discharge experiments, although it has very limited but rare advantages [114]. A high flux of electrons can be obtained from a negative DC electrical discharge in gas or liquids [115]. The negative DC performance further depends upon the electrodes assembly and discharge creating reactor types [116]. Lot of work has been done on creating negative DC discharge for various industrial and environmental research application purposes [117]. For example in an early submerged capillary point-shaped electrode discharge reactor the discharge with gas injection through the capillary, causes enhancement of the interfacial area for mass transfer [118]. The emission spectra results suggested that the major radical species produced from such system were hydroxyl radicals, ozone and atomic hydrogen [119]. However, in some applications like phenol degradation, modeling results showed that only aqueous electrons and hydroxyl radicals are dominantly responsible for organic removal in pulseless discharge [120].

Capillary discharge has advantage of the possibility of using many capillaries in parallel combination [120]. Some researchers described a wire-plate type reactor over the treated water displaying superior treatment performance by negative DC discharge. When applying a high negative DC voltage onto the wire cathode, energetic electrons drifting along the electric field can induce dissociation and ionization of oxygen with O-based active species (O_3 , OH radical and O etc.) generation. These species initiate reactive OH radical production when reaching the interfacial water and dissolving into it. With such electrode configuration a large volume of water or polluted gas can be exposed to electrical discharges [121]. So this reactor configuration along with negative DC, it can be an efficient assembly for continuous treatment of wastewater.

3.2 Experimental set-up

This setup presents an effective method of generating an underwater capillary discharge at low power through gas injection (O_2 , air) and generating OH radicals. A flowing water (0.1 L/min) discharge was created in a quartz capillary tube ($\Phi= 4$ mm outer; $\Phi= 2$ mm inner; thickness = 2 mm) by applying a continuous negative DC voltage (0 – 4 kV) across tungsten electrodes ($\Phi = 0.5$ mm) separated by a variable distance (1 – 2 mm) in the pin-pin electrode configuration. The air- and oxygen-injected capillary discharges at a constant water flow rate, similar gas injection variation rates, and two different inter electrode gaps were compared. Fig. 3.1 shows a schematic of the experiment set-up that was used for this experiment. A visual view of the discharge is shown in Fig. 3.2 The inter electrode gap where the plasma was generated was varied from 1 – 2 mm, and the inlet contained water. A liquid flow meter and controller (Dwyer-RM Series) was used to control the flow rate of water at 0.1 L/min through plasma generating quartz capillary tube. An air compressor (CROX-RX47L) was used to provide an air stream controlled by an air regulator, and the flow rate of air was measured with an air flow meter (KOFLOC-1600) for different adjusted flow values (100 – 800 sccm). A mass flow controller (LINE TECH M3030V), along with a mass flow control and display unit (FM-30VP), was used to control and provide the oxygen flow rate for different adjusted values (100 – 800 sccm). An Avantes Avaspec-NIR256 miniature fiber-optic spectrometer was used to record the emission spectrum of the OH radicals and other reactive oxidants under different experimental conditions. A high-speed camera, (PHOTRON, FASTCAM-SA4), with a 500-fps efficiency was used to take the images of the discharge structure under different gas injection rates and gap distances.

3.3 Methodology

Two tungsten electrodes were inserted in the quartz tube, and one electrode was connected to the negative DC power supply source while the other was connected to the same source's ground terminal. An injection syringe was used to inject air and oxygen, respectively. A powerful compressor was used

to provide the air stream filtered by a ceramic fiber filter, and the air stream was allowed to pass through an air regulator that provided the desirable flow of air into the air flow meter. The oxygen was provided by using mass flow controllers (MFCs), and the status of the flow rate at any instant could be observed through the display unit of the MFC. The water in a small tank with a one liter water reservoir was allowed to enter the quartz capillary tube through the liquid flow meter that measured the flow rate of liquid. When the gas and the liquid simultaneously entered the quartz tube, in the liquid, the gas generated bubbles, and these bubbles participated mainly in breaking down the liquid. The air and oxygen stream was injected in the range of 100 – 800 sccm, in 100 sccm intervals. The electrical data were recorded using a digital oscilloscope with high- voltage and large-current probes, and with a data storage device facility. The breakdown voltage and the discharge current for the 1 and the 2 mm inter electrode gaps for both air and oxygen addition was recorded. The images of the discharge structure were taken with a high-speed camera with a 500-fps rate to study the illumination intensity and the expansion of discharge structure. The emission spectrum of the OH radicals was recorded with a spectrometer after the discharge had occurred. Under all the presented experimental conditions, the electrical, spectral, and imaging data were taken simultaneously to study, compare, and present the results.

The Gaussian de-convolution method was applied to the spectral lines to determine, compare, and present the increase in the concentration of the OH radicals for oxygen and air injection, separately.

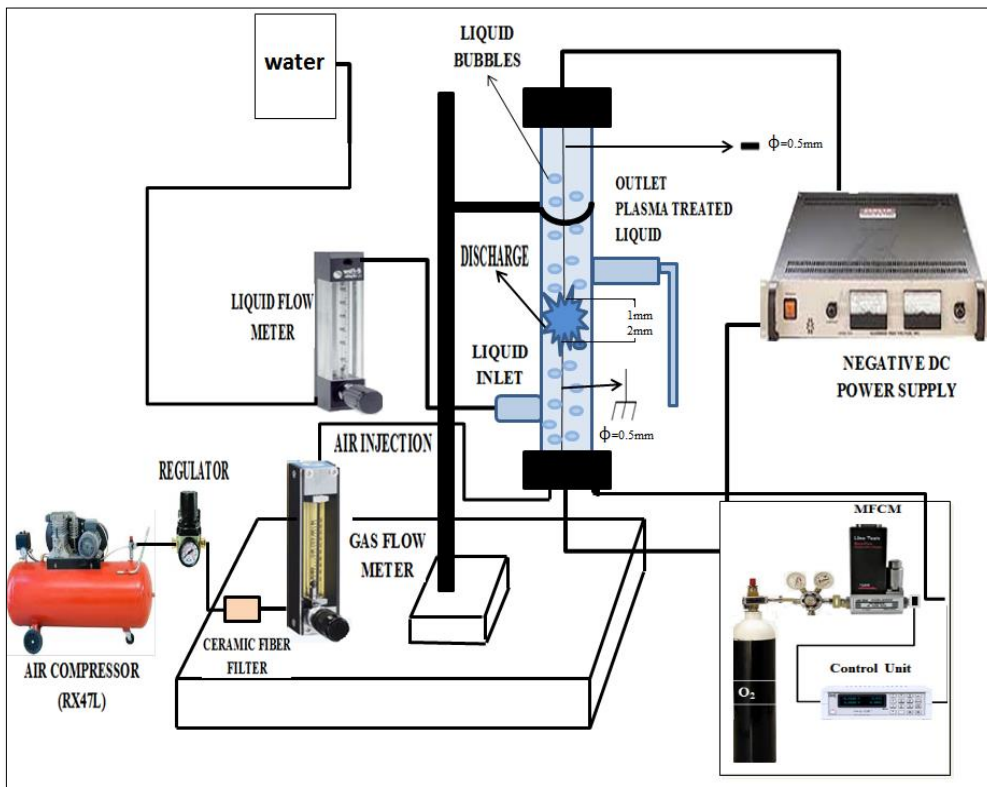


Fig. 3.1. (Color online) Schematic view of the experiment set-up.

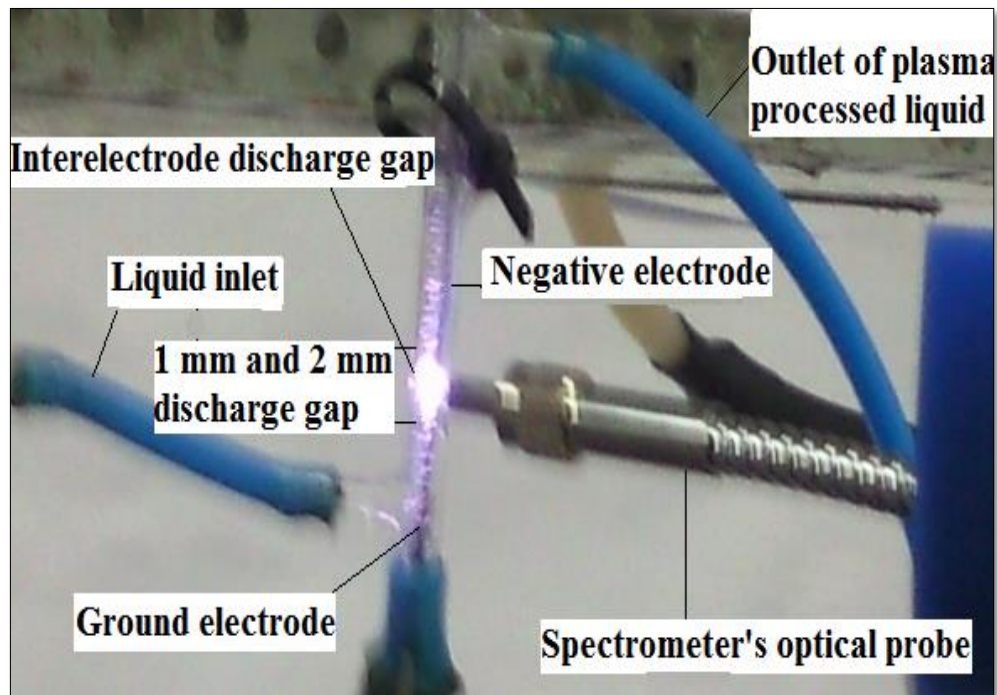


Fig. 3.2 (Color online) Visual view of capillary discharge.

3.4 Results and discussion

The results were analyzed using electrical, spectroscopic, and imaging diagnostic techniques. A reduction in the breakdown voltage with increasing gas injection rate was shown. Compared to air, oxygen was proven to be more effective for generating an underwater discharge of a pulsating nature with the characteristics of high energy per pulse, higher power per pulse, short pulse width, and short pulse repetition rate. The emission spectrum of the oxygen-injected discharge showed a higher concentration of OH radicals than that of the air-injected discharge. The imaging diagnostic results showed that the discharge was brighter and more expanded when oxygen was added than it was when air was added.

3.4.1 Electrical diagnostics

The electrical results for the flowing water capillary discharge at two different inter electrode gaps and various gas injection rates were observed and compared. The Tektronix P6015A (high voltage probe) and Tektronix P6021 (large-current probe) designed via inductive coupling and Hall-effect coupling, respectively, were used to measure the breakdown voltages and the discharge currents for two different inter electrode gaps and various gas injection rates.

I. Volt-Ampere characteristic curves

Fig. 3.3 (a, b) shows some typical voltage and current waveforms for an air-injected discharge, and Fig. 3.4(a, b), shows for an oxygen-injected discharge.

A water plasma discharge follows a mechanism of bubble and gas channel formation inside the gas-injected liquid and the occurrence of plasma inside these bubbles and gas channels, whose implosion participates in liquid plasma generation. Two types of bubbles are formed in the water-carrying current: micro bubbles, which are generated as a result of the joule heating effect (due to the applied electrical energy) and whose density is higher around the electrode tips (because the energy is

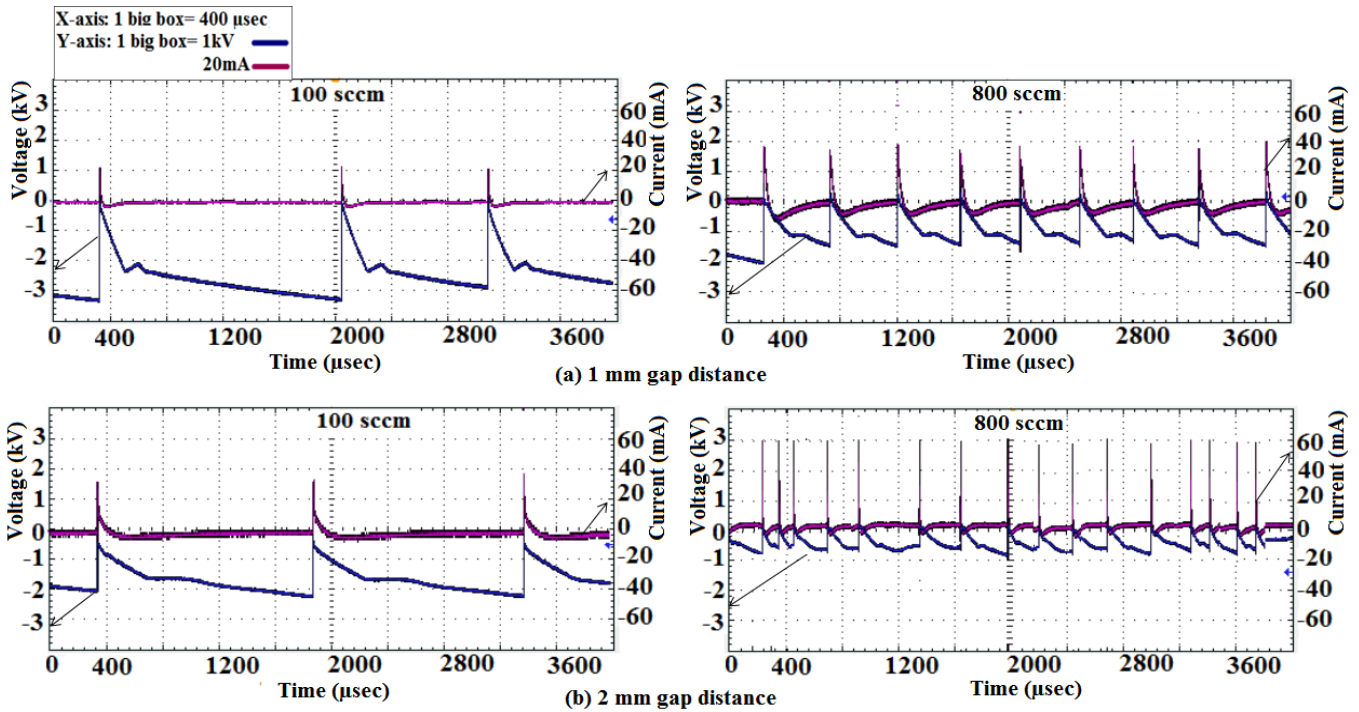


Fig. 3.3 (Color online) IV characteristics of air-injected discharges with (a) 1-mm and (b) 2-mm gap distances.

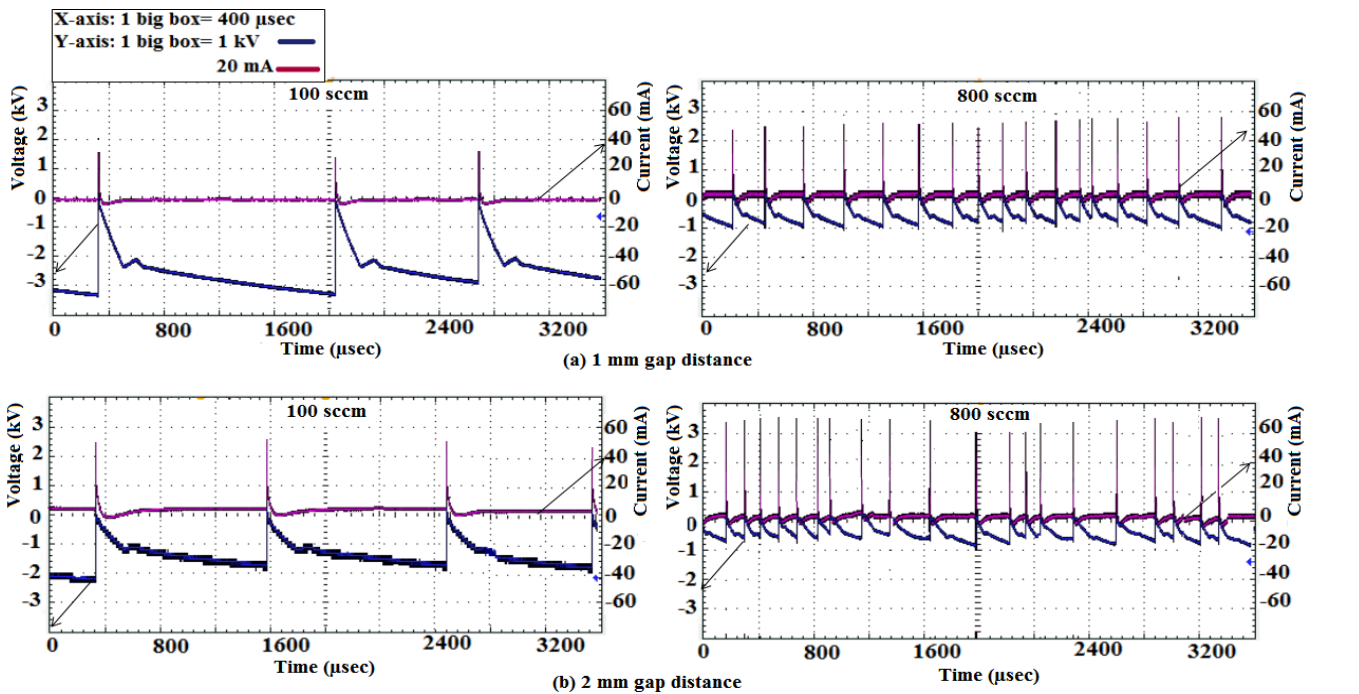


Fig. 3.4 (Color online) IV characteristics of oxygen-injected discharges with (a) 1-mm and (b) 2-mm gap distances.

sufficient to boil the water there), and large size bubbles, which are generated by the gas injection. The injection of gas also generates gas channels, with various shapes and sizes inside the liquid. Inside the gas channels and gas bubbles exist conduction electrons, and the gas is ionized and a plasma discharge occurs. The population of charged particles and the rate of ionization inside the bubbles and the gas channels depend on the sizes of the bubbles and gas channels. The larger the gas channels and bubbles are, the higher the density of the charge carriers and the ionization rate inside them. The bubbles move randomly inside the quartz tube and change their positions randomly and quickly. When a bubble comes to the inter electrode gap, a discharge occurs through the bubble because the dielectric strength of the gas bubble is less than that of water. However other bubbles pass the electrodes, so the encounter between bubble and the electrode is a statistical one. In each gas channel and bubble where the gas breakdown mechanism occurs, at the time of breakdown, the discharge current raises and the voltage drops. The implosion of bubbles and gas channels contributes to the plasma formation inside the liquid.

The generation of both bubbles and gas channels, the occurrence of plasma inside these bubbles and gas channels, and their implosion is a repeated periodic process; therefore, the discharge is pulsating. Although a negative DC is applied, the discharge is pulsating, with a microsecond time difference between discharge occurrences and microsecond pulse discharge duration.

II. Time between occurrence of discharge pulses

Fig. 3.5 (a, b) show the average time difference between the occurrences of discharge pulses at various gas injection rates and inter electrode gaps. At higher gas injection rates, the sizes of the bubbles and the gas channels increase; therefore, the volume of ionized gas inside these bubbles and gas channels becomes larger. This increases the number of water breakdown inside the gas channels

and gas bubbles; therefore, the time between the discharge pulses becomes short, and a high-frequency discharge is obtained.

III. Breakdown voltage

As the electron impact collision also causes ionization, the higher electron density inside the liquid or gas drastically enhances the ionization. The oxygen-injected discharge carries more conduction electrons inside the gas channels and gas bubbles; therefore, compared to air, a slightly higher-frequency discharge is obtained, which is more effective for water sterilization. The breakdown voltage as a function of the gap distance and gas injection rates is presented in Figs. 3.6 (a, b). An increase in the gas injection rate causes reduction in the breakdown voltage for both oxygen and air because of the increase in the density of water bubbles, which plays a vital role in causing water breakdown.

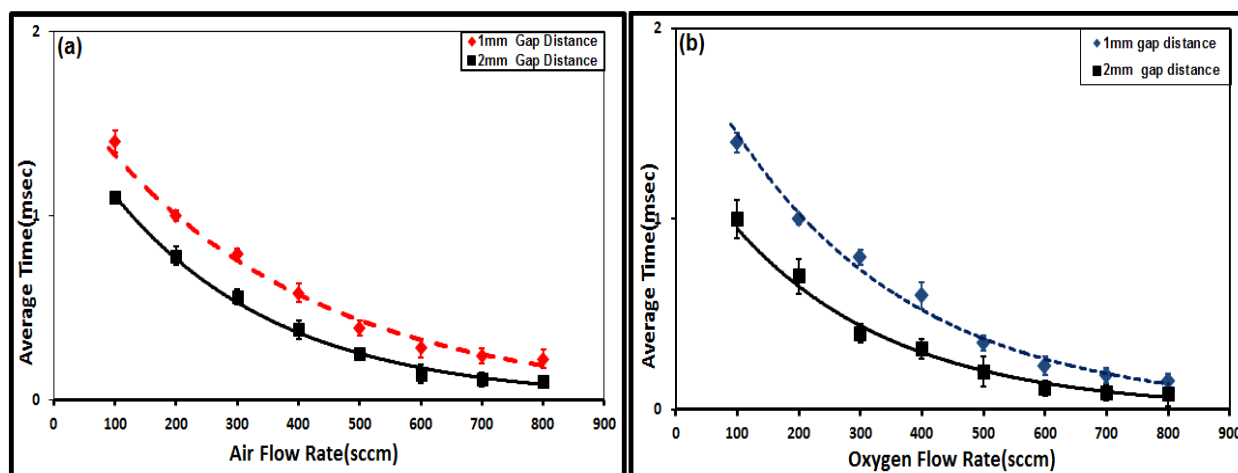


Fig. 3.5 (Color online) Average time interval as a function of the gas flow rate for two different gap distances: (a) air and (b) oxygen.

The breakdown voltages for oxygen and air were compared, and in the case of oxygen injection, a lower breakdown voltage is observed to be needed compared to nitrogen-containing air. The reason for this is that for plasma generation, ionization is important in a gas plasma, liquid plasma, and liquid-gas plasma. Thus, due to the low ionization energy for oxygen (13.61 eV), a lower ionization potential

(provided by electrical energy) is required compared to air. Air consists of nitrogen as a major element, and the electronic configuration of nitrogen is $(1s^2 2s^2 2p^3)$ while that of oxygen is $(1s^2 2s^2 2p^4)$; therefore, the fourth electron in the oxygen atom's outer level has to pair up with one of the others, and this introduces repulsion, which makes it easier to remove it at a lower ionization potential provided by the electrical energy. While in the case of nitrogen, which is a major element of the air used in this work, a higher ionization potential (14.53 eV) is needed because the p-orbital is more stable than it is in oxygen, as in oxygen, it is half-filled; therefore, the ionization energy becomes less in oxygen than in air. Also, the dielectric strength, (breakdown voltage) of air (0.97) and nitrogen (1.00) are more than that of oxygen (0.92), so air-containing bubbles require more voltage for creating a breakdown compared to oxygen-containing bubbles [122].

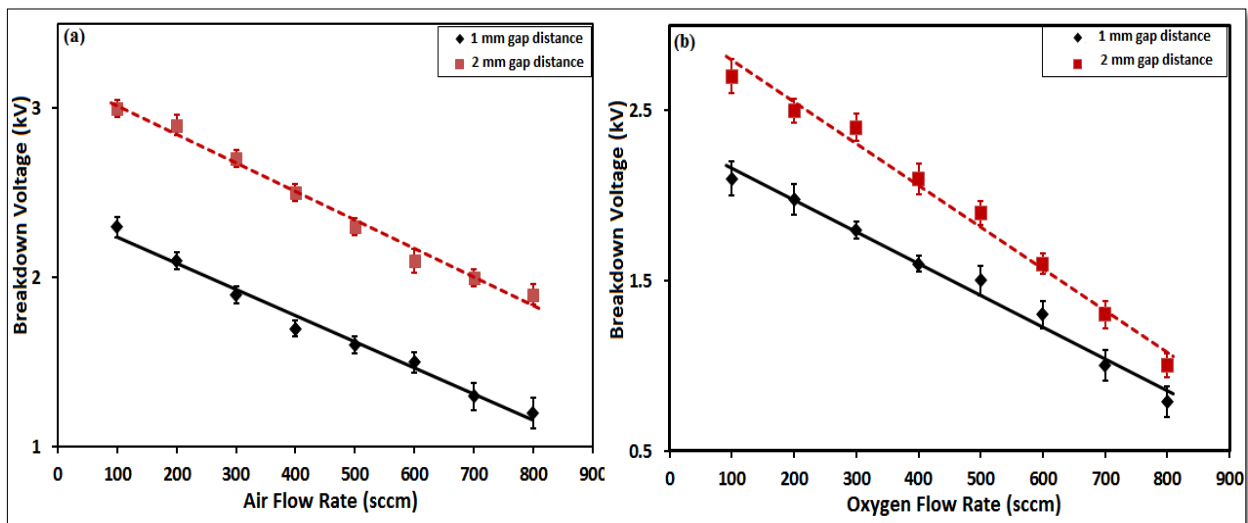


Fig. 3.6 (Color online) Breakdown voltage as a function of the gas flow rate at two different gap distances: (a) air and (b) oxygen.

IV. Energy of discharge pulses

Fig. 3.7 (a, b) show the average energy per pulse for various gas injection rates and two different gap distances.

Due to the elongation of the gas channels and the increase in the number density of bubbles, the discharge current inside these bubbles and gas channels becomes higher. An oxygen-injected discharge has more energy per pulse than an air-injected discharge because of the large number of conduction electrons and large discharge current inside the gas channels and bubbles and because of the liquid medium in the gap between the two electrodes.

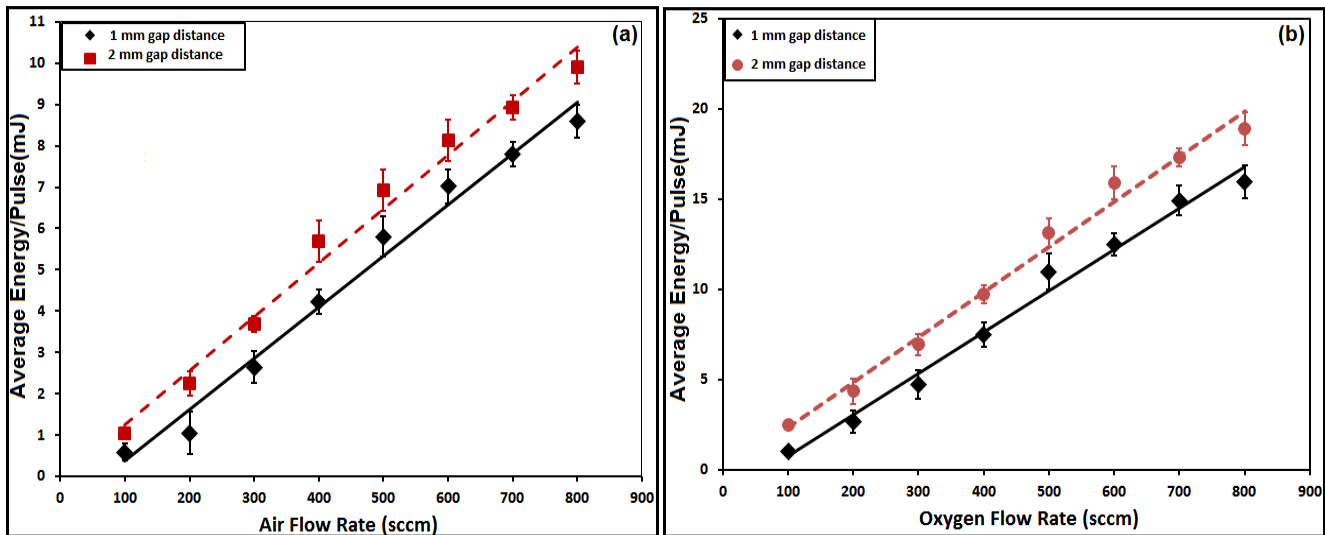


Fig. 3.7 (Color online) The average energy per pulse at different gas flow rates for 1-mm and 2-mm gap distances (a) air injected and (b) oxygen injected.

V. Discharge pulse duration

Fig. 3.8 (a, b) show the variation of the discharge pulse duration calculated based on the calculations of full width at half maximum (FWHM) for the IV curves of electrical outcomes.

At higher gas injection rates, the discharge current increases, and some part of voltage drops rapidly; thus the discharge is no longer continuous and so the pulse width decreases. In an oxygen-injected discharge, the conductivity is higher than it is in an air-injected discharge; therefore the pulse width in an oxygen-injected discharge is shorter than that in an air-injected discharge.

IV. Power of discharge pulses

Fig. 3.9 (a, b) show the variation of the average power of the pulses with gas and gap distance variations.

In a unit time at high gas injection rates, the occurrence of discharge pulses and the energy per pulse increase; therefore, the average power of the pulses rises. Because the frequency of discharge pulses increases at 2 mm inter electrode gap, the average power of the discharge pulses is more than it is for a 1 mm gap distance.

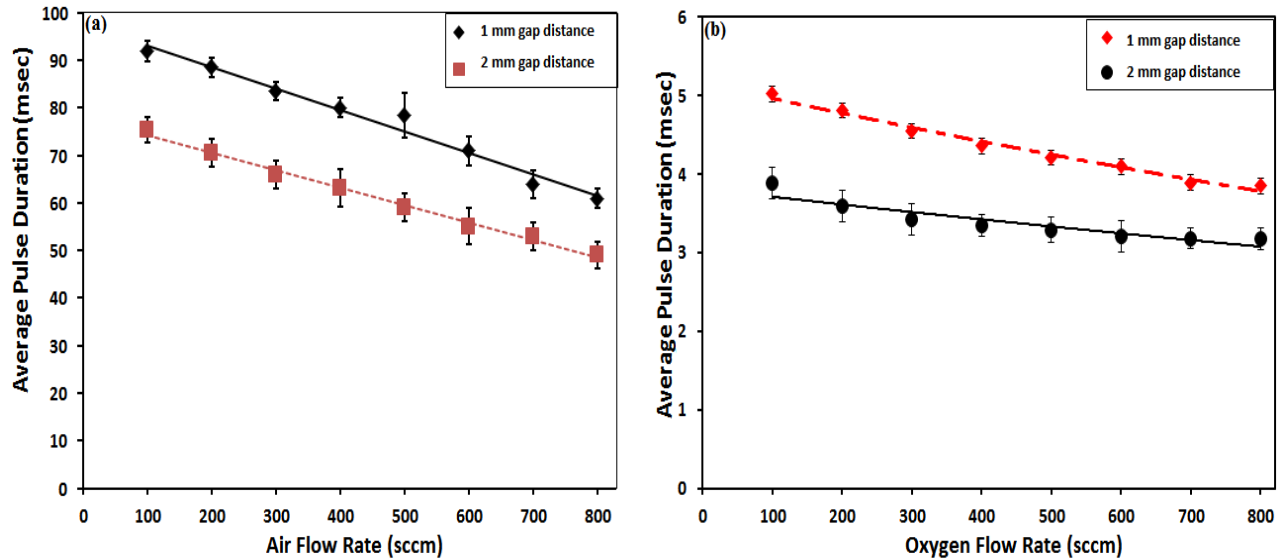


Fig. 3.8 (Color online) Average pulse duration as a function of the gas flow rate for 1-m and 2-mm gap distances: (a) air and (b) oxygen.

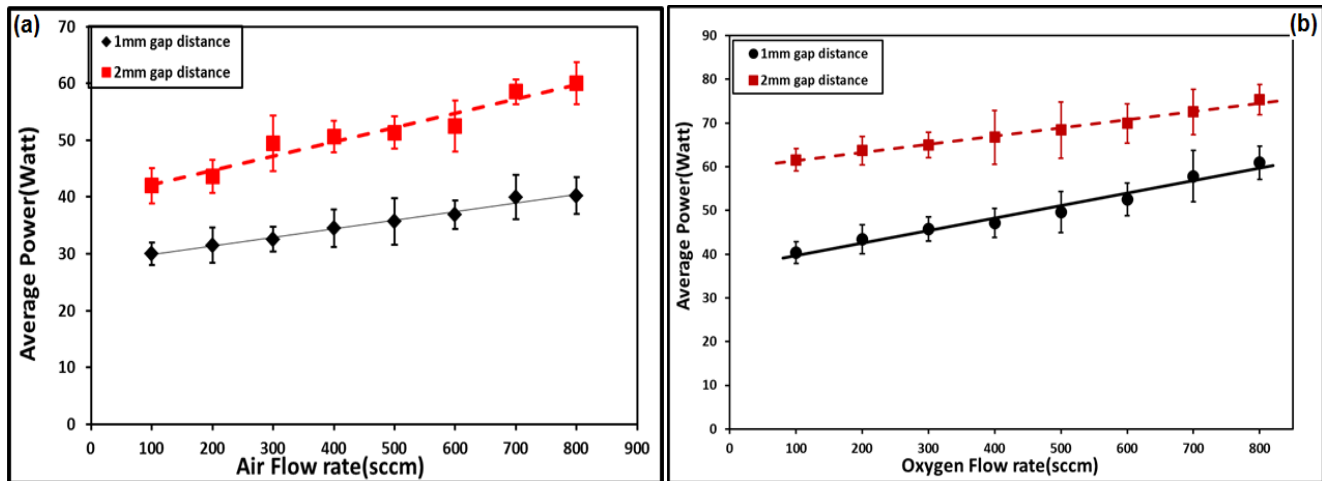


Fig. 3.9 (Color online) Average power of the pulses occurring per second as a function of the gas flow rate for 1-mm and 2-mm gap distances: (a) air and (b) oxygen.

The electrical results prove that with the increasing gas injection rate, the breakdown voltage, the time interval between pulse occurrences, and the discharge pulse width decreases, but the average power of the pulses increases; the frequency of the discharge pulses increases as well, giving rise to a stronger discharge.

3.4.2. Spectral diagnostics

a). Emission Spectroscopy

When plasma was generated between the two electrodes inside the quartz tube, the emission spectrum of $OH\cdot$ radicals and other reactive oxidant species was obtained. This spectrum consisted of a wavelength range greater than 250 nm and less than 900 nm, with $OH\cdot$ radical peak at 309 nm, a Balmer α -peak at 656 nm, and a Balmer β -peak at 486 nm of hydrogen and highly reactive oxygen peak at 777 and 844 nm [123]. Along with this, some other peaks were observed, which were produced in large quantities as a result of the discharge produced inside the capillary tube. Fig. 3.10 (a, b) show the spectral results obtained from air-injected plasma.

The spectral results also show that an increase in the gas injection rate causes an increase in the reactive oxygen and hydrogen species, which react with the water molecules and sterilize water. The comparison of the air and the oxygen spectra proved that $OH\cdot$ radicals had a high concentration in the case of oxygen injection because more ionization took place in the case of oxygen atoms compared to nitrogen containing air, which were due to the oxygen injected discharge having more energy per pulse and a higher frequency. Fig. 3.11 (a, b) shows the spectral peaks of the oxygen-injected plasma. The concentration of $OH\cdot$ radicals was higher at higher gas injection rates and long gaps because the bubble density and the length of the gas channel increased with increasing gas injection rates.

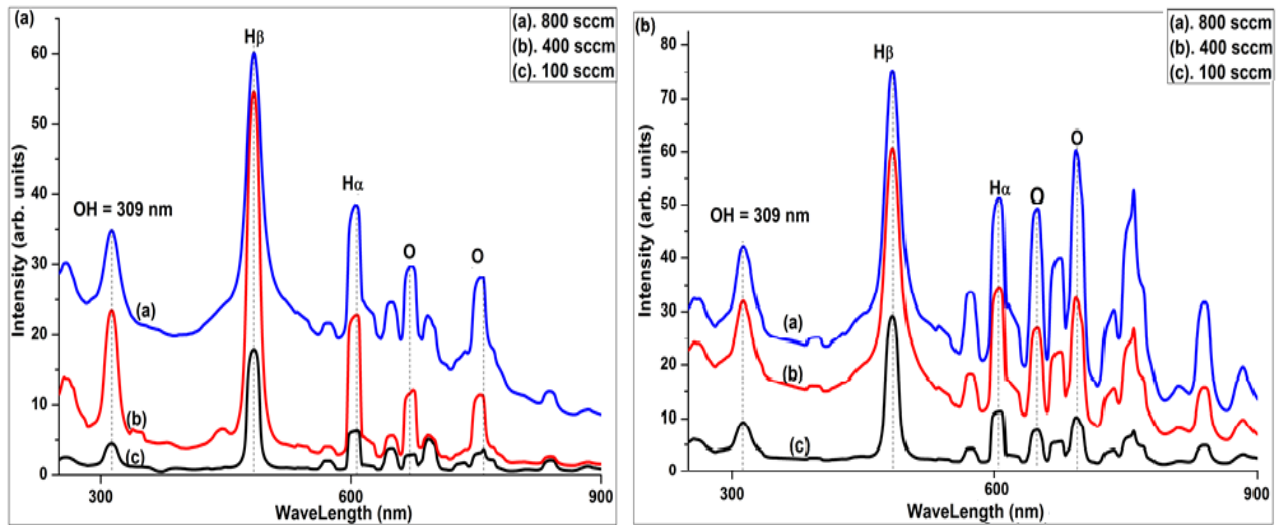


Fig. 3.10 (Color online) Emission spectrum of OH radicals for (a)1-mm and (b) 2-mm inter electrode gaps and various air injection rates.

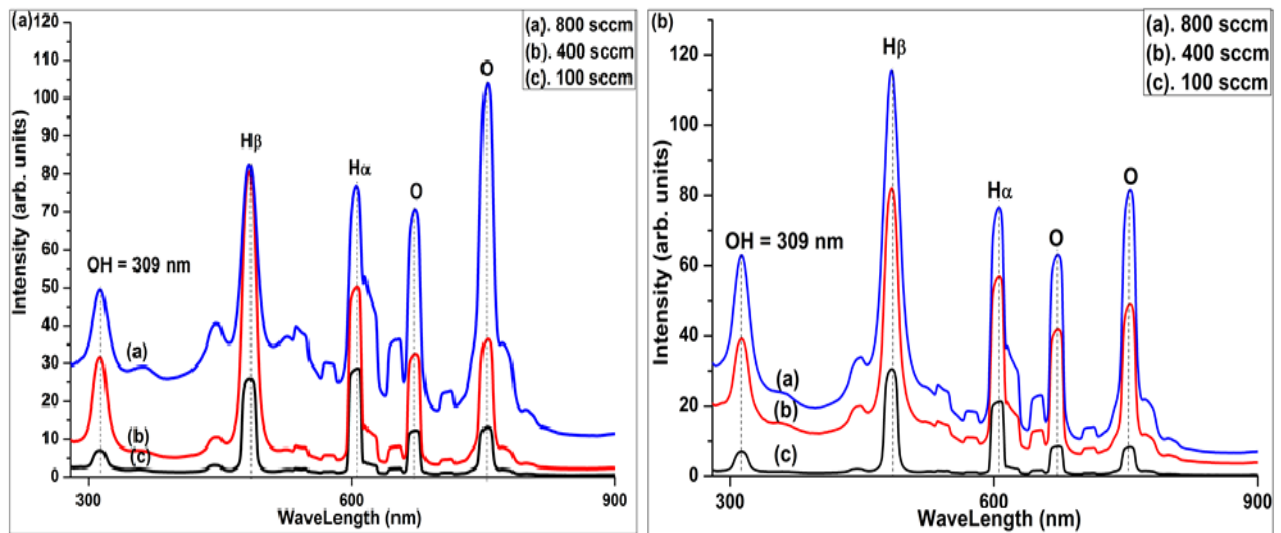


Fig. 3.11 (Color online) Emission spectrum of the OH radicals for (a) 1-mm and (b) 2-mm inter electrode gaps and various oxygen injection rates.

Also at a low voltage and less power consumption, more OH radicals were obtained while at a long gap distance, as the discharge zone increased, a higher dissociation of water molecules into OH radicals and other reactive species occurred.

b). Gaussian Function and $OH\cdot$ Radicals

The concentration of $OH\cdot$ radicals was calculated via a Gaussian de-convolution by using the following equation [124]:

$$\int_{-\infty}^{\infty} Fi(x)dx = A_i\sigma_i\sqrt{2\pi}. \quad (1)$$

The calculations are the concentration of the $OH\cdot$ radicals for the 1 and the 2 mm inter electrode gaps at various air and oxygen injection rates.

Fig. 3.12 (a, b) shows the concentration of the $OH\cdot$ radicals for different air and oxygen injection rates for the 1 and the 2 mm gaps, respectively. The results prove that an increase in oxygen injection rate causes an increase in the yield of $OH\cdot$ radicals compared to air injection.

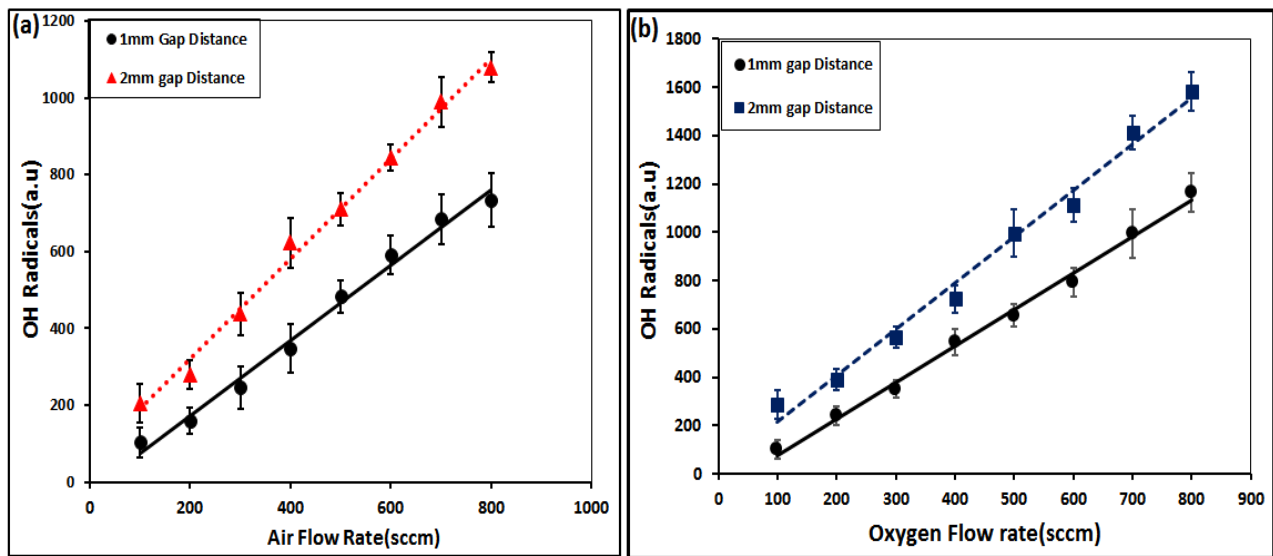


Fig. 3.12 (Color online) Concentration of $OH\cdot$ radicals by using a Gaussian function for various gas injection rates and two different inter electrode gap distances: (a) air injection and (b) oxygen injection.

3.4.3. Imaging diagnostics

(a) High Speed camera Imaging

In an air injected discharge, the discharge current, frequency of discharge pulses, energy per pulse, and the average power of discharge pulses are less than they are for an oxygen-injected discharge. Also the illumination intensity of oxygen-injected discharge is higher compared to that of an air-injected discharge.

Figs. 3.13 (a, b) and 3.14 (a, b) present typical images of the fully developed discharge structures at various oxygen and air-injected rates, respectively, at two different inter electrode gaps.

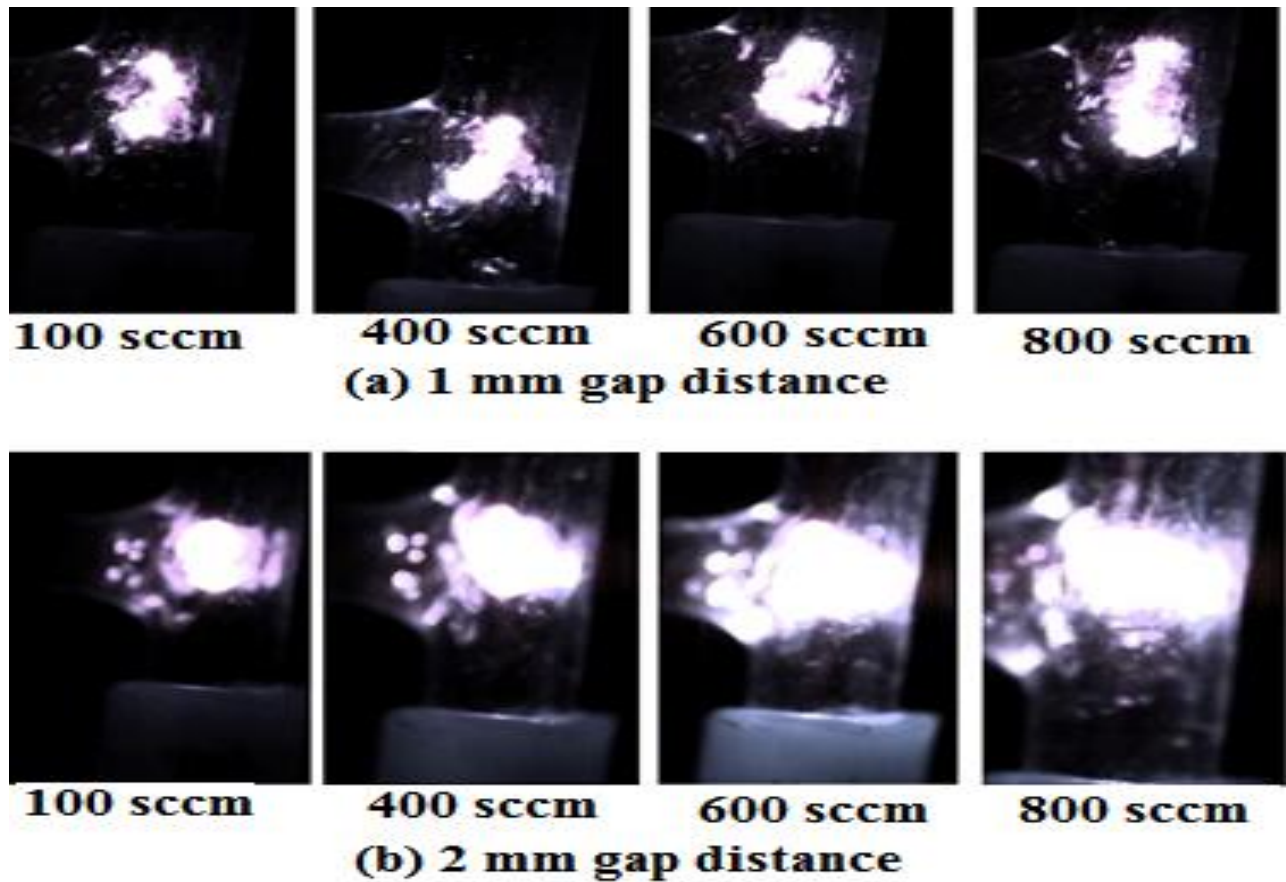


Fig. 3.13 (Color online) Oxygen injected discharges.

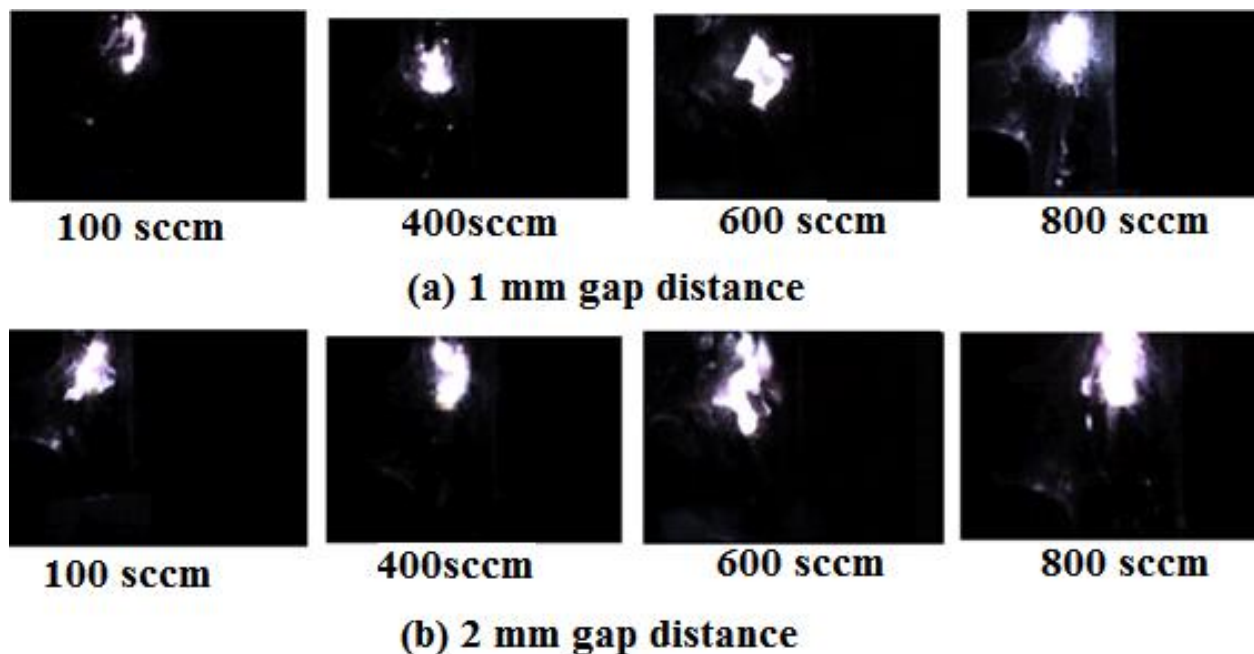


Fig. 3.14 (Color online) Air injected discharges.

In the oxygen-injected discharge the emission of radiations, ozone generation and the yield rate of oxidant species are more than they are in an air-injected discharge. The highly luminous oxygen-injected discharge is more useful for generating $OH\cdot$ radicals and water disinfection compared to air-injected discharge.

The discharge expands more with increasing gas injection rate in the case of oxygen-injected discharge than it does in an air-injected discharge. The high-intensity radiation emitted from the broader oxygen-injected discharge can generate more $OH\cdot$ radicals, as discussed previously for better sterilization of water on the generation of oxidant species. This means that an oxygen-injected discharge is better for the sterilization of water.

(b) Thermal camera Imaging

The images taken by thermal video system (TV-BM002) that indicates the shapes of varying discharge structure. Fig. 3.15 (a-f) and Fig 3.16 (a-f) shows the discharge structure obtained for at variable inter-electrode gap length. The discharge expands slowly in the surrounding regions and in the

direction of flow of water due to increase in water temperature and increase in number density of gas bubbles and gas channels within capillary at higher gas injection rates.

At 2mm gap distance and higher gas injection rates, since the elongation of gas channels and size of gas bubbles increased therefore expanded discharge was observed. Moreover at the center of discharge region (in front of electrodes) the temperature is high and while discharge expands then towards sides the temperature reduced. Brighter portion of discharge indicates more intense and high temperature discharge. The thermal imaging system represents the variation in temperature of plasma from central core to the edges.

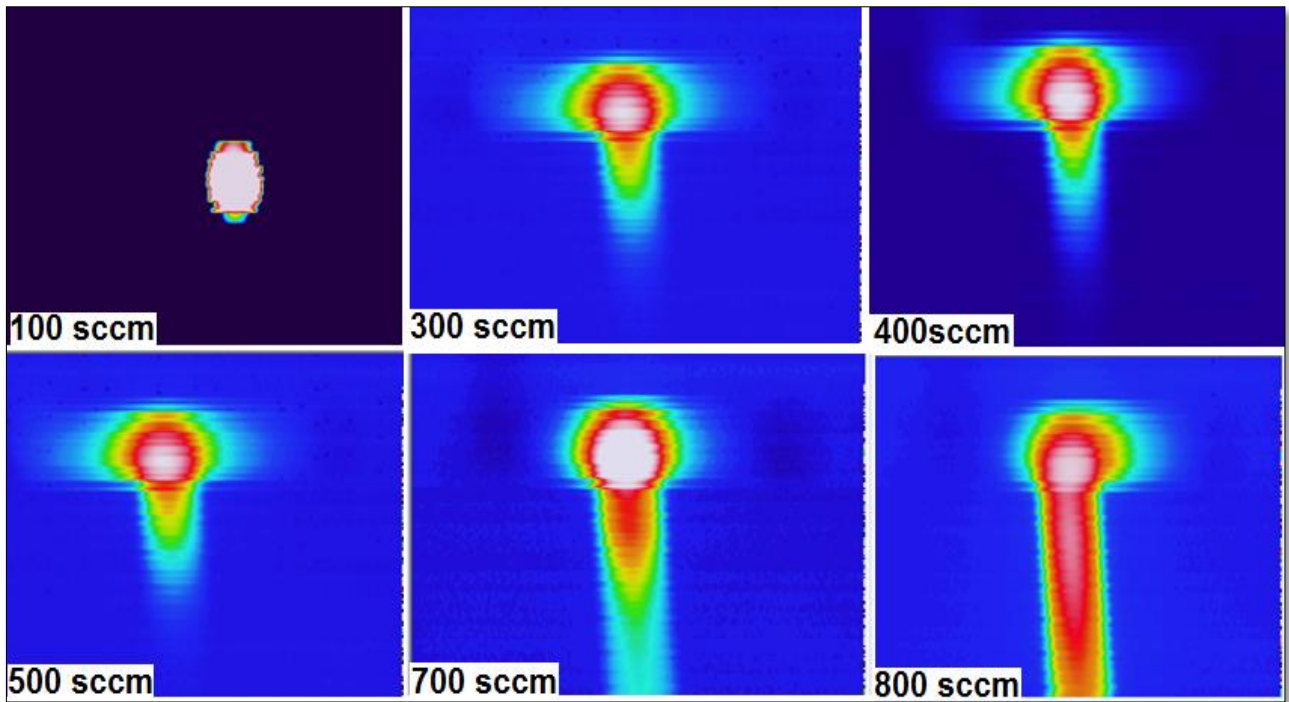


Fig 3.15 The discharge structure at 2mm Inter-electrode gap distance for various air injection rates.

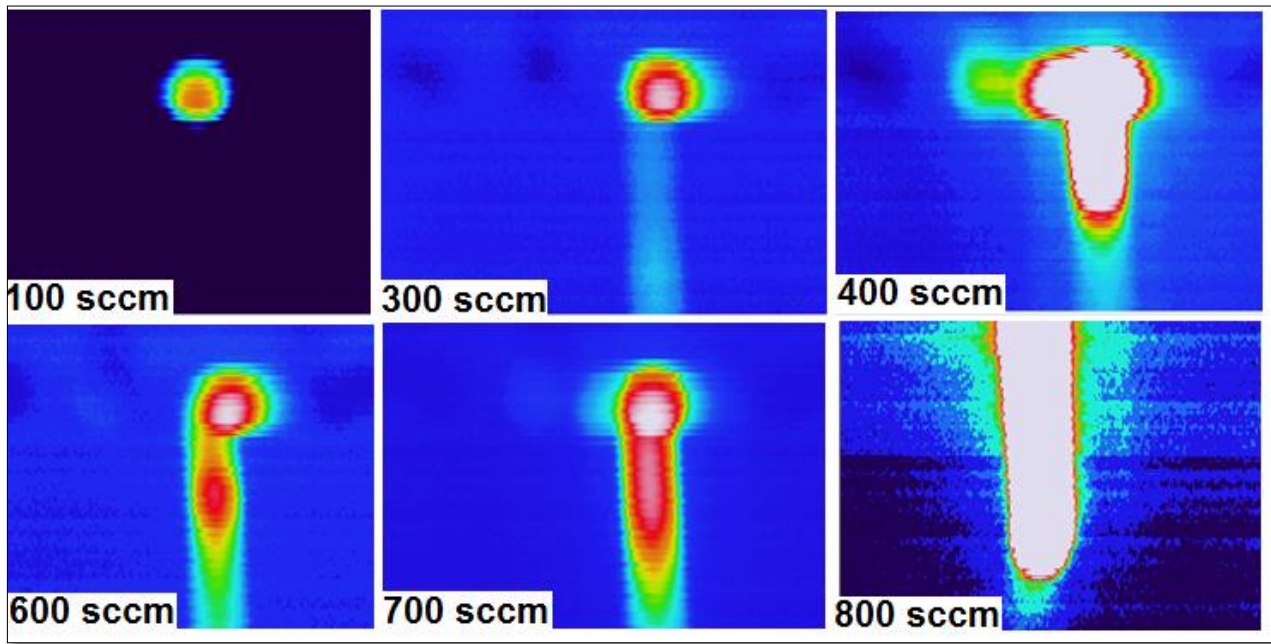


Fig 3.16 The discharge structure at 2mm Inter-electrode gap distance for various oxygen injection rates.

3.5. Conclusions

Long gap oxygen injected underwater capillary discharge is an effective method of generating high concentration of $OH\cdot$ radicals in flowing water capillary discharge. The issue of high power consumption could be resolved by injecting gas in water medium. Compared to air more highly powerful and energetic discharge pulses could be obtained after oxygen injection.

4. Appraisal of Plasma Electron Temperature and Number Density and Their Effect on Chemical Reactive Species in a Gas Injected Negative DC Underwater Capillary Discharge

4.1 Introduction

Liquid plasma plays a vital role in a large type of industrial and environmental applications, including sterilization of drinking water to make it free from dangerous bacteria, to remove odor from drinking water, sea water blasting used in ships, for cooling water treatment to reduce calcium carbonate precipitation and hardness, chemical applications by generating direct discharge in liquid chemicals, biological applications, medical applications and also in polymer industry [125-128]. Therefore different kind of applications in underwater discharge relies on measurement of basic plasma parameters such as, T_e , N_e and yield rate of highly reactive species [129]. Due to high dielectric constant of water electrical power consumption for generating plasma in water is most challenging issue and since last few decades many techniques including pulse-power technology, high frequency alternating current, and wave heating were adopted and tested to check required input power reduction [130-132]. For this reason rapid information concerning T_e and N_e is often used as the first step in solving power consumption problem and suggesting an effective way of generating plasma in water. Some techniques like Thomson scattering and probe method used for finding T_e and N_e , but have some disadvantages. Thomson scattering is an expensive way and having complicated experimental assembly, in spite of its accuracy, precision and spatial and temporal resolution [133]. In probe method like Langmuir probe the plasma stability altered by probe and also the results may not too accurate as the changing distance of probe tip from plasma region alters the calculated values [134], moreover sputtering from the probe tip due to high temperature takes place. Also due to small gap and short discharge period, the measurement of such plasma characteristics by probe method is extremely

difficult and inaccurate. Generally statistical techniques (Stark broadening, intensity ratio method) on hydrogen emission lines can be effective to determine physical characteristics of plasma conveniently.

Optical emission spectroscopy (OES) is an effective technique for the determination of physical characteristics of plasma and correlating to the chemical reactive species yield rate in plasma. By comparing emission intensities of hydrogen Ballmer spectral lines ($H_{\beta}=486.127$ nm and $H_{\alpha}=656.285$ nm) and considering plasma approximation in *local thermodynamic equilibrium* (LTE) the electron temperature can be estimated [135]. Based on the relative intensities of emission lines, this spectroscopic technique can be used to measure T_e in plasma [136]. The Stark broadening method can be applied to determine N_e using various relations available in literature [137]. A relation from Gig-Card theory was applied on H_{β} lines to determine N_e [138]. The method is technically relevant and would act as baseline data for relating the physical and chemical characteristics of underwater plasma discharge.

The scope of this work was to determine and compare the effect of electron temperature (T_e) and number density (N_e) on the yield rate and the concentration of chemical reactive species ($\cdot\text{OH}$, H_2O_2 and O_3) in argon, air and oxygen injected negative dc (0-4kV) flowing water (0.1L/min) capillary discharge. The discharge was created in a quartz capillary tube (inner $\Phi=2$ mm, outer $\Phi=4$ mm, thickness=1mm), across tungsten electrodes ($\Phi=0.5$ mm) separated by a variable distance (1-2mm) in pin-pin electrode configuration, with various gas injection rates (100-800sccm). Optical emission spectroscopy (OES) of the hydrogen Ballmer emission lines were carried out to investigate their line shapes and intensities as functions of the discharge parameters such as type of gas, gas injection rates and two different inter electrode gaps. The intensity ratio method on hydrogen emission lines was used to calculate T_e and relation from Gig-Card theory was applied on hydrogen Ballmer β lines for determining N_e . The effect of T_e and N_e on chemical reactive species was evaluated and presented. The enhancement in yield rate of chemical reactive species with increase in electron temperature and at

higher gas injection rates, higher power of discharge pulses and larger inter-electrode gap was revealed. The oxygen injected discharge proved effective for high concentration of chemical reactive species. This method offers a convenient way of determining relation between the physical and chemical characteristics of flowing water gas injected negative dc capillary discharge.

4.2 Materials and methods

Fig. 4.1 shows a schematic of the experiment set-up that was used for this experiment. A visual view of the discharge is shown in Fig. 4.2. The inter electrode gap where the plasma generated was varied from 1 – 2 mm, and the inlet contained water. A liquid flow meter and controller (Dwyer-RM Series) was used to control the flow rate of water at 0.1 L/min through plasma generating quartz capillary tube. An air compressor (CROX-RX47L) was used to provide an air stream controlled by an air regulator, and the flow rate of air was measured with an air flow meter (KOFLOC-1600) for different adjusted flow values (100 – 800 sccm). A mass flow controller (LINE TECH M3030V), along with a mass flow control and display unit (FM-30VP), was used to control and provide the argon and oxygen flow rates for different adjusted values (100 – 800 sccm). An Avantes Avaspec-NIR256 miniature fiber-optic spectrometer (having specification of spectral resolution 0.04-20nm, slit size 500 μ m having 1200 lines/mm) was used to record the emission spectrum of Hydrogen Ballmer lines under different experimental conditions.

Two tungsten electrodes were inserted in the quartz tube, and one electrode was connected to the negative DC power supply source while the other was connected to the same source's ground terminal. An injection syringe was used to inject argon, air and oxygen. The water from a small tank reservoir was allowed to enter the quartz capillary tube through the liquid flow meter that measured the flow rate of liquid.

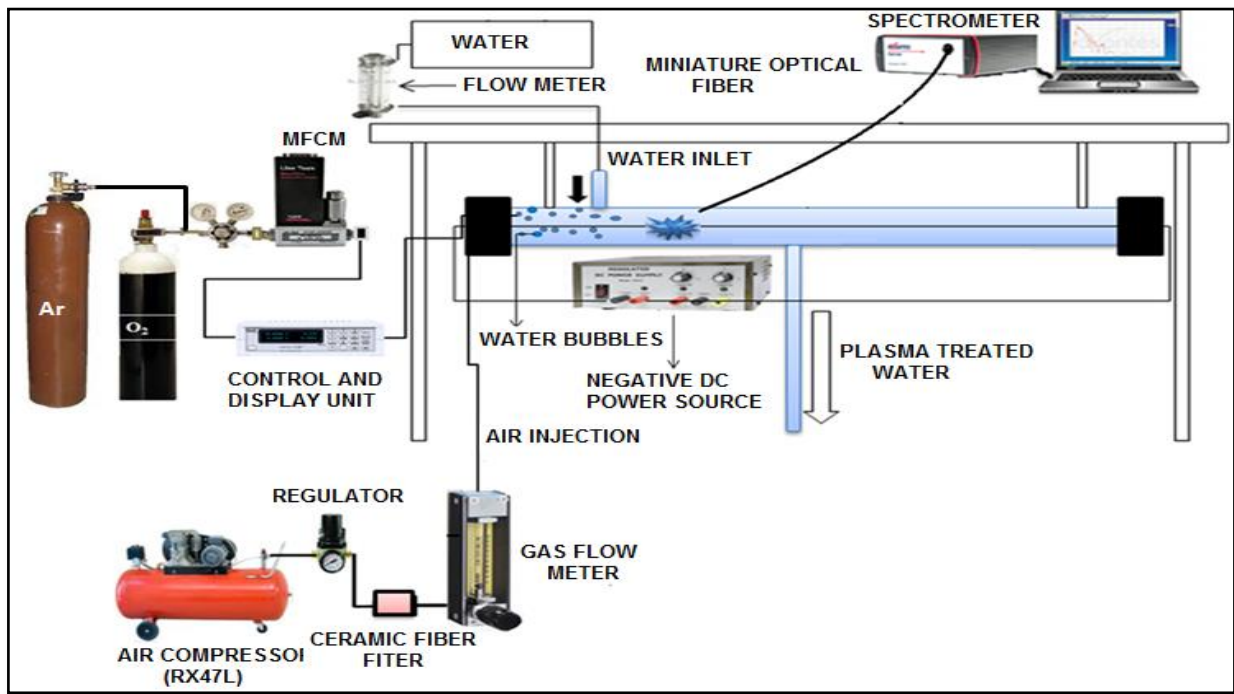


Fig. 4.1 Experimental Setup for underwater capillary Discharge.

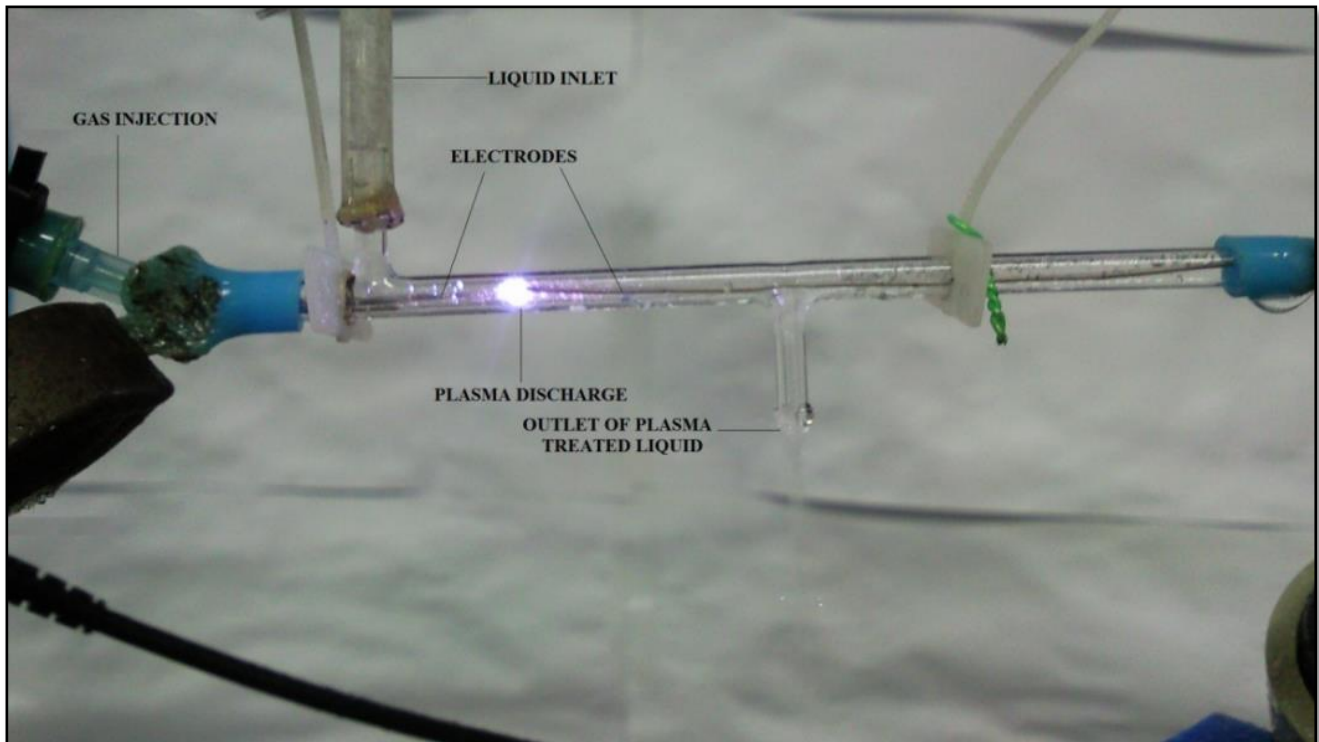


Fig. 4.2 Visual view of the discharge

When the gas and the liquid simultaneously entered the quartz tube, in the liquid, the gas generated bubbles, and these bubbles participated mainly in breaking down the liquid. The air, argon and oxygen stream were injected in the range of 100 – 800 sccm, in 100 sccm intervals. The electrical data was recorded using a digital oscilloscope with high- voltage and large-current probes, and with a data storage device facility. The emission spectrum of hydrogen Ballmer lines was recorded with a spectrometer when discharge occurred. Under all the presented experimental conditions, the electrical and spectral data were taken simultaneously to study, compare, and present the results.

4.3 Results and discussion

4.3.1. Electrical Results

A digital oscilloscope Tektronix (DPO-2024) was used for observing Volt-Ampere characteristics. A high voltage probe (Tektronix P6015A) and a large-current probe (Tektronix P6021) designed via inductive coupling and Hall-effect coupling, respectively, were used to measure the breakdown voltages and the discharge currents for two different inter electrode gaps and various gas injection rates. The underwater plasma discharge follows a mechanism of bubbles and gas channels formation inside the gas-injected water and the occurrence of plasma discharge inside these bubbles and gas channels, whose implosion participated in underwater discharge occurrence. The generation of both bubbles and gas channels, the occurrence of plasma inside these bubbles and gas channels, and their implosion was a repeated periodic process; therefore, the discharge was pulsating [139]. Fig. 4.3 represents a typical Volt-Ampere characteristics curve. The streamers propagation was a major phenomenon in plasma discharge occurrence. In case of water medium the streamers exhibit less branching and slow propagation compared to gas medium. In this experiment both water and gas bubbles exists, therefore under influence of applied electric field a quick breakdown and fast streamers propagation appears in gas medium compared to water medium where it was slow.

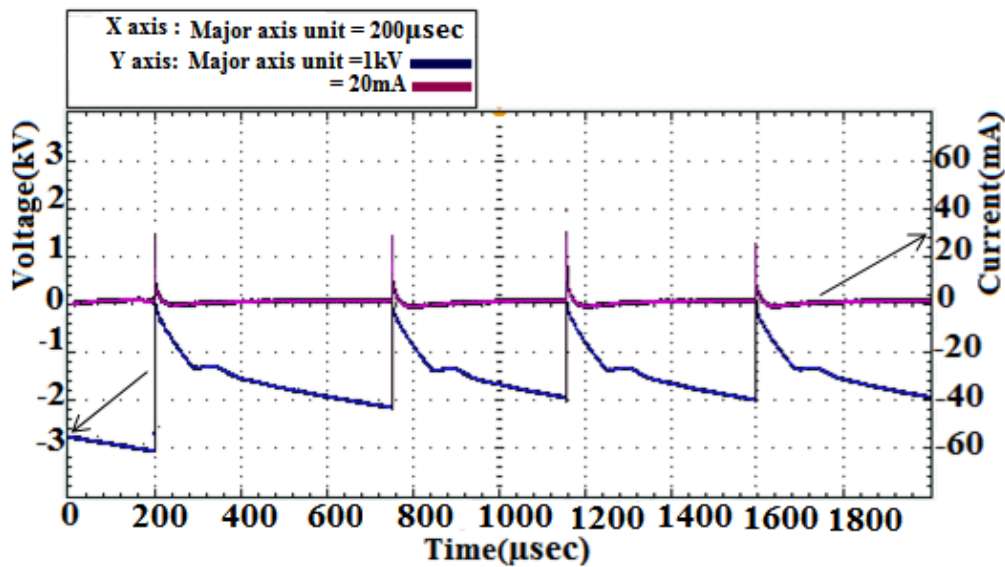


Fig. 4.3 (Color online) Typical Volt-Ampere characteristics of the gas injected discharge.

At high gas injection rate the elongation of gas channels and increase in size of gas bubbles resulted to the high frequency discharge pulses. Moreover the breakdown voltage directly related to the dielectric strength of medium. Although water having high dielectric strength (65-70) kV/mm, but gas injection reduced the dielectric strength due to the existence of gas bubbles and gas channels due to gas injection. The dielectric strength of argon relative to nitrogen is (0.18) and for oxygen is 0.92kV/mm; while for air it is (0.97-1.4) kV/mm [140]. At higher gas injection rates the increased size of gas channels and bubbles reduced the dielectric strength of overall water medium, hence breakdown voltage lessened. Fig. 4.4 (a, b) represents the variation of breakdown voltages under different experimental conditions. Comparing the breakdown voltage of gas injected discharge, argon injected discharge presented lowest while air injected discharge resulted highest breakdown voltage but oxygen positioned at intermediate among these three gasses. It was observed that with increase in gas injection in water, the breakdown voltage reduced.

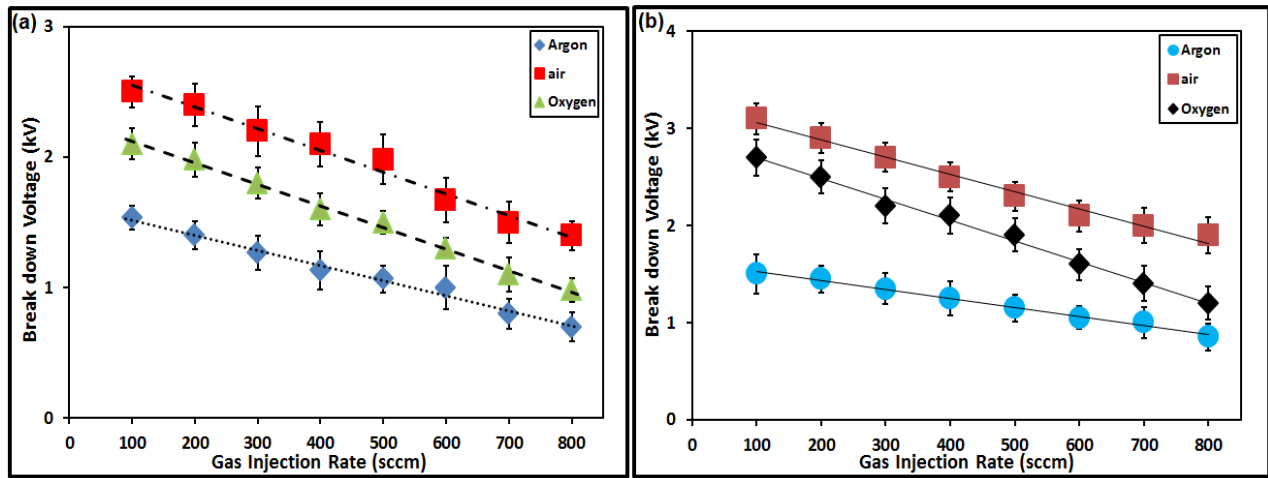


Fig. 4.4 (Color online) Break down voltage (a) 1-mm and (b) 2-mm gap distance.

The higher gas injection rate increased the gaseous medium in water therefore frequency of discharge pulses raised, also the energy per pulse increased due to high gas injection rates, both factors resulted in an increase in power of discharge pulses. Fig. 4.5 represents the variation in power of discharge pulses under different experimental conditions. The power of oxygen injected discharge compared to argon and air was larger due to high energy and frequency of discharge pulses. At 2mm gap distance compared to 1mm gap distance the power was higher as more intense discharge was obtained.

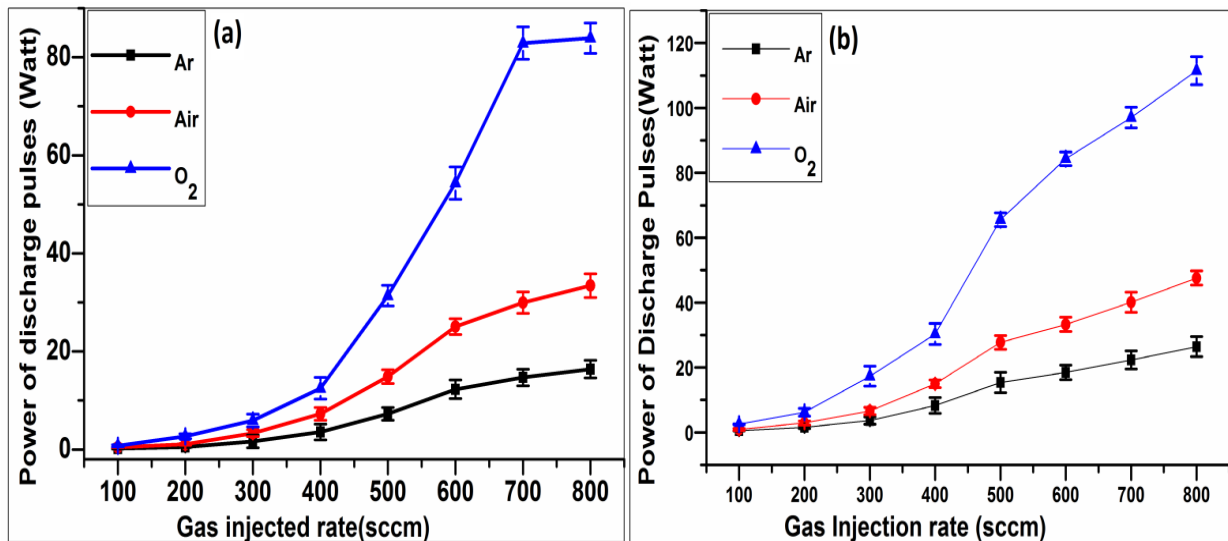


Fig. 4.5 (Color online) variation in power of discharge pulses under different gas injection rates (a) 1-mm and (b) 2mm gap distance.

4.3.2 Hydrogen emission profiles

The hydrogen emissions profiles were recorded as a function of gas injection rates and different inter electrode gaps. Fig. 4.6 (a, b) shows typical emission spectrum of argon injected discharge, while Fig. 4.7 (a, b) shows typical emission spectrum of air injected and Fig. 4.8 (a, b) is for representing emission spectrum of oxygen injected discharge at 1mm and 2mm inter electrode gap distance respectively.

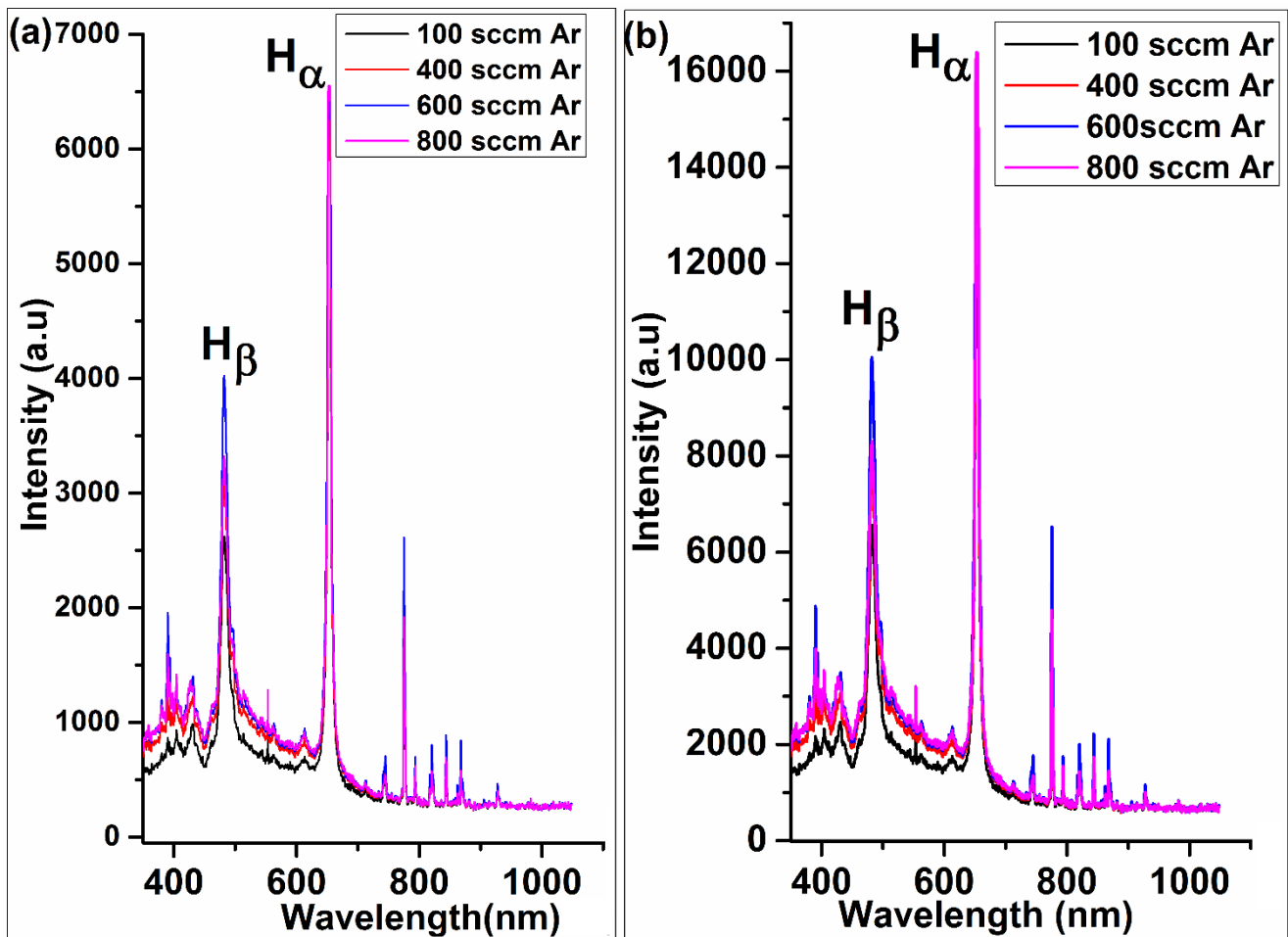


Fig. 4.6 (Color online) Emission spectrum of hydrogen lines at various argon injection rates. (a) 1-mm and (b) 2-mm inter-electrode gaps.

The results demonstrated that the intensity of oxidant species generated by the discharge significantly depend upon the type of gas, gas injection rates and inter electrode gap distances. With increase in gas injections rates and inter-electrode gap distances the strength of discharge and plasma generated

electric fields rises that enhances intensity of spectrum. The emission intensity of oxygen injected discharge proven to be higher compared to argon and air. The main factor that influenced the emission intensity was power of discharge pulses. As in Fig. 4.5(a, b) power of oxygen injected discharge pulses was observed higher compared to air and argon, this resulted in an increase in emission intensity of discharge. The ascent in intensity of emission spectrum with increase in gas injection rates and power of discharge pulses corresponded to an inflation in electron energy distribution function (EEDF), that was highest in oxygen injected discharge and lowest in argon injected discharge and air injected discharge had intermediate values in this experiment. The increase in emission intensity resulted in high electron temperature.

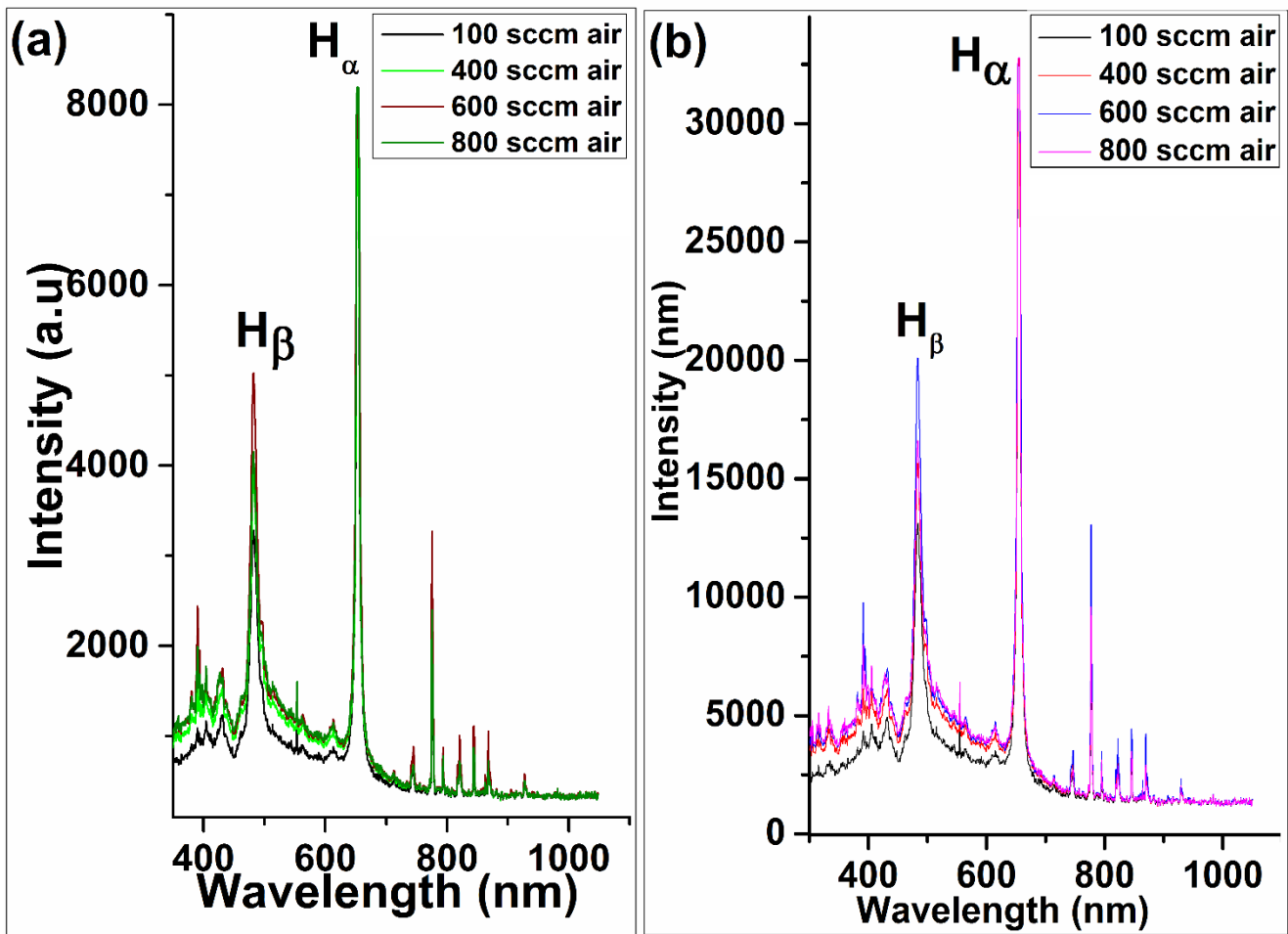


Fig. 4.7(Color online) Emission spectrum of hydrogen lines at various air injection rates. (a) 1-mm and (b) 2-mm inter-electrode gaps .

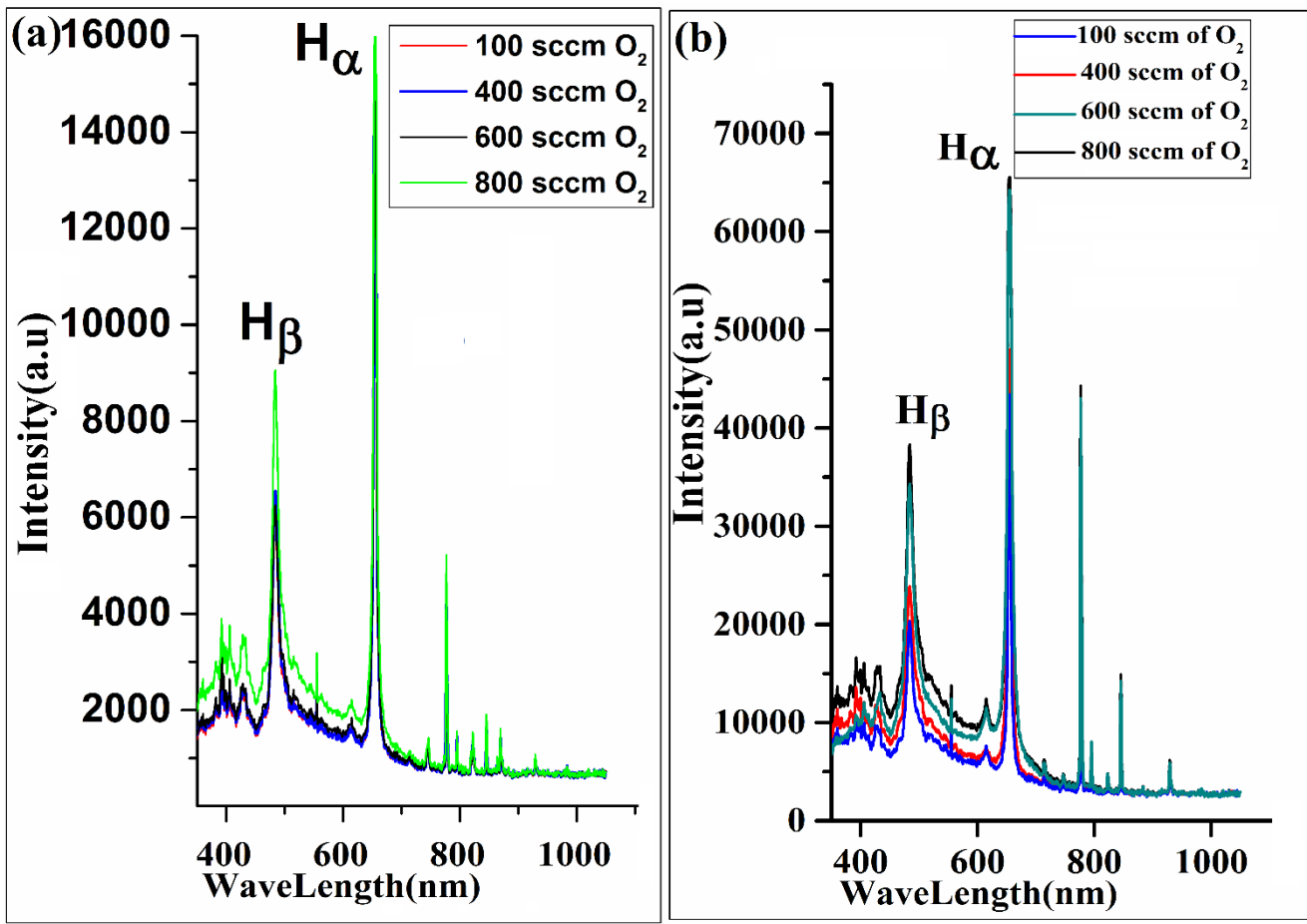


Fig. 4.8 (Color online) Emission spectrum of hydrogen lines at various oxygen injection rates. (a) 1-mm and (b) 2-mm inter-electrode gaps

4.3.3 Calculation of electron temperature (T_e)

Since the free electrons are responsible for the excitation of atoms and molecules, therefore T_e and T_{ext} are inter-related. The emission lines intensity provides physical characteristics of plasma. If the condition of LTE for population densities of upper energy levels of two lines is fulfilled then intensity ratio method is straight forward for the determination of T_e [141]. Considering the intensity of each hydrogen emission spectral line (Ballmer region), the electron temperature was calculated by using relation [142]:

$$T_e = \frac{\Delta E}{\ln \left[\frac{A_1 g_1 \lambda_2 I_2}{A_2 g_2 \lambda_1 I_1} \right] K} \dots \dots \dots (1)$$

Where I , λ , g , K and A are intensity, wavelength, statistical weight, Boltzmann constant and transition probability respectively. The two hydrogen lines 2s-4p transitions for Ballmer- β and 2s-3p for Ballmer- α were used and the numerical values for above relation were taken from NIST database [143]. The intensity of these lines was obtained from the emission spectrum by considering the integration over hydrogen emission profiles and by normalizing instrumental sensitivity with same profiles spectral response.

The emission spectrum was taken after discharge occurrence under different experimental conditions. Depending upon the experimental conditions there was a variation in the intensity and broadness of spectral peaks. Fig. 4.9 represents the electron temperature, its variation under different gas injection rates at 1mm and 2mm inter electrode gaps. The results demonstrated that due to increase in gas injection rate (100-800 sccm), power of discharge pulses and emission intensity of spectrum the electron temperature rises.

In oxygen injected discharge, compared to air and argon, high electron temperature exists due to increase in power of discharge pulses, as discussed in Fig. 4.5. The presence of oxygen-related ions can effectively participate in increasing gas temperature. The expansion of discharge can reduce its

temperature, but the oxygen-related ions seems to be responsible for an overall increase in gas temperature, that prevents lowering electron temperature due to expansion [144].

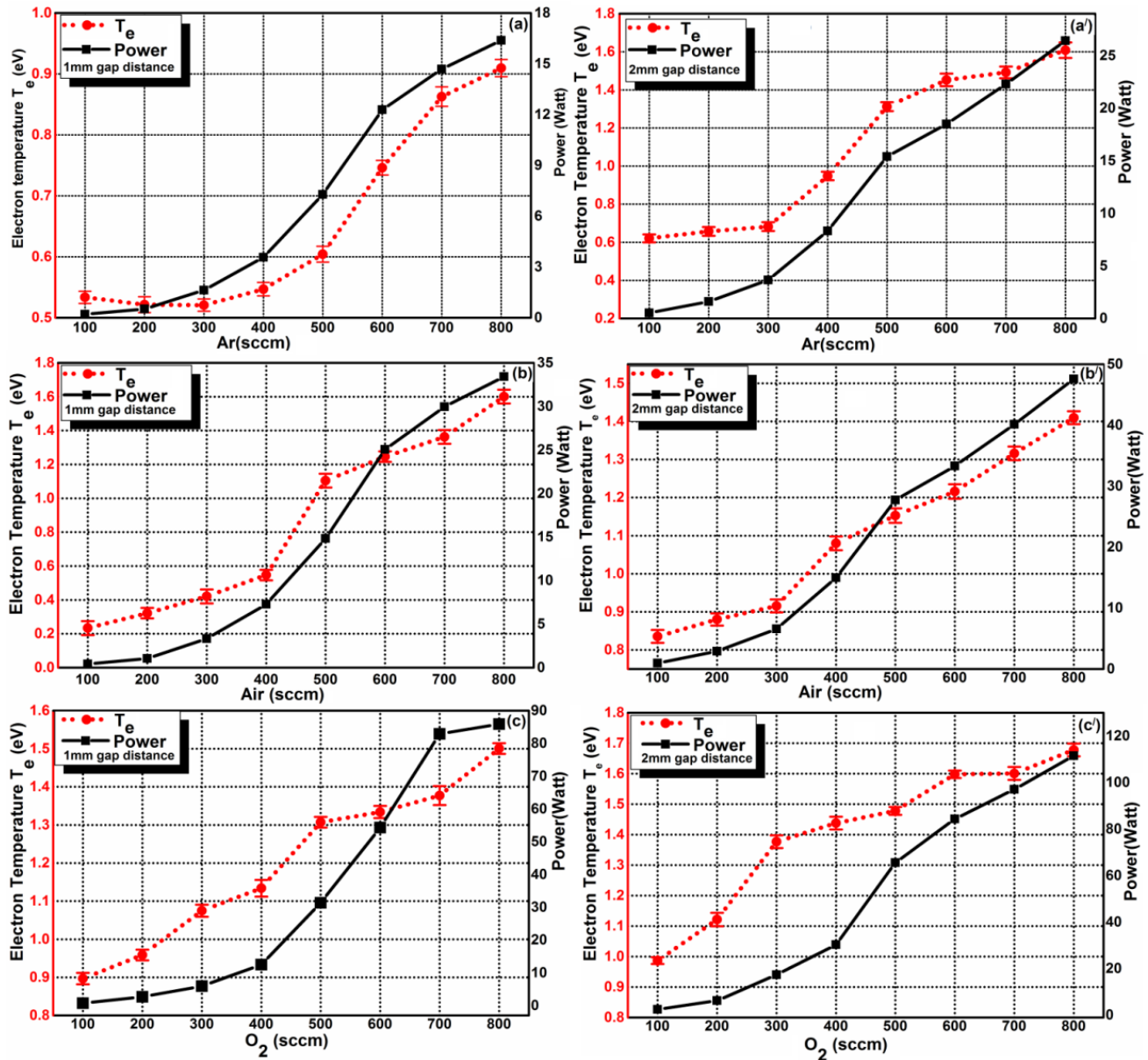


Fig. 4.9 (Color online) Electron Temperature for various gas injection rates and power of discharge pulses at 1-mm and 2-mm gap distances.

4.3.4 Calculation of Electron Number Density (N_e)

Spectra of the discharge have been used to estimate the average electron density from Stark broadening. The emission spectrum of H_β that have probability of broadening due to various factors was used. The most dominant effects are local broadening mechanisms that include mainly Doppler broadening, Stark broadening, and Vander-wales broadening. The mechanisms like Doppler broadening provide Gaussian profiles, while Vander-wales broadening and Stark broadening provides Lorentzian profiles. The Doppler broadening was calculated by relation [145]:

$$\Delta\lambda_D = 7.16 \times 10^{-7} \lambda_0 \sqrt{\frac{T_g}{M}} \dots \dots \dots (1)$$

$T_g =$ gas temperature , $M =$ atomic mass of emitter in atomic mass unit.

The Vander wall broadening was calculated by relation [146]:

$$\Delta\lambda_{vdW} = A P T_g^{-0.7} \dots \dots \dots (2)$$

$T_g =$ gas Temperature, $A =$ Vander wall coefficient having different values ($N_2/Air = 3.6$, $Ar = 5.24$, $O_2 = 1.32$); $P =$ pressure measured in bar.

Since plasma is in water having density high and gas injection increase the strength of discharge that raises the chemical reactions both recombination and ionization therefore , therefore it is estimated that plasma temperature can be equal to gas temperature.

The stark broadening was calculated by FWHM of Ballmer β spectral lines. The Coulomb interaction among the light emitting atoms and some charged particles, like electrons, line broadening can occur due to the Stark effect. The mechanisms like Doppler broadening provided Gaussian profiles, while Vander walls broadening and Stark broadening provided Lorentzian profiles. The convolution of these two phenomena resulted in Voigt profile, that was calculated by following relation [147]:

$$\Delta\lambda_{Voigt} \approx \left[\left\{ \frac{\Delta\lambda_{Lorentz}}{2} \right\}^2 + \Delta\lambda^2_{Gauss} \right]^{\frac{1}{2}} + \frac{\Delta\lambda_{Lorentz}}{2} \dots \dots \dots (3)$$

The de-convolution of Lorentzian from Voigt profile provided Stark FWHM. Since our plasma has environment of low temperature and high density, therefore other broadening mechanisms were minor and ignorable therefore only stark broadening was considered. The stark broadening (FWHM of H_{β}) having Lorentzian profile was used in this research work for finding electron number density, and following relation was used for determining the electron density [148]:

$$N_e = 10^{16} X [\Delta\lambda^{stark}(H_{\beta})]^{1.55} (\text{cm}^{-3}) \dots\dots\dots (4)$$

$\Delta\lambda^{FWHM}$ is measured in nanometers.

Fig. 4.10 represents values of electron number density under different experimental conditions. At higher gas injection rates with increase in power of discharge pulses the electron number density increased.

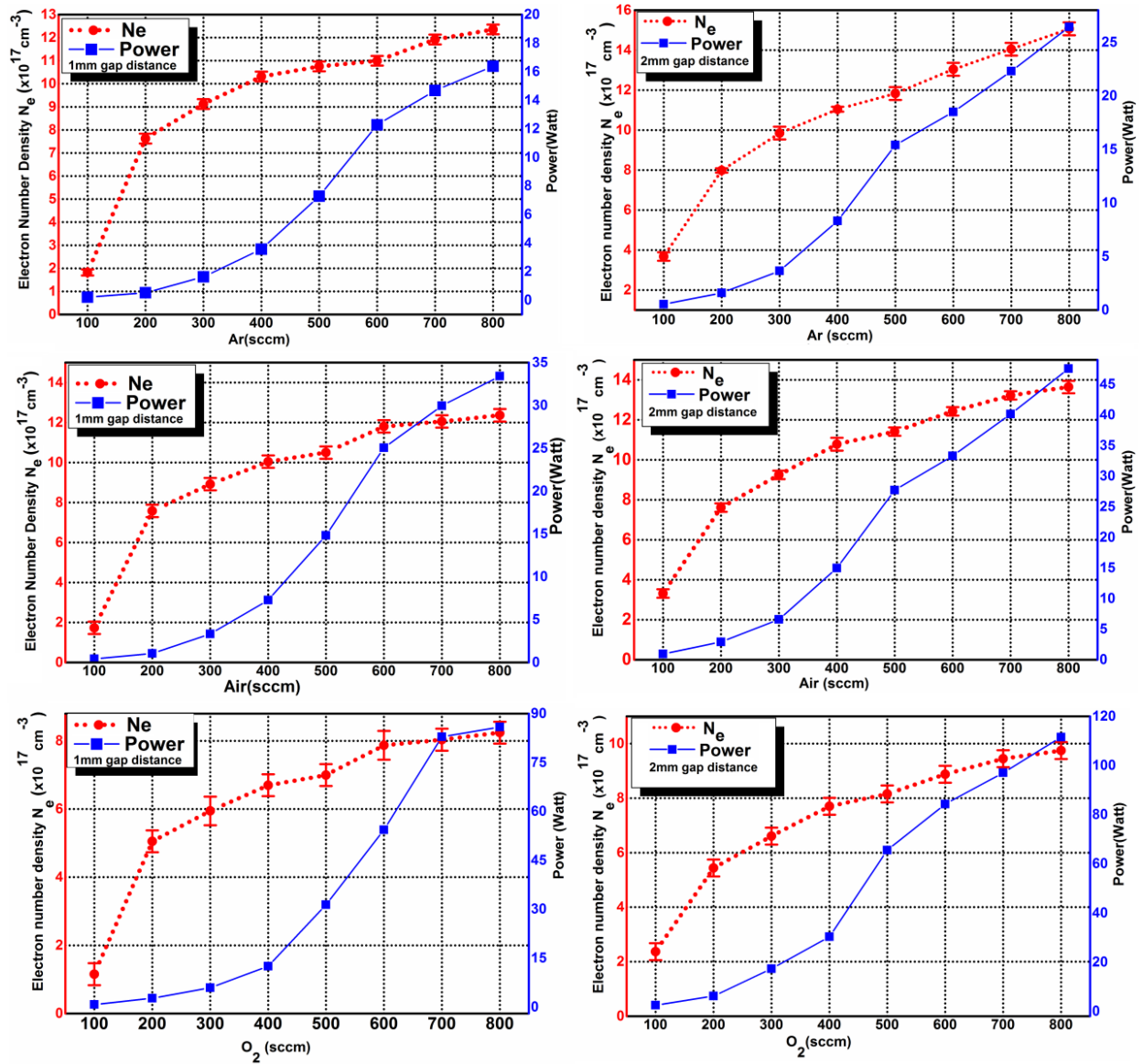


Fig. 4.10 (Color online) Electron number density under different experimental conditions and inter-electrode gap distances.

Comparing the ionization energies of three injected gases (Ar = 15.7596eV, air = 14.53eV and O_2 = 13.6181eV) the lowest ionization energy needed by oxygen, therefore in oxygen injected discharge, the electron collisions with oxygen effectively promoted many positive and negative ions like O^+ , O^{+2} , O^{+4} , O^{+3} , O^{-2} , O^{-1} . Oxygen being an electronegative gas, its injection in water resulted to the formation of high density of negative ions in the plasma that caused decrease in the plasma electron density. Since some part of oxygen exists in air also, it also reduced electron number density; therefore argon

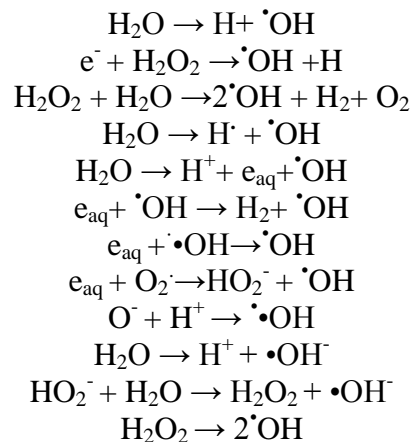
injected underwater discharge outcome highest electron number density and oxygen injected underwater discharge gave lowest electron density, while air existed at intermediate of two gasses when three of them were compared. Although the power of discharge pulses was highest in oxygen injected discharge, but the probable power consumption was in forming ions, the excess of oxygen ions resulted to the decrement of electron number density in oxygen bubbles containing discharge.

4.3.5 Effect of Electron Temperature on Chemical Reactive Species

The increase in electron temperature and number density caused increase in yield rate of highly reactive chemical oxidant species $\bullet\text{OH}$, H_2O_2 and O_3 .

i. $\bullet\text{OH}$ Radicals

The $\bullet\text{OH}$ radicals, due to high redox potential among oxidant species (2.80V) is of large interest in liquid plasma for environmental, medical, biological and other advance applications. When plasma occurred in water, some chemical reactions took place that caused generation of $\bullet\text{OH}$ radicals. The dissociation of water molecule by applied electric field, by electron impact dissociation, through plasma generated shock waves, dissociation of hydrogen peroxide and ultra violet (UV) radiations caused the generation of $\bullet\text{OH}$ radicals. Some typical chemical reactions that probably take place in underwater discharge for $\bullet\text{OH}$ radical's generation are given as [149]:



In case of gas injected discharge where bubbles and gas channels exist in water, the generation of $\bullet\text{OH}$ radicals and their yield rate depend upon type of gas and gas injection rate. Since the life time of $\bullet\text{OH}$ radicals is very short $\sim 10^{-8}$ sec, therefore convenient method for its detection is emission

spectroscopy. Fig. 4.11(a, b) represents the emission spectrum of $\cdot\text{OH}$ radicals ($\lambda=309\text{nm}$) generated by argon injection, while Fig. 4.12 (a, b) shows $\cdot\text{OH}$ radicals emission spectrum of air injected discharge and oxygen injected results of $\cdot\text{OH}$ radicals are represented in Fig. 4.13 (a, b) at 1 and 2-mm inter-electrode gaps respectively.

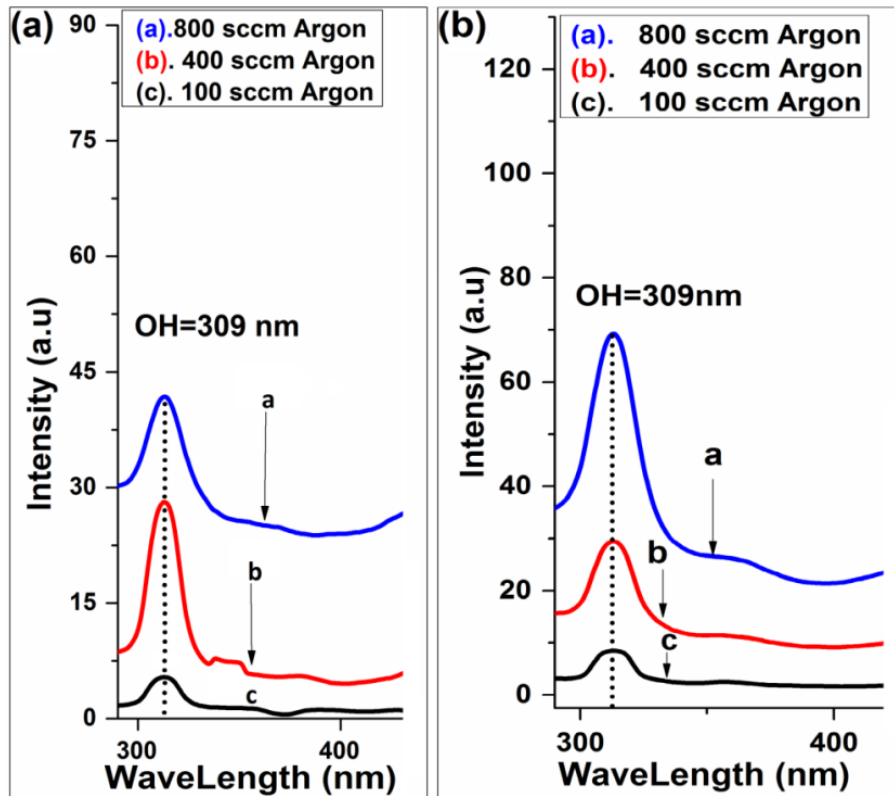


Fig. 4.11 (Color online) Emission spectrum of OH radicals for various argon injection rates at (a) 1-mm and (b) 2-mm inter electrode gap distances.

In case of argon injection since it is non-reactive gas therefore the chemical reactions are not too high. Only electric field dissociation and electron impact dissociation in water mainly participated in generating reactive species specially $\cdot\text{OH}$ radicals. Fig. 4.14 (a-f) represents the concentration of $\cdot\text{OH}$ radicals, calculated by applying Gaussian distribution function on emission spectrum peak of $\cdot\text{OH}$ radicals (at 309 nm), as a function of electron temperature and electron number density.

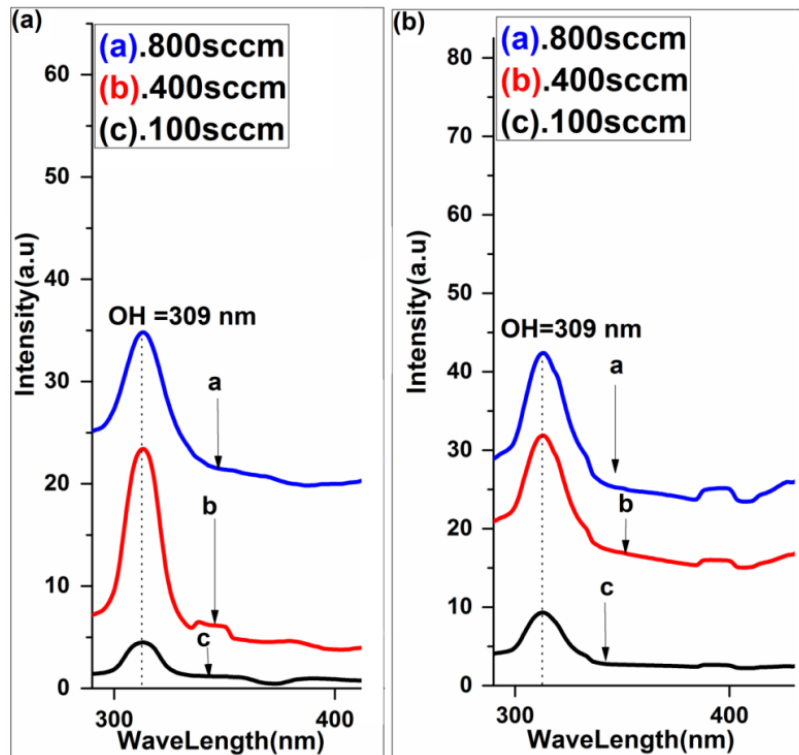


Fig. 4.12 (Color online) Emission spectrum of OH radicals for (a) 1-mm and (b) 2-mm inter electrode gaps and various air injection rates.

The results showed that with increase in electron temperature and electron number density and at long gap distance more $\cdot\text{OH}$ radicals can be induced. The oxygen injected discharge compared to argon and air, higher concentration of $\cdot\text{OH}$ radicals can be induced. The $\cdot\text{OH}$ radicals were formed mainly due to dissociation of H_2O_2 , which was highly influenced by nitrogen existence. Since air contains high concentration of nitrogen (78%) therefore air injected discharge produced lowest concentration of $\cdot\text{OH}$ radicals among three gasses. T_e was highest in oxygen injected discharge and concentration of $\cdot\text{OH}$ radicals as well. While N_e was highest in argon injected discharge but even concentration of $\cdot\text{OH}$ radicals proven to be less compared to O_2 injected discharge.

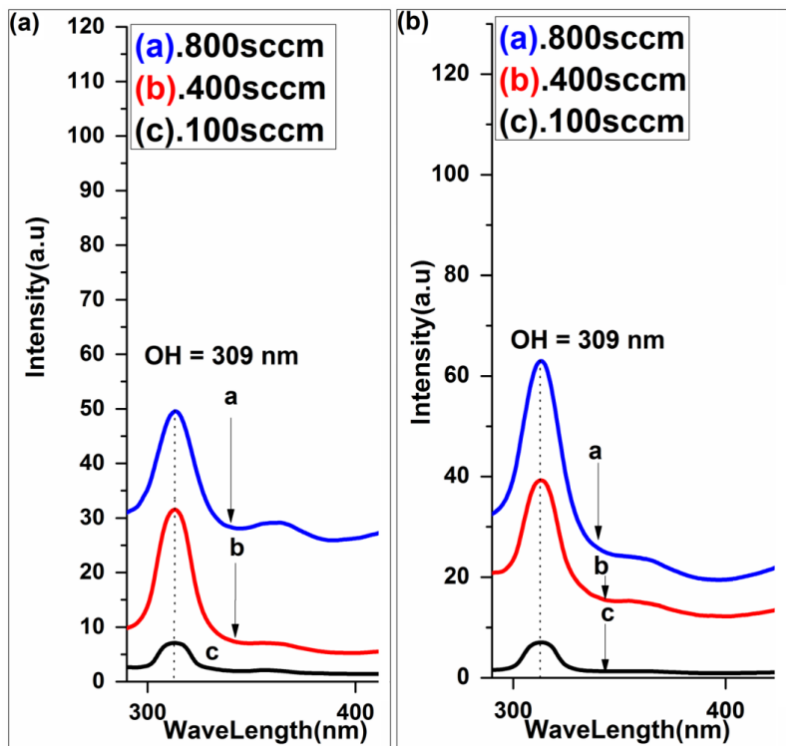


Fig. 4.13 (Color online) Emission spectrum of OH radicals for various oxygen injection rates at (a) 1-mm and (b) 2-mm inter electrode gap distances.

ii. *Hydrogen peroxide*

Hydrogen peroxide (H_2O_2) with redox potential (1.78V) is stable and highly reactive oxidant specie, which can be generated in water after plasma discharge occurrence. Unlike $\cdot OH$ radicals whose life time is very short, it is stable and can be detected in water, long time after plasma processing. H_2O_2 plays a vital role in disinfection of water. Several methods exist for the detection of H_2O_2 generated in water after plasma treatment [150], but the most dominant method is colorimetric method proposed by Eisenberg [151]. In this research same photometric analysis for the determination of H_2O_2 generated in water was adopted after occurrence of plasma discharge.

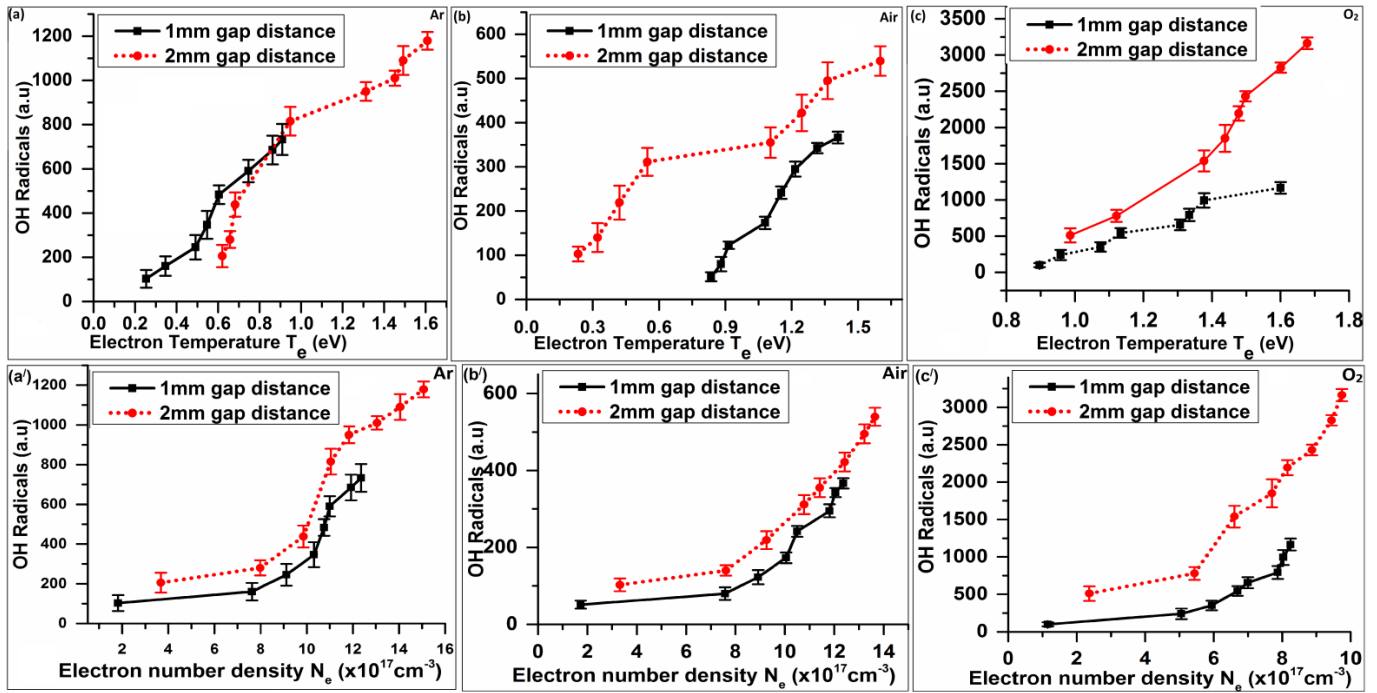
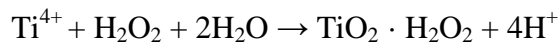


Fig. 4.14 (Color online). Concentration of OH radicals by using Gaussian function (a-c) Electron temperature dependent (d-f) Electron number density dependent for 1 mm and 2 mm gap distances.

In this method sample of plasma treated water with equal amount of titanium sulfate reagent (purchased from Kanto chemicals co. Inc. Tokyo, Japan). The hydrogen peroxide generated by water plasma reacts with titanil ions and a yellow color complex solution of pertitanic acid was formed, under following chemical reaction [152];



The absorption spectrum of this yellow color complex solution was measured at 407 nm. The absorbance at this wave length corresponds to the concentration of H_2O_2 generated in water as result of plasma discharge.

Since the discharge was created after three different gasses injection at different gas injection rates 100 to 800 scm, therefore the amount of hydrogen peroxide varies with gas injection. Fig. 4.15 (a-d) represents the absorption spectrum of pertitanic acid yellow complex solution and resulted H_2O_2 concentration at 1mm and 2mm inter electrode gap distances respectively for different values of

electron temperature. Fig. 4.16 (a-c) represents the variation in concentration of H_2O_2 under different values of electron number density. At large inter-electrode gap and highest oxygen injection rate resulted in maximum concentration of hydrogen peroxide in plasma treated water. The presence of nitrogen in water due to air injection will suppressed hydrogen peroxide. The amount of hydrogen

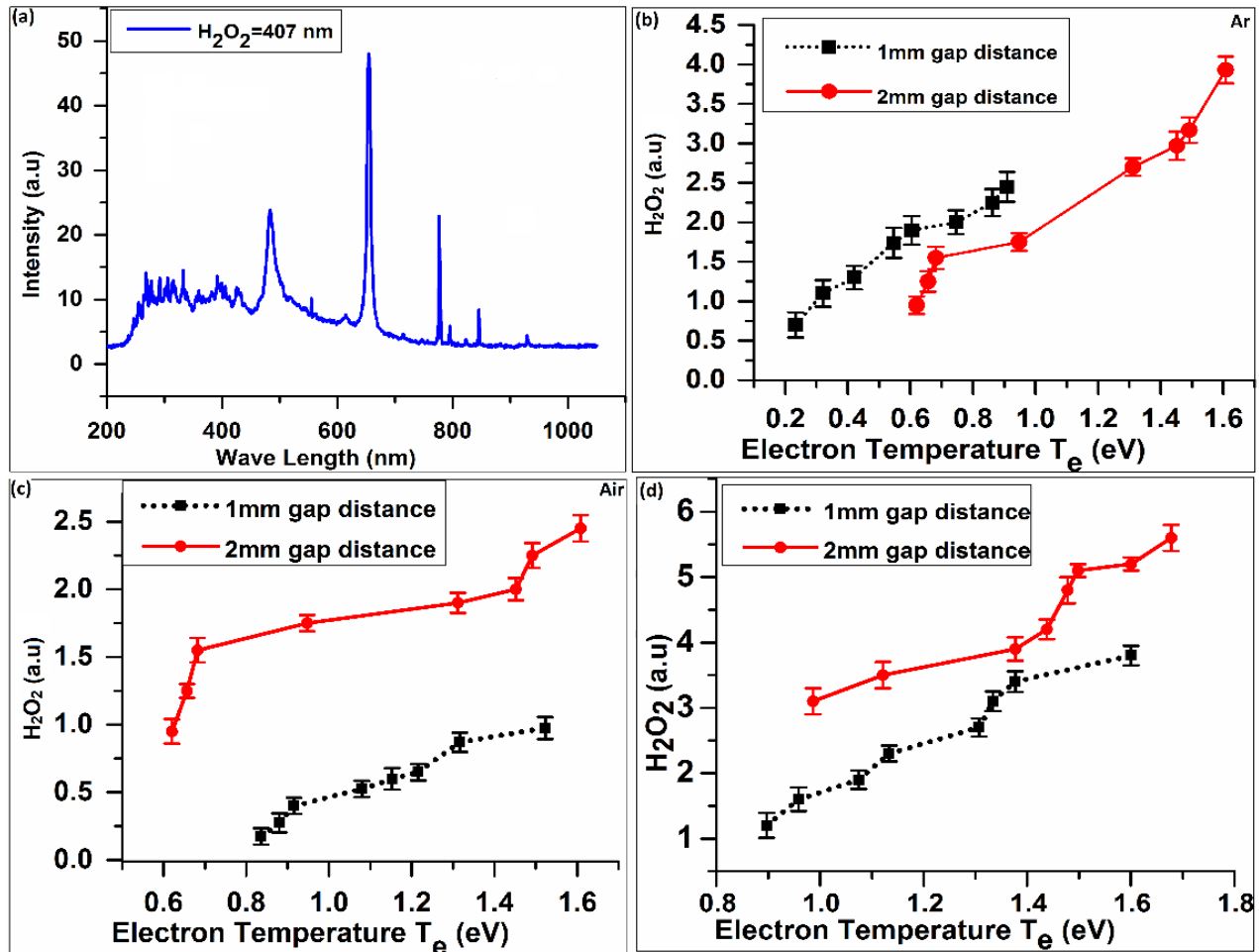


Fig. 4.15 (Color online) (a) Absorption spectrum of pertitanic acid yellow complex solution (b-d) Electron temperature dependent Hydrogen peroxide concentration.

peroxide formed by oxygen injection was highest and approximately same amount was observed with argon injection. The H_2O_2 resulted to be in direct relation with T_e as well.

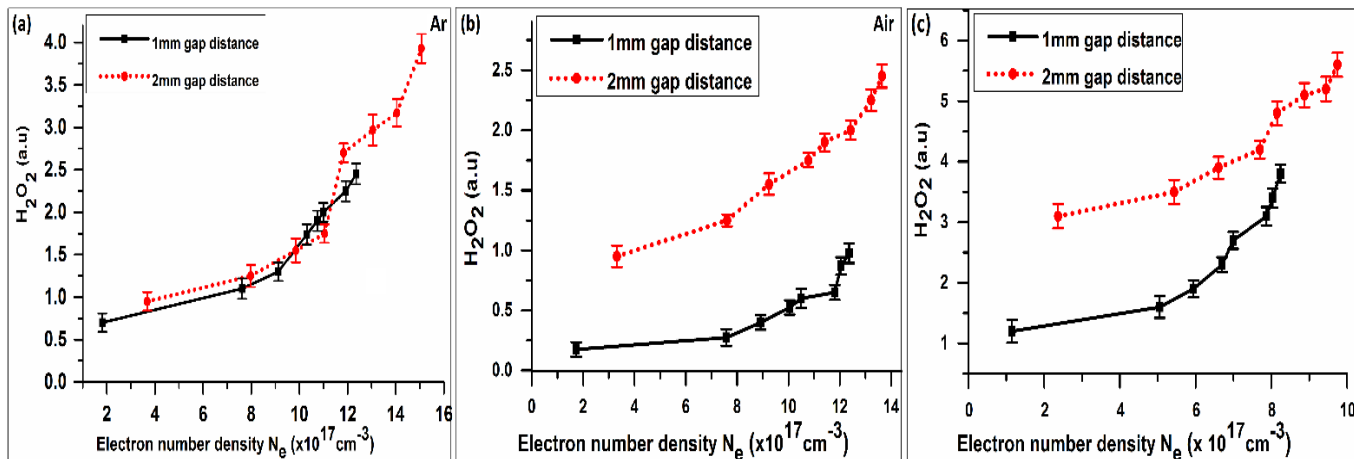


Fig. 4.16 (a-c). (Color online) Electron Number density dependent Hydrogen peroxide concentration.

iii. Ozone

As a result of plasma discharge occurrence in water, ozone has also been detected. The redox potential of Ozone (2.07V) [137] is although less than $\cdot\text{OH}$ radicals but it can be detected in water after plasma processing. Ozone can induce $\cdot\text{OH}$ radicals also after reacting with H_2O_2 . Ozone formation is possible in water as well as gas ozone; therefore in this experiment since gas bubbles generated by argon, air and oxygen exists within water therefore ozone can be detected in dissolved water. A common method presented by Hoigne [153] called indigo method was used in this research for ozone measurement. Two solutions were prepared for quantitative measurement of ozone [154].

Solution 1: 1ml of phosphoric acid (H_3PO_4), (purchased from Daejung chemical and metal co. LTD. Korea) was mixed with 620 mg of indigo reagent (purchased from Daejung chemical and metal co. LTD. Korea) in glass volumetric flask of 1 liter size, then flask was filled with distilled water.

Solution 2: 28 g of sodium di-hydrogen phosphate (NaH_2PO_4), (by SIGMA-ALDRICH, Korea), 35 g of H_3PO_4 were mixed together in 1 liter size volumetric flask, and filled up with 1 liter distilled water.

For reagent preparation 1ml of each solution was taken and mixed with 12.5 ml distilled water. This gave us indigo color liquid solution. The absorption spectrum of this solution gave us blank or reference absorbance (at 600 nm), represented by A_1 . To determine ozone concentration first 1 liter of plasma treated water and then 12.5ml of this treated water sample was taken and mixed with 1ml of

each solution (solution 1 and solution 2) presented above. The addition of plasma treated water removed the indigo color from the water having 1ml of each solution. The absorbance spectrum (at 600 nm), of this sample gave us another absorbance reference A_2 . The differences between the two absorbance's were calculated by $\Delta A = A_2 - A_1$. The equation applied to calculate the ozone concentration is expressed as [155]:

$$O_3(ppmw) = \frac{100 \cdot \Delta A}{fbV} \dots\dots\dots (1)$$

ΔA = difference in absorbance; b = path length of cuvette in cm; V = volume of sample; f = experimentally obtained factor = 0.42.

Fig. 4.17 (a-d) represents the typical absorption spectrum of solution and ozone concentration at 1mm and 2mm inter electrode gaps respectively at different electron temperatures. The results demonstrated that with increase in electron temperature and larger inter-electrode gaps, higher concentration of ozone exists. Compared to other two gasses oxygen proved to be powerful ozone generating gas. Oxygen injection generated almost twice ozone then other gasses. Fig. 4.18 (a-c) represents the concentration of ozone dependent on electron number density. The results showed that increase in electron temperature caused increase in ozone yield rate. Oxygen injected discharge generated more ozone despite of having low electron number density. As the atomic oxygen reacted with water molecules and molecular oxygen to form ozone therefore generation of O_3 can be more effective in the presence of oxygen gas bubbles in water compared to air and argon. Also the reaction rate co-efficient for forming ozone through dissociation or recombination was higher in oxygen injected discharge, compared to argon and nitrogen containing air. Moreover the energetic electrons and UV radiations cause dissociation of oxygen molecules that cause ozone generation. Compared to oxygen, argon is a chemically inert gas therefore when pulsed discharges take place; argon was dissociated to excite electrons; resulting high electron number density in discharge containing argon bubbles. Since nitrogen and argon can have some catalytic effects on the generation of ozone. In the case of air

injection that contains nitrogen as major part, such an effect probably due to reaction of nitrogen atoms and nitrogen molecules in electronically excited state with oxygen (produced by splitting of water molecules and some concentration existing in air), that results the generation of additional oxygen atoms for ozone generation.

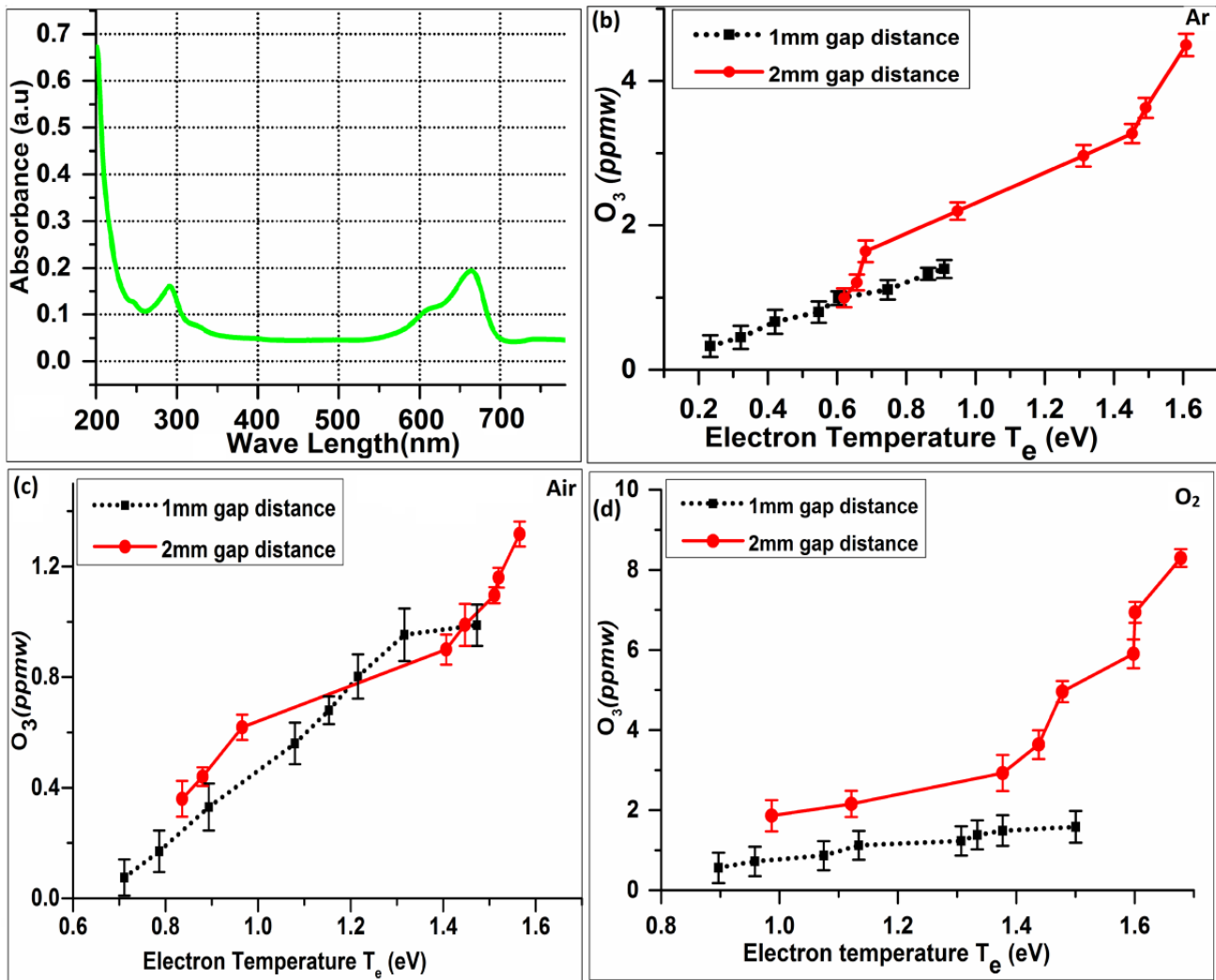


Fig. 4.17 (Color online) (a) Absorption spectrum of ozone containing water sample (b-d) Electron temperature dependent ozone concentration.

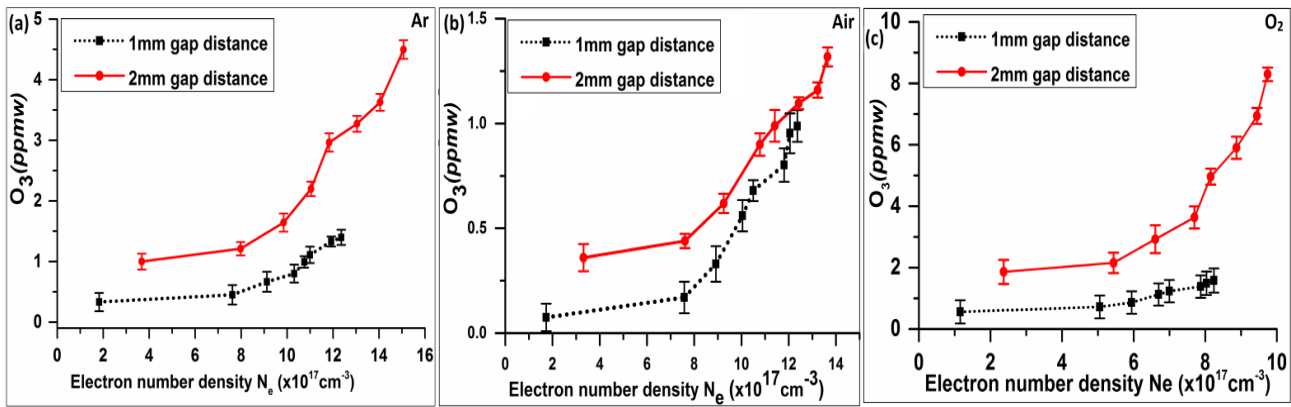


Fig. 4.18 (a-c) (Color online) Electron Number density dependent ozone concentrations.

But, at higher specific energy densities in the discharge nitrogen existing in air that can destroy ozone by quenching of oxygen atoms. Comparison among three gasses showed that oxygen was best for generating ozone and due to nitrogen air was not too favorable.

4.4 Conclusions

Following were deduced from the experiment:

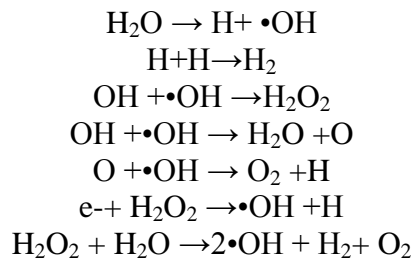
1. The average electron number density was observed 10^{17} cm^{-3} , and electron temperature was 0.5-1.6eV under different experimental conditions.
2. Increase in gas injection rate increases the power of discharge pulses, which result in an increase in electron temperature and number density.
3. The electron temperature of oxygen injected discharge proved highest then air and argon due to high emission intensity of hydrogen Ballmer lines.
4. The chemicals reactions that took place after discharge occurrence affected by electron temperature rather than electron number density.
5. The electronegative characteristic of oxygen reduced the electron number density; therefore argon contains highest electron number density then oxygen and air.
6. The oxidant reactive species ($\bullet\text{OH}$, O_3 and H_2O_2) has direct relation with T_e , for Ar, air and O_2 .

5. High Frequency Underwater Capillary Discharge

5.1 Diagnostics of Argon Injected Hydrogen Peroxide Added High Frequency Underwater Capillary Discharge

1. Introduction.

The generation of reactive species like $\bullet\text{OH}$ radicals, ozone, reactive hydrogen and oxygen through electrical discharge in water is of large interest and has been widely investigated by many researchers [156-158]. Through various diagnostics phenomena different kinds of reactive species were detected [159-160]. Among them ozone and $\bullet\text{OH}$ radicals are of larger interest due to high redox potential (2.07V and 2.80V respectively) and their high sterilization rate [161]. These reactive species have wide range of environmental, biological, medical, Nano-technology and industrial applications [162-167]. $\bullet\text{OH}$ radicals are widely used for controlling environmental pollution including drinking water and waste water treatment [168]. High redox potential reactive species are useful in blood treatment and *E. coli* degradation when generated in water and other liquids through electrical discharge [169-170]. Synthesis of Nano-particles and polymers surface modifications is another useful application of underwater plasma discharge and these reactive species can act as antibacterial agents [171-172]. The hydroxyl radicals can be generated by various mechanisms [173] else than electrical discharge in water, but researchers proved that the electrical discharge method is most effective method where high intensity of $\bullet\text{OH}$ radicals can be obtained [174-175]. Therefore in this research electrical discharge in water was used to induce highly reactive oxidant species especially $\bullet\text{OH}$ radicals. When plasma generated then highly intensive shock waves, high temperature, strong electric field generation and electron impact dissociation can cause water molecule to split into $\bullet\text{OH}$, other reactive species, ionization and excitation process. Under various chemical reactions the splitting and recombination of generated radicals and ionic species takes place to form $\bullet\text{OH}$, ozone and H_2O_2 . Following are some common chemical reactions that occur in aqua system while inducing some highly reactive oxidant species [176]:



In the table 5.1.1 the possible chemical reactions list, that takes place when discharge occurs in liquid is shown [177].

Reactants	Products
$2\text{H}_2\text{O}$	$\rightarrow \text{H}_2\text{O}_2 + \text{H}_2$
H_2O	$\rightarrow \text{H}^+ + \text{e}_{\text{aq}}^- + \cdot\text{OH}$
$\text{e}_{\text{aq}}^- + \cdot\text{OH}$	$\rightarrow \text{H}_2 + \text{OH}^-$
$\text{e}_{\text{aq}}^- + \cdot\text{OH}$	$\rightarrow \text{OH}^-$
$\text{e}_{\text{aq}}^- + \text{HO}_2$	$\rightarrow \text{HO}_2^-$
$\text{e}_{\text{aq}}^- + \text{O}_2$	$\rightarrow \text{HO}_2^- + \text{OH}^-$
$\text{e}_{\text{aq}}^- + \text{H}_2\text{O}_2$	$\rightarrow \text{OH}^- + \text{OH}^-$
$\text{e}_{\text{aq}}^- + \text{HO}_2^-$	$\rightarrow \text{O}^- + \text{OH}^-$
$\text{e}_{\text{aq}}^- + \text{O}_2$	$\rightarrow \text{O}_2^-$
$\text{e}_{\text{aq}}^- + \text{H}^+$	$\rightarrow \text{H}^-$
$\text{e}_{\text{aq}}^- + \text{H}_2\text{O}$	$\rightarrow \text{OH}^- + \text{H}^-$
2e_{aq}^-	$\rightarrow \text{H}_2 + 2\text{OH}^-$
2H^-	$\rightarrow \text{H}_2$
$\text{H}^- + \cdot\text{OH}$	$\rightarrow \text{H}_2\text{O}$
$\text{H}^- + \text{HO}_2$	$\rightarrow \text{H}_2\text{O}_2$
$\text{H}^- + \text{O}_2^-$	$\rightarrow \text{HO}_2^-$
$\text{H}^- + \text{H}_2\text{O}_2$	$\rightarrow \text{H}_2\text{O} + \cdot\text{OH}$
$\text{H}^- + \text{O}_2$	$\rightarrow \text{HO}_2^-$
$\text{OH}^- + \text{H}^-$	$\rightarrow \text{e}_{\text{aq}}^- + \text{H}_2\text{O}$
$\cdot\text{OH} + \cdot\text{OH}$	$\rightarrow \text{H}_2\text{O}_2$
$\cdot\text{OH} + \text{O}^-$	$\rightarrow \text{HO}_2^-$
$\cdot\text{OH} + \text{HO}_2$	$\rightarrow \text{O}_2 + \text{H}_2\text{O}$
$\cdot\text{OH} + \text{O}_2^-$	$\rightarrow \text{O}_2 + \text{OH}^-$
$\cdot\text{OH} + \text{H}_2\text{O}_2$	$\rightarrow \text{HO}_2^- + \text{H}_2\text{O}$
$\cdot\text{OH} + \text{HO}_2^-$	$\rightarrow \text{HO}_2^- + \text{OH}^-$
$\cdot\text{OH} + \text{H}_2$	$\rightarrow \text{H}^- + \text{H}_2\text{O}$
$\cdot\text{OH} + \text{OH}^-$	$\rightarrow \text{O}^- + \text{H}_2\text{O}$
2O^-	$\rightarrow \text{OH}^- + \text{HO}_2^-$
$\text{O}_2^- + \text{O}^-$	$\rightarrow \text{O}_2 + 2\text{OH}^-$
$\text{O}^- + \text{H}_2\text{O}_2$	$\rightarrow \text{O}_2^- + \text{H}_2\text{O}$
$\text{O}^- + \text{HO}_2^-$	$\rightarrow \text{O}_2^- + \text{OH}^-$

Table 5.1.1 The possible chemical reactions list that takes place when discharge occurs in liquid (Dors et al., Chen et al., Grymonpre et al., Mok et al ;2005, 2002, 2009, 2001, 2008 respectively).

The addition of hydrogen peroxide in water can enhance the reaction rates for generating $\cdot\text{OH}$ radicals and other reactive species. In this research the standard value of hydrogen peroxide (0.35ml/L) [178] was added at different amounts starting from (0-0.35) ml/L. This addition enhanced the yield rate of $\cdot\text{OH}$ radicals. It is important to measure the intensity of reactive species especially $\cdot\text{OH}$ radicals. Several methods exist for the measurement of $\cdot\text{OH}$ radicals among them the most convenient method is optical emission spectroscopy (OES) [179]. Beside that other complicated methods like spin-trap electron-spin resonance (ESR) [180], indirect measurement of $\cdot\text{OH}$ radicals using chemical probe [181], laser induce fluorescence (LIF) [182] and $\cdot\text{OH}$ radicals dissolved in liquid were observed indirectly using fluorescent properties of hydroxyl-terepethalic acid (HTA) formed in the reaction of Terepethalic acid (TA) [183]. Among all of them OES is simple and convenient method that was used in this experiment. The properties of $\cdot\text{OH}$ radicals and other reactive species observed by several researchers by different mechanisms. Table 5.1.2 represents the properties of reactive species generated by electrical discharge in water [184].

This research work is useful to present the effect of H_2O_2 addition in water along with plasma discharge to enhance the yield of $\cdot\text{OH}$ radicals. Also the electrical characteristics of H_2O_2 added water discharge were presented.

2. Experiment Set-up

Fig. 5.1.1 represents the experimental set-up used while Fig. 5.1.2 shows the visual view of the discharge. The inter-electrode gap where plasma generated was kept 10mm, a liquid flow meter and controller (Dwyer-RM series) was used to control the flow rate of water (0.1L/min). Hydrogen peroxide (H_2O_2) was added to the water reservoir that was to be treated at standard rates starting from 0ml/L to 0.35ml/L. A conductivity meter (OAKTON-CON6) was used for observing conductivity of water during experiment specially after adding hydrogen peroxide. Mass flow controller (LINE TECH M3030V) along with display unit was used to control and provide Argon gas.

Species	Formula	Standard Electrochemical Potential (V)	pH (where present)	Role
Hydroxyl Radical	$\cdot\text{OH}$	+2.59	pH < 11.9	Strong oxidant
Hydrogen Peroxide	H_2O_2	+1.77	pH < 11.6	Strong oxidant Week reductant
Superoxide anion	O_2^-	-0.33	pH < 4.8	Week reductant
Perhydroxyl radical	$\text{HO}_2\cdot$	+1.49	pH < 4.8	Strong oxidant
Hydroperoxide anion	HO_2^-	+0.88	pH > 11.6	Week oxidant Week reductant
Singlet oxygen	$^1\text{O}_2$			
Ozone gas	O_3	+2.07		Strong oxidant
Atmospheric oxygen (normal triplet form)	O_2	+1.23		Week oxidant
Solvated electrons	$e_{(\text{aq})}^-$	-2.77	pH > 7.85	Strong reductant

Table 5.1.2. Properties of selected species involved in advance oxidation process (AOP) are through electrical discharge in water discharge (Buxton et al., 1998; Lide, 2006; Petri et al., 2011).

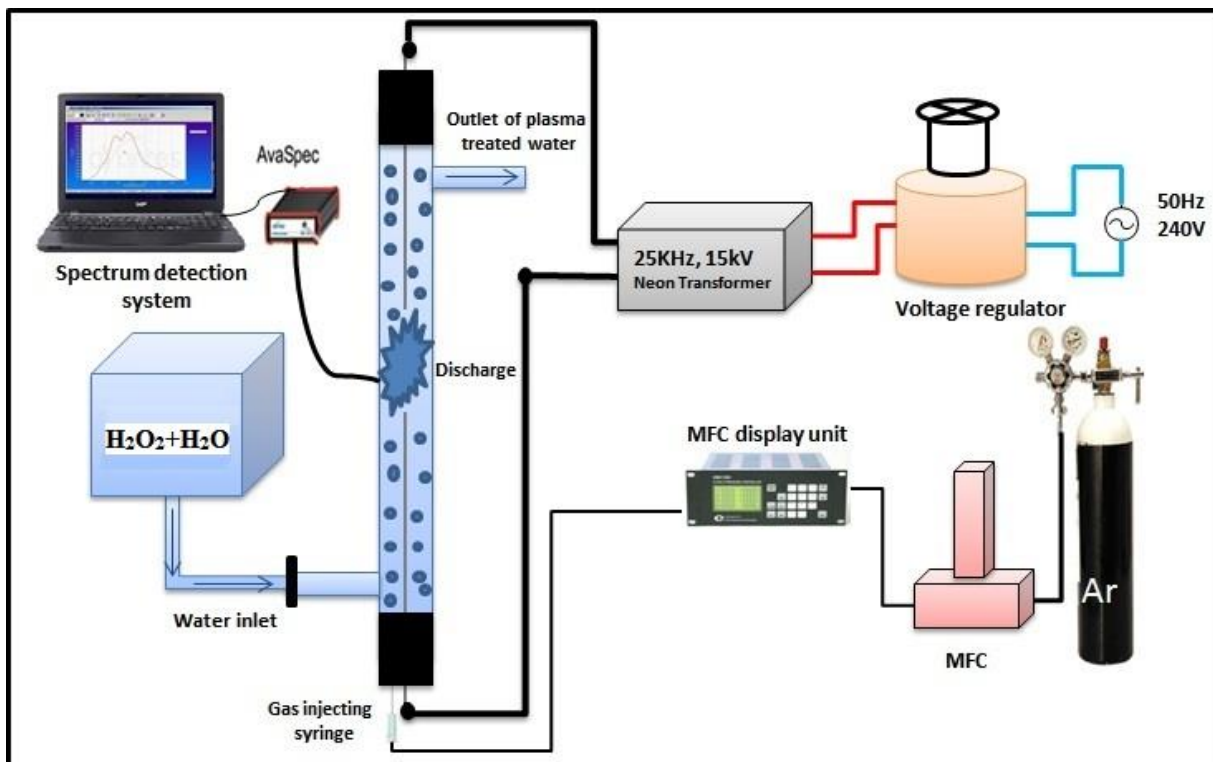


Fig. 5.1.1. (Color online) Schematic view of experiment set-up.



Fig. 5.1.2. (Color online) Visual view of the capillary discharge.

A Neon transformer (15 kV, 25 kHz) was used to provide required input power for generating discharge at 10 mm inter-electrode gap in tap water. A Tektronix digital oscilloscope (DPO 2024) with high voltage and current probes and having data storage facility was used for recording Volt-Ampere characteristics. An Avantes Avaspec-NIR256 miniature fiber-optic spectrometer was used to record the emission spectrum of hydrogen emitted lines.

A mixture of water and hydrogen peroxide was taken in one liter water tank (H_2O_2 was added for different amounts), and water was allowed to flow through the quartz tube. The two terminals of electrodes were connected at the output of the Neon transformer. The discharge was created inside capillary between two electrodes carrying flowing water and after discharge occurrence the electrical and spectral data was recorded. The electrical data taken by oscilloscope was evaluated by Matlab codes to find volt-ampere characteristic curves, electrical power of discharge pulses, frequency of discharge pulses and time difference between the occurrences of discharge pulses under different experimental conditions. Argon gas was injected at 0-500sccm injection rates through injection syringe and bubbles were created to reduce required power for generating discharge in flowing water long gap discharge. The emission spectrum was recorded to find the intensity of $\cdot OH$ radicals and other reactive species. The Gaussian distribution was applied on $\cdot OH$ emission spectrum peaks to determine the intensity of $\cdot OH$ radicals. The results were tabulated and presented graphically as well. Under different experimental conditions, electrical and spectral data was taken simultaneously, compared and presented.

3. Results and discussion

3.1. Electrical results

Fig. 5.1.3 represents typical Volt-Ampere characteristics of non-gas injected discharge for different amounts of hydrogen peroxide addition. The addition of hydrogen peroxide does not influence remarkably water conductivity; therefore the required breakdown voltage was almost same as without

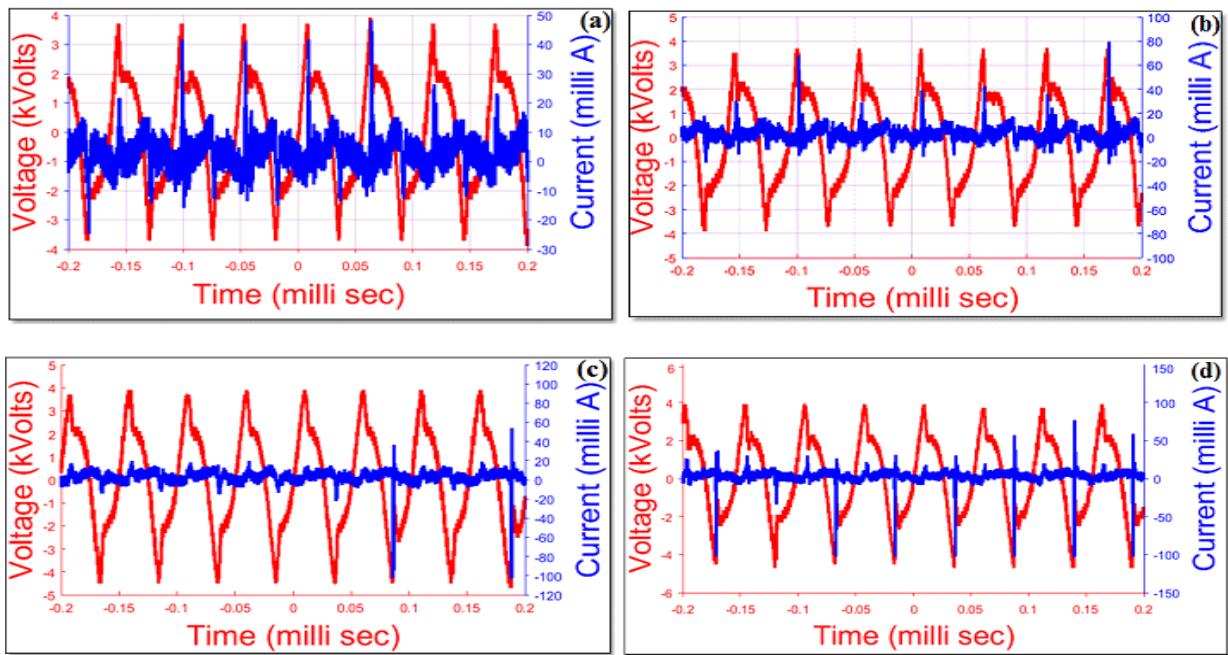


Fig. 5.1.3. (Color online) Typical Volt-Ampere characteristics of non-gas injected discharge for different amounts of hydrogen peroxide addition (a) 0ml/l H_2O_2 (b) 0.05 ml/L H_2O_2 (c) 0.20 ml/L H_2O_2 (d) 0.35 ml/L H_2O_2 .

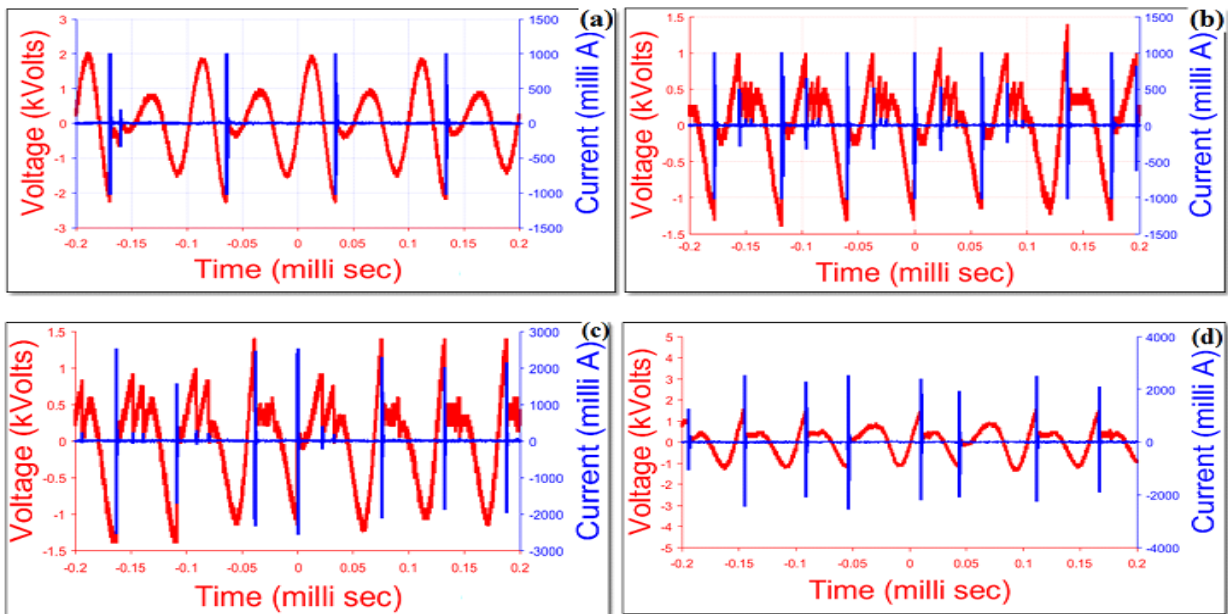


Fig. 5.1.4. (Color online) Typical Volt-Ampere characteristics of 500 sccm Ar gas injected discharge for different amounts of hydrogen peroxide addition (a) 0ml/l H_2O_2 (b) 0.05 ml/L H_2O_2 (c) 0.20ml/L H_2O_2 (d) 0.35 ml/L H_2O_2 .

argon injection. Fig. 5.1.4 represents typical Volt-Ampere characteristics of argon injected discharge for various amounts of hydrogen peroxide addition. The addition of argon gas generated bubbles and gas channels drastically reduced the required breakdown voltage due to small dielectric constant of gas compared to pure water medium having high dielectric strength. When no gas was injected, after applying electrical fields across the electrodes, the joule's heating cause evaporation and micro bubbles generation that assist the discharge occurrence process. Moreover electron impact dissociation was another cause of electrical breakdown in water medium. In volt-ampere curves the sharp peaks represents the stage when evaporation, micro bubbles density and electron density due to electron impact dissociation was at maximum, after discharge occurrence the voltage drops and discharge current rises. Sharpe peaks represents quick breakdown process. After argon injection, bubbles and gas channels were generated, that participated mainly in creating low voltage breakdown. Discharge occurred within that bubbles and channels and inside water or liquid-gas interface. The generation of bubbles and gas channels, occurrence of discharge in theses gas channels and bubbles and in liquid-water interface was a quick and random process, so underwater discharge was of pulsating nature. The addition of argon gas generated bubbles and gas channels that drastically reduced the required breakdown voltage due to small dielectric constant of gas compared to pure water medium having high dielectric strength. Fig. 5.1.5 represents the reduction in breakdown voltage. Due to high dielectric constant of pure water medium, the required breakdown voltage was larger compared to the gas injected discharge, where gas channels and gas bubbles created low voltage breakdown. With increase in gas injection rate, breakdown voltage reduced enormously.

Fig. 5.1.6 represents the variation in electrical power of the discharge pulses, under different experimental conditions.

The addition of hydrogen peroxide had no remarkable effect on the breakdown voltage therefore, the electrical power of discharge pulses depends upon the medium of discharge i.e. pure water medium or argon injected medium. In case of argon injection due to rise in bubbles size and number density, and gas channels, the discharge strength increased and dimensionally more expanded discharge was

obtained. This increased the strength of electrical power of discharge pulses. The electrical power of pulses becomes higher with increase in gas injection rates.

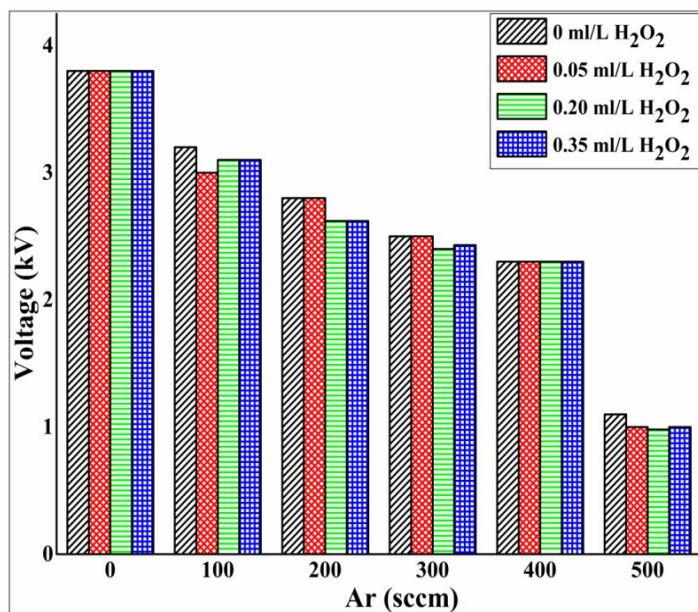


Fig. 5.1.5. (Color online). Variation in breakdown voltage for different Ar injection rates and various hydrogen peroxide addition.

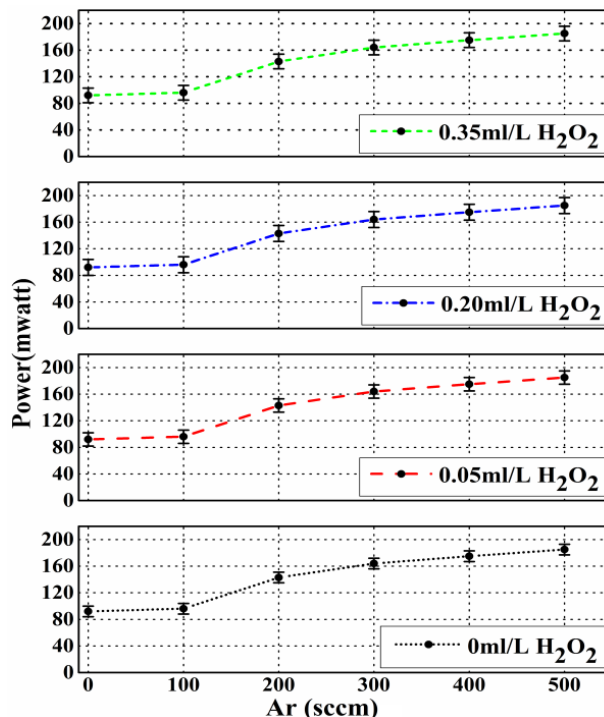


Fig.5.1.6. (Color online). Variation in electrical power of discharge pulses for different Ar injection rates and various hydrogen peroxide additions.

Fig. 5.1.7 shows the variation of discharge pulse frequency. Due to argon injection high frequency of discharge pulses were obtained compared to the pure water discharge. The increase in gas injection rate can cause high frequency discharge. The time difference between the occurrences of discharge pulses under different experimental conditions is shown in Fig. 5.1.8. After gas injection quick discharge pulses were obtained compared to the non-gas discharge.

The results presented that without gas injection high break down voltage was needed, while after argon injection that is non-reactive the chemical characteristics of discharge were not altered, but the physical characteristics varied. At higher gas injection rates the breakdown voltage reduced, electrical

power of discharge pulses raised, frequency was increased while time difference between occurrences of discharge pulses reduced. The addition of hydrogen peroxide had no remarkable influence on the electrical characteristics of the discharge.

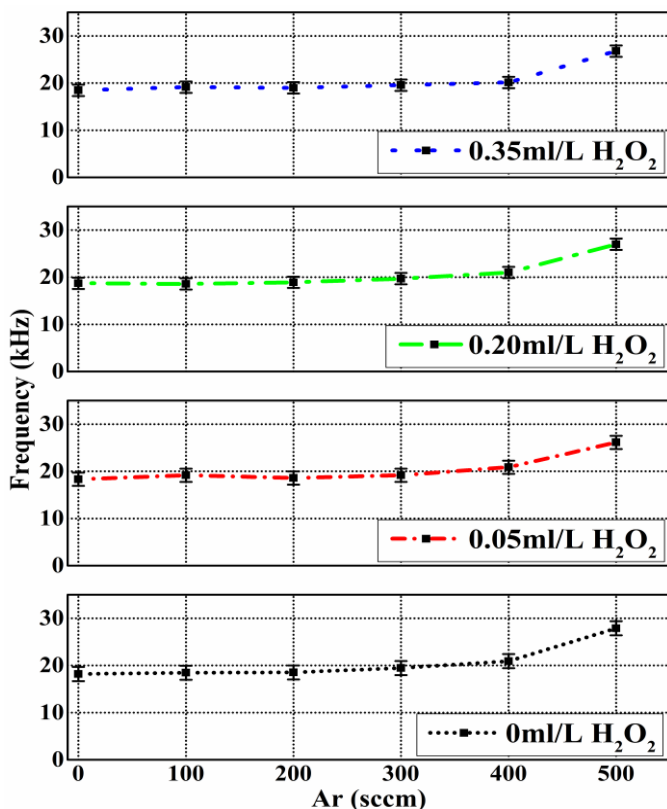


Fig. 5.1.7. (Color online). Variation in frequency of discharge pulses for different Ar injection rates and various hydrogen peroxide additions.

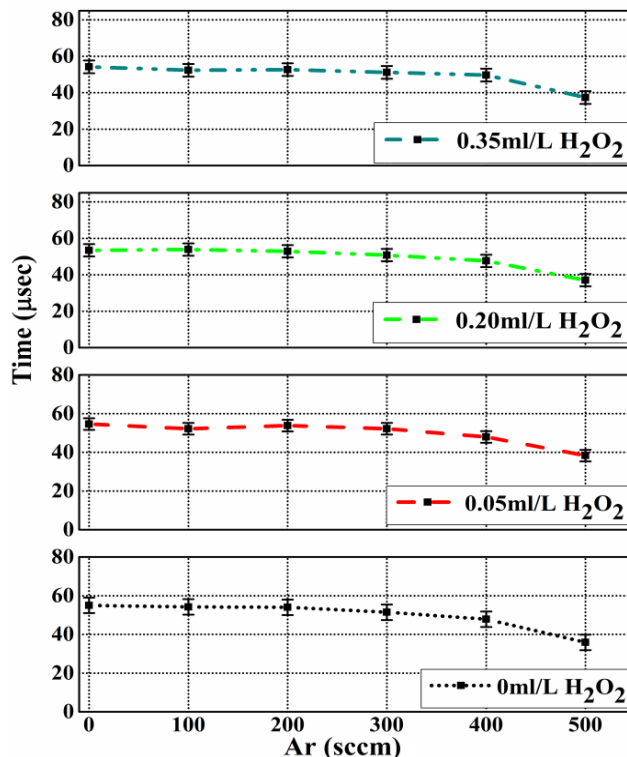


Fig. 5.1.8. (Color online). Average time difference between the occurrence of discharge pulses for different Ar injection rates and various hydrogen peroxide additions.

3.2. Spectral results

Fig. 5.1.9 (a-d) represents the emission spectrum results of the discharge. The emission spectrum was obtained after discharge occurrence by setting spectrometer wavelength range 250-1000 nm. The peaks of $\cdot\text{OH}$ radicals at 309 nm, H_α at 656 nm and reactive oxygen at 777 nm and 844 nm were observed more dominant among required reactive species peaks. The intensity of $\cdot\text{OH}$ radicals and other

reactive species was too high when H₂O₂ was added. Fig. 5.1.9 (a) represents the emission spectrum without hydrogen peroxide addition. Without H₂O₂ addition only the splitting of water molecule by electrical field, ultra violet (UV) radiations and electron impact dissociation caused the generation of these reactive species. Fig. 5.1.9 (b) represents the emission spectrum at 0.05ml/L hydrogen peroxide addition. While Fig. 5.1.9 (c) for 0.20 ml/L hydrogen peroxide addition and Fig. 5.1.9 (d) for 0.35ml/L hydrogen peroxide addition. Comparison outcome that the [•]OH radicals, reactive hydrogen and reactive oxygen were quite high for the case of hydrogen peroxide addition.

The results also demonstrated that with increase in argon gas injection since the strength of the discharge, electrical power of discharge pulses and frequency of discharge pulses was high, therefore intensity and concentration of reactive species increased as well. The addition of hydrogen peroxide along with argon injection generated more reactive species. Fig. 5.1.10 represents the concentration of OH radicals by applying Gaussian distribution function on [•]OH radical's emission peaks at 309nm [185]:

$$\int_{-\infty}^{\infty} F_i(x) = A_i \sigma_i \sqrt{2\pi} \dots \dots \dots (1)$$

Increase in argon injection and hydrogen peroxide addition resulted in high concentration of OH radical's.

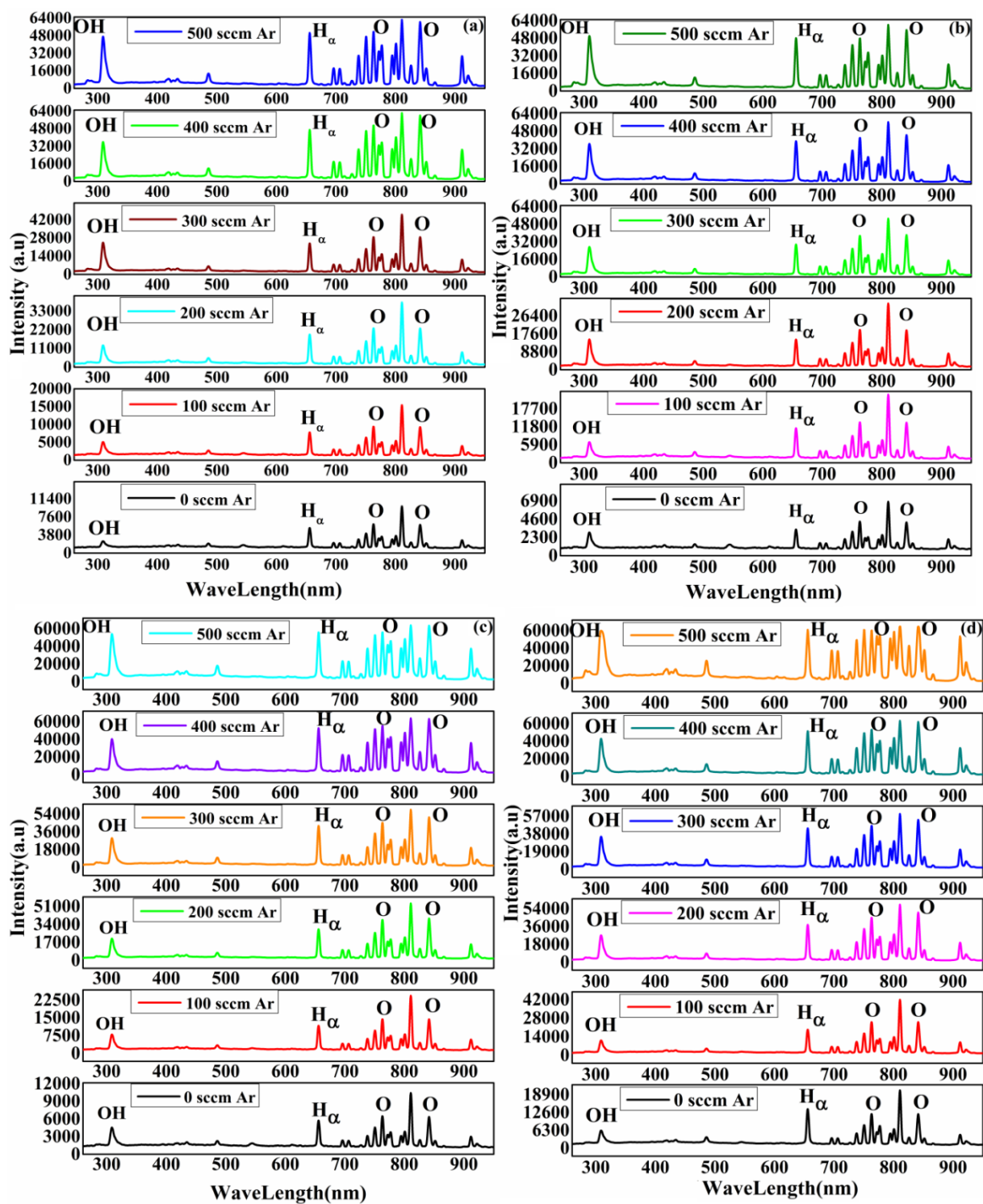


Fig. 5.1.9. (Color online). Emission Spectrum of •OH radicals and other reactive species for different Ar injection rates and various hydrogen peroxide addition (a) 0ml/l H₂O₂ (b) 0.05 ml/L H₂O₂ (c) 0.20 ml/L H₂O₂ (d) 0.35 ml/L H₂O₂.

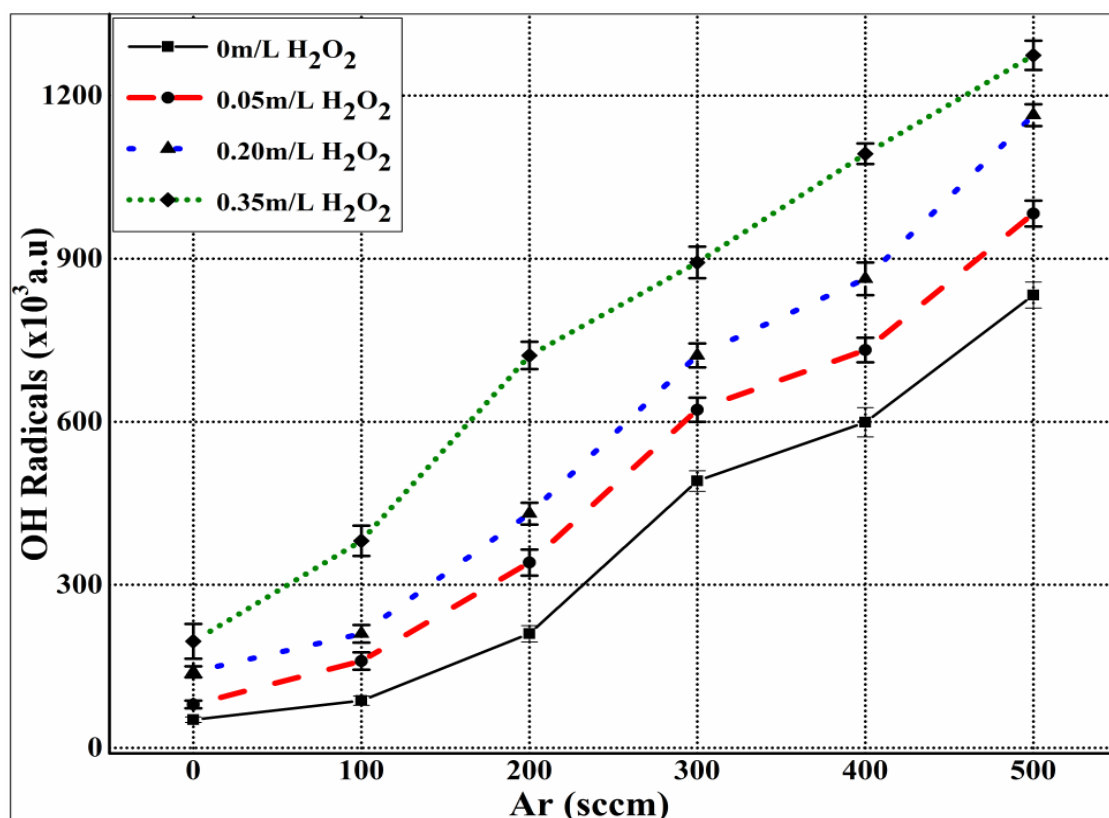


Fig. 5.1.10. (Color online). Variation in concentration of •OH radicals for different Ar injection rates and various hydrogen peroxide addition.

At larger argon injection rates, since power of discharge pulses and frequency of discharge pulses was observed increasing therefore, higher dissociation rate of water molecules was obtained, that resulted in higher concentration of •OH radicals.

4. Conclusions.

1. The addition of hydrogen peroxide along with argon injection generated stronger plasma and high intensity of reactive species especially •OH radicals.
2. Addition of hydrogen peroxide effected chemical properties and have no remarkable effect on electrical characteristics, especially conductivity of water.
3. Argon gas injection generated bubbles and gas channels that reduced the required breakdown voltage for long gap flowing water discharge.
4. The frequency and electrical power of discharge pulses increased while time difference between the occurrence of discharge pulses and breakdown voltage was reduced at higher argon injection rates.

5.2 Effect of Water Conductivity on the Generation of OH· Radicals in High Frequency Underwater Capillary Discharge

1. Introduction:

Generation of non-thermal plasma by electrical discharge in water for various industrial, environmental and biomedical applications becomes one of the interesting topics since last few decades [186-190]. The high dielectric strength of water cause large power consumption, therefore overcoming such problem is a challenging issue in underwater plasma discharge. The introduction of gas bubbles and gas channels and induction of plasma within these gas bubbles and channels drastically reduced the required input power due to less dielectric strength of gas [191]. The type of gas, gas injection rate and injection mechanisms enormously affect the physical and chemical characteristics of plasma discharge. In this research we injected non-reactive gas argon for generating gas bubbles and channels to reduce power. We consider known reaction rate equations to explain the reaction kinetics of reactive species for Ar injected discharge as explained in table 5.2.1 [192, 193]. The de-excitation of these energetic reactive species from higher to lower energy states can cause the emission of ultra-violet (UV) radiations [194]. Underwater plasma discharge also known as electrohydraulic discharge generates plasma streamers. The propagation of these streamers results in generation and propagation of shock waves [195]. Underwater discharge also generates oxidant species like OH·, O, O₃, H₂O₂ and H due physical and chemical reactions that take place as result of electrical discharge in water. The concentration of chemical reactive species (OH·, O, O₃, and H) can be measured by emission and absorption spectrums [196-199]. The shockwave intensity and propagation velocity can be measured by hydrophones and various pressure measurement devices [200]. The generation of all these outputs from underwater plasma discharge depends upon the chemical characteristics of water especially on water conductivity. Two important issues of water conductivity are related to the electrical discharge in water [201].

- 1). The breakdown voltage
- 2). Discharge current.

The discharge current in water transferred by solvated ions and both positive and negative streamers propagate. These solvated ions occupy in the streamers during their propagation and strongly influence the electrical discharge. In pure water medium, higher breakdown voltage required due to high dielectric strength of water. The injection of gas and generation of gas bubbles and gas channels leads to the reduction of breakdown voltage due to less dielectric constant of gas compared to liquid. In underwater discharge two types of current exists [202].

Reactants	Products
$\text{Ar} + e$	$\rightarrow \text{Ar} (^3\text{P}) + e$
$\text{H}_2\text{O} + e$	$\rightarrow \text{H} + \text{OH} + e$
$\text{OH} + \text{OH}$	$\rightarrow \text{H}_2\text{O}_2$
$\text{OH} + \text{O}_3$	$\rightarrow \text{HO}_2 + \text{O}_2$
$\text{OH} + \text{HO}_2$	$\rightarrow \text{H}_2\text{O} + \text{O}_2$
$\text{OH} + \text{H}_2\text{O}_2$	$\rightarrow \text{HO}_2 + \text{H}_2\text{O}$
$\text{O} + \text{O}_2$	$\rightarrow \text{O}_3$
$\text{O} + \text{O}_3$	$\rightarrow \text{O}_2 + \text{O}_2$
$\text{O} (^1\text{D}) + \text{H}_2\text{O}$	$\rightarrow \text{OH} + \text{OH}$
$\text{O} + \text{HO}_2$	$\rightarrow \text{H} + \text{O}_2$
$\text{H}_2\text{O} + \text{Ar} (^3\text{P})$	$\rightarrow \text{H} + \text{OH} + \text{Ar}$
$\text{O}_2 + \text{Ar} (^3\text{P})$	$\rightarrow \text{O} + \text{O} (^1\text{D}) + \text{Ar}$
$\text{H} + \text{O}_3$	$\rightarrow \text{OH} + \text{O}_2$
$\text{H} + \text{HO}_2$	$\rightarrow \text{H}_2\text{O} + \text{O}$
$\text{H} + \text{HO}_2$	$\rightarrow \text{OH} + \text{OH}$
$\text{H} + \text{HO}_2$	$\rightarrow \text{O}_2 + \text{H}_2$
$\text{HO}_2 + \text{HO}_2$	$\rightarrow \text{H}_2\text{O}_2 + \text{O}_2$

Table 5.2.1. Reactions considered in non-gas and Argon gas injected discharge.

1). The conduction current that obeys Ohm's laws as $I = \frac{V}{R}$ and the current density of

conduction current is given as $J_c = \sigma \vec{E}$;

2). The apparent current produced by time varying electrical field known as displacement

current having current density given by $J_d = \epsilon \frac{\partial \vec{E}}{\partial t}$.

For less conductivity like in tap water the conduction current density reduces resulting in no discharge initiation or low discharge power. In this case displacement current ' J_d ' caused by variation in electric field and dependent upon dielectric strength of water becomes more dominant. With increase in conductivity, conduction current ' J_c ' becomes more dominant due to reduction in resistive strength of water. When the conductivity is much higher more conduction current increases those results in larger dissociation of water molecule and generation of reactive species in large concentration. Therefore conductivity directly influences the breakdown phenomena, initiation of discharge, nature of current at various stages in discharge and sustaining the discharge.

This research work presents the effects of water conductivity on various phenomena like breakdown voltage, electrical power of discharge pulses and concentration of OH^\cdot radicals. To increase the conductivity we added H_2SO_4 because sulfate ions do not react effectively with OH^\cdot and H^\cdot radicals. The injecting of argon gas bubbles reduced required break down voltage in pure water medium. The injection of this argon gas enhanced electron impact ionization due to existence of gas bubbles and gas channels [203]. A comparison was made between gas injected and non-gas injected discharge at various conductivities and inter-electrode gaps.

2. Experimental set-up:

Fig. 5.2.1 shows a schematic of the experimental set-up that was used for this experiment. A visual view of the discharge is shown in Fig. 5.2.2.

The inter-electrode gaps where plasma generated were varied for different distances 1, 4, 7 and 10mm. A liquid flow meter and controller (Dwyer-RM Series) was used to control the flow rate of water of 0.1 L/min through plasma generating quartz tube. A mass flow controller (LINE TECH M303V) along with mass flow control and display unit (FM-30VP) was used to control argon flow rate for adjusted value of 200 sccm. The required input power for generating discharge was provided by a neon transformer (15kV output voltage, and 25 kHz output frequency). An Avantes Avaspec-NIR256

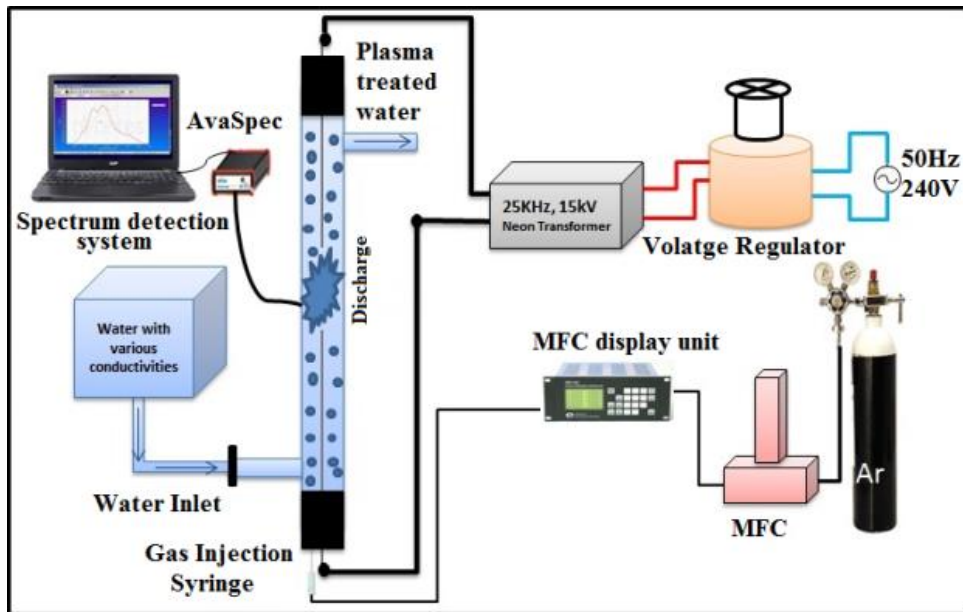


Fig. 5.2.1: (Color online) Schematic view of experiment set-up.

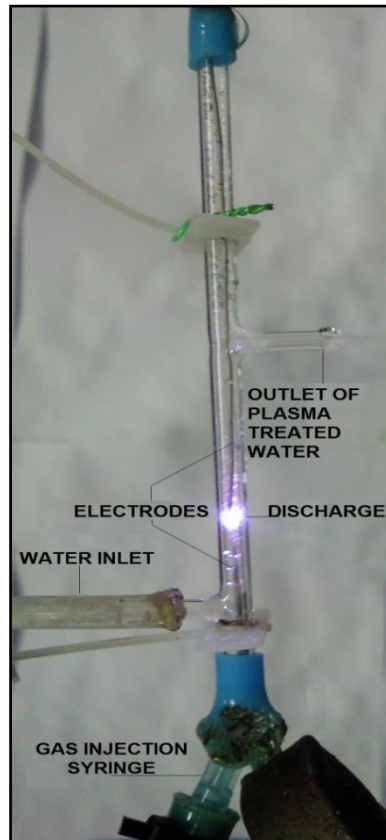


Fig. 5.2.2: (Color online) Visual view of the capillary discharge.

miniature fiber-optic spectrometer was gas and water simultaneously entered the quartz tube, in the liquid, the gas generated bubbles, which played a vital role in creating breakdown in water.

The argon injection rate was fixed at 200 sccm and water flow rate was also kept constant at 0.1 L/min. H_2SO_4 was added to enhance the conductivity of water according to required experimental conditions.

A Tektronix digital oscilloscope (DPO-2024) with high voltage and current probes and having data storage device facility was used for observing and recording Volt-Ampere characteristics. After allowing water to flow through quartz tube argon gas was injected and when bubbles were created, high voltage and high frequency input power was given and discharge was ignited.

After discharge occurrence the electrical and spectral data (emission spectrum) was taken simultaneously, used to record the emission spectrum of $\text{OH}\cdot$ radicals and other oxidant species (reactive hydrogen and oxygen) at different inter-electrode gaps and various conductivities.

3. Methodology:

Two tungsten electrodes attached to the Neon transformer were inserted in quartz tube. A tank having water with different conductivities (by adding H_2SO_4) was used to deliver continues supply of water during discharge. The argon gas was injected by using an injection syringe and gas flow rate was controlled by using mass flow controllers (MFCs). When the The complex wave forms of electrical data were obtained and numerical methods were applied to calculate power of discharge pulses and breakdown voltage under various experimental conditions. The computational method was applied to emission spectral lines to determine the concentration of $\text{OH}\cdot$ radicals for the various conductivities, non-gas and gas injected discharges and different inter-electrode gaps.

4. Results and discussion:

The results were analyzed by the electrical and spectral diagnostic techniques.

4.1. Electrical Results

The electrical results for four different inter-electrode gaps (1, 4, 7 and 10) mm and at various conductivities were observed and compared. A high voltage probe (Tektronix P6015A) and a current

probe (Tektronix P6021) were used to measure the breakdown voltages and discharge currents. Fig. 5.2.3 (a, b) shows typical Volt-Ampere characteristics under different experimental conditions.

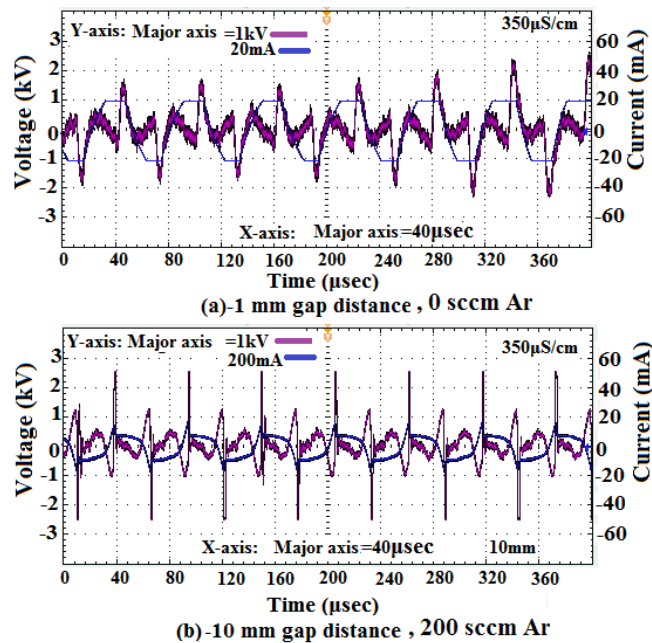


Fig. 5.2.3 (a, b) (Color online) Typical Volt-Ampere characteristics for non-gas and Argon injected values at different gap distances.

The applied voltage was sinusoidal and having high frequency but due to special liquid plasma characteristics the output appeared complex wave form when plasma occurred. The plasma discharge in water consists of many complex physical phenomena. The bearing of plasma in water obeys electron impact dissociation process and discharge in bubbles, either created by Ohmic heating or by external gas injection. We presented two cases: A gas injected discharge and non-gas injected discharge at various conductivities. When 25 kHz voltage was applied across two tungsten electrodes, then the streamers propagated between two electrodes and heating phenomena started that generated micro-bubbles, at break down voltage the discharge occurred inside these bubbles, the implosion of these bubbles participated in occurrence of discharge in water. Also the electron impact dissociation participated in creating breakdown inside liquid. In case of gas injection the bubbles of larger size compared to bubbles generated by Ohmic heating were generated that created discharge more effectively. The generation of bubbles and gas channels, occurrence of discharge within that bubbles was a random process therefore the nature of discharge was pulsating. The plasma generation and

nature of discharge depends upon the size of bubbles, number density of bubbles and statistical probability of bubbles existence between two electrodes. The bubble generation in turn depends upon the gas injection rate and Ohmic heating rate which depends upon the conductivity of water and applied electric field value. The sharp peaks in discharge pulses represent the stage when bubbles fully exists between the electrodes and discharge occurs within that bubbles, at this stage voltage drops and discharge current rises. The procedure was quick and random therefore arbitrary and sharp pulses were obtained.

Fig. 5.2.4 represents the variation in breakdown voltage for different experimental conditions. In case of non-gas injection, the required breakdown voltage was high, but if compared to argon injection the required breakdown voltage even at long gap distance reduced enormously. When no gas was injected input power had to do two works: 1) Ohmic heating of water to create micro bubbles: 2) the creation of breakdown inside these micro bubbles and in the water at the interface of these bubbles through electron impact dissociation, and variation of electrical field across the electrodes.

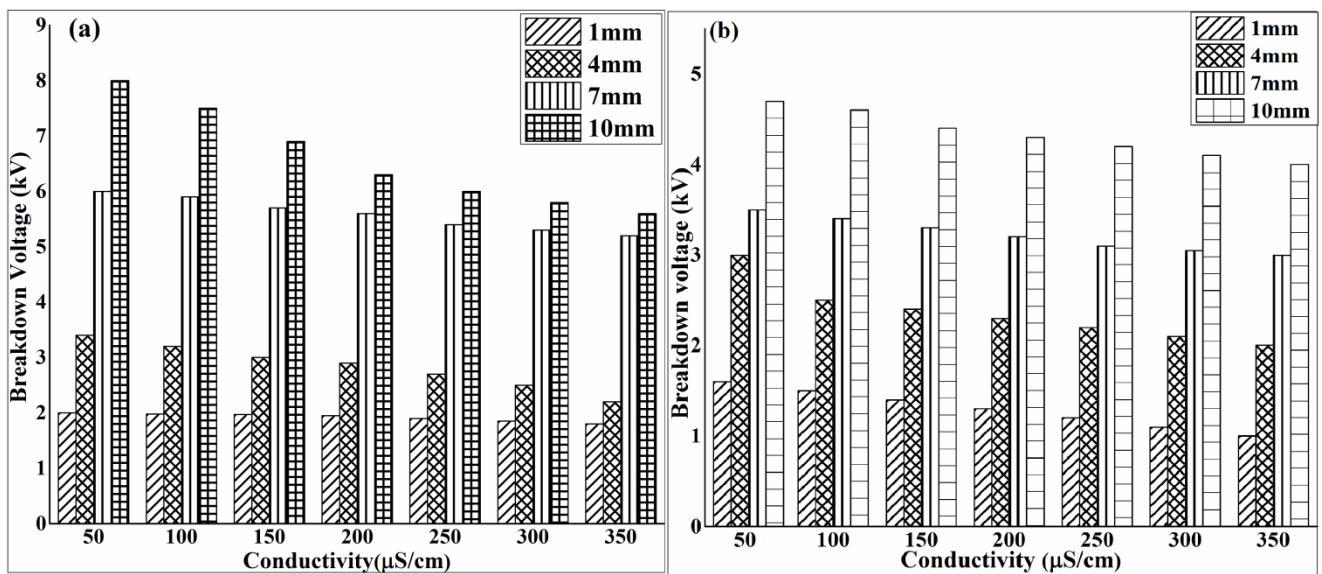


Fig. 5.2.4 (Color online) Variation of breakdown voltage at various conductivities and different inter-electrode gaps (a) No gas injection (b) 200sccm Argon injection.

In this experiment since water was flowing through capillary tube continuously, therefore heating phenomena, and generation of micro-bubbles was not dominant. The micro-bubbles existed in the

surrounding of the discharge region along the walls of the capillary tube. Therefore in the absence of the external gas injection the discharge occurred due to electron impact dissociation and applied electric field across electrodes. At low conductivities the water resistance was higher, so conduction current reduced therefore higher breakdown voltage was essential. At higher conductivities the conduction current increased, Ohmic heating raised, evaporation increased and all these processes enhanced the discharge occurrence process; therefore less breakdown voltage was needed at higher conductivities.

When argon gas was injected, it generated bubbles and gas channels inside liquid and in the region where electric field was dominant. These bubbles and gas channels reduced the required breakdown voltage as the dielectric strength of gas is much less than water. Therefore the required input breakdown voltage was higher in pure water medium compared to gas injected medium.

At higher conductivities although the breakdown voltage reduced but it can be scaled down more drastically by injecting external gas more preferably non-reactive gas like argon. The breakdown voltages in this research article were compared to other previous research performed by AC with less frequency [203] and results proved that high input frequency dissociated water molecule more effectively at lower breakdown voltage and less power consumption.

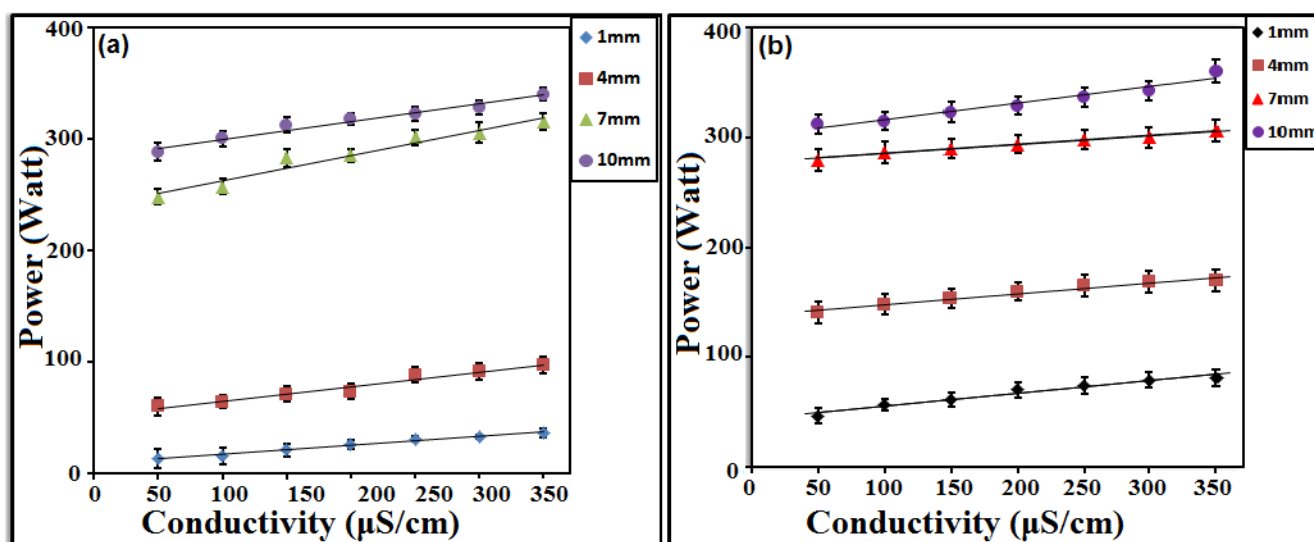


Fig. 5.2.5 (Color online) Variation in average electrical power of discharge pulses at various conductivities and inter-electrode gaps (a) Non-gas injected (b) 200sccm Argon.

With increase in water conductivity, electrical power of discharge pulses increased and more intense discharge (intense UV radiations) was obtained.

Fig. 5.2.5 represents the variation in electrical power of discharge pulses under different experimental conditions. Since the discharge wave forms were complex wave forms therefore, the power was calculated by $P_{avg}=V_{rms} \times I_{rms}$. The results represented that with increase in water conductivity the power of discharge pulses increased and comparison of non-gas and gas-injection emanated that the power of discharge pulses in gas injected case were much higher than non-gas injected discharge. In case of no-gas injection where the discharge occurred due to electron impact dissociation in pure water medium, the gap distance contained water only, the dielectric constant was higher therefore the strength of discharge was weak and discharge pulses comprised of less power.

In gas injected case, as in this experiment 200sccm argon was injected the gas channels and gas bubbles filled the gap distance between two electrodes and more powerful discharge pulses were obtained.

4.2.Spectral results

The emission spectrum was taken after discharge occurrence at different inter-electrode gaps and various conductivities for non-gas as well as argon injection.

Fig. 5.2.6 represents typical emission spectrum of various reactive species at 1-mm and 10-mm inter-electrode gaps and various conductivities without injecting any stream of gas, while Fig. 5.2.7 represents the 200sccm argon injected typical spectrum under similar conditions.

When plasma was generated between two electrodes then emission spectrum of reactive oxidant species specially $\text{OH}\cdot$ radicals were recorded. The spectral range consists of 250-1000nm, with $\text{OH}\cdot$ radicals (309nm), reactive hydrogen ($\text{H}_\alpha = 656\text{nm}$, $\text{H}_\beta = 486\text{nm}$) and reactive Oxygen (777nm and 844nm). Special focus was on $\text{OH}\cdot$ radicals having high redox potential (2.87V) while other hydrogen, oxygen and remaining reactive species can also be seen in the emission spectrum.

In both cases non-gas and argon injected, the statistical probability of the bubbles existence between the electrodes was small; therefore weak discharge occurred at small gap distance with less electrical

power of discharge pulses compared to long gap distance. The electrical field variation in long gap distance and electron impact dissociation was higher than short gap distance.

The argon gas injection was kept constant to produce approximately uniform size of bubbles and gas channels while conductivity was varied from tap water conductivity ($\sim 50\mu\text{S/cm}$) to higher conductivity ($350\mu\text{S/cm}$). Short intervals of conductivity ($50\mu\text{S/cm}$) were taken to determine the variation in OH \cdot radical's intensity with increase in conductivity.

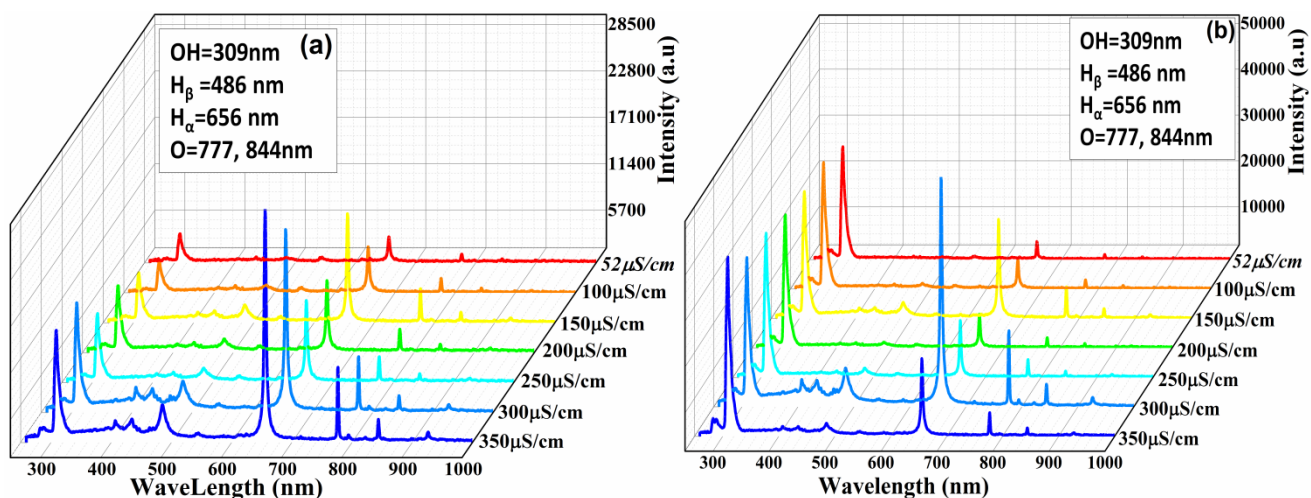


Fig. 5.2.6 (Color online) Emission spectrum of OH \cdot radicals at various conductivities for (a) 1-mm (b)-10mm Inter-electrode gaps without argon gas injection.

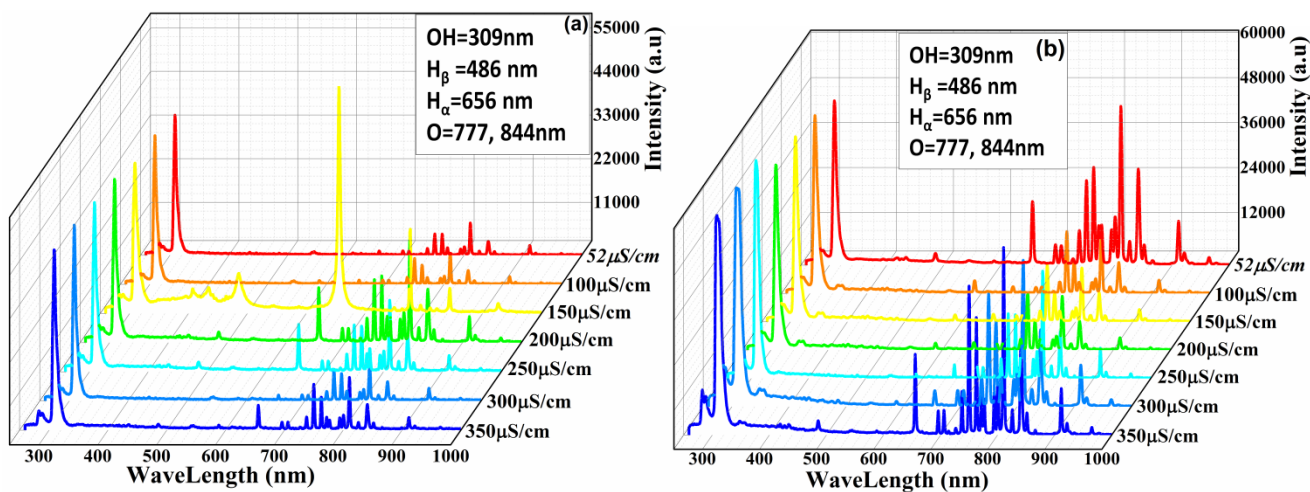


Fig. 5.2.7 (Color online) Emission spectrum of OH \cdot radicals at various conductivities for (a) 1-mm (b) 10-mm inter-electrode gaps at 200 sccm argon gas injections.

The results demonstrated that increase in conductivity increased OH[•] radical's concentration and this concentration was observed higher in case of argon injection and at long gap distance. The probable reason was electron impact dissociation of water molecule under argon injection.

The concentration of OH radicals was calculated by computational method (MS Excel) using emission spectrum's area under the curve of OH radicals at 309 nm.

Fig. 5.2.8 represents the variation in concentration of OH radicals under different experimental conditions.

At higher conductivities the emission peak of OH radical's was high and comparatively broader lines were obtained than low conductivity.

Argon injected discharge resulted more intense discharge compared to non-gas injected discharge, therefore higher OH[•] radical's concentration with Argon injection was obtained, compared to non-gas injection.

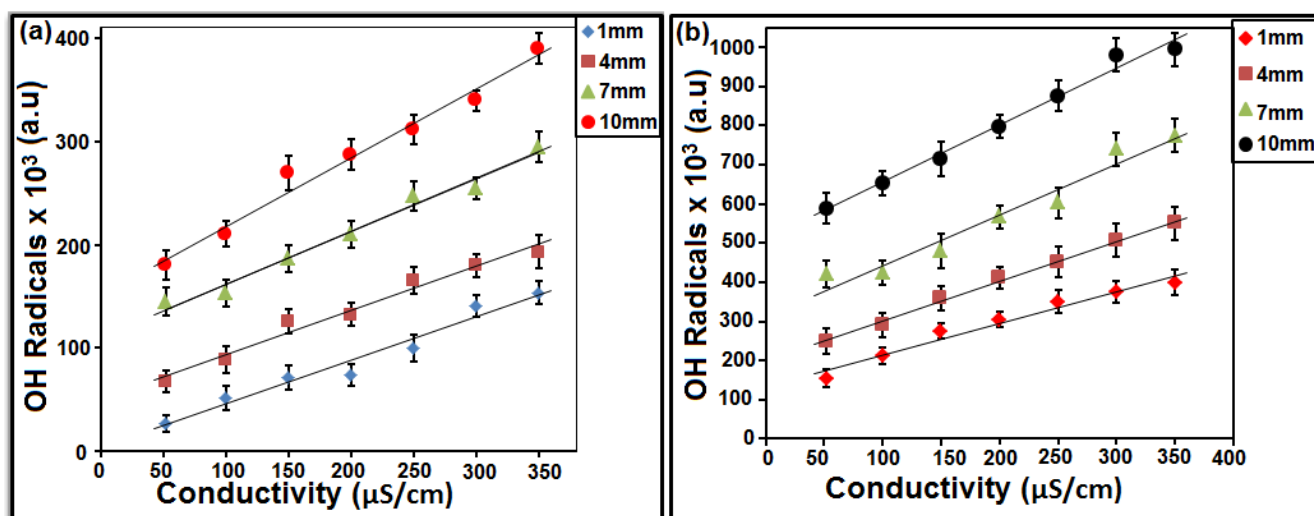


Fig. 5.2.8 (Color online) Concentration of OH[•] radicals for various conductivities and different inter-electrode gaps (a) non gas injection (b) 200sccm Argon injection.

discharge compared to non-gas injected discharge, therefore higher OH[•] radical's concentration with Argon injection was obtained, compared to non-gas injection.

5. Conclusions

1. At large conductivities less breakdown voltage was needed, that can be more reduced by injecting gas from external source
2. At large conductivities, electrical power of discharge pulses was observed higher.
3. Long gap discharge, with argon injection and with high frequency source produce high concentration of OH radicals, compared to non-gas injected and short gap distance.
4. The problem of power consumption at large gap distances and at low or high conductivities can be solved by using high frequency source.
5. High frequency source proved useful for creating long gap flowing water discharge at less Power consumption and less breakdown voltage.

6. Large Volume Underwater Plasma Discharge

1. Introduction

High frequency underwater plasma discharge is of technological larger interest for industrial, biological, medical and environmental applications [204-207]. The sterilization of drinking water and industrial waste water treatment is some dominant applications of underwater plasma discharge [208-211]. High frequency, high-voltage underwater plasma discharge generated directly in water proved to be an effective waste water treatment method. The high frequency and high voltage pulses are able to concentrate a strong electric field between the two electrodes inserted in water for creating breakdown and to initiate discharge within water medium [212]. The occurrence of discharge in water interacts with water molecules and initiates various physical and chemical processes in water such as shock waves of several mega Pascal, strong electric fields of several kV/cm, intense UV radiations, high redox potential chemical reactive species like O_3 , $OH\cdot$ radicals, reactive hydrogen, reactive oxygen, hydrogen peroxide etc. [213-216]. These reactive species generated by the electrical discharge in water chemically react and then degrade the organic pollutants contained in the water. The injection of gas to produce bubbles in water influence physical properties of plasma as well as yield rate of chemical reactive species. Since the dielectric strength of water is higher, therefore in order to reduce the required input power to induce discharge in water medium and to lower the dense effects of water, gas bubbles can be introduced [217]. The presence of gas bubbles makes it possible to easy initiation of ionization and electron avalanche process [218].

Due to high dielectric strength of water the power consumption, required high breakdown voltage especially in large volume of water make it a challenging issue for the researchers. The injection of gas bubbles and generation of gas streamers with in liquid and generation of plasma within such bubbles and gas channels drastically reduced the required input power for generating discharge in large volume of water due to less dielectric strength of gas compared to water[219]. In the absence of gas bubbles the required breakdown voltage was observed approximately above 40kV and required current from power source was observed above 100A [220]. The capillary discharge method with gas injection is a

convenient method for generating discharge in water at low power [221]. Even the assembly of electrodes like pin to pin, pin to plate could affect the required input power [222].

In this research we adopted a new mechanism of multiple capillaries connection in parallel. As in our previous research we proved that at the flow rate of 0.1 L/min the flowing water sterilization is possible, therefore we extended our research to some higher volume. We connected twenty capillaries in parallel and each capillary was able to flow maximum up-to 0.2 L/min, and therefore we were able to sterilize 4 L/min water with these capillaries at comparatively low power compare to other mechanisms. In our previous research we also proved that oxygen is the best gas among other gasses for producing reactive oxidant species like $OH\cdot$, H_2O_2 , and O_3 . Therefore we used oxygen in this research for producing highly oxidant reactive species in large volume discharge.

The aim of this research was to provide a different convenient mechanism and idea for sterilizing large volume of water at lower power. This research will provide a baseline data for large scale applications.

2. Experimental set-up

Fig. 6.1 shows the schematic of the experimental set-up used in this research. The visual view of multiple capillary discharges is shown in Fig. 6.2. Twenty capillaries were connected in parallel. The capillary tubes were chosen of size; $\Phi = 4\text{mm}$ outer; $\Phi = 2\text{mm}$ inner and thickness = 1mm. A Neon transformer was used for applying high frequency (25 kHz) and variable voltage (15kV) across tungsten electrodes ($\Phi = 0.5\text{mm}$) inserted in each capillary. The inter electrode gap where the plasma generated, was 10mm for each capillary. A liquid flow meter and controller (Dwyer-RM Series) was used to control the flow rate of water at 0.2 L/min through plasma generating quartz capillary tube. A mass flow controller (LINE TECH M3030V), along with a mass flow control and display unit (FM-30VP), was used to control the oxygen flow rate (100 – 800 sccm) with interval of 100 sccm, through an injection syringe. The electrical results were recorded by a Tektronix digital oscilloscope (DPO-2024) with high voltage and current probes and having data storage facility was used for recording Volt-Ampere characteristics.

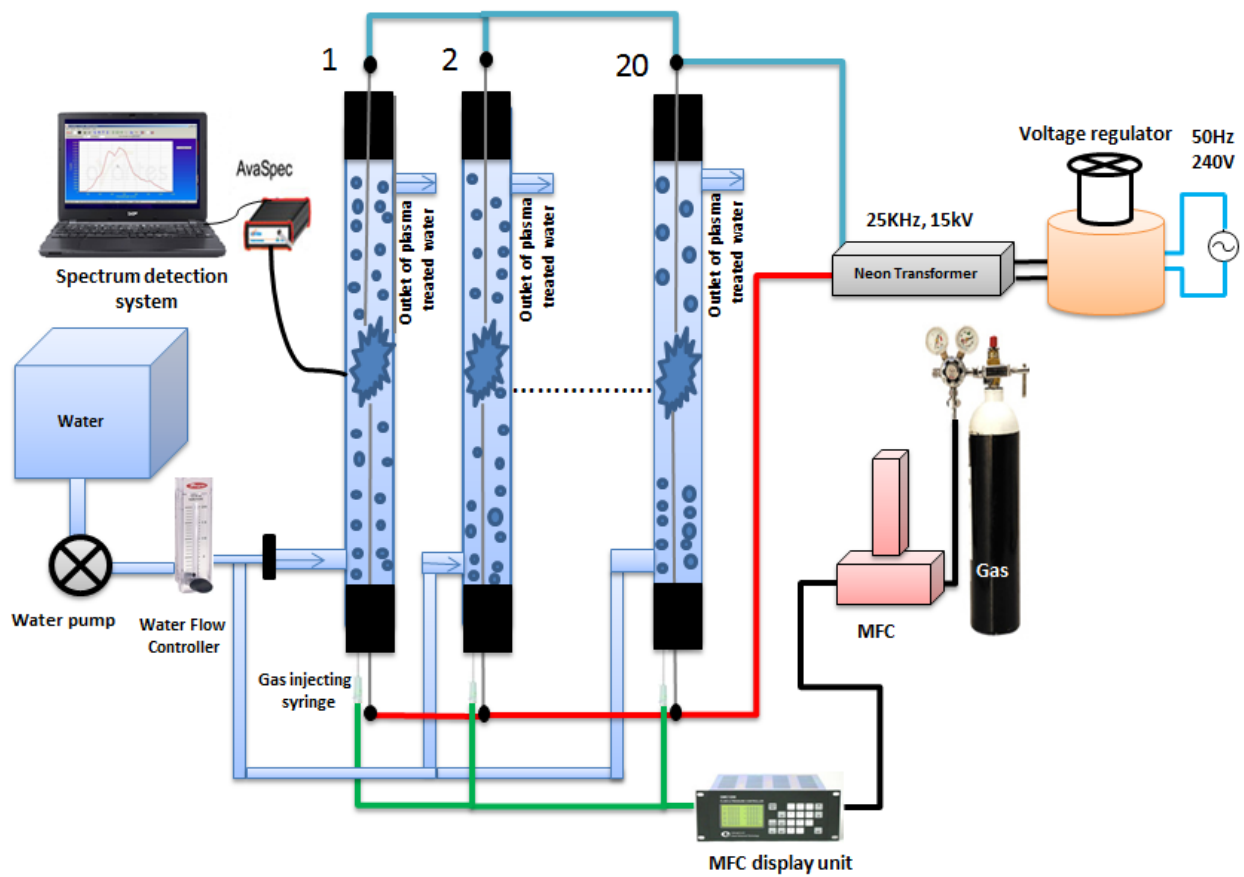


Fig. 6.1 Schematic diagram of experimental set-up.

The variation in break down voltages and average power of discharge pulses were calculated and presented. An Avantes Avaspec-NIR256 miniature fiber-optic spectrometer was used to record the emission spectrum of discharge under different experimental conditions. The spectrum provides the concentration of reactive species under different experimental conditions.

3. Results and discussion

(a) Electrical results

Fig. 6.2 (a) represents the typical volt-ampere characteristics curves obtained by voltage and current probes for parallel capillaries assembly while fig. 6.2 (b) demonstrates the breakdown voltage. With increase in gas injection rate the required breakdown voltage reduced enormously, while discharge current rises. The existence of many capillaries and having single cathode and Anode makes the discharge pulses of complex and irregular nature. The large flowing water discharge was fluctuating and carrying noise of spark.

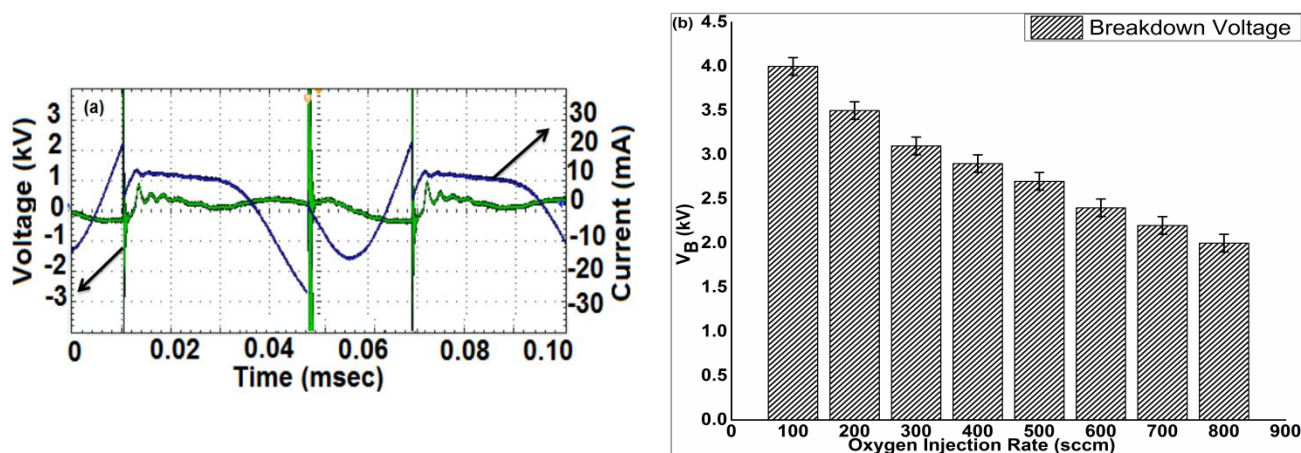


Fig. 6.2 (Color online) (a) Typical volt-ampere characteristics curve (b) Variation in Breakdown Voltage; for parallel capillaries assembly.

(b) Spectral Results

Fig. 6.3 represents an emission spectrum of discharge obtained after discharge occurrence. The strength of discharge was observed same for all capillaries under similar experimental conditions

therefore the emission spectrum was observed similar under one experimental condition in all capillaries. At larger gas injection rates since more hydrogen peroxide could be generated in water;

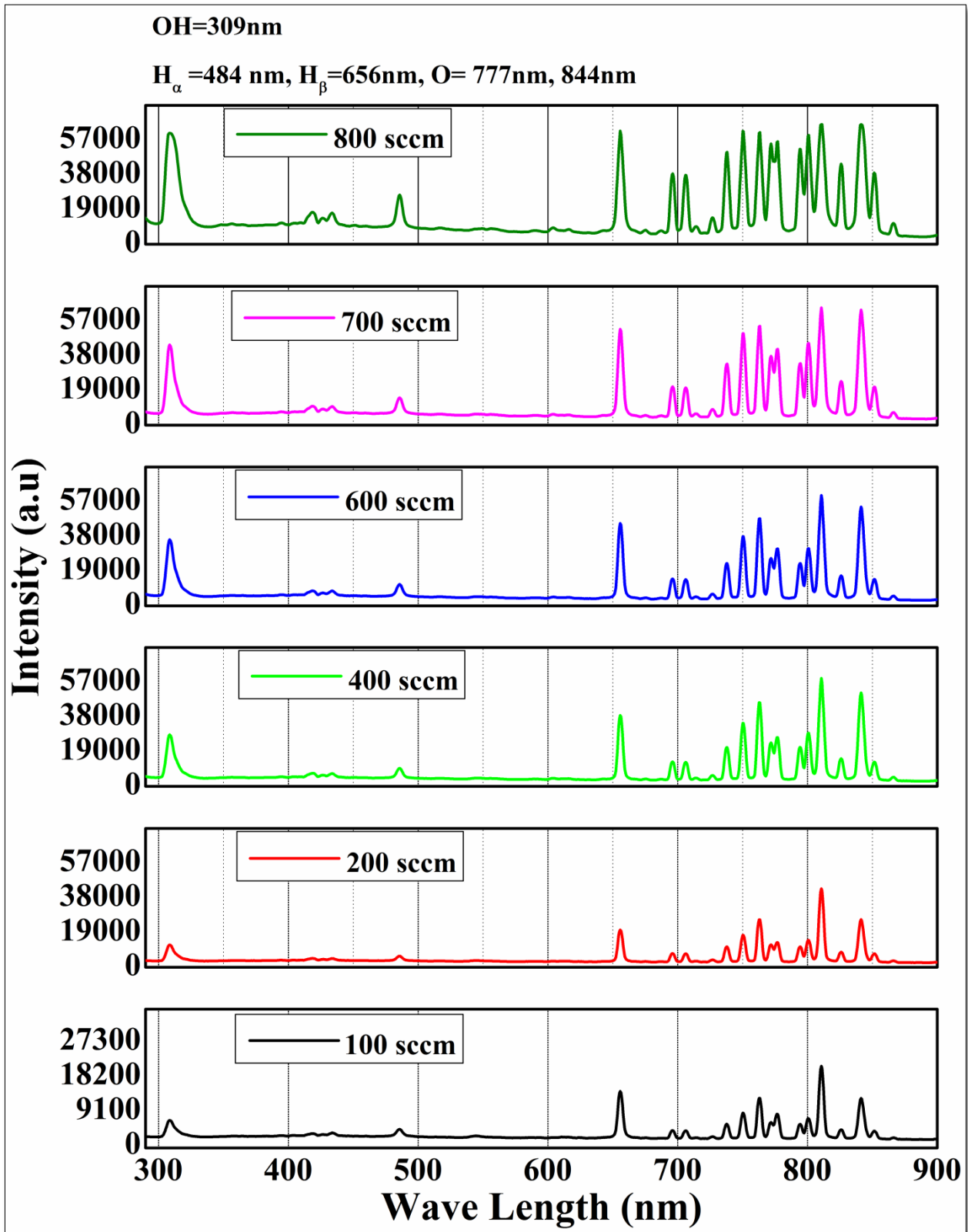


Fig. 6.3 Emission spectrum of oxygen Injected large volume capillary discharge.

also strength of discharge raises therefore high concentration of $OH\cdot$ radicals (at 309nm) was observed from the emission spectrum. Along with $OH\cdot$ radicals the reactive hydrogen (486nm, 656nm) and reactive oxygen (777nm, 844nm) can also be observed.

In our previous section (chapter 4) we presented the concentration of ozone and hydrogen peroxide as well. It was proved that oxygen injected discharge could induce high concentration of $OH\cdot$ radicals, H_2O_2 and O_3 . Therefore multiple capillaries could yield such high concentration of these reactive species.

In this part of research we focused on $OH\cdot$ radicals only due to their high redox potential and quick chemical reaction ability that is too useful for flowing water discharge.

4. Conclusions

Connection of multiple capillaries could work as large volume flowing water discharge. The injection of oxygen gas not only could reduce the required input power but also it could induce high concentration of $OH\cdot$ radicals.

7. High Frequency Underwater Plasma Discharge Application in Antibacterial Activity

7.1 Introduction

Treatment of water by plasma technology to inactivate dangerous bacteria like *E. coli* is a profitable and impressive non-chemical method [223-226]. The occurrence of discharge in water engendered highly reactive species like ozone (O_3), $OH\cdot$ radicals, reactive oxygen (O), reactive hydrogen (H), hydrogen peroxide (H_2O_2), ultra violet (UV) radiations and shock waves of several mega Pascal [227, 228]. Depending upon their redox potential (for oxidant species) and their intensity (for UV and Shock waves), each of these play a vital role in the inactivation of *E. coli* [229-231]. $OH\cdot$ radicals have high redox potential but have very short life time of $\sim 10^{-8}$ sec [232], therefore they react quickly for a short time, compared to other reactive species like ozone and H_2O_2 , those have long half-lives and react adequately as well [233]. They can be used for treatment of large volume of contaminated water [234]. Conventionally ozone can be generated in air and mixed in water for sterilization. Ozone can also be generated inside water like H_2O_2 by water dissociation process through electrical discharges [235-237]. Several chemical reactions take place simultaneously for generating $OH\cdot$ radicals and recombination of these $OH\cdot$ radicals with hydrogen, oxygen and other $OH\cdot$ radicals to generate ozone and hydrogen peroxide [238-240], reducing pH of water at the same time. When low pH of water reservoir is maintained the microbial activity of plasma treated water can be extended over long time after treatment [241]. Several electrode configurations and plasma generating mechanisms in water exist [242-244], and each mechanism generates different loads of oxidant species. Among them it is found that the discharge created in water is more competent than the discharge existence over the surface of water [208]. The occurrence of discharge within water causes dissociation of water molecules, formation of oxidant species and emission of UV and shock waves within water medium. These offer effectiveness of water treatment by plasma technology. The injection of oxygen compared to other non-reactive gas can generate more reactive oxygen, ozone and $OH\cdot$ radicals, which are more effective for *E. coli* sterilization in water. The dominant reason why oxygen is superior feed gas compared to air that contains 70% nitrogen, for generating reactive species in water especially ozone

generation [245, 246] is; 1). Oxygen fed plasma system can generate twice ozone and other reactive species that is highly effective for water sterilization; 2) its high chemical reactivity for generating oxidant species.

Since water is having high dielectric strength, therefore power consumption in underwater discharge is also a confront affair. To conquer such problem the gas bubbles and gas channels can be formed by oxygen injection. Due to low dielectric strength of gas, the occurrence of discharge in gas channels and bubbles at low power consumption takes place. In this research work, oxygen was injected for creating bubbles and channels. The oxygen injection was not only effective for reactive species generation but also useful for reducing required input power. Oxygen being electronegative gas, presence of oxygen bubbles and channels containing plasma, acts as a source of electronegative species, originate an increase of the electric field strength. Therefore, the mean electron kinetic energy increased and this lead to an increase of the excitation temperature and rise in electron density.

Several oxidant species contribute to inactivate *E. coli* through different mechanisms.

Ozone (O_3) causes *E. coli* inactivation through chemical reaction. Compared to other Gram-positive *E. coli* like cocci (Staphylococcus and streptococcus), bacillae (Bacillus) and Myco *E. coli* those are resistant to O_3 , *E. coli* being Gram negative bacillae is very sensitive to inactivation by O_3 [247]. O_3 damages the membrane of *E. coli* and also causes loss of cell numbers. By mutating of *E. coli*, it causes membrane damage [248].

H_2O_2 is also an athletic oxidizing agent for water disinfection, but its effect on *E. coli* is minimal because relatively high concentration is desired for sterilization, and considerable contact time is needed [249]. The addition of H_2O_2 elevates the chemical reactions for generating O_3 , and $OH\cdot$.

The highly reactive OH radicals engage in aqua purification by forming double strand break (DSB) in DNA cells of *E. coli*, which causes segregation of DNA molecule from each other near cell walls, whereas the number of DSB formed by single $OH\cdot$ radical is autonomous of molecular weight of DNA [250].

The underwater discharge emits highly intense UV radiations, which may outcome residual effect that is harmful for *E. coli* [251]. The plasma generated reactive oxygen proved highly practical for *E. coli* disinfection [252].

The shock waves transmitted by plasma discharge can also eradicate the membrane of *E. coli* by immobilize it to reinvigorate themselves, preserve the safety and quality, also provide a novel approach for solving sterilization process [253].

Literature review demonstrated that the waste water treatment and sterilization of drinking water by ordinary advance oxidation processes (AOP's) is not too effective as it cannot generate high intensity and concentration of oxidant species that are necessary for the inactivation of hazard species from water. The advantages of such AOP's are also restricted [254-256]. Generation of all above cited reactive species by initiating discharge with in water and its application on *E. coli* treatment proved effective compared to pure chemical and traditional methods.

Plasma discharge is a novel disinfection and effectual inactivation approach to treat microorganisms in aqueous systems. Inactivation of Gram-negative *Escherichia coli* (*E. coli*) by generating high frequency, high voltage, oxygen (O_2) injected and hydrogen peroxide added (H_2O_2) discharge in water was achieved. The effect of H_2O_2 dose and oxygen injection rate, on electrical characteristics of discharge and *E. coli* disinfection has been reported. Microbial log reduction dependent on H_2O_2 addition with O_2 injection was observed. The time variation of the inactivation efficiency quantified by the log reduction of the initial *E. coli* population on the basis of optical density (OD) measurement was reported. The analysis of emission spectrum recorded after discharge occurrence illustrated the formation of oxidant species ($OH\cdot$, H and O). Interestingly the results demonstrated that O_2 injected and H_2O_2 added, underwater plasma discharge had fabulous impact on the *E. coli* sterilization. The oxygen injection notably reduced the voltage needed for generating breakdown in flowing water and escalated the power of discharge pulses. No impact of hydrogen peroxide addition on breakdown voltage was observed. A significant role of oxidant species in bacterial inactivation also has been identified. Furthermore the *E. coli* survivability in plasma treated water with oxygen injection and

hydrogen peroxide addition drastically reduced to zero. The time course study also showed that the retardant effect on *E. coli* colony multiplication in plasma treated water was favorable, observed after long time. High frequency underwater plasma discharge based biological applications is technically relevant and would act as baseline data for the development of novel antibacterial processing strategies.

This research work payoff underwater plasma discharge application in *E. coli* disinfection through oxygen and hydrogen peroxide addition to water. The comprehensive aftermath of all reactive species generated by plasma discharge, on *E. coli* inactivation was reviewed and conferred.

7.2. Materials and methods

7.2.1 *E. coli* strains and growth conditions

Representative Gram-negative *E. coli* were procured from the American Type Culture Collection (ATCC[®] 25922[™]). The strains of *E. coli* were revived on Mueller-Hinton (MH) (Fluka, Sigma-Aldrich, Ireland Ltd.) efficient agar plates. Overnight (16 to 18 h) *E. coli* cultures were grown aerobically at 37°C, with rotation 250 rpm on moving shaker, in TSB supplemented with 5% NaCl, MH broth for *E. coli* strains. After 24 hours *E. coli* culture was stored at -20° C for next *E. coli* coliform assays.

a. Micro-well dilution coliform assay

Minimum inhibitory dose (MID) of plasma treatment was determined by the micro-well dilution method in culture broth as previous study [257, 258]. To test the ability of the plasma to kill large amounts of colony forming *E. coli*, overnight grown colonies of *E. coli* were diluted in sterile LB medium (1 colony in 1 µL). This suspension was diluted 1/100 in sterile medium and seeded in 96 well plate (Nunc[™], Wiesbaden, Germany). Wells were incubated at 37 °C for 24 hours in LB medium broth. Anti *E. coli* activity was studied by observing the *E. coli* growth and turbidity in different treated and untreated wells. The plates were read for turbidity by measuring the optical density (OD) at 595 nm on a micro plate reader (Model-680, Bio-Rad). MID of plasma was read as the lowest dose for

which no turbidity is appeared (Transmittance > 90% of a media control well). All test groups were performed in triplicate.

b. Agar-well diffusion coliform assay

The antimicrobial activity was determined as earlier reported method in agar well diffusion method [259, 260][240, 241], with some modifications. The *E. coli* suspension water was prepared in different group (without hydrogen peroxide and without oxygen injection, with hydrogen peroxide and with oxygen from 100 -800 sccm) as water sample with nutrient medium. Next, the *E. coli* were streaked on Luria-Bertani (LB) agar (1% (w/v) bacto-tryptone and 0.5% (w/v) bacto-yeast extract along with 1% (w/v) NaCl and 4.5% (w/v) nutrient agar) and were incubated aerobically at 37 °C for overnight in CO₂ incubator for 24 hours. Penicillin-Streptomycin was used as positive control and PBS only as negative control. Next day, all plates take off and calculated inactivation efficiency of growing colonies as follow [261]:

$$\eta = \left(1 - \frac{N_t}{N_o}\right) \times 100 \% \dots\dots\dots (1)$$

Where η is the inactivation efficiency of *E. coli*, N_o is the initial concentration of *E. coli* (in colony forming unit per milliliter), and N_t is the concentration of *E. coli* after treatment time t (in colony forming unit per milliliter).

The abatement of number of colonies in plasma processed water under different experimental conditions was determined by $\ln \frac{N}{N_o}$ [262] ;(N = after treated colonies, N_o = before treated Colonies).

7.3. Experiment set-up and methology

The discharge was initiated in capillary tube ($\Phi=4\text{mm}$ outer; $\Phi=2\text{mm}$ inner and thickness =1mm). A Neon transformer was used for applying high frequency (25 kHz) and variable voltage (15kV) across two tungsten electrodes ($\Phi=0.5\text{mm}$). Fig. 7.1 presents a schematic of the experimental set-up that was used for this experiment, also a visual view of the discharge is shown in Fig. 7.2. The inter electrode gap where the plasma generated, was 10mm.

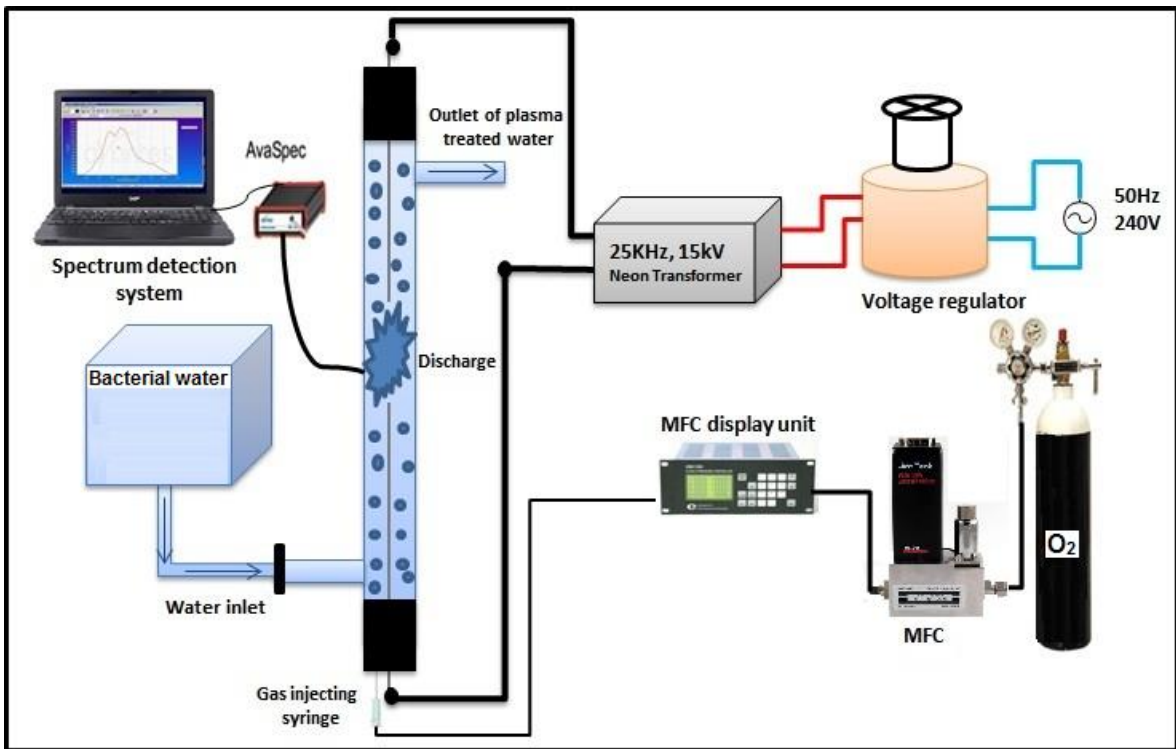


Fig. 7.1 (Color online) Schematic view of experiment set-up.

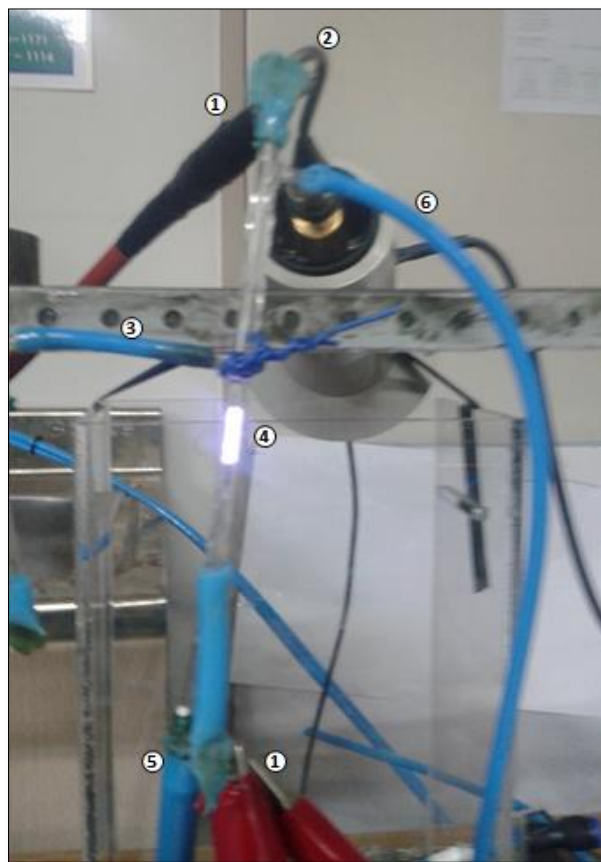


Fig. 7.2 (Color online) Visual view of the capillary discharge. 1. Electrodes connections. 2. High Voltage probe. 3. Water Inlet. 4. Discharge Region. 5. Oxygen Injection Syringe. 6. Water Outlet.

A liquid flow meter and controller (Dwyer-RM Series) was used to control the flow rate of water at 0.1 L/min through plasma generating quartz capillary tube. A mass flow controller (LINE TECH M3030V), along with a mass flow control and display unit (FM-30VP), was used to control the oxygen flow rate (100 – 800 sccm) with interval of 100 sccm, through an injection syringe. An Avantes Avaspec-NIR256 miniature fiber-optic spectrometer was used to record the emission spectrum of discharge under different experimental conditions. The spectrum provides the concentration of reactive species under different experimental conditions.

The *E. coli* containing water was treated under different experimental conditions including with and without oxygen injection and with and without hydrogen peroxide addition. The standard amount of hydrogen peroxide (0.35ml/l) [263][244] was added for generating high concentration of chemical reactive species.

The water (*E. coli* mixed) in a small tank with a one liter water reservoir was allowed to enter the capillary tube, and oxygen was injected by injecting syringe. When the oxygen and liquid simultaneously enter the quartz tube, in the water, the oxygen generated bubbles participate mainly in creating breakdown in water. The electrical data was observed and recorded using a digital oscilloscope with high- voltage and large-current probes, and with a data storage device facility. The emission spectrum was taken to observe the concentration of oxidant species generated in water after discharge occurrence.

The treated water was tested immediately after plasma treatment and after every 12 hours up-to 72 hours was tested to detect the regeneration of *E. coli* in water, and further disinfection rate due to existence of hydrogen peroxide in water.

7.4. Results and discussion

The electrical, spectral and *E. coli* diagnostics were carried out to study the results, physical and chemical procedures culpable for *E. coli* inactivation, under distant experimental conditions.

7.4.1. Volt-Ampere characteristics

A digital oscilloscope (Tektronix DPO-2024) was used for observing and reporting Volt-Ampere characteristics of underwater plasma discharge. A high voltage probe (Tektronix P6015A) and a large-current probe (Tektronix P6021), were used to determine the breakdown voltages and the currents for 10 mm long gap discharge at various experimental frameworks. Fig. 7.3(a-d) represents typical Volt-Ampere characteristic curves under different experimental conditions.

The eminent dielectric strength of water requires large break down voltage and higher power consumption. In order to apprehend this challenge, gaseous mediums are usually introduced in water where plasma needs to be produced. Two types of bubbles exists; a). Micro bubbles. b) Bubbles generated by external gas injection. The process of generation of micro bubbles depends upon the conductivity of water and whereabouts of water (static or flowing). At high conductivity and static reservoir of water these micro bubbles yield rate is dominant and having high number density. In order to generate micro bubbles the boiling of water is necessary and also higher conductivity is useful. These micro bubbles play a vital role in igniting plasma discharge. But since in this research water conductivity is very low (tap water) and water is flowing (heating process is almost negligible) therefore the number density of micro bubbles (generated by joule's heating) is very small, just around the tip of electrodes small number of micro bubbles exists, therefore the participation of these micro bubbles is negligible. Therefore external injection of oxygen gas drastically reduced the required high breakdown voltage. The formation of bubbles and oxygen channels, occurrence of discharge inside these bubbles and oxygen channels was an abrupt and arbitrary phenomenon; therefore nature of discharge was pulsating and having short pulse duration, as can be seen from oscillograms.

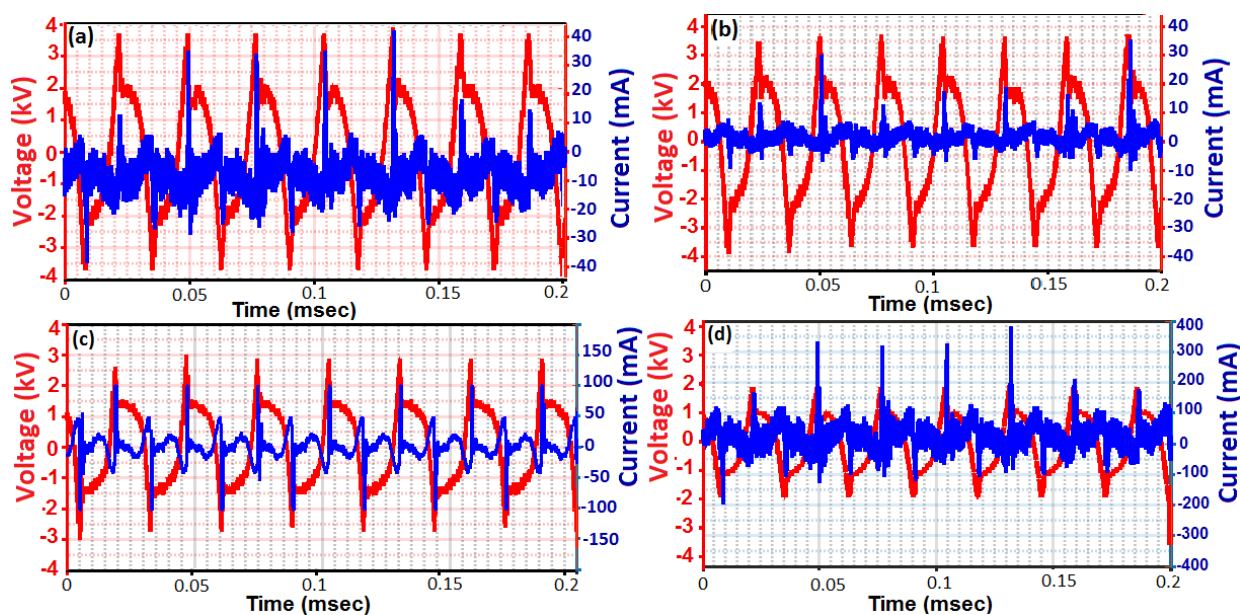


Figure 7.3 (color online) Dependence of typical Volt-Ampere characteristics of High Frequency Underwater Plasma Discharges occurred in bubbles containing water without and with H_2O_2 addition on oxygen injected rate (rate of O_2 -injection).

- (a): rate of O_2 -injection – 0 sccm, and H_2O_2 addition - 0 ml/L;
- (b): rate of O_2 -injection – 100 sccm, and H_2O_2 addition - 0.35 ml/L;
- (c): rate of O_2 -injection – 600 sccm, and H_2O_2 addition - 0.35 ml/L;
- (d): rate of O_2 -injection – 800 sccm, and H_2O_2 addition - 0.35 ml/L

Fig. 7.4(a, b, c) represents the breakdown voltage, power of discharge pulses and energy of discharge pulses under different oxygen injection rates. With increase in oxygen injection rates the breakdown voltage was reduced and higher power of discharge pulses were perceived. The existence of oxygen channels and bubbles between two electrodes reduced the density of medium and thus the breakdown occurred at low voltage. At higher oxygen injected rates the size of channels and bubbles was larger thus limited breakdown voltage was required. Since the discharge current was observed high at higher oxygen injection rates (as shown in oscillograms), so power of discharge pulses heightened as well. The increase in power of discharge pulses resulted to the corresponding increase in energy of discharge pulses as well. Both increase in power and energy aid a critical role in disinfecting *E. coli*.

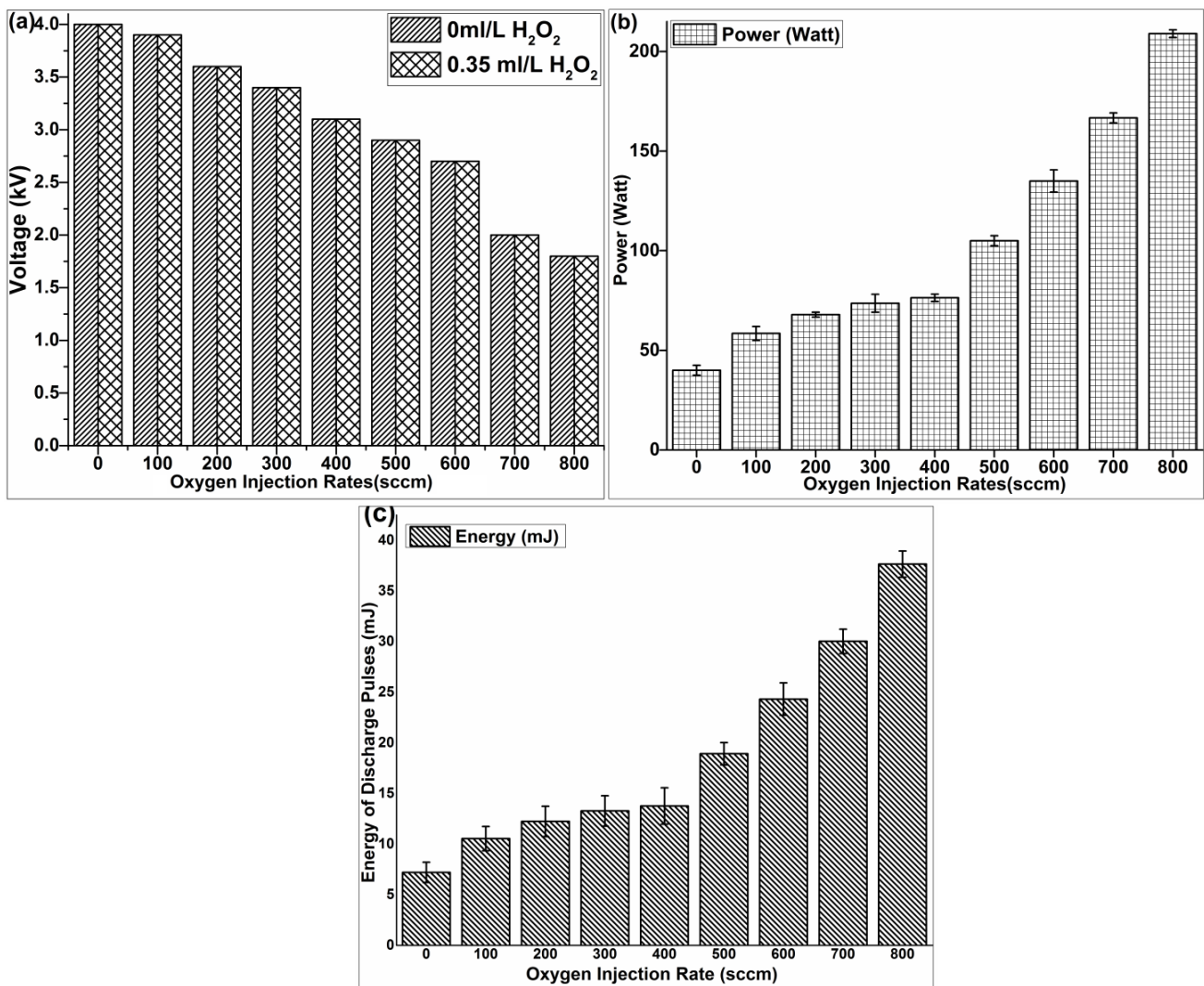


Fig. 7.4 Dependences of electrical parameters due to oxygen injected bubbles and increasing in power and in energy of discharge pulses on oxygen injection rate.

(a): variation in breakdown voltage in presence and absence of hydrogen peroxide addition;

(b): increasing in power of discharge pulses;

(c): increase in energy of discharge pulses.

7.4.2. Spectral

The optical emission spectroscopy (OES) has been widely exercised to interrogate the highly reactive species provoked in underwater plasma discharge [263]. In this experiment, the emission spectrum emitted from the discharge was checked to scrutinize the clustering of reactive species produced by plasma discharge under different experimental conditions. Fig. 7.5 (a-f) represents emission spectrum of eminently reactive chemical species. The spectra represented vigorous atomic lines emissions due to the existence of hydrogen and oxygen radicals, originated from the dissociation of water molecules. The vivid peaks of hydrogen Ballmer lines (H_{α} =656nm and H_{β} =484 nm) were present. The broadening of hydrogen Ballmer lines (H_{α} and H_{β}) were observed, which may be due to several broadening mechanisms including natural broadening, Doppler broadening, Stark /pressure/collisional broadening, instrumental broadening and Vander-wales broadening [265-267], and are useful for determining physical characteristics (electron temperature and number density) of plasma discharge under various conditions. In the infrared region, many vivid lines were perceived due to atomic oxygen. In UV range at 309 nm $OH\cdot$ radicals peaks were inspected. No distinctive lines due to metal ablation from electrodes were present in the spectra. The emission spectrum represents a cumulative contribution of all oxidant species necessary for *E. coli* disinfection. Beside these oxidant species, some consequential oxidants like H_2O_2 and O_3 are may be generated due to possible chemical reactions [268, 269], when the discharge occurs in water. Although their quantitative or qualitative analysis, that require chemical probe method [270, 271], for observing their dissolved amount in water, was not conferred in this article to desist chemical effects on *E. coli*, but their actuality in plasma treated water was scrutinized by innumerable researchers.

The vitality of plasma discharge and the generation of chemical reactive species were detected more at higher oxygen injection rate. The admixing of hydrogen peroxide along with oxygen injection enhanced the concentration of reactive species. Although each oxidant specie have different redox

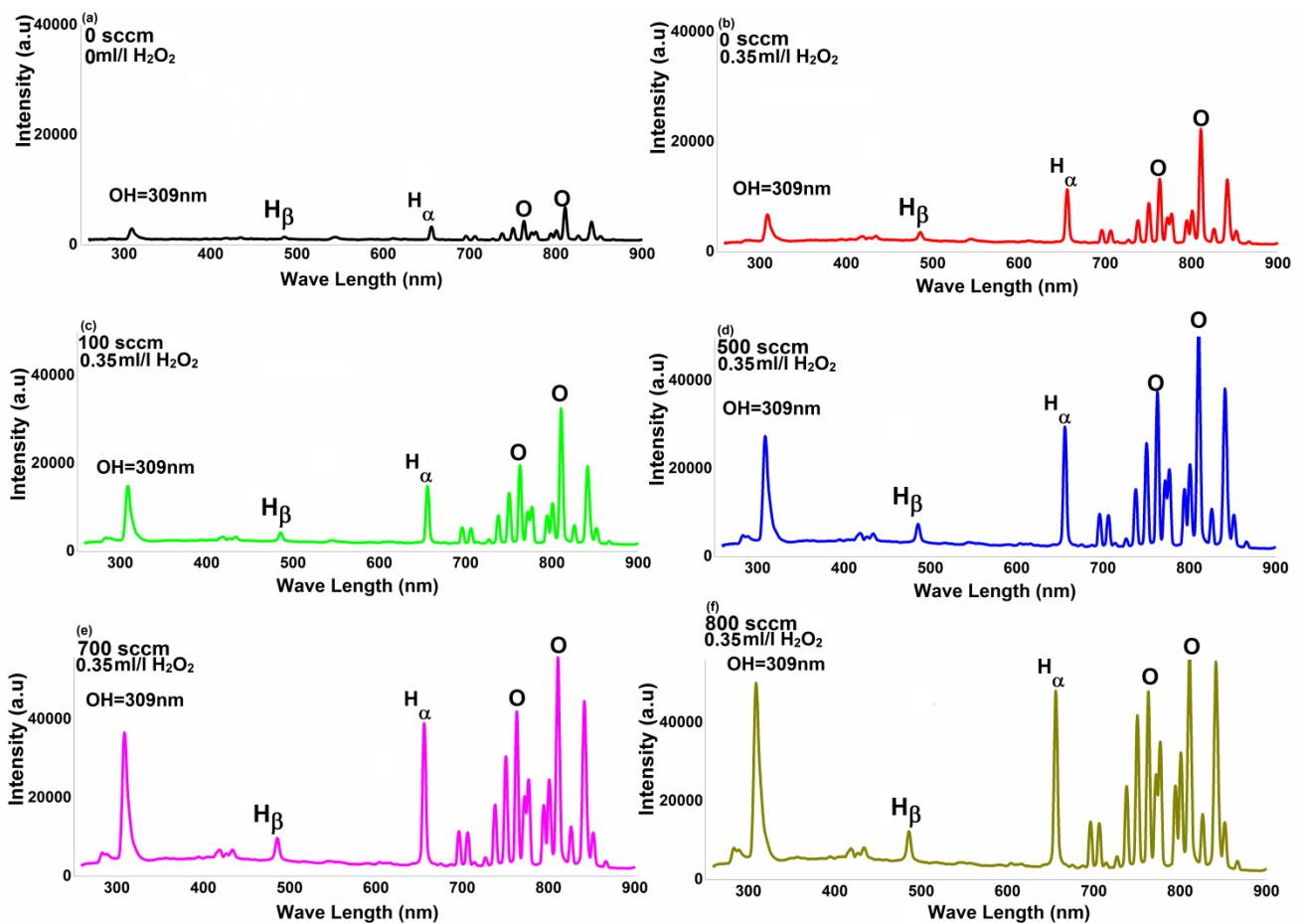


Fig. 7.5 (color online) The typical optical emission spectra of reactive chemical species useful for *E. coli* inactivation which have enhanced yield rate due to mixing H_2O_2 and O_2 and have been observed in High Frequency Underwater Plasma Discharges for various values of O_2 injection rates and H_2O_2 additions in water, accordingly, (a), (b), (c), (d), (e) and (f).

potential and inactivation power, but individual effects are not abundant, the existence of all of them (H_2O_2 , O_3 , H , OH^\cdot , O) participate to inactivate *E. coli*. The concentration of reactive species was low with the absence of O_2 and H_2O_2 , but it was enhanced at higher oxygen injection rate and hydrogen peroxide inclusion. OH^\cdot radicals due to high redox potential (2.70V) can massacre *E. coli* and virus effectively by wrecking their cell membranes or walls [272]. The plasma generated H_2O_2 and O_3 in water can contribute to *E. coli* inactivation.

7.4.3 Ozone concentration

The concentration of ozone was determined by indigo method as presented in chapter 4 of this thesis.

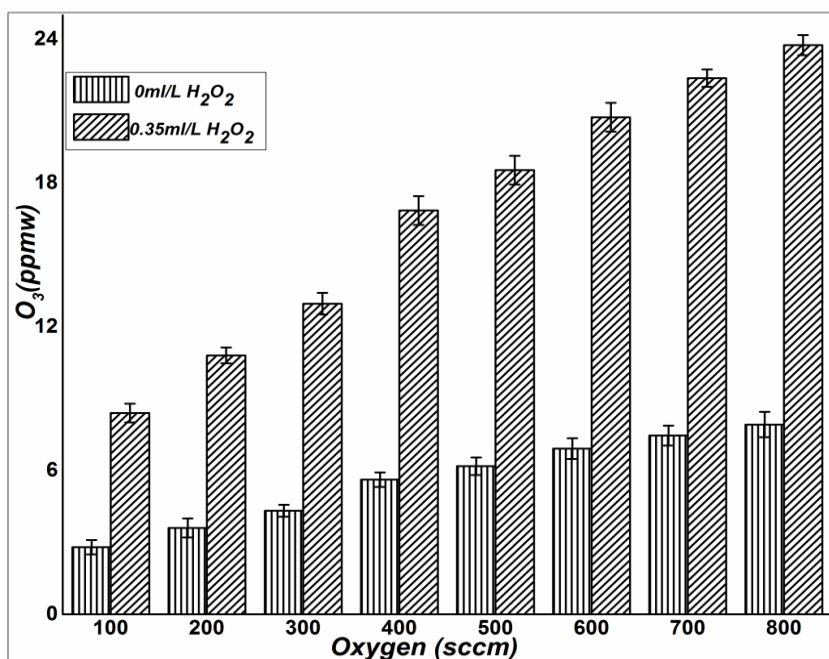


Fig. 7.6 Concentration of ozone (O₃) generated by underwater capillary discharge under different experimental conditions.

Figure 7.6 represents the concentration of ozone measured during different experimental conditions. Ozone (O₃) causes *E. coli* inactivation through chemical reaction. *E. coli* being Gram negative is very sensitive to inactivation by O₃ and it damages the membrane of *E. coli* and also causes loss of cell numbers. By mutating of *E. coli*, it causes membrane damage [247, 248]. At higher oxygen injection rates and in the presence of hydrogen peroxide the bacteria was observed effectively treated by plasma discharge as can be seen from agar plates in coming results.

7.4.4 Plasma discharge inhibits rapid propagation and inactivation of *E. coli*

A 100 µl of *E. coli* (liquid form) was added to one liter of water reservoir and the water was rotated at 250 rpm on moving shaker for overnight. The *E. coli* were active in this form and then under different experimental conditions the water was treated. The treated water was again rotated through shaker and

then spreaded over the LB agar plates the growth of *E. coli* was determined as process mentioned in section 2.

The colony forming unit (CFU), for different results was computed by relation [273]:

$$CFU = \frac{(Number\ of\ colonies) \times (Dilution\ factors)}{V_o} \dots\dots\dots (2)$$

Since 100µl of liquid *E. coli* was added to 1 liter water reservoir, therefore the dilution factor (DF) is 1.0001units/volume; $V_o=1$ L and number of colonies were counted by manual counting method.

Fig. 7.7(a) represents pure *E. coli* Strain concentration in water before plasma treatment, while Fig. 7.7(b) represents untreated water and *E. coli* before plasma treatment without oxygen injection and without H₂O₂ addition and Fig. 7.7(c). After Plasma Treatment without oxygen injection and H₂O₂ addition while Fig. 7.7(d) after plasma treatment without oxygen injection and 0.35ml/L of H₂O₂ addition in untreated water. The results showed that pure *E. coli* making high concentration of colonies, too numerous to count (TNTC) , while when 1 liter of water with DF=1.0002 units/Volume, is added then number of colonies were 350.002 CFU, after plasma treatment without oxygen and without hydrogen peroxide addition the colonies reduced to 300 CFU, and after 0.35ml/l of H₂O₂ the colonies remain 120 CFU. In Fig. 7.8 (a-d) the typical results of pure *E. coli* strain, oxygen injected discharge results, without any addition of hydrogen peroxide were represented. The oxygen addition generated reative species including ozone and OH· radicals that played an important role in sterilizing of *E. coli*. Fig. 7.9(a-d) represents the inactivation results of oxygen injected and hydrogen peroxide added discharge. Fig. 7.10 (a, b) represents the *E. coli* inactivation efficiency of underwater plasma discharge under different expeimental conditions and $\log \frac{N}{N_o}$ (kill rate) of *E. coli* respectively.

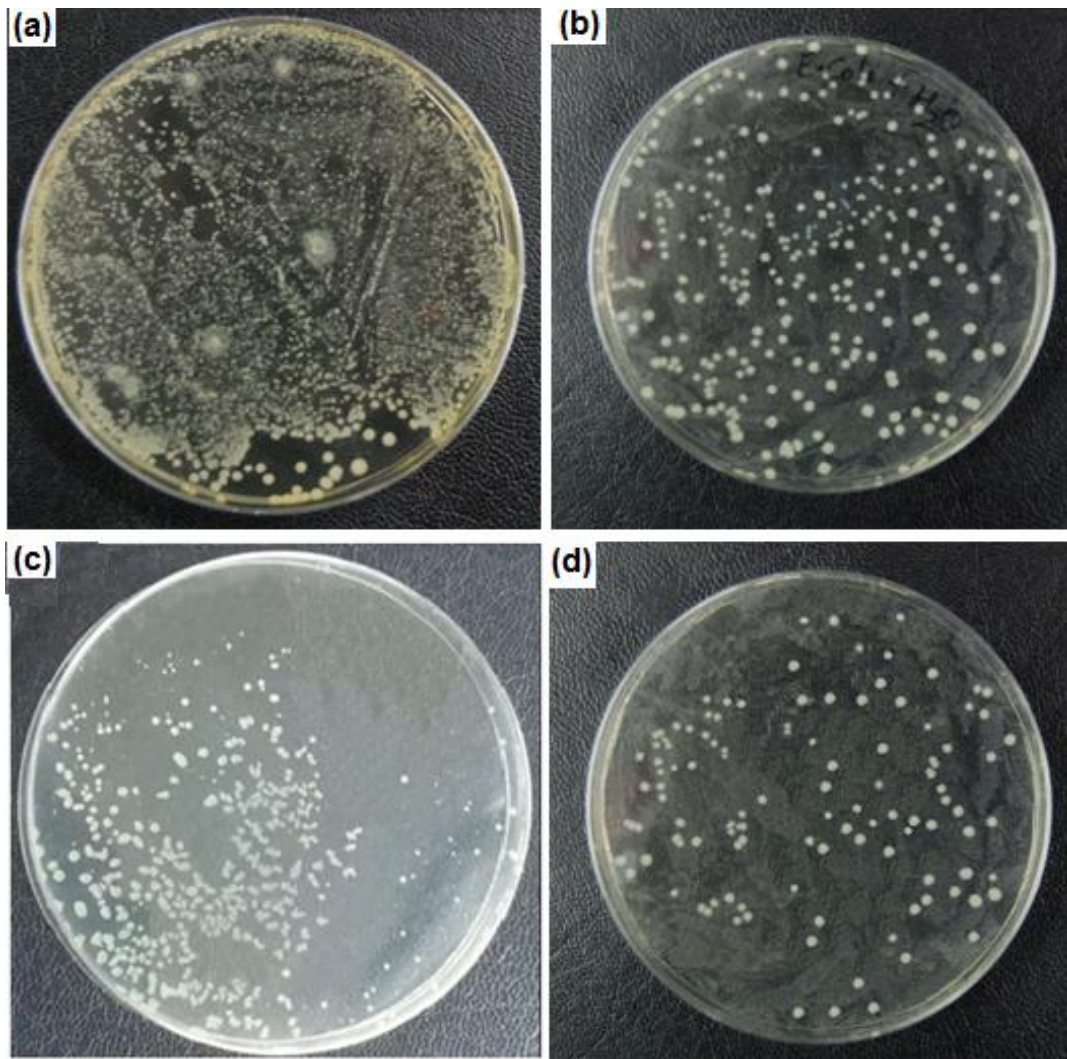


Fig. 7.7 Visual comparison of *E. coli* colonies concentration existence.

- (a): High concentration of *E. coli* colonies in agar plate with pure *E. coli* Strain concentration too numerous to count (TNTC).
- (b): Reduced to countable colonies after mixing 100 μ l of strain to 1 liter water, before plasma treatment.
- (c): the countable colonies after Plasma Treatment without oxygen injection and 0 ml/L H_2O_2 ;
- (d): the countable colonies after Plasma Treatment without oxygen injection and with 0.35ml/L H_2O_2 .

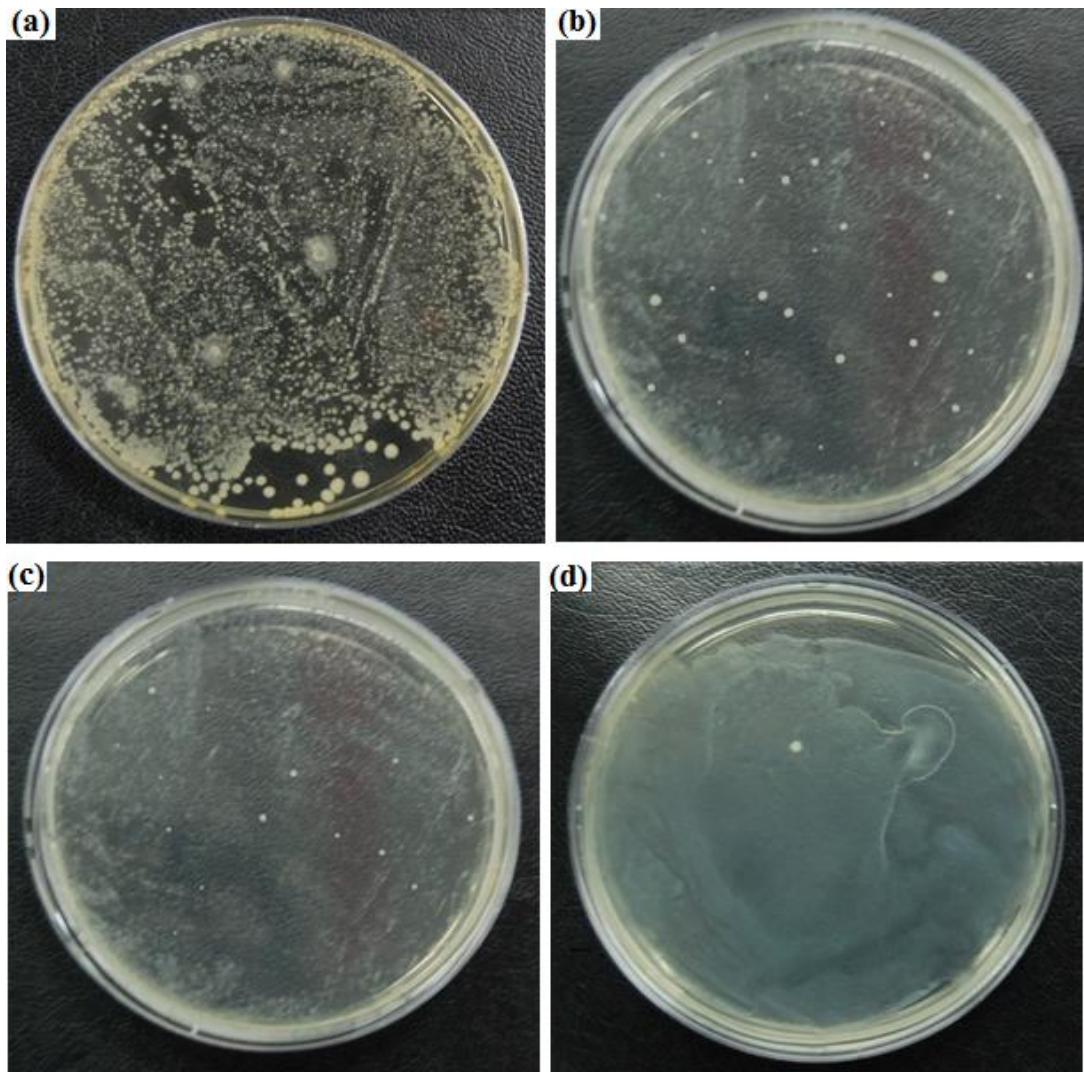


Fig. 7.8 Typical results of ineffective action on *E. coli* by plasma treatment without any addition of hydrogen peroxide.

- (a): after plasma treatment of pure *E. coli* strain concentration in water;
- (b): after plasma treatment with 100 sccm O₂ injection;
- (c): after plasma treatment with 400 sccm O₂ injection;
- (d) after plasma treatment with 800 sccm O₂ injection.

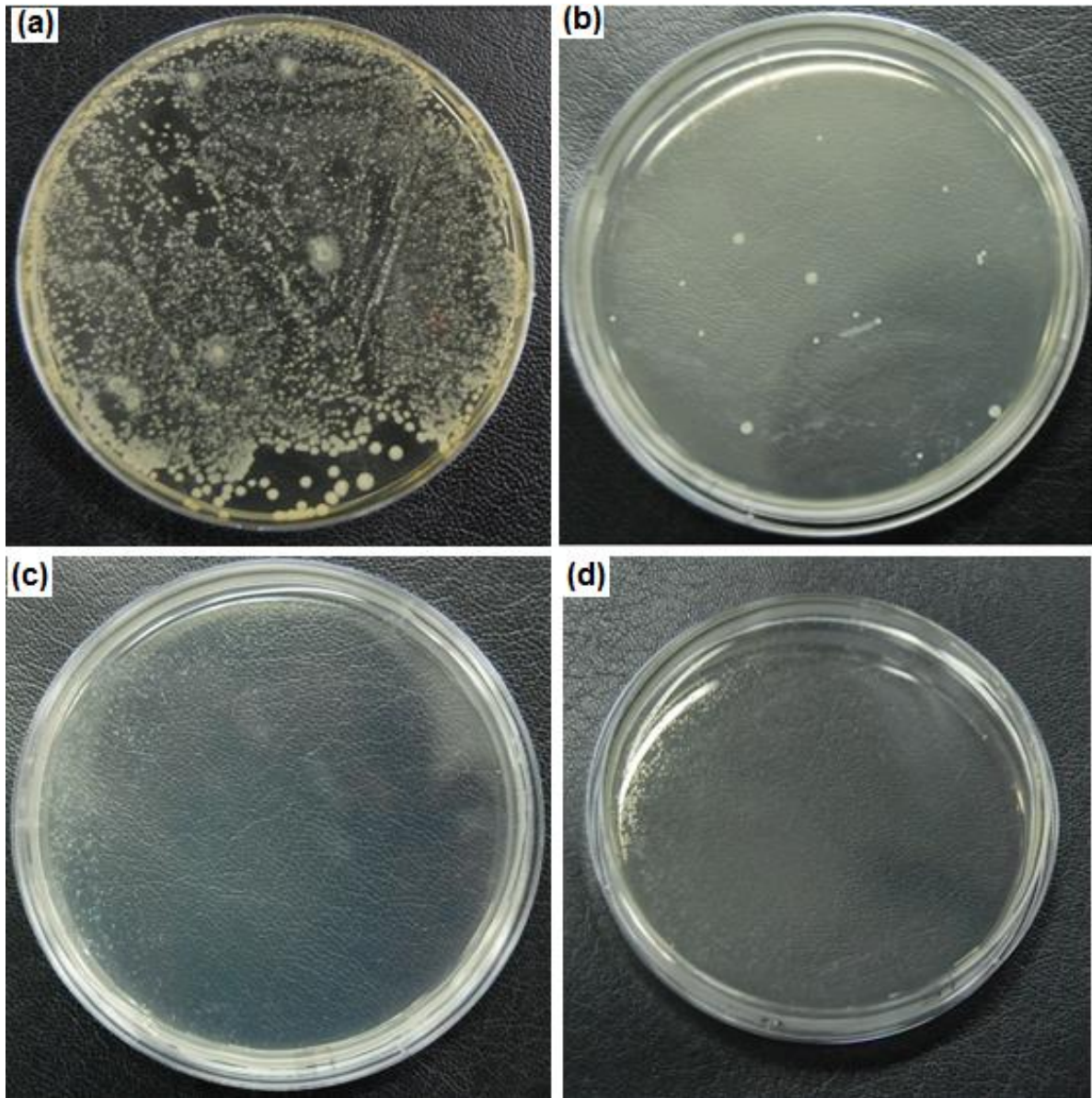


Fig. 7.9 Typical examples of the effective inactivation of *E. coli* by plasma treatment in discharges with the H_2O_2 -adding in water and injection of O_2 .

- (a): after plasma treatment of pure *E. coli* strain concentration in water;
- (b): after plasma treatment with 100 sccm O_2 injection and adding of 0.35 ml/L H_2O_2 ;
- (c): after plasma treatment with 400 sccm O_2 injection and adding of 0.35 ml/L H_2O_2 ;
- (d) after plasma treatment with 800 sccm O_2 injection and adding of 0.35 ml/L H_2O_2 .

The samples of plasma treated water were tested after each 12 hours intervals, up-to 72 hours, without H₂O₂ addition and with H₂O₂ addition, under different oxygen injected rates respectively. The results demonstrated that with increase in oxygen injection rate and hydrogen peroxide addition, the inactivation efficiency increased, while the kill rate was also higher as represented by logarithmic ratio of number of colonies after plasma treatment to the initial number of colonies before treatment.

In the current study, we also conducted growth kinetic study of *E. coli* proliferation and inhibition by various experimental conditions (various oxygen injection and H₂O₂ addition rates) for plasma treatment. The *E. coli* survival percentage was calculated by relation:

$$\% \text{ of Survival } E. coli = \frac{OD \text{ of test group} - OD \text{ of blank}}{OD \text{ of control} - OD \text{ of blank}} \times 100 \dots \dots \dots (3)$$

The OD of Blank was (0.033-0.034, average=0.0335), OD of control was 1.13, while of OD test group varies for different plasma treatment conditions. Fig. 7.11 represents typical images of water samples and *E. coli* strain under different plasma treatment conditions. The addition of hydrogen peroxide and oxygen injected discharge sterilized water more effectively.

Fig. 7.12 represents kinetics of *E. coli* growth and *E. coli* survivability under different treatment conditions. Our findings showed that oxygen injected and H₂O₂ added discharge revealed higher anti-*E. coli* cytotoxic then other only oxygen injected, only H₂O₂ added or discharge at absence of both.

It can be estimated from results that without oxygen injection and H₂O₂ addition, only electrical field, emitted shock waves due to plasma and ultraviolet (UV) radiations participate mainly in *E. coli* inactivation and reactive species generation as well. The direct interaction of shockwaves with the microorganisms existing in water, splitting of their DNA structure making them disables to regenerate themselves. The scattering of microorganism's colonies takes place within liquid, thus exposure to their inactivation factors raises.

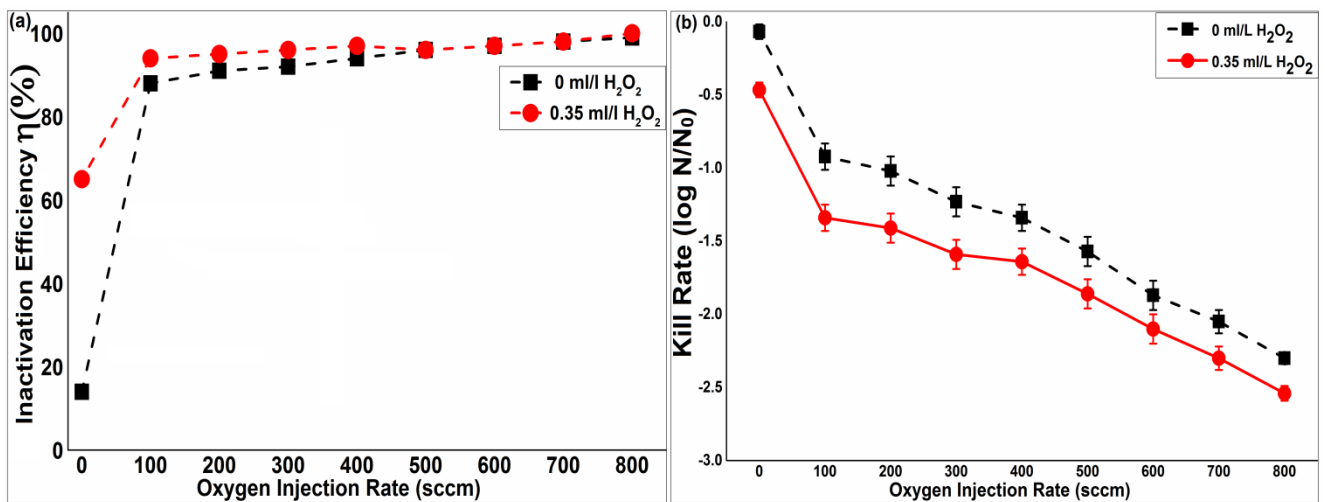


Fig. 7.10 (color online) Dependences of the *E. coli* inactivation efficiency, η and the Kill rate, $\log \frac{N}{N_0}$ (the reduction in *E. coli* colonies) versus the rate of O₂-injection in underwater plasma discharges with the add of H₂O₂ in water.

(a): *E. coli* inactivation efficiency, η ;

(b): the Kill rate of *E. coli* colonies.

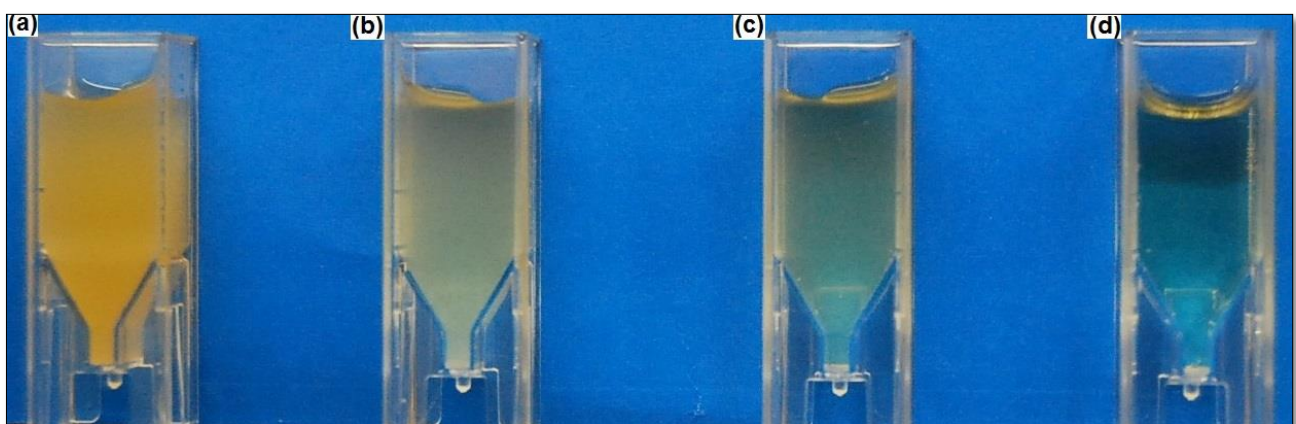


Fig. 7.11 Typical images of untreated and treated water samples.

(a): sample with Pure *E. coli* strain;

(b): sample with untreated water containing *E. coli*;

(c): sample with H₂O₂ mixed water containing *E. coli* which treated by plasma discharge without oxygen injection;

(d): sample with H₂O₂ mixed water containing *E. coli* which treated by plasma discharge with oxygen injection. The oxygen injected and H₂O₂ mixed plasma discharge effectively sterilized water from *E. coli*.

The existence of high voltage across the electrodes and large current with in discharge, cause the formation of thermal plasma channel, which emits highly intensive UV radiations, effective for *E. coli* inactivation.

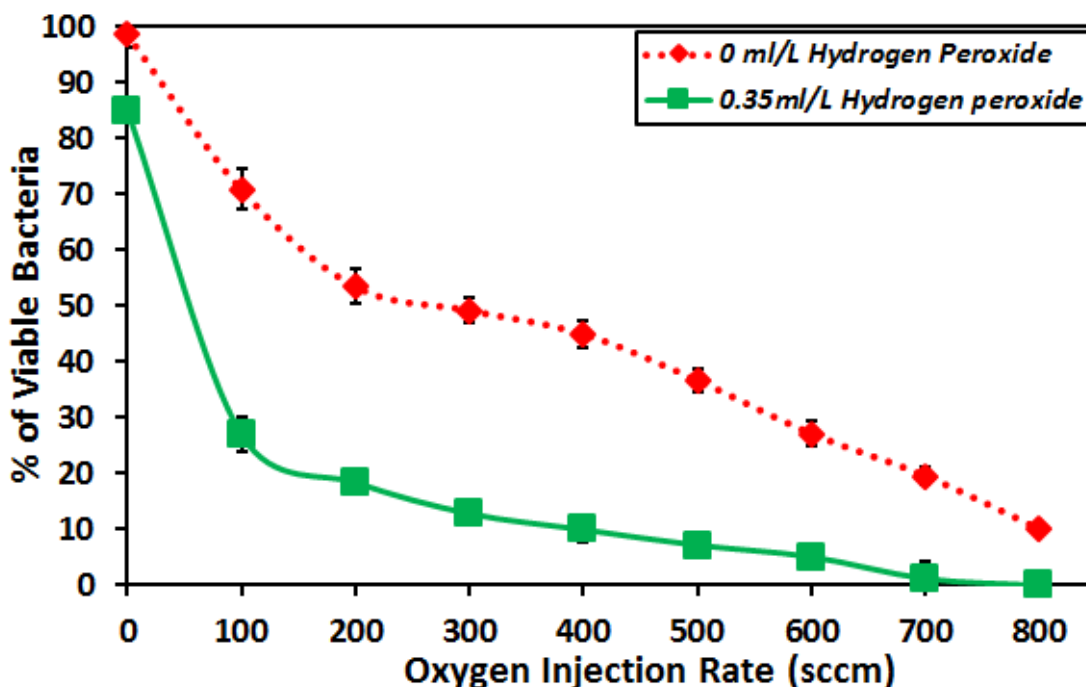


Fig. 7.12 (Color online) The % of viable bacteria in water containing *E.coli* after its underwater discharge treatment versus the rate of oxygen injection for two conditions related to adding of hydrogen peroxide in the water.

The *E. coli* inactivation results were effective after plasma treatment. The colonies were enumerated after every 12 hours, from same agar plates and new agar plates prepared from same water samples preserved at -20⁰C, and it was found that there was no remarkable effect of *E. coli* rebirth even after 72 hours. The percentage of *E. coli* viability was reduced significantly due to oxygen injection and H₂O₂ addition simultaneously.

7.5 Conclusions

- 1). Oxygen injected, H₂O₂ added underwater plasma discharge is a non-toxic and effective method for *E. coli* inactivation.
- 2). The injection of oxygen (100 -800) sccm and standard amount of H₂O₂ (0.35 ml/L) addition

enhanced the concentration of ozone, $OH\cdot$ radicals, reactive oxygen, reactive hydrogen, intensity of shock waves and UV radiations that raised the inactivation efficiency and reduced drastically the survival rate of *E. coli* to zero.

- 3). At high oxygen injection rate, strength of discharge, power of discharge pulses and *E. coli* inactivation efficiency was high, while required breakdown voltage was reduced.
- 4). After plasma treatment no remarkable re-growth of *E. coli* takes place in the water.

8 Summary

Use of underwater plasma discharge for sterilization of drinking water, waste water treatment and for other industrial application is a well-known, non-toxic and quick method. Due to high dielectric strength of water the power consumption is the major issue that needs to be resolved for its applications on large scale. Among them the relation between physical characteristics of underwater plasma discharge and yield rate of oxidant species is very important. A flowing water gas injected and non-gas injected capillary discharge is suitable for such diagnostics and testing for various applications. The experiments were performed by using negative DC power source and high frequency power source separately, under different types of gasses (argon, air and oxygen) at various gas injection rates and different inter-electrode gap distances. The addition of hydrogen peroxide was also tested to compare the effect of only underwater discharge to hydrogen peroxide added discharge on the production rate of oxidant species. The electrical and chemical characteristics of tap water and high conductivity water were tested and the application of capillary discharge on Gram- negative *Escherichia coli* (*E. coli*) was performed.

The results are composed of three sections; section one negative DC, second section high frequency AC and third section application of bacterial disinfection.

In first part of section one, the flowing water capillary discharge was created by using negative DC after injecting air and oxygen. Compared to other research on underwater plasma discharges, where high voltage sources that can deliver large power are needed, in this research the required power consumption to generate and sustain the plasma was drastically reduced by using gas injection. Compared to air, oxygen is more effective for creating low-voltage breakdown and inducing a high concentration of $\text{OH}\cdot$ radicals. Based on the characteristics of the discharge observed in the experiment conducted in this study, including the current transfer by electrons, the gap bridging by the discharge current, the ionization of the gap inside the channel and water bubbles, the emission of strong, but short-lived, UV rays, the increase in energy per pulse, and the average power of the discharge pulses occurring in one second, we were able to categorize the discharge as a pulsed arc plasma discharge.

Water sterilization using plasma-assisted technology is maximum, quick, and more effective than that using only chemical method.

In second experiment of first section, using negative DC a relation between physical; and chemical characteristics was made. The electron temperature and electron number density was calculated by using intensity-ratio method and Gig-Card theory respectively. The average electron number density was observed 10^{17} cm^{-3} , and electron temperature was 0.5-1.6 eV under different experimental conditions. Increase in gas injection rate increased the power of discharge pulses, which resulted in an increase in electron temperature and number density. The electron temperature of oxygen injected discharge proved highest then air and argon due to high emission intensity of hydrogen Ballmer lines. The chemicals reactions that took place after discharge occurrence affected by electron temperature rather than electron number density. The electronegative characteristic of oxygen reduced the electron number density; therefore argon contains highest electron number density then oxygen and air. The oxidant reactive species ($\cdot\text{OH}$, O_3 and H_2O_2) has direct relation with T_e , for argon, air and O_2 .

In first experiment of second section, diagnostics of argon injected hydrogen peroxide added high frequency underwater capillary discharge was performed. The addition of hydrogen peroxide along with argon injection generated stronger plasma and high intensity of reactive species especially $\cdot\text{OH}$ radicals. Addition of hydrogen peroxide effected chemical properties and have no remarkable effect on electrical characteristics, especially conductivity of water. Argon gas injection generated bubbles and gas channels that reduced the required breakdown voltage for long gap flowing water discharge. The frequency and electrical power of discharge pulses increased while time difference between the occurrence of discharge pulses and breakdown voltage was reduced at higher argon injection rates.

In second experiment of second section, Effect of Water Conductivity on the Generation of $\text{OH}\cdot$ Radicals in High Frequency Underwater Capillary Discharge was tested. At large conductivities less breakdown voltage was needed, that can be more reduced by injecting gas from external source. At large conductivities, electrical power of discharge pulses was observed higher. Long gap discharge, with argon injection and with high frequency source produce high concentration of $\text{OH}\cdot$ radicals,

compared to non-gas injected and short gap distance. The problem of power consumption at large gap distances and at low or high conductivities was solved by using high frequency source. High frequency source proved useful for creating long gap flowing water discharge at less power consumption and less breakdown voltage.

In third experiment of second section the large volume of water was treated by connecting twenty capillaries in parallel. The previous research demonstrated that oxygen injected discharge is highly useful therefore 100-800 sccm of oxygen was injected into the capillary tubes. The increase in gas injection rate not only reduced the required input power enormously low but also increased oxidant species especially OH[·] radicals. The connection of many capillaries in parallel is an effective way of large volume water treatment.

In section three, application of high frequency underwater plasma discharge in antibacterial activity was performed. Oxygen injected, H₂O₂ added underwater plasma discharge was used to inactivate Gram-negative *E. coli*. Oxygen injected, H₂O₂ added underwater plasma discharge is a non-toxic and effective method for *E. coli* inactivation. The injection of oxygen (100 -800) sccm and standard amount of H₂O₂ (0.35 ml/L) addition enhanced the concentration of ozone, OH[·] radicals, reactive oxygen, reactive hydrogen, intensity of shock waves and UV radiations that raised the inactivation efficiency and reduced drastically the survival rate of *E. coli* to zero. At high oxygen injection rate, strength of discharge, power of discharge pulses and *E. coli* inactivation efficiency was high, while required breakdown voltage was reduced. After plasma treatment no remarkable re-growth of *E. coli* takes place in the water.

Acknowledgements

This study was supported by Plasma Diagnostics Using Fast Thomson Scattering through the National Research Foundation of Korea (NRF) funded by Ministry of Education, Science and Technology (2014M1A7A1A03045383) and Priority Research Centers Program through the National Research Foundation of Korea (NRF) funded by Ministry of Education, Science and Technology (2010-0020077).

References

- [1] [https://en.wikipedia.org/wiki/Plasma_\(physics\)](https://en.wikipedia.org/wiki/Plasma_(physics))
- [2] F. F. Chen, "Plasma Physics and Controlled Fusion", Plenum Press, 1929.
- [3] <http://web.ornl.gov/sci/fed/Theory/tt/ttmcp/plasma.htm>
- [4] https://en.wikipedia.org/wiki/Induction_plasma
- [5] [http://www.plasma-universe.com/Plasma_classification_\(types_of_plasma\)](http://www.plasma-universe.com/Plasma_classification_(types_of_plasma))
- [6] [https://en.wikipedia.org/wiki/Plasma_\(physics\)](https://en.wikipedia.org/wiki/Plasma_(physics))
- [7] [https://en.wikipedia.org/wiki/Plasma_\(physics\)](https://en.wikipedia.org/wiki/Plasma_(physics))
- [8] Micro capillary dielectric barrier plasma jet discharge characterization by optical Spectroscopy, Ph.D. Dissertation, July 2011, pp 16-17.
- [9] A. Saeed, Dr. Thesis, 2013, Optimization study of N₂_H₂ mixture pulse DC plasma ionnitridding reactor, pp.17.
- [10] Y. C. Hong, H. J. Park, B. J. Lee, W. S. Kang and H. S. Uhm, Phys. Plasmas. 17,5 (2010).
- [11] J. G. Jacangelo, D. J. Askenazer and K. Schwab, J. Water Health. 04,1 (2006).
- [12] G. C. Windham, K. Waller, M. Anderson, L. Fenster, P. Mendola and S. Swan, J. Environ. Health. 111, 935 (2003).
- [13] K. P. Cantor, C. F. Lyunch, M. E. Hildesheim, M. Dosemeci, J. Lubin, M. Alavanja and G. Craun, Am J. Epidemiol. 9, 21 (1998).
- [14] United States Environmental Protection Agency (USEPA) Report No. EPA-815-R-99-014 (1999).
- [15] J. Baron and M. M. Bourbigot, Wat. Res. 30, 2817 (1996).
- [16] R. Sommer, M. Lhotsky, T. Haider and A. Cabaj, J. Food Prot. 63, 1015 (2000).
- [17] C. V. Sonntag, G. Mark, R. Mertens, M. N. Schuchmann and H. P. Schuchmann, J. Water Srt-Aqua. 42,201 (1993).
- [18] C. Collivignarelli and S. Sorlini, Water Sci Technol. 49,51 (2004).
- [19] R. Munter and Proc. Estonian, Acad. Sci. Chem. 50, 59(2001).
- [20] P. C. Fung, K. M. Sin and S. M. T. Sui, Color Technol. 116, 170 (2000).
- [21] T. Blume, I. Martinez and U. Neis, The Hamburg-Harburg Reports on Sanitary engineering 35, 117 (2002).
- [22] United State Environmental Protection Agency (USEPA). Report No. EPA 815-R-06-009 (2005).
- [23] M. A. Malik, U. Rahman, A. Ghaffar and K. Ahmed, Plasma Sources Sci. Technol. 10, 82 (2001).
- [24] S. Gasanova, Ph.D. Dissertation, (Institute of Instrumental Analytical Chemistry, The University of Duisburg-Essen, 2013), Chap. 1, p. 29.
- [25] M. J. Kirkpatrick and B. R. Locke, Ind. Eng. Chem. Res. 44, 4243 (2005).
- [26] A. J. Bard and M. A. Fox, Acc. Chem. Res. 28, 141(1995).
- [27] M. S. Banu, P. Sasikala, A. Dhanapal, V. Kavitha, G. Yazhini and Lavanya Rajamani, IJETED. 4, 9 (2012).
- [28] B. R. Locke, P. Sunka, M. R. Hoffmann and J. S. Chang, Ind. Eng. Chem. Res. 45, 882 (2006).
- [29] Young Yang, Young I Cho, Alexander Friedman, "Plasma Discharge in Liquid, water treatment and applications", CRC press, 2012.

- [30] K.V. Dubovenko, L.P. Trofimova, S.G. Poklonov, Plasma Science, 1998. 25th anniversary. IEEE Conference Record - Abstracts. 1998 IEEE International on Date 1-4 June 1998.
- [31] A. Grinenko, A. Sayapin, V. T. Gurovich, S. Efimov, J. Felsteiner, and Ya. E. Krasik, J. Appl. Phys. 97, 023303 (2005).
- [32] M. Sato, T. Ohgiyama, and J. S. Clements, IEEE Trans. Ind. Appl. 32 (1): 106-112, 1996.
- [33] B. Sun, M. Sato and J.S. Clements, J. Appl. Phys. 32. 1908-1915, 1999.
- [34] H. M. Jones and E. E. Kunhardt, J. Appl. Phys. 77, 795. (1995).
- [35] Young I Cho and Alexander A. Friedman, "Application of pulse spark discharges for scale prevention and continuous filtration methods in coal-fired power plant", Final Technical Report October 2008 —June 2012.
- [36] H. Akiyama, Steramer discharge in liquid and their applications, IEEE Trans. Dielect. Elect. Insul. Vol. 07 (5), 2000.
- [37] Petr Lukes, Martin Clupek, Vaclav Babicky and Pavel Sunka, Plasma Sources Sci. Technol. 17 (2008) 024012 (11pp).
- [38] M. Radmilovi´c-Radjenovi´c, B. Radjenovi´c, M. Klas, A. Bojarov and S. Matej´cik, "acta Physica slovacica vol. 63 No. 3, 105 – 205 June 2013.
- [39] Naddeo V, Cesaro A, Mantzavinos D, Fatta- Kassinos D, Belgiorno V, Global NEST Journal, Vol 16, No 3, pp 561-577, 2014.
- [40] B. R. Locke, M. Sato, P. Sunka, M. R. Hoffmann, J.-S. Chang, Ind. Eng. Chem. Res. 2006, , 882- 905.
- [41] W G Graham and K R Stalder, J. Phys. D: Appl. Phys. 44 (2011) 174037 (8pp).
- [42] Yong Yang, "Plasma Discharge in Water and Its Application for Industrial Cooling Water Treatment", Drexel University, Doctor Thesis, June 2011.
- [43] Yong Cheol Hong, Sang Ju Lee, Ye Jin Kim, and Bong Ju Lee, IEEE Trans. Plas. sci. 39(11), November 2011.
- [44] Ing. Zdenka Kozakova, Dr. thesis, Electrical Discharge in water Solutions, 2011.
- [45] Mi-jung um, Seong-hoon yoon, Chung-hak lee, Kun-yong chung and Jae-jin kim, wat. res. 35(17), pp. 4095–4101, 2001.
- [46] J. R. Lucas, High Voltage Engineering, 2001.
- [47] Erik Wagenaars, Dr. Thesis, Plasma Breakdown of Low-Pressure Gas Discharges, 2006.
- [48] Jianqi Qin and Victor P Pasko, J. Phys. D: Appl. Phys. 47, pp. 9, 2014.
- [49] Ing. Petr Hoffer, Dr. Thesis, Shock waves generated by corona-like discharges in water, 2014.
- [50] Yong Yang, Young I. Cho, Alexander Fridman, Plasma Discharge in Liquids, pp. 40, CRC Press, 2012.
- [51] S. B. Gupta, Dr. Thesis, Investigation of a Physical Disinfection Process Based on Pulsed Underwater Corona Discharges, 2007.
- [52] Yong Yang, Young I. Cho, Alexander Fridman, Plasma Discharge in Liquids, pp. 40-44, CRC Press, 2012.
- [53] P Sunka, V Babicky, M Clupek, P Lukes, M Simek, J Schmidt and M Cernak, Plasma Sources Sci. Technol. 8, 1999.
- [54] Yong Yang, Dr. Thesis, Plasma Discharge in Water and Its Application for Industrial Cooling Water Treatment, 2011.
- [55] E. A. Sisein, Sch. Acad. J. Biosci. 2, 110 (2014).
- [56] P. S. Monks, Chem. Soc. 34, 376 (2005).

- [57] <http://courses.seas.harvard.edu/climate/eli/Courses/EPS281r/Sources/OH-reactivity/www.atmosphere.mpg.de-oxidation-and-OH-radicals.pdf>
- [58] Mayank Sahni and Bruce R. Locke, *Plasma process and Ploymers*, 03(9), pp. 668-681, 2006.
- [59] <http://www.atmosphere.mpg.de>.
- [60] D. I. Jang; S. B. Lee; Y. S. Mok; D. L. Jang, *Int. J. chem. Environ. Eng.* 04, pp.150 2013.
- [61] Svetlana Gasanova, Dr. Thesis, 2013, Aqueous-phase electrical discharges: generation, Investigation and application for Organics removal from water.
- [62] Svetlana Gasanova, Dr. Thesis, Aqueous-phase electrical discharges: generation, investigation and application for organics removal from water, 1988.
- [63] Mitsuru Tahara, Masaaki Okubo, *Proc. Joint Electrostatics Conference*, 2012.
- [64] A. Rodríguez, R. Rosal, J. A. Perdigon-Melon, M. Mezcuca, A. Aguera, M. D. Hernando, P. Leton, A. R. Fernandez-Alba, E. García-Calvo, *Hdb Env Chem.* 5, (2008): pp.127–175.
- [65] Rein MUNTER, *Proc. Estonian Acad. Sci. Chem.* 50(2), pp.59–80, 2001.
- [66] S Okazaki, M Kogoma, M Uehara and Y Kimura, *J. Phys. D: Appl. Phys.* 26(5), 1993.
- [67] W. H. glaze, Joon-Wun Kang, D. H. Chapin, *Ozone science and engineering*, 9, pp. 335-352.
- [68] <https://www.ucar.edu/communications/gcip/m1sod/m1pdfc2.pdf>
- [69] L. Schone and H. Herrmann, *Atmos. Chem. Phys.* 14, pp.4503–4514, 2014.
- [70] W.L. Morgan, L.A. Rosocha, *Chemical Physics*, 398, pp.255–261, 2012.
- [71] R. C. Spitzer, T. J. Orzechowski, D. W. Phillion, R. L. Kauffman and C. Cerjan, *J. Appl. Phys.* 79, pp.2251, 1996.
- [72] V M Donnelly, M V Malyshev, M Schabel, A Kornblit, W Tai, I P Herman and N C M Fuller, *Plasma Sources Sci. Technol.* 11, 2002.
- [73] Petr Lukes, Martin Clupek, Vaclav Babicky and Pavel Sunka, *Plasma Sources Sci. Technol.* 17, 2007.
- [74] Kazuo Umezawa, Satomi Asai, Sadaki Inokuchi, Hayato Miyachi, *Curr Microbiol* , 64(6) pp. 581–587, 2012.
- [75] Haibin Zhou, Yongmin Zhang, Hengle Li, Ruoyu Han, Yan Jing, Qiaojue Liu, Jiawei Wu, Youzhi Zhao, and Aici Qiu, *IEEE Trans. Plas. Sci.* 43(12), 2015.
- [76] Ravi Shankar, U.Kaushik, and Shayeeb A Bhat, *International Journal of Innovation and Applied Studies* ISSN 2028-9324, 6(4), pp. 941-958, 2014.
- [77] N. Smith,¹ G. N. Sankin, W. N. Simmons, R. Nanke, J. Fehre, and P. Zhong, *Rev Sci Instrum.* 83(1),2012.
- [78] M. S. Banu, P. Sasikala, A. Dhanapal, V. Kavitha, G.Yazhini and Lavanya Rajamani, *IJETED.* 4(9), (2012).
- [79] Seiji Samukawa, Masaru Hori, Shahid Rauf, Kunihide Tachibana, Peter Bruggeman, Gerrit Kroesen, J Christopher Whitehead, Anthony B Murphy, Alexander F Gutsol, Svetlana Starikovskaia, *J. Phys. D: Appl. Phys.* 45 ,2012.
- [80] Indrek jogi, R. Brandenburg, A. Schwock, D. Cameron, J. Jasowiak and K. Ulrich, *Plasma Treatment for Environment Protection*, 2012.
- [81] Tetsu Mieno, *Plasma Science and Technology - Progress in Physical States and Chemical Reactions*, Chapter 16, 2016.
- [82] Yong Yang, Dr. Thesis, *Plasma Discharge in Water and its Application for Industrial Cooling water Treatment*, 2011.

- [83] Y. S. Lee, H. K. Han and C.J. Cheong, JEB, 36, pp. 591-595, 2015.
- [84] S. B. Gupta, Investigation of a Physical Disinfection Process Based on Pulsed Underwater Corona Discharges, Ph.D. Thesis, September 2007.
- [85] <http://www.newagepublishers.com/samplechapter/000357.pdf>
- [86] <https://arxiv.org/ftp/arxiv/papers/1305/1305.6335.pdf>
- [87] <http://meettechniek.info/measurement/theory-definitions.html>
- [88] <https://www.itp.uni-hannover.de/~zawischa/ITP/atoms.html>
- [89] https://en.wikipedia.org/wiki/Emission_spectrum
- [90] <http://www.pa.msu.edu/courses/2013spring/PHY252/Lab10.pdf>
- [91] Ji Hun Kim, Yoon Ho Choi, and Y. S. Hwang, "Electron density and temperature measurement method by using emission spectroscopy in atmospheric pressure non-equilibrium nitrogen plasmas", PHYSICS OF PLASMAS 13, 093501 2006.
- [92] F. Deeba, A. Qayyum and Nasir Mahmood, "Optical Emission Spectroscopy of 2.45 Ghz Microwave Induced Plasma", Journal of Research in Spectroscopy, Vol. 2015 (2015).
- [93] https://en.wikipedia.org/wiki/Emission_spectrum.
- [94] Ing. Zdenka Kozáková, "Electric Discharges in Water Solutions", Ph.D. thesis, 2011.
- [95] Kazuki Kozue, Shinichi Namba, Takuma Endo, Ken Takiyama, and Naoki Tamura, "Spectroscopic Observation of He Arcjet Plasma Expanding through a Converging and Diverging Slit Nozzle", ENGINEERING JOURNAL Volume 17 December 2013.
- [96] <https://hal.archives-ouvertes.fr/hal-00986714/document>
- [97] Muhammad Waqar Ahmed, Jong-Keun Yang, Young-Sun Mok and Heon Ju Lee, "Underwater Capillary Discharge with Air and Oxygen Addition", JKPS, Vol. 65, No. 9, November 2014, pp. 1404~1413.
- [98] <https://arxiv.org/pdf/1604.07659.pdf>
- [99] J Tores, J M palomares, A Sola, J J A M van der Mullen and A Gamero, J. Phys. D: Appl. Phys. 40, (2007), 5936.
- [100] Spectral Lines Broadening, Hans R. griem, Appendix III. page 316(a), ACADEMIC PRESS New York and London 1974.
- [101] D. M. Devia, L. V. Rodriguez-Restrepo and E. restrepo-Parra, A Review ing.cienc., 11 (21), pp. 239-267, (2015).
- [102] <https://www-amdis.iaea.org>
- [103] W. L. Wiese and J. R. Fuhr, J. Phys. Chem. Ref. Data, 38(3), (2009).
- [104] Yong Yang, "Plasma Discharge in Water and Its Application for Industrial Cooling Water Treatment", Ph.D. thesis, 2011.
- [105] Y. C. Hong, H. J. Park, B. J. Lee, W. S. Kang and H.S. Uhm, Phys. Plasmas. 17, 5(2010).
- [106] George Eisenberg. Ind. Eng. Chem. Anal. Ed. 15 (5), pp. 327-328, (1943).
- [107] F De Baerdemaeker, M Simek and C Leys. J. Phys. D: Appl. Phys., 40 pp. 2801-2809, (2007).
- [108] H. Bader, J. Hoigne. Water Res., 15, pp.449-456, (1981).
- [109] I.V. Timoshkin, M.J. Given, M.P. Wilson, T. Wang, S.J. MacGregor and N. Bonifaci, "Optical emission from spark discharge in water: evaluation of plasma temperature", 22nd International Symposium on Plasma Chemistry July 5-10, 2015; Antwerp, Belgium.
- [110] Method 1103.1: Escherichia coli (E. coli) in Water by Membrane Filtration Using membrane-Thermotolerant Escherichia coli Agar (mTEC), USEPA, March 2010.

- [111] C. Fuchsluger, M. Preims, I. Fritz, "Automated measurement and quantification of heterotrophic bacteria in water samples based on the MPN method", *J Ind Microbiol Biotechnol* (2011) 38:241–247.
- [112] <http://www.moldbacteriaconsulting.com/bacteria/heterotrophic-plate-count>
- [113] <http://www.mpi-bremen.de/Binaries/Binary13037/Wachstumsversuch.pdf>
- [114] <http://www.physics.csbsju.edu/370/jcalvert/dischg.htm.html>
- [115] Bo Jiang, Jingtang Zheng, Shi Qiu, Mingbo Wu, Qinhui Zhan, Zifeng Yan, Qingzhong Xue, "Review on electrical discharge plasma technology for wastewater Remediation", *Chemical Engineering Journal* 236 (2014) 348–368.
- [116] M. Goldman, A. Goldma' and R. S. Sigmond, "The corona discharge, its properties and specific uses", *Pure & Appl. Chem.*, Vol. 57, No. 9, pp. 1353—1362, 1985.
- [117] Torgeir Bakke, Jarle Klungsøyr, Steinar Sanni, "Environmental impacts of produced water and drilling waste discharges from the Norwegian offshore petroleum industry", *Marine Environmental Research* 92 (2013).
- [118] Bo Jiang, Jingtang Zheng, Shi Qiu, Mingbo Wu, Qinhui Zhang, Zifeng Yan, Qingzhong Xue, *Chemical Engineering Journal* 236 (2014) 348–368.
- [119] Dong Nam Shin, Chul Woung Park, and Jae Won Hahn, *Bull. Korean Chem. Soc.* Vol. 21, No. 2, 2000.
- [120] Jufang ZHANG, Jierong CHEN, Xiaoyong LI, "Remove of Phenolic Compounds in Water by Low-Temperature Plasma: A Review of Current Research", *J. Water Resource and Protection*, 2009, 2, 99-109.
- [121] B. R. Locke, M. Sato, P. Sunka, M. R. Hoffmann, J.-S. Chang, *Ind. Eng. Chem. Res.* 2006, 45, 882-905.
- [122] *CRC Handbook of Chemistry and Physics, Dielectric Strength of Insulating Material*, (CRC Press LLC 2000), p. 2.
- [123] D. Zaharie-Butucel and S. D. Anghel, *Rom. Journ. Phys.* 59, 757(2014).
- [124] https://en.wikipedia.org/wiki/Gaussian_function
- [125] J. G. Jacangelo, D. J. Askenaizer and K. Schwab. *J. Water Health.* 04, , pp.1-9, (2006).
- [126] Yong Yang, Physical and chemical mechanisms of direct and controllable plasma interaction with living objects Dr. Thesis, Drexel University, Chap. 6, pp. 73, (2011).
- [127] Paul Rumbach, Megan Witzke, R. Mohan Sankaran, David B. Go, *Proc. ESA Annual Meeting on Electrostatics*, (2013).
- [128] Bruce R. Locke, *I.J.PEST*, 06, 4074, (2012).
- [129] Sang-Heon Song, Yang Yang, Pascal Chabert, and Mark J. Kushner, *Phys. Plasmas*.21, 093512, (2014).
- [130] Ruma, P Lukes, N Aoki, E Spetlikova, SHR Hosseini, T Sakugawa and H Akiyama, *J. Phys. D: Appl. Phys.* 46, (2013).
- [131] Ivana Halamová, Anton Nikiforov, František Krčma, Christophe Leys, *J. Phys. D, Conference Series* ,516-012007, (2014).
- [132] Ji Liangliang, Zou Shuai, Shen Mingrong and Xin Yu, *Plasma Sci. Technol.* 14, 111, (2013).
- [133] S.G. Belostotskiy, R. Khandelwal, Q. Wang, V.M. Donnelly, D.J. Economou, and N. Sadeghi, *Appl.Phys.Lett.* 92, 6, (2008).
- [134] F. Soberon and V. Prada, 2005 Plasma Transport and Development of Plasma Kinetics in ARIS Dr. Thesis, School of Physical Sciences, Dublin City University.

- [135] P. Bruggeman, D. Schram, M.Á. González, R. Rego, M.G. Kong, and C. Leys, *Plasma Sources Sci. Technol.* 18, 025017, (2009).
- [136] D.E. Kelleher, W.L. Wiese, V. Helbig, R.L. Greene, and D.H. Oza, *Phys. Scr.* 75, (1993).
- [137] Z. Mijatovic, D. Nikolic, R. Kobilarov, M. Ivkovic, J. Quant. Spectrosc. Radiat. Transfer, 111, pp. 990-996, (2010).
- [138] Marco A. Gigosos, Manuel A. Gonzalez, Valentín Cardenoso, *Acta, Part B.* 58, pp.1489-1504, (2003).
- [139] M.W. Ahmed, J.-K. Yang, Y.S. Mok, Y.-H. Yu and H.J. Lee, *J. Korean Phys. Soc.* 65, 1404, (2014).
- [140] http://chemistry.mdma.ch/hiveboard/rhodium/pdf/chemical-data/diel_strength.pdf
- [141] D. M. Devia, L. V. Rodriguez-Restrepo and E. restrepo-Parra, *A Review ing.cienc.*, 11 (21), pp. 239-267, (2015).
- [142] <https://www-amdis.iaea.org>
- [143] W. L. Wiese and J. R. Fuhr, *J. Phys. Chem. Ref. Data*, 38(3), (2009).
- [144] Davide Mariotti, A Yoshiki Shimizu, Takeshi Sasaki, and Naoto Koshizaki, *J. Appl. Phys.* 101(1), (2007).
- [145] S Hofmann, A F H van Gessel, T Verreycken and P Bruggeman, *Plasma Sources Sci. Technol.* 20 065010 pp. 12, (2011).
- [146] P J Bruggeman, N Sadeghi, D C Schram and V Linss, *A review Plasma Sources Sci. Technol.*, 23 023001 pp.32, (2014).
- [147] R Miotk, B Hrycak, M Jasinski and J Mizeraczyk, *J. Phys. conf. ser.* 406 012033, (2012).
- [148] M. Jasinski, Z. Zakrzewski, J. Mizeraczyk, *Czech. J. Phys.* 56, (2006).
- [149] S Mededovic and B R Locke. *J. Phys. D: Appl. Phys.* 40 7734-7746, (2007).
- [150] Philip J. Brandhuber, Gregory Korshin. *Methods for detection of residual concentration of hydrogen peroxide in advance oxidation processes*, water Reuse foundation, Alexandria, VA, 2009.
- [151] George Eisenberg. *Ind. Eng. Chem. Anal. Ed.* 15 (5), pp. 327-328, (1943).
- [152] F De Baerdemaeker, M Simek and C Leys. *J. Phys. D: Appl. Phys.*, 40 pp. 2801–2809, (2007).
- [153] H. Bader, J. Hoigne. *Water Res.*, 15, pp.449-456, (1981).
- [154] S. B. Gupta, Dr. Thesis, Institut für Hochleistungsimpuls- und Mikrowellentechnik, pp. 42, (2007).
- [155] Jacek MAJEWSKI, *Methods for measuring ozone concentration in ozone-treated water* ISSN 0033-2097, R. 88NR 9b/2012.
- [156] Mayank Sahni and Bruce R. Locke , “Quantification of Hydroxyl Radicals Produced in Aqueous Phase Pulsed Electrical Discharge Reactors”, I & EC research, 2006.
- [157] Petr Lukes, Martin Clupek, Vaclav Babicky, Vaclav Janda and Pavel Sunka,” Generation of ozone by pulsed corona discharge over water surface in hybrid gas–liquid electrical discharge reactor”, *J. Phys. D: Appl. Phys.*, 2005.
- [158] Robert J. Wandell, Bruce R. Locke,” Hydrogen Peroxide Generation in Low Power Pulsed Water Spray Plasma Reactors”, *Ind. Eng. Chem. Res.*, 2014.
- [159] Mitsuru Tahara, Masaaki Okubo,” Detection of Free Radicals Produced by a Pulsed Streamer Corona Discharge in Solution Using Electron Spin Resonance”, Proc. 2012 Joint Electrostatics Conference.
- [160] Vít Jirasek, Petr Lukes, Halyna Kozak, Anna Artemenko, Martin Clupek, Bohuslav

- Rezek, Alexander Kromka ,” Filamentation of diamond nanoparticles treated in underwater corona discharge”, 2015.
- [161] United States Environmental Protection Agency (USEPA) Report No. EPA-815-R-99-014(1999).
- [162] S. Li, I. V. Timoshkin, M. Maclean, S. J. MacGregor, M. P. Wilson, M. J. Given, T. Wang and J. G. Anderson,” Fluorescence Detection of Hydroxyl Radicals in Water Produced by Atmospheric Pulsed Discharges”, IEEE Transactions on Dielectrics and electrical insulation, 2015.
- [163] Yong Yang, Young I. Cho, Alexander Friedman, Plasma Discharge in Liquid: Water Treatment and Applications”, by CRC Press, January 24, 2012.
- [164] Xiujuan J. Dai, Cormac S. Corr, Sri B. Ponraj, Mohammad Maniruzzaman, Arun T. Ambujakshan, Zhiqiang Chen, Ladge Kviz, Robert Lovett, Gayathri D. Rajmohan, David R. de Celis, Marion L. Wright, Peter R. Lamb, Yakov E. Krasik, David B. Graves, William G. Graham, Riccardo d’Agostino, Xungai Wang,” Efficient and Selectable Production of Reactive Species Using a Nanosecond Pulsed Discharge in Gas Bubbles in Liquid”, Plasma Process. Polym. 2016.
- [165] Genki Saito and Tomohiro Akiyama,” Nanomaterial Synthesis Using Plasma Generation in Liquid”, Journal of Nanomaterials, 2015.
- [166] W F L M Hoeben, E M van Veldhuizen, W R Rutgers and G M W Kroesen,” Gas phase corona discharges for oxidation of phenol in an aqueous solution”, *Phys. D: Appl. Phys.* Nov. 1999.
- [167] Joanna Pawlat, Dr. Thesis, “Electrical discharges in humid environments Generators, effects, application”, Lublin University of Technology, Poland.
- [168] Masayuki Sato,” Environmental and biotechnological applications of high-voltage pulsed discharges in water”, *Plasma Sources Sci. Technol.* Oct. 2007.
- [169] M. Sato,” Degradation of organic contaminants in water by plasma”, International Journal of Plasma Environmental Science and Technology Vol. 03, No.1, MARCH 2009.
- [170] P. Baroch, T. Takeda, M. Oda, N. Saito and O. Takai,” Degradation of Bacteria Using Pulse Plasma Discharge in Liquid Medium”, 27th international power modulator symposium, 2006.
- [171] Paul Y. Kim, Yoon-Sun Kim, Il Gyo Koo, Jae Chul Jung, Gon Jun Kim, Myeong Yeol Choi, Zengqi Yu, George J. Collins*,”Bacterial Inactivation of Wound Infection in a Human Skin Model by Liquid-Phase Discharge Plasma”, PloS One, 2011.
- [172] Vasil I. Parvulescu, Plasma Chemistry and catalysis in Gases and Liquids, Wiley-VCH,Germany, 2012.
- [173] Magnus Ingelman-Sundbergz and Inger Johansso,” Mechanisms of Hydroxyl Radical Formation and Ethanol Oxidation by Ethanol-inducible and Other Forms of Rabbit Liver Microsomal Cytochromes”, 1984.
- [174] J. Kornev, N. Yavorovsky, S. Preis, M. Khaskelberg, U. Isaev & B.-N. Chen,” Generation of Active Oxidant Species by Pulsed Dielectric Barrier Discharge in Water-Air Mixtures”, Ozone: Science and Engineering, 2007.
- [175] Pankaj Attri , Yong Hee Kim , Dae Hoon Park , Ji Hoon Park , Young J. Hong , Han Sup Uhm , Kyoung-Nam Kim , Alexander Friedman & Eun Ha Choi,” Generatio mechanism of hydroxyl radical species and its lifetime Prediction during the plasma-

- initiated ultraviolet (UV) photolysis”, Scientific Reports, 2015.
- [176] Svetlana Gasanova, Dr. Thesis, Aqueous-phase electrical discharges: generation, investigation and application for Organics removal from water, 2013.
- [177] Shigeo Daito, Fumiyoshi Tochikubo and Tsuneo Watanabe,” Improvement of NO_x Removal Efficiency Assisted by Aqueous-Phase Reaction in Corona Discharge”, Jpn. J. Appl. Phys. 2000.
- [178] Dip. Ing. Dr. Otto Zajic,” Disinfection of Drinking Water with Hydrogen Peroxide / Silver”, Fourth International Water Technology Conference IWTC 99, Alexandria, Egypt, 1999.
- [179] Dong Nam Shin, Chul Woung Park, and Jae Won Hahn,” Detection of OH (A²S+) and O (¹D) Emission Spectrum Generated in a Pulsed Corona Plasma”, Bull. Korean Chem. Soc., 2000.
- [180] Weiwei He, Yitong Liu, Wayne G. Wamer, Jun-Jie Yin, “Electron spin resonance spectroscopy for the study of nanomaterial-mediated generation of reactive oxygen species”, journal of food and drug analysis, 2014.
- [181] Michael S. Elovitz¹ and Urs von Gunten,” Hydroxyl Radical/Ozone Ratios During Ozonation Prozesse”, 1998.
- [182] Ryo Ono, and Tetsuji Oda,” Measurement of Hydroxyl Radicals in an Atmospheric Pressure Discharge Plasma by Using Laser-Induced Fluorescence”, IEEE Transactions on Industry Applications, 2002.
- [183] Seiji Kanazawa, Hirokazu Kawano, Satoshi Watanabe, Takashi Furuki, Shuichi Akamine, Ryuta Ichiki, Toshikazu Ohkubo, Marek Kocik and Jerzy Mizeraczyk,” Observation of OH radicals produced by pulsed discharges on the Surface of a liquid”, Plasma Sources Sci. Technol. Vol. 20, No. 03, Jan. 2011.
- [184] Petr Lukes, Martin Clupek, Vaclav Babicky, Vaclav Janda and Pavel Sunka,” Generation of ozone by pulsed corona discharge over water surface in hybrid gas–liquid electrical discharge reactor”, J. Phys. D: Appl. Phys. 2004.
- [185] Muhammad Waqar Ahmed, Jong-Keun Yang, Young-Sun Mok and Heon Ju Lee*, ”Underwater Capillary Discharge with Air and Oxygen Addition”, Journal of the Korean Physical Society, 2014.
- [186] B.R. Locke, M. Sato, P. Sunka, M.R. Hoffmann, and J.S. Chang, (2006) “Electrohydraulic discharge and non-thermal plasma for water treatment” Industrial and Engineering Chemistry Research. Vol. 45, No. 3, Jan 2006, pp 882-905
- [187] Michel Moisan, Jean Barbeau, Marie-Charlotte Crevier, Jacques Pelletier, Nicolas Philip, Bachir Saoudi, (2002) “Plasma Sterilization methods and mechanisms” Pure and Applied Chemistry, Vol. 74, No. 3, Jan 2002, pp 349-358
- [188] D. M. Willberg , P. S. Lang , R. H. Höchmer , A. Kratel , and (1996)“Degradation of 4-Chlorophenol, 3,4-Dichloroaniline, and 2,4,6-Trinitrotoluene in an Electrohydraulic Discharge Reactor” Environmental Science and Technology, Vol. 30, No. 8, July 1996, pp 2526-2534
- [189] Le C. Lei ,* Yi Zhang , Xing W. Zhang , Ying X. Du , Qi Z. Dai , and Song Han, (2007) “Degradation Performance of 4-Chlorophenol as a Typical Organic Pollutant by a Pulsed High Voltage Discharge System” Industrial and Engineering Chemistry Research, Vol. 46, No. 17, May 2007, pp 5469-5477
- [190] Zhiyong Zhou, Xiaying Zhang, Ying Liu, Yuepeng Ma, Shuaijun Lu, (2015) “ Treatment of azo dye (Acid Orange II) wastewater by pulsed high-voltage hybrid gas–liquid

- discharge” RSC Advances, Vol. 5, No. 88, August 2015, pp 71973-71979
- [191] Muhammad Waqar Ahmed, Jong-Keun Yang, Young-Sun Mok, Young-Hun Yu, Heon- Ju Lee, , (2014)” Underwater capillary discharge with air and oxygen addition” Journal of Korean Physical Society, Vol. 65, No. 9, November 2014, pp 1404-1413
- [192] S Collette, T Dufour and F Reniers, (2016)” Reactivity of water vapor in an atmospheric argon flowing post-discharge plasma torch” Plasma Sources Science and Technology, Vol. 25, No. 02, April 2016, pp 025014
- [193] <http://digital.csic.es/bitstream/10261/35135/1/Tanarro-Pressure%20effects-PSST-11.pdf>
- [194] Petr Lukes, Martin Clupek, Vaclav Babicky and Pavel Sunka, (2008) “ Ultraviolet radiation from the pulsed corona discharge in water” Plasma Sources Science and Technology, Vol. 17, No. 02, May 2008, pp 4012
- [195] Haibin Zhou, Ruoyu Han, Qiaojue Liu, Yan Jing, Jiawei Wu, Yongmin Zhang, Aici Qiu, Youzhi Zhao, (2015) “Generation of Electrohydraulic Shock Waves by Plasma-Ignited Energetic Materials: II. Influence of Wire Configuration and Stored Energy” IEEE Transactions on Plasma Science, Vol. 43, NO. 12, December 2015, pp 4009-4016
- [196] Peter Bruggeman and Daan C Schram, (2010) “On OH production in water containing atmospheric pressure plasmas” Plasma Sources Science and Technology, Vol. 19, No. 04, May 2010, pp 5025
- [197] Peter Bruggeman, Daan Schram, Manuel Á González, Robby Rego, Michael G Kong and Christophe Leys, (2009) “Characterization of a direct dc-excited discharge in water by optical emission spectroscopy” Plasma Sources Science and Technology, Vol. 18, No. 02, pp 5017
- [198] L Li, A Nikiforov, Q Xiong, X Lu, L Taghizadeh and C Leys, (2012) “Measurement of OH radicals at state $X^2\Pi$ in an atmospheric-pressure micro-flow dc plasma with liquid electrodes in He, Ar and N_2 by means of laser-induced fluorescence spectroscopy” J. D. Appl. Phys. Vol. 45, No. 12, February 2012, pp5201
- [199] Kai-Yuan Shih and Bruce R. Locke, (2011) “Optical and Electrical Diagnostics of the Effects of Conductivity on Liquid Phase Electrical Discharge” IEEE Transactions on Plasma Science, , March 2011, Vol. 39, No. 3, pp 883-892
- [200] S. H. R. HOSSEINI, S. Iwasaki, T. Sakugawa and H. Akiyama, (2011)” Characteristics of Micro Underwater Shock Waves Produced by Pulsed Electric Discharges for Medical Applications” Journal of Korean Physical Society, DOI: 10.3938/jkps.59.3526, Vol. 59, No. 6, December 2011, pp 3526-3530
- [201] Branislav Pongrac, Hyun-Ha Kim, Nobuaki Negishi, and Zdenko Machala, (2014)” Influence of water conductivity on particular electrospray modes with dc corona discharge – optical visualization approach” The European Physical Journal D, Vol. 68, No. 8, August 2014, pp 224
- [202] Paul Ceccato, (2010) “Filamentary plasma discharge inside water: initiation and propagation of a plasma in a dense medium” Ph.D. Report, Jan 2010, pp 37-80.
- [203] <http://www.ispc-conference.org>
- [204] Bing Sun, Masayuki Sato and J S Clements, *J. Phys. D: Appl. Phys.* 32 1908.
- [205] E Stoffels, I E Kieft, R E J Sladek, L J M van den Bedem, E P van der Laan and M Steinbach, *Plasma Sources Sci. Technol.* **15** S169.
- [206] David B Graves, . *Phys. D: Appl. Phys.* **45** 263001.
- [207] A. K. Sharma, B.R. Locke, P. Arce, and W.C. Finney, Hazardous Waste and Hazardous

- Materials. 2009, 10(2), pp. 209-219.
- [208] Kevin Hsieh, Huijuan Wang, Bruce R. Locke, Journal of Hazardous Materials. Nov 2016, **317**. Pp. 188-197.
- [209] Jennifer Pascal, Rocío Tíjaro-Rojas, Mario A. Oyanader, Pedro E. Arce European Journal of Engineering Education. 2016, pp. 1-20.
- [210] Fei Dai, Xiangru Fan, Gunnar R. Stratton, Christopher L. Bellona, Thomas M. Holsen, Bernard S. Crimmins, Xiaoyan Xia, Selma Mededovic Thagard Journal of Hazardous Materials. May 2016, 308. pp. 419-429.
- [211] Yongjun Shen, Lecheng Lei, Xingwang Zhang, Jiandong Ding Plasma Science and Technology. 2014, **16**, pp. 1020-1031.
- [212] A Fridman, A Chirokov and A Gutsol, *J. Phys. D: Appl. Phys.*, 2005, 38.
- [213] P Sunka, V Babicky, M Clupek, P Lukes, M Simek, J Schmidt and M Cernak, *Plasma Sources Sci. Technol.* **8** 258, 1999.
- [214] <http://www.ispc-conference.org/ispcproc/papers/23.pdf>
- [215] A Yu Nikiforov, Ch Leys, *Plasma Sources Sci. Technol.* **16**, 2007.
- [216] Bruce R Locke and Kai-Yuan Shih, *Plasma Sources Sci. Technol.* **20**, 2011.
- [217] B S Sommers and J E Foster, *Plasma Sources Sci. Technol.* **23**, 2014.
- [218] Kunihide Tachibana, Yuki Takekata, Yusuke Mizumoto, Hideki Motomura and Masafumi Jinno, *Plasma Sources Sci. Technol.* **20**. 2011.
- [219] Yong Yang, Ph.D. Thesis, “Plasma Discharge in Water and Its Application for Industrial Cooling Water Treatment”, Drexel University, 2011.
- [220] Yong Cheol Hong, Sang Ju Lee, Ye Jin Kim, and Bong Ju Lee, IEEE TRANSACTIONS ON PLASMA SCIENCE, **39** (11), 2011.
- [221] M. W. Ahmed, J. K. Yang, Y. S. Mok, H. J. Lee, Y.H. Yu, JKPS, **65**(9), 2014, pp. 1404-1413.
- [222] W. A. Kearsley Etal, Underwater spark discharge sound-producing system, **3**, 1966.
- [223] Yong Cheol Hong, Hyun Jae Park, Bong Ju Lee, Won-Seok Kang, and Han Sup Uhm, *Phys. Plasmas* **17**, (2010).
- [224] Ruobing Zhang, Liming Wang, Yan Wu, Zhicheng Guan, and Zhidong Jia, IEEE Trans. Plasma Sci. **34**, 2006.
- [225] Cui-hua Wang, Yan Wu, Guo-Feng Li, *J. ELECTROSTAT* **66**, 71–78 (2008).
- [226] D. Ziuzina, S. Patil, P.J. Cullen, K.M. Keener and P. Bourke, *Journal of Applied Microbiology*, **114**, (2013).
- [227] P Sunka , V Babick’y, M Clupek , P Lukes, M Simek , J Schmidt and M Cernak, *Plasma Sources Sci. Technol.* **8** (1999).
- [228] Ing. Zdenka Kozáková, Ph.D. Thesis, Brno University of Technology, Faculty of Chemistry, 2011.
- [229] M. Sato, *I.J.PEST.* **3**,(2009).
- [230] S. H. R. Hosseini, S. Iwasaki, T. Sakugawa and H. Akiyama, *J Korean Phys Soc.* **59**, No. 6, (2011).
- [231] M. W. Ahmed, Jong-Keun Yang, Young-Sun Mok and Heon Ju Lee*, *J Korean Phys Soc.* **65**, (2014).
- [232] Tomasz Izdebski, Mirosław Dors, Jerzy Mizeraczyk, *Eur. Chem. Bull.*, **3**(8), 811-814 (2014).
- [233] B Eliasson, M Hirth and U Kogelschatz, *J. Phys. D: Appl. Phys.* **20** (1987).

- [234] Noriyuki Suetsugu, Takeshi Higa, Sam-Geun Kong, and Masamitsu Wada, *Plant Physiology*, **2**(169)1155-1167, 2015.
- [235] P.A. Balakrishnana, A. Arunagiria, P.G. Raob, *J. ELECTROSTAT* **56**, 77–86 (2002).
- [236] J Kitayama and M Kuzumoto, *J. Phys. D: Appl. Phys.* **32**, pp 3032–3040 (1999).
- [237] Petr Lukes, Austin T. Appleton, and Bruce R. Locke, *IEEE Trans. Ind. Appl.* **40**, (1), 2004.
- [238] Bruce R Locke and Kai-Yuan Shih, *Plasma Sources Sci. Technol.* **20** (2011).
- [239] E Tatarova, N Bundaleska, J Ph. Sarrette and C M Ferreira, *Plasma Sources Sci. Technol.* **23** (2014).
- [240] Petr Lukes, Martin Clupek, Vaclav Babicky, Vaclav Janda and Pavel Sunka, *J. Phys. D: Appl. Phys.* **38** (2005).
- [241] Jean-Thomas Marois-Fiset, Anne Carabin, Audrey Lavoie, and Caetano C. Dorea, *Appl Environ Microbial.* **79**(6): 2107–2109 (2013).
- [242] Nan Jiang, Ailing Ji, and Zexian Cao, *J. Appl. Phys.* **106**, (2009).
- [243] Sun Ja Kim, Tae Hun Chung,* Se Hwan Bae, Sun Hee Leem, *Plasma Process. Polym.* **6**, 2009.
- [244] Mikhail Pekker and Mikhail N Shneider, *J. Phys. D: Appl. Phys.* **48** (2015).
- [245] Stephan Reuter, Jörn Winter, Sylvain Iséni, Ansgar Schmidt-Bleker, Mario Dünnbier, Kai Masur, Kristian Wende, and Klaus-Dieter Weltmann, *IEEE Trans. Plasma Sci.* **43**(9) 2015.
- [246] Shreya Wani, Jagpreet K. Maker, Joseph R. Thompson, Jeremy Barnes and Ian Singleton, *Agriculture*, **5**, 2015.
- [247] Andre Passaglia Schuch, Rodrigo da Silva Galhardo, Keronninn Moreno de Lima-Bessa, Nelson Jorge Schuch and Carlos Frederico Martins Menck, *Photochem. Photobiol. Sci.*, **8**, pp111–120 (2009).
- [248] Rajeshwar P. Sinha, Margit Dautz and Donat-P. Hader, *Acta Protozool.* **40**, pp 187-195 (2001).
- [249] Mojtaba Davoudi, Tahereh Vakili, Abdorrahim Absalan, Mohammad Hassan Ehrampoush and Mohammad Taghi Ghaneian, *Middle-East J. Sci. Res.*, **13** (6): 710-715, 2013.
- [250] Peter Belenky, Jonathan D. Ye, Caroline B.M. Porter, Nadia R. Cohen, Michael A. Lobritz, Thomas Ferrante, Saloni Jain, Benjamin J. Korry, Eric G. Schwarz, Graham C. Walker, and James J. Collins, *Cell Rep.* **13**, 1–13, (2015).
- [251] Michale. G. Simic, Karen A. Taylor, John F. Word “oxygen radicals in biology and medicine”, Plenum press, New York, London, pp. 403, 1987.
- [252] Barbara A. Hamkalo, and P. A. Swenson, *J Bacteriol.* **99**(3), 815–823(1969).
- [253] H. Zuckerman, Ya. E. Krasik, J. Felsteiner, *Innov. Food sci. & emerg. Technol.* **3**, pp.3329–336, 2002.
- [254] S. V. Gudkov, O. E. Karp, S. A. Garmash, V. E. Ivanov, A. V. Chernikov, A. A. Manokhin, M. E. Astashev, L. S. Yaguzhinsky, and V. I. Bruskov, *Mol. BioPhys.* **57**, pp. 1–8. 2012.
- [255] Urs von Gunten, *Water Res.* **37**, pp. 1443–1467, 2003.
- [256] Bum Gun Kwona and Jai H. Lee, *Bull. Korean Chem. Soc.* **27**, pp. 1785-1790, 2006.
- [257] Sankar kumar dey, Debdulal banerjee, Sourav Chattapadhyay and Krishnendu Bikash Karmakar, *IJBPS*, **1**(3), 2010.
- [258] Emima Jeronsia. J, Allwin Joseph, L. and Jerome Das, S., *IJDR*, **5** (10), 2015.
- [259] Priscila Gava Mazzola, Angela Faustino Jozala, Letícia Célia de Lencastre Novaes, Patricia Moriel, Thereza Christina Vessoni Penna, *BJPS*, **45**(2), 2009.
- [260] Kim, Jeong-Keun, Narae Kim, and Young-Hee Lim, *J. Microbiol. Biotechnol.* **20**(1), pp.82–87,

- (2010).
- [261] Ruobing Zhang, Liming Wang, Yan Wu, Zhicheng Guan, IEEE Trans. Plasma Sci. VOL. **34** (4), 2006
- [262] Yong Cheol Hong, Hyun Jae Park, Bong Ju Lee, Won-Seok Kang, and Han Sup Uhm, Phys. Plasmas **17**, 2010.
- [263] Dip. Ing. Dr. Otto Zajic, "Fourth International water Technology Conference IWTC 99", Alexandria, Egypt.
- [264] Ivana Halamova, Anton Nikiforov, Frantisek Krcma, Christophe Leys, J. Phys. **516** (2014).
- [265] J Tores, J M palomares, A Sola, J J A M van der Mullen and A Gamero, J. Phys. D: Appl. Phys. **40**, pp. 5936 2007.
- [266] Spectral Lines Broadning, Hans R. griem, Appendix III. page 316(a), ACADEMIC PRESS New York and London 1974.
- [267] W.L. Wiese, D.E. Kelleher, D.R. Paquette, Detailed Study of the Stark Broadening of Balmer Lines in a High-Density Plasma, Phys. Rev. A. 6 (1972) 1132–1153.
- [268] T. Shirafuji, T. Morita, O. Sakai, and K. Tachibana, Ispc_19, **3**(2009).
- [269] Jufang Zhang, Jierong Chen, Xiaoyong Li, J. Water Resource and Protection, **2**, pp.99-109, 2009.
- [270] George Eisenberg, Ind. Eng. Chem. Anal. Ed., 15 (**5**), pp. 327-328 (1943).
- [271] H. Bader, J. Hoigne, water Res. **15**, pp.449-456 (1981).
- [272] Montgomery, J. M. 1985. Water treatment principles and design. John Wiley, New York, N.Y.
- [273] <http://technologyinscience.blogspot.kr>

Publications

1. **Muhammad Waqar Ahmed**¹, Jong-Keun YANG, Young-Sun MOK, Young-Hun. YU, and Heon-Ju Lee^{*}, "Underwater capillary discharge with air and oxygen addition", JKPS, Vol. 65, No. 9, November 2014.
2. Ulugbek Shaislamov^a, Karthikeyan Krishnamoorthy^b, Sang Jae Kim^b, Amir Abidov^c, Bunyod Allabergenov^c, Sungjin Kim^c, Sooseok Choi^a, Rai Suresh^a, **Waqar Muhammad Ahmed**^a, Heon-Ju Lee^{a*}, "Highly stable hierarchical p-cuo/zno Nano rod/ Nano branch photo electrode for efficient solar energy conversion", International Journal of Hydrogen Energy, Vol.41, No. 4, January 2016.
3. **Muhammad Waqar Ahmed**^a, Sooseok Choi, Konstantin Lyakhov, Ulugbek Shaislamov, Raj Kumar Mongre, Dong Kee Jeong, Rai Suresh. Heon-Ju Lee^{a*}, "High frequency underwater plasma discharge application in antibacterial activity", Plasma physics Reports, 43 (3), 2017 (will be available online from Feb.2017).
4. **Muhammad Waqar Ahmed**¹, Rai Suresh², Jong-Keun Yang², Sooseok Choi², H. J. Lee^{*}, "Effect of water conductivity on the generation of oh· radicals in high frequency underwater Capillary discharge", International Journal of Renewable Energy and Environmental Engineering (IJREE), Vol. 04. No. 02, April, 2016.
5. **Muhammad Waqar Ahmed**¹, Sooseok Choi, Rai Suresh, J.K. Yang, Heon-Ju Lee^{*}, "Diagnostics of argon injected hydrogen peroxide added high frequency underwater capillary discharge", MMSE, Vol.06, Sep. 2016.